



Durham E-Theses

Molecular characterisation of the Polaris locus of Arabidopsis

Casson, Stuart Anthony

How to cite:

Casson, Stuart Anthony (2000) *Molecular characterisation of the Polaris locus of Arabidopsis*, Durham theses, Durham University. Available at Durham E-Theses Online: <http://etheses.dur.ac.uk/4342/>

Use policy

The full-text may be used and/or reproduced, and given to third parties in any format or medium, without prior permission or charge, for personal research or study, educational, or not-for-profit purposes provided that:

- a full bibliographic reference is made to the original source
- a [link](#) is made to the metadata record in Durham E-Theses
- the full-text is not changed in any way

The full-text must not be sold in any format or medium without the formal permission of the copyright holders.

Please consult the [full Durham E-Theses policy](#) for further details.

Molecular Characterisation of the *POLARIS*

Locus of *Arabidopsis*

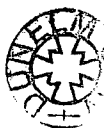
**Thesis submitted for the degree of
Doctor of Philosophy
at the University of Durham**

The copyright of this thesis rests with the author. No quotation from it should be published in any form, including Electronic and the Internet, without the author's prior written consent. All information derived from this thesis must be acknowledged appropriately.

by

**Stuart Anthony Casson B.Sc.
Department of Biological Sciences
University of Durham**

August 2000



17 SEP 2001

Stuart Anthony Casson
Molecular Characterisation of the *POLARIS*
Locus of *Arabidopsis*
ABSTRACT

This study is concerned with the analysis of the AtEM101 promoter trap line of *Arabidopsis thaliana*. AtEM101 seedlings show GUS expression in the tips of both primary and lateral roots, and more weakly in the hypocotyl and cotyledons. GUS activity in mature plants is found variably in both rosette and cauline leaves, stem nodes and also siliques but not other floral organs. Active auxins rapidly upregulate whilst cytokinins downregulate GUS transcript levels. AtEM101 roots are shorter than those of the wild-type, a phenotype which is putatively linked to elevated ethylene levels. AtEM101 roots were also found to be hypersensitive to exogenous cytokinins. Root patterning is not affected, but cells distal to the elongation zone are shorter in the AtEM101 line than the wild-type. The T-DNA in line AtEM101 was found to have inserted in a small, low abundance gene named *POLARIS*, which encodes a putative 36 amino acid polypeptide, which does not share homology to any known genes. *POLARIS* shows unusual genome organisation, with its 5' end overlapping with the 3' end of an upstream gene. Upstream sequence, embedded within the upstream gene, when fused to GUS were able to direct expression in root tips whilst a longer fragment mimics the GUS expression of the AtEM101 line. Retransformation of the AtEM101 line with a wild-type allele of *POLARIS* was able to complement the mutant phenotype indicating that the T-DNA insertion into *POLARIS* is responsible for the AtEM101 phenotype. Overexpression of *POLARIS* resulted in transgenic plants with reduced sensitivity to both cytokinins and ACC. The structure of the *POLARIS* locus and the potential role of *POLARIS* in regulating cytokinin-induced ethylene levels, with regards to the control of root growth, are discussed.

Acknowledgements

Many thanks to my supervisor, Keith Lindsey, for his help and support. His advice and a number of useful discussions has been extremely helpful in the completion of this work.

Also, my thanks to past and present members of the lab. Jen and Marta have been particularly helpful with regards to practical matters. Many thanks also to Paul, whose own work and discussions have been invaluable to this work. To Kez, Kirsty, Gill, Martin, Mags and others, thanks for making my time in the lab enjoyable, and for the odd pint too. Kirsty, my appreciation's for grudgingly giving me your swivel chair. I am very grateful for financial support from the BBSRC and Shell Research in the form of a case studentship, in particular Dr. Glyn Edwards at Shell.

Save the best till last. Should I thank Mike, whom I have far too many hangovers to be grateful for. At least he helped keep me sane whilst writing up. Poorer, but sane. My housemates Mark, Hilary and Beki for putting up with me. And of course to my family. Mum. For your patience, help (not just financial!) and support (again, not just financial!). My gratitude always.

CONTENTS

Page Number

Chapter 1

Introduction.....	1
1.1 The <i>Arabidopsis</i> root.....	1
1.1.1 Embryonic origin of the <i>Arabidopsis</i> root.....	1
1.1.2 The structure of the primary seedling root.....	2
1.2 Mutations affecting root development.....	3
1.2.1 Apical-basal pattern mutants.....	3
1.2.2 Mutations in the <i>GNOM</i> gene affect axis formation.....	4
1.2.3 Mutations in the <i>MONOPTEROS</i> gene disrupt root and hypocotyl formation.....	5
1.2.4 The <i>bodenlos</i> mutation affects primary root formation.....	7
1.2.5 The <i>HOBBIT</i> gene is required for root meristem formation.....	9
1.3 Radial Pattern Mutants.....	10
1.3.1 The <i>woodenleg</i> and <i>gollum</i> mutations affect vascular organisation.....	10
1.3.2 The <i>short root</i> and <i>scarecrow</i> mutations affect endodermis and cortex patterning.....	11
1.3.3 The <i>fass</i> mutant affects morphogenesis.....	12
1.4 Mutants in post-embryogenic root development.....	13
1.4.1 The <i>ROOT MERISTEMLESS</i> genes are involved in cell proliferation in the root meristem.....	14
1.5 Cell Expansion mutants.....	14
1.6 Epidermal Cell Differentiation.....	16
1.7 The Role of Plant Growth Regulators in Root Development.....	20
1.7.1 Auxin as a signal during embryogenesis.....	20
1.7.2 Polar Auxin Transport in the Root.....	25
1.7.3 Auxin Distribution in the Root and its Possible Role in Patterning.....	30
1.7.4 Auxin and Root Growth.....	33
1.7.5 Auxin-Binding Protein – An Auxin Receptor?.....	35
1.7.6 The Auxin Response Pathway.....	37
1.7.7 Ethylene and Root Development.....	41
1.7.8 Ethylene and Auxin Interactions.....	43
1.7.9 Ethylene and Cytokinin Interactions.....	44

1.7.10 Ethylene Signalling.....	47
1.8 The AtEM101 promoter trap line of Arabidopsis.....	50
1.8.1 Isolation of Genes by Promoter Trapping.....	51
1.8.2 Identification and Characterisation of Line AtEM101.....	52
1.8.3 Line AtEM101 has a Short Root Phenotype.....	54
1.8.4 Molecular Characterisation of the <i>POLARIS</i> locus of <i>Arabidopsis thaliana</i>	55
 Chapter 2 Materials and methods.....	 56
2.1 Materials.....	56
2.1.1 Chemicals.....	56
2.1.2 Radiochemicals.....	56
2.1.3 Enzymes.....	56
2.1.4 Kits.....	57
2.1.5 Bacterial strains.....	57
2.1.6 Plasmids.....	58
2.1.7 Bacterial culture media.....	58
2.1.8 Plant material.....	59
2.1.9 Plant culture media.....	59
2.1.10 cDNA libraries.....	59
2.2 Plant transformation.....	59
2.2.1 Mobilisation of binary vectors into <i>Agrobacterium tumefaciens</i>	59
2.2.2 Seed sterilisation and growth conditions.....	60
2.2.3 <i>Arabidopsis</i> transformation: the root explant method.....	60
2.2.4 <i>Arabidopsis</i> transformation: the dipping method.....	62
2.3 GUS enzyme analysis.....	62
2.3.1 Histochemical GUS analysis.....	62
2.4 Histological Examination of Roots.....	63
2.4.1 Fresh Transverse Root Sections.....	63
2.4.2 Examination of Root Tips.....	63
2.4.3 Cell Measurements.....	64
2.5 Extraction and purification of nucleic acids.....	64
2.5.1 Miniprep of plasmid DNA using the Wizard™ minipreps DNA purification system.....	64
2.5.2 Maxipreps of plasmid DNA.....	65
2.5.3 Plant DNA extraction using the Phytopure kit.....	66

2.5.4 A quick DNA extraction method for PCR.....	66
2.5.5 RNA extractions using Guanidine hydrochloride.....	67
2.5.6 RNA extraction using the Qiagen RNeasy kit.....	67
2.5.7 Purification of DNA from agarose gels using the Geneclean II kit.....	68
2.5.8 Purification of DNA using the <i>High Pure</i> PCR Product Purification kit.....	68
2.5.9 Purification of mRNA from total RNA.....	69
2.6 Electrophoresis.....	70
2.6.1 DNA agarose gel electrophoresis.....	70
2.6.2 RNA formaldehyde gel electrophoresis.....	70
2.6.3 Staining of RNA formaldehyde gels.....	71
2.6.4 DNA sequencing gels.....	71
2.6.5 Mini denaturing polyacrylamide gels.....	72
2.7 Nucleic acid hybridisation.....	72
2.7.1 Southern blotting.....	72
2.7.2 Northern blotting.....	73
2.7.3 Colony hybridisation.....	74
2.7.4 Radio-labelling of probes with [³² P]α-dCTP.....	74
2.7.5 End-labelling with [³² P]γ-ATP.....	75
2.7.6 Pre-hybridisation and hybridisation.....	75
2.7.7 Washing conditions.....	76
2.7.8 Ribonuclease protection assays.....	76
2.7.9 Radiolabelling of RNA probes.....	77
2.7.10 Primer extension.....	78
2.7.11 Autoradiography.....	79
2.7.12 Probe stripping.....	79
2.8 cDNA library screening.....	79
2.8.1 Plating lambda phage libraries to generate plaques.....	79
2.8.2 Plaque lifts for hybridisation with DNA probes.....	80
2.8.3 Removal and storage of positive plaques.....	80
2.9 DNA cloning into plasmid vectors.....	80
2.9.1 Digestion of vector and insert DNA with restriction endonucleases.....	80
2.9.2 Dephosphorylation of vector DNA.....	81
2.9.3 T-tailing of vector DNA.....	81
2.9.4 Ligation of DNA fragments.....	81
2.9.5 Ligation of PCR fragments into pCR®2.1-TOPO.....	82
2.9.6 Transformation of <i>E.coli</i> with plasmid DNA by electroporation.....	82

2.9.7 Transformation of TOP10 One Shot™ competent cells.....	83
2.10.1 DNA sequencing.....	83
2.10.2 Manual DNA sequencing.....	83
2.11 Polymerase Chain Reaction	84
2.11.1 Standard PCR.....	84
2.11.2 PCR using Expand™ High Fidelity PCR system.....	85
2.12 Cloning of cDNA ends by RACE.....	85
2.12.1 Cloning of cDNA 3' ends (3' RACE)	85
2.12.2 cDNA synthesis.....	86
2.12.3 Cloning <i>POLARIS</i> and <i>GENE X</i> cDNA clones by 3' RACE.....	86
2.12.4 Cloning of cDNA 5' ends (5' RACE)	87
2.12.5 cDNA synthesis.....	87
2.12.6 Purification of cDNA.....	87
2.12.7 Tailing of cDNA.....	88
2.12.8 Cloning of the <i>POLARIS</i> and GUS-fusion transcripts 5' ends.....	88
2.13 RNA-Specific PCR (RS-PCR)	89
2.13.1 DNase treatment of RNA.....	90
2.13.2 cDNA synthesis.....	90
2.13.3 Amplification of <i>POLARIS</i> cDNA.....	90
2.14 Analysis of proteins.....	91
2.14.1 Protein extraction.....	91
2.14.2 Precipitation of proteins.....	91
2.14.3 Electrophoresis of proteins using the tris-tricine buffer system.....	91
2.14.4 Staining of protein gels.....	93
2.14.5 Blotting of protein gels.....	93
2.14.6 Staining of PVDF membrane for total protein.....	94
2.14.7 Reversible staining of membranes for total protein.....	94
2.14.8 Protein detection by chemiluminescence.....	95
2.14.9 Antibody production.....	96
2.15 Plasmid Construction.....	96
2.15.1 Construction of <i>POLARIS</i> - GFP fusions.....	96
2.15.2 Construction of pCIRCE-NOS.....	97
2.15.3 Construction of pN-POL:GFP.....	97
2.15.4 Construction of pC:GFP:POL.....	97

Chapter 3 The Promoter trap line AtEM101.....	99
3.1 GUS expression pattern of line AtEM101.....	99
3.2 Analysis of the GUS-fusion transcript.....	101
3.2.1 Transcription initiates outside the T-DNA.....	101
3.2.2 Initiation of transcription of the fusion transcript.....	101
3.3 Auxin treatment rapidly upregulates GUS transcript levels.....	102
3.3.1 The effect of inactive auxin analogues on GUS-fusion transcript levels.....	103
3.3.2 Line AtEM101 Shows Normal Auxin Sensitivity.....	104
3.4 Line AtEM101 is defective in ethylene synthesis and is hypersensitive to cytokinins and ACC.....	105
3.5 Histological Examination of AtEM101 Roots.....	106
3.6 Summary.....	107

Chapter 4 Cloning and characterisation of the *POLARIS*

gene.....	109
4.1 Genomic organisation of the <i>POLARIS</i> locus.....	109
4.2 Cloning of the <i>POLARIS</i> gene.....	112
4.2.1 Isolation of a partial cDNA by 3' RACE.....	112
4.2.2 Determining the transcriptional initiation site.....	113
4.2.3 Structure of the <i>POLARIS</i> gene.....	115
4.3 The <i>POLARIS</i> gene putatively encodes a small polypeptide.....	116
4.3.1 The 5' UTR of <i>POLARIS</i> contains small upstream ORFs.....	117
4.3.2 The putative <i>POLARIS</i> polypeptide is undetectable using a polyclonal antibody.....	118
4.4 Expression pattern of the <i>POLARIS</i> gene.....	118
4.5 Summary.....	120

Chapter 5 Cloning and Characterisation of the *POLARIS* Promoter and Preliminary Analysis of the *GENE X* Promoter.....

5.1 Cloning of the <i>POLARIS</i> promoter.....	121
5.2 Auxin response of the <i>POLARIS</i> promoter.....	123
5.2.1 Examination of the auxin response by northern blot analysis.....	125
5.3 Expression pattern of the putative <i>GENE X</i> promoter.....	126
5.4 Summary.....	127

Chapter 6 Complementation of the AtEM101 mutant phenotype and analysis of plants overexpressing <i>POLARIS</i>	129
6.1 Complementation of the AtEM101 mutant phenotype by retransformation with the <i>POLARIS</i> gene	129
6.2 35S: <i>POLARIS</i> seedlings overexpress the <i>POLARIS</i> gene	132
6.3 The effect of overexpressing <i>POLARIS</i> on root growth in light grown seedlings	134
6.4 Root growth of 35S: <i>POLARIS</i> seedlings grown in the presence of ACC and BA in the dark	134
6.5 The effect of auxin treatment on root growth of wild-type and 35S: <i>POLARIS</i> seedlings	135
6.6 Summary	136
Chapter 7 Discussion	137
7.1 Genomic Organisation of the <i>POLARIS</i> Locus	137
7.2 Structure of the <i>POLARIS</i> Transcript	142
7.3 The <i>POLARIS</i> Polypeptide	145
7.4 The <i>pls</i> Phenotype	149
7.5 Expression of <i>POLARIS</i> and the <i>pls</i> Phenotype	154
7.6 Future Work	155
References	160
Appendix	
Appendix I Oligonucleotides	185
Appendix II Complementation Root Length Data	188
Appendix III 35S <i>POLARIS</i> data	189

List of Figures

Title	Page Number
1.1 Structure of the Primary Root of <i>Arabidopsis</i>	3a
1.2 A Model for The Auxin / Ubiquitin Pathway.....	38a
1.3 The Ethylene Response Pathway.....	42a
1.4 Promoter Trap Vector pΔgusBIN19.....	52a
3.1 Histochemical Analysis of GUS Expression in 7 day old AtEM101 Seedlings..	99a
3.2 Time Course of GUS Staining in the Root Tip of AtEM101.....	100a
3.3 Analysis of GUS-fusion transcript levels in organs of the AtEM101 line.....	100b
3.4 Histochemical Analysis of GUS Expression in 3 week old AtEM101 Plants...	100c
3.5 Transcription of the GUS Transcript Initiates Outside of the T-DNA LB.....	101a
3.6 5' RACE on the GUS-Fusion Transcript.....	102a
3.7 Analysis of GUS-Fusion Transcript Levels in Line AtEM101 Following Treatment with Auxin or Cytokinin.....	103a
3.8 GUS-Fusion Transcript Levels Following Treatment with Active and Inactive Auxin Analogues.....	104a
3.9 Expression of an Ethylene-induced GST in AtEM101 Determined by RNA Gel Blot Hybridisation.....	105a
3.10 Histological Comparison of AtEM101 and C24 Roots.....	106a
4.1 Genomic Clone Sequence.....	109a
4.2 Cloning of <i>GENE X</i> by 3' RACE and Analysis of Expression in the AtEM101 line.....	110a

4.3 Primer Sites.....	112a
4.4 Cloning of a Partial <i>POLARIS</i> cDNA by 3' RACE.....	112b
4.5 RNase Protection Assay on AtEM101 and Wild-type RNA.....	114a
4.6 Isolation of the Transcript Start Site of <i>POLARIS</i> by 5'RACE.....	114b
4.7 Southern and northern analysis of <i>POLARIS</i>	115a
4.8 The <i>POLARIS</i> Transcript.....	115b
4.9 Overlap Between the <i>GENE X</i> and <i>POLARIS</i> Transcripts.....	115c
4.10 Secondary Structure Predictions of the Putative <i>POLARIS</i> Polypeptide.....	116a
4.11 Analysis of the <i>POLARIS</i> transcript in various organs by RS-PCR.....	119a
4.12 RS-PCR of the <i>POLARIS</i> transcript following treatment with auxin or ACC.....	119b
5.1 Cloning of the <i>POLARIS</i> Promoter.....	122a
5.2 Histochemical Analysis of GUS Expression in 584POL:GUS Transgenic Lines.....	123a
5.3 Histochemical Analysis of GUS Expression in 1635POL:GUS Transgenic Lines.....	123b
5.4 Auxin response of the 584POL:GUS and 1635POL:GUS Promoters.....	125a
5.5 Isolation and Cloning of the <i>GENEX</i> Promoter.....	126a
5.6 Histochemical Analysis of GUS Staining of <i>GENE X</i> Promoter GUS Primary Transformants.....	127a
5.7 Analysis of <i>GENE X</i> Promoter GUS Staining Patterns in the Root.....	127b
6.1 Cloning of the <i>POLARIS</i> Locus for Complementation of the AtEM101	

Phenotype.....	130a
6.2 Complementation of the AtEM101 Mutant Phenotype.....	131a
6.3. Root Lengths of Independent AtEM101 Lines Retransformed with a Wild-Type Allele of <i>POLARIS</i>	131c
6.4 Complementation of the AtEM101 Mutant Phenotype in Line 113C.....	132a
6.5 Cloning of a Partial <i>POLARIS</i> cDNA for Overexpression.....	132b
6.6 Overexpression of a Partial <i>POLARIS</i> cDNA in Transgenic Plants.....	133a
6.7 Root Growth of 35 <i>SPOLARIS</i> Transgenic Lines in Light Conditions.....	134a
6.8 Root Growth of 35 <i>SPOLARIS</i> Transgenic Plants in the Presence of ACC or BA.....	135a
6.9 The Effect of Overexpressing <i>POLARIS</i> on ACC and BA Sensitivity.....	135b
6.10 Root Growth of 35 <i>SPOLARIS</i> Transgenic Lines in the Presence of NAA....	136a
7.1 <i>POLARIS</i> Genome Organisation and Gene Structure: Potential Problems.....	139a
7.2 Model to Explain the Possible Mode of Action of <i>POLARIS</i> in the Root.....	155a

List of Tables

Table	Title	Page Number
3.1	Root Growth of AtEM101 and C24 on Auxin, BA and ACC.....	104b
3.2	Comparison of Cortical Cell Measurements Between AtEM101 and C24.....	107

ABBREVIATIONS

ACC	1-aminocyclopropane-1-carboxylic acid
AREs	auxin response elements
ARFs	auxin response factors
BA	benzyladenine
Bp	base pair (length of a nucleotide)
BSA	bovine serum albumin
CaMV35s	cauliflower mosaic virus 35S RNA gene
cDNA	complementary DNA
dATP	2'-deoxyadenosine 5'-triphosphate
dCTP	2'-deoxycytidine 5'-triphosphate
dGTP	2'-deoxyguanine 5'-triphosphate
dTTP	2'-deoxythymidine 5'-triphosphate
2,3-D	2,3-dichlorophenoxyacetic acid
2,4-D	2,4-dichlorophenoxyacetic acid
DNA	deoxyribonucleic acid
dNTPs	2'-deoxynucleotide 5'-triphosphates
DTT	dithiothreitol
EDTA	ethylenediaminetetraacetic acid, disodium salt
GUS	β -glucuronidase
<i>gusA</i> (<i>uidA</i>)	gene encoding β -glucuronidase
HCl	hydrochloric acid
HPTII	hygromycin B phosphotransferase
IAA	indole-3-acetic acid
IPCR	inverse PCR

kb	kilobase(s) (length of 1000bp)
KCl	potassium chloride
KOH	potassium hydroxide
LB	T-DNA left border
LiCl	lithium chloride
MgCl ₂	magnesium chloride
mRNA	messenger RNA
1-NAA	1-naphthaleneacetic acid
2-NAA	2-naphthaleneacetic acid
NaCl	sodium chloride
Na ₂ HPO ₄	disodium hydrogen orthophosphate
NaH ₂ PO ₄	sodium dihydrogen orthophosphate
NaOH	sodium hydroxide
NOS	nopaline synthase
NPA	1- <i>N</i> -naphthylphthalamic acid
NPTII	neomycin phosphotransferase
<i>nptII</i>	gene encoding neomycin phosphotransferase
OD	optical density
PCR	polymerase chain reaction
<i>PLS</i>	gene encoding POLARIS
RACE	rapid amplification of cDNA ends
RB	T-DNA right border
RNA	ribonucleic acid
RPA	RNase protection assay
RS-PCR	RNA-specific PCR

SDS	sodium dodecyl sulphate
SE	standard error
SEM	standard error of the mean
T-DNA	transferred DNA
Ter	terminator (transcriptional)
TIBA	triiodobenzoic acid
Ti plasmid	tumour-inducing plasmid
Tris	tris(hydroxymethyl)aminomethane
μg	microgram
X-Gluc	5-brom-4-chloro-3-indoyl β-D-glucuronic acid

KEY TERMS AND GENE AND MUTANT SYMBOLS

Cellular differentiation – the processes by which a cell acquires a specialised identity.

Morphogenesis – the development of shape and structure.

Pattern formation – The establishment of body plan ie. the spatial arrangement of differentiated cell types, tissues and organs.

ABP1	Auxin-binding protein
ACS4	ACC SYNTHASE 4
ACS5	ACC SYNTHASE 5 (allelic to <i>cin5</i> and <i>eto2</i>)
AGR1	AGRAVITROPIC1 (also known as <i>AtPIN2</i> and <i>EIR1</i>)
<i>alf1</i>	<i>aberrant lateral root formation 1</i> (alleic to <i>superroot</i> and <i>rooty</i>)
<i>alf4</i>	<i>aberrant lateral root formation 4</i>
ARF1	ADP-RIBOSYLATION FACTOR1
ARF1	AUXIN RESPONSE FACTOR 1 (also kown as <i>IAA24</i>)
ASK1	<i>Arabidopsis</i> Skp1-like protein1
ASK2	<i>Arabidopsis</i> Skp1-like protein2
<i>AtCUL1</i>	<i>Arabidopsis</i> CULLIN
<i>AtLTP1</i>	LIPID TRANSFER PROTEIN1
<i>AtPIN1</i>	PIN-FORMED 1
<i>AtPIN2</i>	PIN-FORMED 2 (also known as <i>AGR1</i> and <i>EIR1</i>)
<i>AUL1</i>	<i>auxilin-like protein</i>
AUX1	AUXIN RESISTANT 1
<i>axr1</i>	<i>auxin resistant 1</i>
<i>axr3</i>	<i>auxin resistant 3</i>
<i>axr6</i>	<i>auxin resistant 6</i>

<i>bdl</i>	<i>bodenlos</i> (allelic to <i>IAA12</i>)
<i>CCT8</i>	<i>chaperonin subunit 8</i>
<i>CDC53</i>	<i>CELL DIVISION CONTROL PROTEIN 53 (CULLIN A)</i>
<i>cin1-5</i>	<i>cytokinin insensitive1-5</i>
<i>ckr1</i>	<i>cytokinin resistant 1</i>
<i>CLV1</i>	<i>CLAVATA 1</i>
<i>CLV3</i>	<i>CLAVATA 3</i>
<i>CPC</i>	<i>CAPRICE</i>
<i>cob</i>	<i>cobra</i>
<i>CTR1</i>	<i>CONSTITUTIVE TRIPLE RESPONSE1</i>
<i>cud</i>	<i>cudgel</i>
<i>ECR1</i>	<i>PUTATIVE UBIQUITIN ACTIVATING ENZYME E1</i>
<i>EhMCM3</i>	<i>Mini Chromosome Maintenance 3</i>
<i>EhPAK</i>	<i>p21 activated kinase</i>
<i>EIL</i>	<i>EIN3-LIKE</i>
<i>EIN2</i>	<i>ETHYLENE INSENSITIVE 2</i>
<i>EIN3</i>	<i>ETHYLENE INSENSITIVE 3</i>
<i>EIN4</i>	<i>ETHYLENE INSENSITIVE 4</i>
<i>EIR1</i>	<i>ETHYLENE INSENSITIVE ROOT 1</i> (also known as <i>AtPIN2</i> and <i>AGR1</i>)
<i>ERF1</i>	<i>ETHYLENE RESPONSE FACTOR 1</i>
<i>ERS1</i>	<i>ETHYLENE RESPONSE SENSOR1</i>
<i>ERS2</i>	<i>ETHYLENE RESPONSE SENSOR2</i>
<i>eto2</i>	<i>ethylene overproducer 2</i> (allelic to <i>ACS5</i> and <i>cin5</i>)
<i>etr1</i>	<i>ethylene response1</i>
<i>fs</i>	<i>fass</i>

<i>Gea1</i>	<i>Guanine-nucleotide exchange factor of ADP-ribosylation factor1</i>
<i>Gea2</i>	<i>Guanine-nucleotide exchange factor of ADP-ribosylation factor2</i>
<i>GL2</i>	<i>GLABRA2</i>
<i>glm</i>	<i>gollum</i>
<i>gn</i>	<i>gnom</i> (also known as <i>emb30</i>)
<i>Grr1</i>	<i>CYCLIN F BOX PROTEIN</i>
<i>hbt</i>	<i>hobbit</i>
<i>JAK3</i>	<i>Janus kinase 3</i>
<i>lit</i>	<i>lion's tail</i>
<i>mp</i>	<i>monopteros</i>
<i>OTC</i>	<i>ORNITHINE CARBAMOYLTRANSFERASE</i>
<i>PLS</i>	<i>POLARIS</i>
<i>pom1</i>	<i>pom-pom 1</i>
<i>pom2</i>	<i>pom-pom 2</i>
<i>qui</i>	<i>quill</i>
<i>ran1</i>	<i>responsive-to-antagonist1</i>
<i>rcn1</i>	<i>roots curl in NPA</i>
<i>rh6</i>	<i>root hair defective 6</i>
<i>RLF1</i>	<i>Relaxin-like-factor</i>
<i>rml1</i>	<i>root meristemless1</i>
<i>rml2</i>	<i>root meristemless2</i>
<i>rty</i>	<i>rooty</i> (alleic to <i>alf1</i> and <i>superroot</i>)
<i>RUB1</i>	<i>RELATED TO UBIQUITIN</i>
<i>sab</i>	<i>sabre</i>
<i>sar1</i>	<i>suppressor of auxin response</i>

<i>SCR</i>	<i>SCARECROW</i>
<i>Sec7</i>	<i>GUANINE NUCLEOTIDE EXCHANGE PROTEIN FOR ARF</i>
<i>SHR</i>	<i>SHORT ROOT</i>
<i>shy2</i>	<i>short hypocotyl 2 (allelic to IAA3)</i>
<i>SKP2</i>	<i>HOMO SAPIENS S-PHASE KINASE-ASSOCIATED PROTEIN 2</i>
<i>stp1</i>	<i>stunted plant 1</i>
<i>sur1</i>	<i>superroot (allelic to <i>alf1</i> and <i>rooty</i>)</i>
<i>TTG</i>	<i>TRANSPARENT TESTA GLABRA</i>
<i>tir1</i>	<i>transport inhibitor response 3</i>
<i>TRP1</i>	<i>PHOSPHORIBOSYLANTHRANILATE ISOMERASE</i>
<i>Uba2</i>	<i>Ubiquitin-activating enzyme 2</i>
<i>Uba3</i>	<i>Ubiquitin-activating enzyme 3</i>
<i>YEC2</i>	<i>ARF GUANINE-NUCLEOTIDE EXCHANGE FACTOR 2</i>
<i>WER</i>	<i>WEREWOLF</i>
<i>wol</i>	<i>woodenleg</i>

Chapter 1 Introduction

Plant development can be viewed as the processes through which the fertilised zygote gives rise to the mature body form with spatially defined organs consisting of organised, differentiated cells. The study of these processes of pattern formation, morphogenesis and cellular differentiation has been greatly facilitated in recent years through the use of such model plants as *Arabidopsis thaliana*. The small size, rapid life cycle, small genome and abundance of mutants has made *Arabidopsis* an attractive model for studying the genetics of plant development (Meinke *et al.*, 1998; Scheres and Wolkenfelt, 1998; Benfey and Schiefelbein, 1994).

1.1 The *Arabidopsis* Root

The structure and development of both the seedling and mature adult plant is dependent on the activity of the shoot and root meristems, both of which are formed during embryogenesis (reviewed Jürgens *et al.*, 1995; West and Harada, 1993). In particular the root has rapidly become a paradigm for the study of the processes controlling organ development. Compared to other organs the primary root is relatively simple with a uniform structure, defined cell lineage, radial symmetry and few differentiated cell types (Dolan *et al.*, 1993; Scheres *et al.*, 1994; Scheres and Wolkenfelt, 1998). Its transparent nature and the ability to grow large numbers of seedlings together has facilitated the identification of large numbers of mutants with abnormal root development all of which have contributed to a greater understanding of the processes which control plant development (Aeschbacher *et al.*, 1994).

1.1.1 Embryonic origin of the *Arabidopsis* root

One of the most attractive features of using the *Arabidopsis* primary root to study development is that a great deal is known about its origin during embryogenesis and the subsequent cell divisions that result in the tightly defined structure of the seedling primary root.

After fertilisation the zygote undergoes a transverse asymmetric division resulting in a smaller apical cell and a larger basal cell. The apical cell divides to produce the embryo proper which consists of the shoot meristem, cotyledons, hypocotyl, root and root meristem initials. The basal cell divides to form the suspensor, a file of 7-8 cells which is involved in nutrient transfer between maternal tissue and the embryo. The uppermost cell of the suspensor, the hypophysis, divides



to give rise to the quiescent centre of the root meristem and the central root cap. Both the daughter cells of the zygote therefore contribute to the root primordium.

Following the division of the zygote, the apical daughter cell undergoes two vertical divisions perpendicular to each other followed by a transverse division giving rise to the octant stage embryo. The embryo proper is now organised into two tiers of which the upper tier ultimately divides to form the cotyledons and shoot apex. The lower tier (lt) will, by the triangular stage of embryogenesis, have undergone another transverse division, further subdividing the lt into the upper lower tier (ult) and the low lower tier (llt). The llt consists at this point of elongated procambial cells and one layer each of protoderm and ground meristem, each two cells high. The hypophyseal cell meanwhile has divided to give a lens shaped cell upon which the llt sits. There follows defined division of these cell types giving rise to a structure with recognisable root meristem initials (cortical, pericycle, vascular, columella as well as the lateral root cap layer; Scheres *et al.*, 1994). The embryonic root primordium therefore becomes a distinct group of cells by the late heart stage of embryogenesis.

1.1.2 The structure of the primary seedling root

One defining feature of the primary seedling root is its precise radial pattern. In transverse sections of the mature root distal to the root meristem this pattern presents itself as single cell-thick rings of epidermis, cortex, endodermis, and pericycle tissues wrapped around the central stele. The cortex and endodermal layers invariably contain eight cells whilst the pericycle averages twelve cells (Dolan *et al.*, 1993). The epidermis lies on the outer side of the cortex and consists of two cell types, trichoblasts and atrichoblasts. Trichoblasts overlie the anticlinal walls of the two underlying cortical cells and differentiate into cells that produce root hairs whereas atrichoblast cells are positioned above only one cortical cell and do not produce root hairs (Dolan *et al.*, 1994). This radial pattern is maintained throughout the mature primary root and longitudinal sections show cell files of each of the aforementioned cell types extending down to specific sets of cells in the meristematic zone, called initials, which act as the origin of these files (Figure 1.1 a & b).

The root meristem consists of these initials, which generate the specific tissue files by regulated cell divisions, and a central cluster of four cells called the quiescent centre, so called because of their low frequency of mitotic activity. The cells of the meristem are arranged in tiers with the lowest tier consisting of the

initials for the root cap (both columella and lateral) and the epidermis, with the lateral root cap and epidermis appearing to originate from the same initials. The middle tier contains the central quiescent centre cells and flanking them the initials for the cortex and endodermis, whilst the upper tier containing the vascular and pericycle initials is allied with the cells of the stele (Dolan *et al.*, 1993). The root meristem therefore provides new cells which add to the pre-existing files extending back into the mature root. Behind the root meristem is the so called expansion zone in which the newly added cells divide and expand before fully differentiating, in the maturation zone, into the varied cell types of the root. The primary root is therefore a good example of an organ in which all cell developmental stages can be easily identified along its axis.

The primary seedling root with its highly organised and regular cellular pattern is therefore an excellent model for examining plant organ development. Among the major questions currently being addressed are what are the nature of the signals that determine this ordered pattern, how it is maintained, and which genes are involved in controlling these processes? A number of different approaches have been used in order to answer these problems and will be discussed.

1.2 Mutations affecting root development

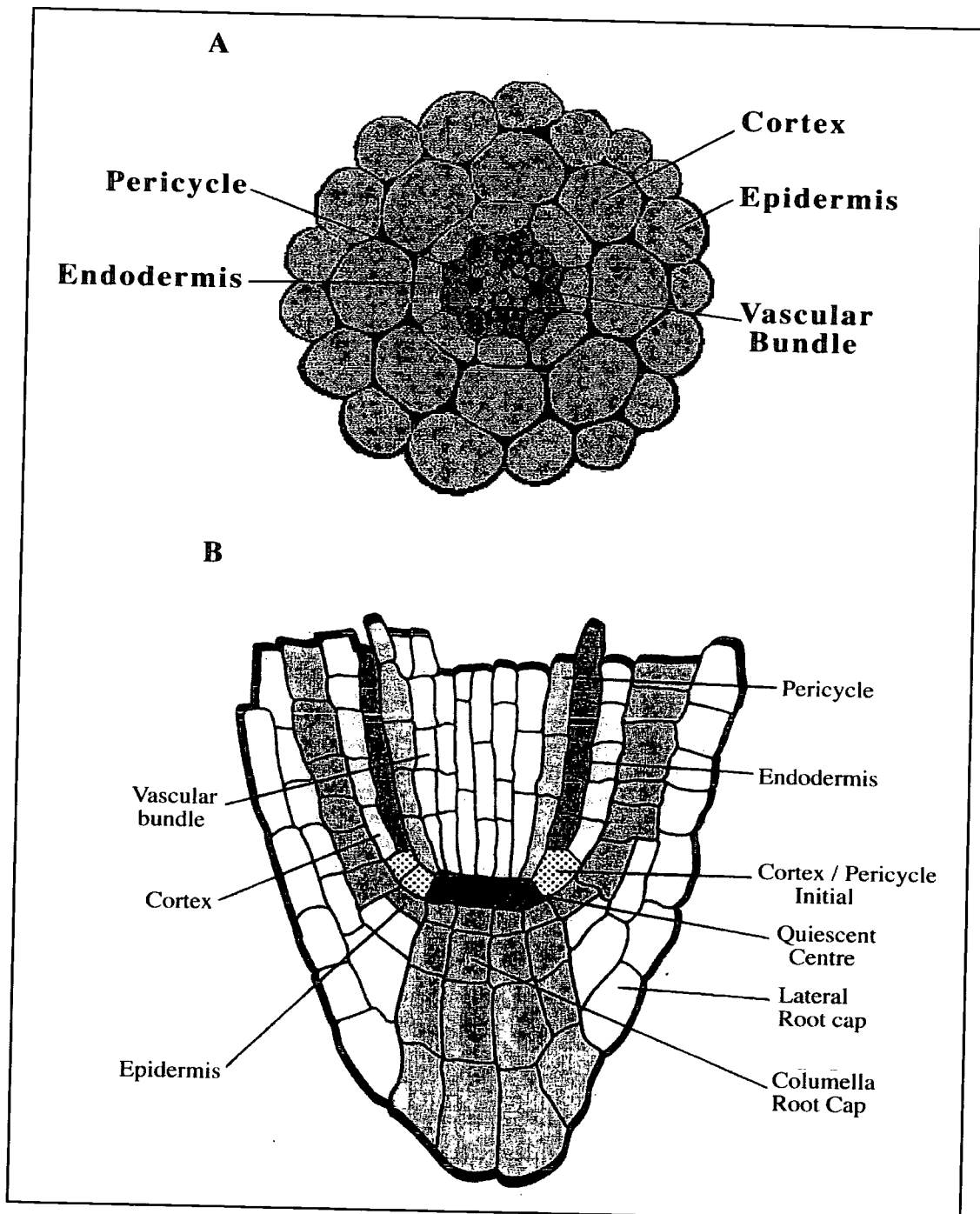
One of the most popular and successful methods of answering questions in plant developmental biology has been the identification and analysis of mutants and the subsequent cloning of the genes involved. The regular patterning of the *Arabidopsis* root makes it particularly amenable to this approach and a number of screens have been performed identifying mutants in apical-basal pattern, radial organisation, morphogenesis and differentiation (Jürgens *et al.*, 1991; Mayer *et al.*, 1991; Scheres *et al.*, 1995; Tanimoto *et al.*, 1995). The identification and analysis of a number of these mutants will be reviewed and where known, the function of the genes discussed.

1.2.1 Apical-basal pattern mutants

One of the most striking features of the seedling body form is the distinct apical-basal axis with the shoot and root meristems located at opposite poles of the seedling. This axis of polarity is established in the earliest stages of embryogenesis with the first division of the zygote which gives rise to a small apical cell and large

Figure 1.1. Structure of the Primary Root of *Arabidopsis*.

- A)** Transverse section from the maturation zone showing the radial pattern of the primary root.
- B)** Longitudinal section of the root tip showing the initial cells flanking the quiescent centre.



basal cell. As described previously, the apical cell produces most of the embryo whilst the basal cell gives rise to the suspensor and the very basal part of the embryo. A number of mutants have been identified in various aspects of pattern formation and some of these will be discussed concentrating on their role in root development.

1.2.2 Mutations in the *GNOM* gene affect axis formation

Studies of the *gnom* mutant of *Arabidopsis* indicate that defects in this gene disrupts the formation of a stable axis (Mayer *et al.*, 1991; Mayer *et al.*, 1993; Vroeman *et al.*, 1996). The mutant phenotype is first evident at the division of the zygote. Instead of an asymmetrical division, the zygote divides to give rise to an apical cell that is only slightly smaller than the basal cell. Subsequent cell divisions are perturbed and by the putative heart stage the mutant embryo lacks the cell pattern characteristic of the root meristem primordia and also the cotyledonary primordia (Mayer *et al.*, 1993). This phenotype would indicate that a functional GNOM protein is required at multiple stages in the development of the embryo, with defects in GNOM function disrupting the processes required for axis formation, though not necessarily directly. The effects of disrupting GNOM function on axis formation was examined by analysis of the AtLTP1 lipid transfer protein expression pattern in *gnom* mutants using an AtLTP1 promoter-GUS fusion (Vroeman *et al.*, 1996). Ordinarily, AtLTP1 is expressed from the early globular stage in protoderm tissue, along the entire apical-basal plane before later becoming confined to the apical region of the embryo. In a *gnom* background in the most severe ball-shaped embryos expression was found to occur in three separate patterns. The first resembled the wild-type expression and was restricted to the apical region of the embryo whilst in the second the polarity was reversed such that expression was in the basal region. The final expression pattern was diffuse throughout the whole embryo. These results indicated that *gnom* embryos can have no or reversed apical-basal patterning (Vroeman *et al.*, 1996).

Mutant *gnom* seedlings carrying the same allele display a high degree of variability ranging from ball-shaped, in which there is no apparent apical-basal polarity, to cone shaped seedlings with fused cotyledons. The root is deleted in all of these cases with the cotyledons strongly reduced or eliminated. Notably, even in the most severe ball shaped *gnom* seedlings, radial patterning is still evident distinguishing apical-basal pattern formation from that of radial patterning (Mayer *et al.*, 1991). This was also supported by the expression of the AtLTP1 promoter-

GUS reporter which though defective in apical-basal expression showed normal radial expression (Vroeman *et al.*, 1996).

The wild type gene was cloned using a T-DNA insertion line and found to encode a polypeptide with partial homology to the yeast Sec7p protein (Shevell *et al.*, 1994; Achstetter *et al.*, 1988) and also to the yeast proteins YEC2, Gea1p and Gea2p (Busch *et al.* 1996; Jurgens *et al.*, 1997; Steinmann *et al.*, 1999). The Sec7p protein is involved in protein transport in the yeast secretory pathway whilst Gea1p acts as a guanine-nucleotide exchange factor of ADP-ribosylation factor (ARF)1, which is involved in vesicle budding (Peyroche *et al.*, 1996). The implication that secretion and vesicle trafficking may be required for axis formation suggests parallels with *Fucus*, a brown alga. *Fucus* zygotes, like *Arabidopsis*, divide asymmetrically to form a large thallus cell and a smaller rhizoid cell each of which has different developmental fates. Axis formation occurs in response to an external stimulus such as light and is followed by axis fixation which involves the targeted secretion of specialised vesicles (F granules), containing cell wall components, to a target site (Quatrano and Shaw, 1997; Shaw and Quatrano, 1996). Treatment of *Fucus* zygotes with brefeldin A (BFA), which blocks Golgi mediated secretion, preventing targeted vesicle deposition, resulted in the inhibition of axis fixation and also the proper orientation of the first division plane (Shaw and Quatrano, 1996). Defective axis formation/fixation in *gnom* mutants indicate that a similar mechanism may be present in higher plants and as such the *GNOM* gene may be a component of a similar pathway.

1.2.3 Mutations in the *MONOPTEROS* gene disrupts root and hypocotyl formation

Mutations in the *MONOPTEROS* (*MP*) gene result in seedlings that lack a hypocotyl, root and root meristem, though root formation can be induced in tissue culture (Berleth and Jürgens, 1993). The mutant phenotype of *mp* seedlings can be traced back to the octant stage of embryogenesis where, instead of two tiers of four cells each, the embryo consists of four tiers. By the heart stage it is apparent that the lower tier cells have not elongated to form their characteristic cell files and behave more like upper tier cells whilst the hypophysis has not undergone the usual division pattern that results in the formation of part of the root meristem. The *mp* phenotype indicates that the *MP* gene is required for specification of the basal region of the embryo, that which gives rise to the seedling root. The fact that root

regeneration can be induced in tissue culture indicates that the role of the *MP* gene in root formation is restricted to the embryo (Berleth and Jürgens, 1993).

Another interesting feature of *mp* plants is the defects displayed by adult plants which could be generated because of the ability of the *mp* mutants to form roots in tissue culture. One of the most pronounced abnormalities was that of inflorescence development. Flowers were found to form almost exclusively in terminal positions and the flowers themselves were abnormal often lacking outer whorl organs. This phenotype is reminiscent of the *pin formed* mutant (*pin1* ; Goto *et al.*, 1991) and also wild-type plants treated with polar auxin transport inhibitors (Okada *et al.* 1991). When tested it was shown that *mp* plants were defective in polar auxin transport and subsequent investigation showed that *mp* plant were also defective in vascular development with defective alignment and connection of vascular cells which was most pronounced in leaf margins (Przemeck *et al.*, 1996). This defect in vascular patterning has its origins in embryogenesis since *mp* embryos lack a distinct vascular primordium at the heart stage (Berleth and Jürgens, 1993). Amongst the numerous *mp* alleles, those with the most severe basal embryo defects also exhibit the strongest vascular and inflorescence mutant phenotypes. This suggests that the same underlying mechanism is responsible for this range of phenotypes. It was therefore hypothesised that the *MP* gene plays an important role in cell polarity determination with the inability to form basal embryo structures and vascular cell alignment a secondary consequence (Przemeck *et al.*, 1996).

The link between basal body formation, vascular patterning and auxin transport in the *mp* mutant became clearer with the cloning of the *MP* gene (Hardtke and Berleth, 1998). It was found to encode a polypeptide with homology to *ARF1*, a transcription factor that binds to auxin response elements in the promoters of auxin inducible genes (Ulmasov *et al.*, 1997). Analysis of the expression pattern of the *MP* transcript by *in situ* hybridisation showed that the message accumulates initially in subepidermal cells of globular stage embryos but is gradually confined to more central domains along the cotyledonary midlines and embryo axis until in mature embryos expression is restricted to provascular tissue. The same pattern emerged in developing adult organs with expression being gradually restricted to provascular tissue (Hardtke and Berleth, 1998). The expression of *MP* throughout the globular embryo is inconsistent with it having a role solely in basal embryo organisation and more likely indicates the requirement for correct polarity determination during hypocotyl and root axis formation during embryogenesis. Similarly, the formation of contiguous vascular elements is likely

dependent on correct polarity determination. The defects in polar auxin transport of *mp* plants and the homology of the *MP* polypeptide to *ARF1* suggests that *MP* influences basal embryo pattern formation and vascular development by its involvement in polarity determination potentially in response to auxin signals. It is possible that *MP* activates downstream events in response to the gradual canalisation of polar auxin flow in developing embryos and organs or alternatively, may actually be involved in the canalisation of auxin flow (Hardtke and Berleth, 1998; Nelson, 1998).

Whilst initial studies indicated that *MP* is required for basal patterning of the embryo and hence seedling root development, further study as described indicates that this is a secondary consequence and not the primary role of the gene. It does however introduce the subject of plant hormones and their role in root development, a subject which is highlighted when considering the *bodenlos* mutant discussed next and reviewed in more detail in a later section.

1.2.4 The *bodenlos* mutation affects primary root formation

The *bodenlos* (*bdl*) mutant was identified in an EMS screen for seedlings displaying abnormal seedling root development (Hamann *et al.*, 1999). The *bdl* phenotype segregated as a single recessive mutation but appeared somewhat variable and was separated into 'weak' and 'strong' classes. The weak *bdl* phenotype resembled the *hobbit* mutant (Willemsen *et al.*, 1998) in that the seedling lacked a root meristem and most of the rest of the root except for at the hypocotyl/root junction. The strong phenotype was more reminiscent of the *mp* mutant (Berleth and Jürgens, 1993), with no hypocotyl, root and root meristem apparent and also with a reduction in the vasculature of the cotyledons.

The defects observed in *bdl* seedlings were traced back to the apical daughter cell of the zygote which was seen to divide horizontally instead of vertically. The differences between the weak and strong phenotypic classes became apparent at later stages of embryogenesis, though both phenotypic classes resulted in embryos in which the hypophyseal cell region did not undergo the usual stereotyped division pattern which would explain the apparent lack of a quiescent centre and root meristem in the *bdl* seedlings.

bdl seedlings of both strong and weak phenotypes could form secondary roots which arose from divisions in the pericycle in the basal region of the seedling. Therefore, like *mp*, the *bdl* mutation only appears to affect root formation during embryogenesis. This allowed the study of adult *bdl* plants which appeared defective

in apical dominance (an auxin mediated process in which the shoot apex inhibits axillary bud growth) and also vascular development. The similarities of the *bdl* phenotype with that of *mp* raised the possibility that *bdl* mutants show some defects in their response to auxin. In comparisons with both wild-type and *auxin resistant 1* (*axr1*, Lincoln *et al.*, 1990) seedlings it was found that *bdl* seedlings were, like *axr1* seedlings, resistant to auxin in various assays.

To understand further the interactions and role of the *BODENLOS* gene in basal embryo development and auxin response double mutants were produced with the *mp* and *axr1* mutants. The *bdl:mp* embryos initially resembled both single mutants before deviating at the heart stage where the cotyledonary primordia did not bulge outwards as in the single mutants. The seedlings of the double mutant lacked roots and had severely reduced cotyledons unlike *mp* with its fused cotyledons and *bdl* with either one or two cotyledons. This phenotype, consisting basically of an elongated hypocotyl, was not considered to be simply an additive effect of the two mutations but indicative of a more complex genetic interaction. The severely reduced cotyledon phenotype of the *bdl:mp* seedling was interpreted as an additive effect of the two mutations in the apical region of the seedling whereas the presence of the hypocotyl, which is absent in *mp* seedlings, indicated a suppression of the *mp* phenotype by *bdl* in the central region. Therefore from analysis of the *bdl:mp* double mutants it was interpreted that *bdl* affects the whole apical-basal axis. Interestingly double mutants between *bdl* and *axr1* resulted in seedlings that resembled *mp* embryos suggesting that the *axr1* mutation enhances the apical-basal defects of *bdl*.

The *bdl* mutant appears to be very much like the *mp* mutant in that it is required for primary root formation in the embryo. The phenotype of the double mutant indicates that they act in distinct but interacting pathways. The insensitivity of *bdl* seedlings to exogenous auxin, along with the phenotypes of adult plants which show reduced apical dominance and defective vascular development, again as with *mp*, indicates a role for auxin in apical-basal pattern formation. As with *mp* embryos, it may be that auxin is required early in embryogenesis as a signal to establish polarity and that if that signal is disturbed it results in defective patterning of the basal region of the embryo thus affecting formation of the seedling root. It has recently been reported that the *BDL* gene is *IAA12* (Hamann, AUX 2000, EMBO workshop, Corsica) which provides further support for such a role for auxin.

1.2.5 The *HOBBIT* gene is required for root meristem formation

Unlike the *gnom*, *mp* and *bdl* mutants which show large-scale embryo phenotypes, mutations in the *HOBBIT* (*HBT*) gene result in more restricted phenotypes. The *hbt* mutant was identified in a screen for genes involved in the embryonic specification of the root meristem (Willemsen *et al.*, 1998). Strong mutant alleles were represented by seedlings with very short roots but with normal radial patterning. Irregular cell divisions were found in the columella and quiescent centre and the layer of lateral root cap appeared to be missing. These irregularities in cell division were found to correlate with cell differentiation defects. Starch granules normally found in columella root cap cells were missing in strong *hbt* mutants as was the expression of GUS markers normally expressed in these cells. A lateral root cap marker was also found not to be expressed in strong *hbt* mutants. Therefore, *hbt* mutants appear to be defective not only in root meristem activity but also in columella and lateral root cap cell identity.

The initial defect in *hbt* mutants was traced back to early embryogenesis and was shown to be due to abnormal hypophyseal cell development. At the globular stage the hypophysis normally undergoes an asymmetric division, producing a lens shaped cell which will give rise to quiescent centre and columella precursors. This division is either absent in *hbt* mutants or is accompanied by further divisions and since the hypophysis gives rise to the quiescent centre and columella, this defect correlates with the lack of these cells in *hbt* seedlings.

Analysis of later stage *hbt* embryos revealed that defects were not only limited to the hypophyseal cell region but also in the adjacent cell tier. Division of epidermal cells that normally occur in the wild-type to give rise to the lateral root cap were either skewed or absent. Mature *hbt* embryos also show a reduction of cell numbers in cortical cell files in the root apex that indicates that little or no mitosis occurred in the cells flanking the hypophyseal cell region earlier in embryogenesis, cells which are the root meristem initials in the wild-type. Taken together, the absence of mitotically active root meristem cells and a lateral root cap in *hbt* mutant embryos, indicates that the identity of root meristem initials is not properly specified in this mutant.

A feature of the *hbt* mutation that distinguishes it from such mutants as *mp*, is that the *hbt* mutant is unable to produce normal roots in tissue culture. *hbt* seedlings readily produce callus when transferred onto callus inducing media but when this callus is transferred to root inducing media, the resulting roots show a

similar phenotype to the seedling root and therefore also must require *HBT* gene activity for their formation, even though their developmental context is different.

The phenotype of *hbt* mutants indicates that this gene is required for the correct formation of the hypophysis in the embryo and the subsequent specification of the progeny of the hypophysis, the quiescent centre and columella, in the seedling. Later in embryogenesis the development of the cell tier above the hypophyseal region, which gives rise to the root meristem initials, is also defective with reduced mitotic activity of these cells. *HBT* gene activity is therefore also required for a mitotically active root meristem and lateral root cap formation as well as development of the hypophyseal cell region. This raises two possibilities as to the mode of *HBT* gene action. One is that *HBT* is required for specifying hypophyseal cell derivatives, root meristem initials and the lateral root cap. The other alternative is that *HBT* action is required for specifying the hypophysis and that later in embryogenesis, the *HBT* expressing cells in the hypophyseal cell region signal to the immediately adjacent upper tier to initiate meristem initial activity and lateral root cap development (Willemsen *et al.*, 1998; van den Berg *et al.*, 1998). The fact that tissue culture derived *hbt* roots share the seedling phenotype indicates that the *HBT* gene is required for root meristem formation regardless of the developmental stage.

1.3 Radial Pattern Mutants

As well as displaying a defined apical-basal axis *Arabidopsis* seedlings also show radial patterning, which is highly evident in the primary root (Figure 1.1 a). As reviewed earlier, the primary seedling root consists of a number of defined tissues organised in concentric layers with the epidermis, cortex, endodermis and pericycle surrounding the central vascular cylinder (Dolan *et al.*, 1993). This radial pattern of the primary root relates to the arrangement of sets of initials present by the early torpedo stage, after the apical-basal axis has been defined. As well as mutants affecting the apical-basal axis of development, a second class of pattern mutants affecting the radial organisation of the root have been identified (Benfey *et al.*, 1993; Scheres *et al.*, 1995) and will be discussed.

1.3.1 The *woodenleg* and *gollum* mutations affect vascular organisation

The *gollum* (*glm*) and *woodenleg* (*wol*) mutants were isolated in a screen for seedlings displaying retarded root growth resulting from defects in radial organisation (Scheres *et al.*, 1995). Cross sections of seedling roots in the differentiation zone, which contains single layers of defined cell number of the

aforementioned cell types, showed that *glm* mutants lack the usual organisation of pericycle and vascular tissue. These defects are also evident in the hypocotyl of *glm* seedlings where the pericycle layer is incomplete. The root of *wol* seedlings were found to contain vascular tissue with fewer cells than the wild-type, a defect again observed in the lower hypocotyl. The vascular cells that were present were all found to differentiate into xylem elements, though in the upper hypocotyl the number of vascular cells was found to increase and phloem elements were present.

The defects observed in the seedling primary root could be traced back to the embryo in both *glm* and *wol* mutants. *gol* mature embryos displayed the same lack of organisation of the pericycle and vascular tissue as found in the seedling whilst *wol* embryos had a reduced number of cells in the pericycle with approximately half the number of the wild-type. The defects in radial organisation were also not restricted to embryogenesis but also to lateral roots formed post-embryogenesis. This would indicate that these genes are required for correct radial organisation of the root (and lower hypocotyl) at all developmental stages.

1.3.2 The *short root* and *scarecrow* mutations affect endodermis and cortex patterning

The *short root* (*shr*) mutant was identified in independent screens for seedlings displaying defective root development (Benfey *et al.*, 1993; Scheres *et al.*, 1995), showing noticeably shorter roots than the wild-type. When compared to the wild-type primary root the *shr* root appears to lack the usual small, densely cytoplasmic cells characteristically found in the meristematic and expansion zones. Longitudinal sections of *shr* root tips confirmed that there were relatively few cells of the correct size and shape in these regions. Analysis of transverse sections revealed that the roots were missing the endodermal cell layer as well as having fewer cells in the stele (Benfey *et al.*, 1993). Analysis of *shr* embryos revealed that, at the early heart stage, the periclinal division that doubles the ground meristem layer does not occur such that by the torpedo stage only one ground tissue layer is present (Scheres *et al.*, 1995).

Transverse sections of the seedling primary root of the *scarecrow* (*scr*) mutant indicated that a ground tissue layer was missing. Suberin staining for the presence of the casparian strip (Esau, 1977), a suberized region present in the endodermis, indicated that this was present in the remaining cell layer. This was initially perceived to indicate that the cortex layer was missing in *scr* mutants

(Scheres *et al.*, 1995). The embryonic origin of the *scr* phenotype was, as with the *shr* mutant, absence of a periclinal division of the ground meristem layer.

1.3.3 The *fass* mutant affects morphogenesis

fass (*fs*) mutant seedlings appear compressed in the apical-basal axis whilst conversely enlarged radially. Though the shape of *fs* seedlings is extremely abnormal, they contain all the major organs of the wild-type seedling and in the correct pattern. Analysis of *fs* embryos showed that they exhibited major alterations in the pattern and number of cell divisions from the early stages of embryogenesis. The cell wall of *fs* embryos is variably orientated following division of the zygote and subsequent cell divisions produced defective cell shapes and arrangements such that by the heart stage none of the primordia of the seedling organs could be morphologically distinguished. However, whilst cell shape and cell wall orientation appear defective, the daughter cells of the zygote are polarised indicating that mutation of *FASS* does not affect cell polarity. Given that *fs* mutants displayed defective morphogenesis whilst maintaining correct pattern it was determined that mutations in the *FASS* gene affect morphogenesis but not pattern formation (Torres-Ruiz and Jürgens, 1994).

The roots of *fs* seedlings were found to contain a large excess of cells with multiple cortical layers and an enlarged vascular cylinder. Though the endodermis and pericycle contain increased cell numbers they still appear as single cell layers (Scheres *et al.*, 1995). The *wol*, *shr* and *scr* mutants all lack a specific cell division during embryogenesis that is linked to the loss of one of the radial cell types in the seedling root (and hypocotyl). The absence of a particular cell type could be because the genes are required for the production of cells in these regions and are therefore involved in morphogenesis. The alternative is that these genes are required for the patterned specification of the missing cell type (pattern formation). By crossing each into the *fs* mutant background with its increased cell numbers in the radial axis it was hoped to resolve between the two possibilities. It was found that *fs* was epistatic to both *scr* and *wol* such that the double mutant seedlings all displayed a *fs* phenotype with the missing cell layers present. The progeny of the *fs* and *shr* cross appeared phenotypically similar to *fs* single mutants, however, staining for suberin revealed that the double mutants still lacked the endodermis layer. Therefore, whilst the extranumerary cell divisions in the double mutant gave rise to multiple ground tissue layers, the extra divisions did not lead to formation of the endodermis. This would suggest that the *SHR* gene is required for radial pattern formation whilst

WOL and *SCR* are required for the cell divisions that give rise to the missing cell type in the respective mutants (Scheres *et al.*, 1995).

More recently, further information about the function of the *SCR* gene has been determined (Di Laurenzio *et al.*, 1996). The presence of the casparian strip in the remaining ground tissue layer in *scr* seedling roots had resulted in the conclusion that this tissue layer was endodermis (Scheres *et al.*, 1995). Another endodermal tissue specific marker, the JIM13 antibody (Knox *et al.*, 1990) which recognises an arabinogalactan epitope, gave a positive result supporting the previous assumption. However, the use of a cortex and epidermal cell specific marker, the CCRC-M2 antibody which recognises a cell wall carbohydrate epitope (Freshour *et al.*, 1996), revealed that the mutant cell layer in *scr* mutants also has cortex attributes and thus is heterogeneous. The *SCR* gene therefore regulates the asymmetric cell division of the cortical/endodermal initial but does not play a role in cell specification (Di Laurenzio *et al.*, 1996). Cloning of the gene has revealed it to be a novel polypeptide with domains suggesting it functions as a transcription factor. *In situ* hybridisation experiments indicate that the *SCR* transcript is found in the ground tissue of heart stage embryos prior to division. After division, expression was found primarily in the endodermis which was also the case in mature roots. Taken together it is hypothesised that the *SCR* gene function is to establish the polarity of the initial cell prior to division or is required to generate an external influence that has an effect on asymmetric cell division (Di Laurenzio *et al.*, 1996).

1.4 Mutants in post-embryogenic root development

The previous sections have detailed the importance of embryonically active genes and processes for the correct pattern and development of the root. However, upon maturation the embryo enters a dormancy stage before post-embryonic development can begin following imbibition and germination of the seed. This results in activation of the embryonically derived apical meristems which generate new cells for growth and formation of the adult organs of the plant. A number of mutants have been isolated in various aspects of post-embryonic root development (Benfey *et al.*, 1993; Galway *et al.*, 1994; Cheng *et al.*, 1995; Masucci *et al.*, 1996; Schneider *et al.*, 1997; Wada *et al.*, 1997) and will be summarised.

1.4.1 The *ROOT MERISTEMLESS* genes are involved in cell proliferation in the root meristem

The *root meristemless* (*rml*) mutants were isolated as seedling mutants in which root growth was seen to arrest within 4 days post-germination (Cheng *et al.*, 1995). Mutations in two distinct genes *RML1* and *RML2* gave rise to similar but subtly different phenotypes with *rml1* roots being slightly shorter than those of *rml2*. The roots of the *rml* mutants were missing the rapidly dividing, cytoplasmically dense cells of the meristematic zone indicating a defect in cell division activity. Sections of young seedling roots post-germination revealed that whereas the wild-type epidermal and cortical cells have divided, so increasing cell number along the root axis, no such divisions occur in *rml1* and *rml2* roots. Furthermore, the cellular arrangement is the same in *rml* seedling roots 4 days post-germination as it is in the embryonic root. Analysis of cell file numbers in both the root and hypocotyl of *rml* seedlings and mature embryos revealed that cell division was not occurring post-germination. Interestingly, the roots and hypocotyl were found to elongate indicating that cell elongation occurs in the absence of cell division

Older *rml* seedlings appeared to have differentiated epidermal and cortical cells at the root apex instead of meristematic cells. This would indicate that lack of cell division in the meristem leads to the terminal differentiation of cells at the root apex. Lateral roots of both *rml1* and *rml2* were able to initiate but, as with the primary root, they did not develop properly and ceased cell division activity soon after emergence. Interestingly, the number of cells in epidermal and cortical cell files was the same in arrested lateral roots as in the primary root.

The fact that the embryonic pattern of *rml* embryos is indistinguishable from that of the wild-type indicates that the *RML* gene products are not required for embryonic root patterning or morphogenesis. Therefore, the *RML* genes are required for cell proliferation in the root meristem post-embryogenically. Furthermore, the fact that both primary and lateral roots of *rml* mutants cease cell division at a defined cell number suggests that root development, regardless of its developmental context, must reach a defined point or unit before *RML* gene activities are required (Cheng *et al.*, 1995).

1.5 Cell Expansion mutants

Whilst root development is obviously very dependent on correct patterning and cell division, another critical parameter for determining correct organ shape is

cell expansion. Manipulation of the cell wall and internal cytoskeleton must play an important role in this process but little is known about the molecular mechanisms that control the degree and direction of expansion. Mutants displaying defects in root cell expansion have been isolated on the basis of their increase in diameter (Baskin *et al.*, 1992; Benfey *et al.*, 1993; Hauser *et al.*, 1995).

The *cobra* (*cob*), *cudgel* (*cud*), *lion's tail* (*lit*), *pom-pom 1+2* (*pom1+2*) and *quill* (*qui*) mutants were all isolated in screens for roots that showed reduced elongation along with variability in their diameter (Benfey *et al.*, 1993; Hauser *et al.*, 1995). The expanded phenotype of these mutants was dependent on a maximum growth rate of the root and they therefore represent conditional root expansion mutants. Cell length measurements of epidermal, cortical and endodermal cells indicated that mutants displayed large reductions in cell elongation. The length of wild-type root epidermal, cortical and endodermal cells is significantly greater than their diameter and indicates the direction of expansion. The epidermal cells of *cob*, *qui* and *cud* mutants were found to have a greater diameter than length indicating a reversal of the polarity of expansion. The epidermal cells of *lit* and *pom-pom* had similar lengths and diameters which was also the case for cortical and endodermal cells of all the mutants. These mutants were further classified by calculating their cell volumes such that they fell into three classes. The first class, consisting of the *lit* mutant, had smaller cell volumes than the wild-type indicating a defect in cell expansion such that normal cell volumes are not achieved. The volume of *cob* epidermal cells was equivalent to the wild-type indicating that the defect they showed was probably in regulating the polarity of cell expansion. The final class, consisting of the *qui* and *cud* mutants, had greater cell volumes than the wild-type indicating a possible loss of expansion control. Measurements of hypocotyl cell lengths indicated little difference to the wild-type suggesting that the defects in cell expansion affected primarily the root. The conditional phenotype of these mutants indicates that the mutations affect some component that is limiting for cell expansion in rapidly growing roots but that redundant processes substitute for the mutant genes in slower growing roots. Redundancy of function was supported by double-mutant analysis which showed that combinations of the different mutants resulted in loss of the conditional phenotype (Hauser *et al.*, 1995).

Another expansion mutant, *sabre* (*sab*) was isolated by the same researchers (Benfey *et al.*, 1993) and differed from the others in two respects. Firstly, the increase in root diameter was fairly uniform along the length of the root, and secondly the phenotype was not conditional on a maximal root growth rate.

Transverse sections revealed that, as with the other mutants, abnormal expansion was most prominent in one cell layer, the cortex in the case of *sab*. Another feature that distinguishes the *sab* mutant was that the phenotype could be partially rescued by manipulation of plant growth regulator levels. Silver ions, which inhibit ethylene perception, when added to growth media resulted in *sab* mutant seedling roots appearing more like wild-type. This would indicate that the *SABRE* gene in part must be involved in counteracting the effects of ethylene on promoting radial expansion of certain cells. The *SABRE* gene has been cloned and found to encode a novel polypeptide which is proposed to play a role in cell elongation, counterbalancing ethylene induced radial expansion (Aeschbacher *et al.*, 1995).

Analysis of the mutant *stunted plant 1* (*stp1*; Baskin *et al.*, 1995) has revealed another interesting feature about the control of cell expansion. In wild-type roots the length of cells increases (to a limit) as the distance from the root apex increases. However, it was found that in *stp1* roots, whilst the cells at or close to the apex were of similar size to wild-type, the cell lengths did not then increase appreciably with distance from the apex. Further experiments showed that rates of expansion in the region of rapid elongation were slower in *stp1* roots than in the wild-type yet the rate of expansion was the same in dividing cells of *stp1* and wild-type. This therefore indicates that the mechanism of cell expansion in the rapidly dividing cell population at the root tip differs from that of the non-dividing cell in the rapid elongation zone. *STP1* is therefore believed to be required for cell elongation in rapidly elongating, but not dividing cells (Baskin *et al.*, 1995). This would correlate with observations of the conditional *cobra* mutant in which seedlings were transferred from conditions permissive to normal growth to restrictive conditions. Following transfer, cells in the elongation zone were seen to undergo radial expansion rather than elongation. Cells in the meristematic zone and above the elongation zone did not display abnormal expansion. Therefore the *cob* phenotype was restricted to the rapidly elongating cells (Hauser *et al.*, 1995).

1.6 Epidermal Cell Differentiation

The epidermal cell layer of the *Arabidopsis* root consists of two cell types, those bearing root hairs (trichoblasts) and hairless cells (atrachoblasts). Immature epidermal cells that overlie the junction between the two underlying cortical cells will differentiate into root hair cells, whilst those cells contacting only a single cortical cell differentiate into hairless cells resulting in files of hair cells separated by one or two hairless cell files. The two kinds of epidermal cells can be distinguished at an

early stage prior to hair emergence. In the meristematic zone hair forming cells appear shorter with increased cytoplasmic density (Dolan *et al.*, 1994). The simplicity of epidermal cell patterning has made it particularly amenable to mutant analysis and a number of genes have now been identified which play a role in determining the fate of epidermal cells (Schneider *et al.*, 1997; Wada *et al.*, 1997; Lee and Schiefelbein, 1999; Walker *et al.*, 1999).

The *TRANSPARENT TESTA GLABRA1* (*TTG1*) locus has been shown to regulate a number of developmental processes in *Arabidopsis* such as production of seed mucilage and anthocyanin pigments. Several of the processes are confined to the epidermal cell layer of various organs including root epidermal cells. In *ttg1* extra root hairs appear in the atrichoblast cell files indicating that the wild-type *TTG1* gene functions as a negative regulator of hair development in the root (Galway *et al.* 1994). The *TTG1* gene has been shown to encode a putative Wd40 repeat protein (Walker *et al.*, 1999). Such proteins have been shown to be involved in signalling, cell cycle regulation and transcriptional repression and implicates *TTG1* as having a role in signal transduction to downstream transcription factors. Interestingly, overexpression of the maize *R* gene in *ttg1* plants results in suppression of the *ttg1* mutant phenotype (Galway *et al.*, 1994). The maize *R* gene is a *myc*-like basic helix-loop-helix (bHLH) transcriptional activator (Ludwig *et al.*, 1989). The fact that overexpression is able to suppress the *ttg1* phenotype indicates that an *R* gene homologue may act in *Arabidopsis* either downstream or in parallel to the *TTG1* gene (Galway *et al.*, 1994).

Mutations in a second gene, *GLABRA2* (*GL2*), also result in ectopic root hair production on atrichoblasts and like *TTG1* also affects seed mucilage production and epidermal cell patterning in various organs. The *GL2* gene has been cloned and is known to encode a homeodomain-containing protein and is putatively a transcription factor (Rerie *et al.*, 1994). Hair and hairless cells in the root epidermis can, as previously described, be distinguished by differences in cell morphology. Closer examination of the root epidermal cells of *gl2* mutants and wild-type revealed that there was no significant difference in the arrangement and morphology of cells. Therefore, whilst ectopic root hairs were forming on epidermal cells in hairless cell positions, these cells did not exhibit all of the other cellular characteristics of hair cells indicating *gl2* mutations affect only some hairless cell differentiation processes (Masucci *et al.*, 1996). Examination of *GL2* expression patterns in the root revealed that the transcript was most abundant in differentiating hairless cells. Together with the *gl2* mutant phenotype this would suggest that *GL2*

functions to suppress hair formation in differentiating hairless cells (Masucci *et al.*, 1996). Interestingly, expression of *GL2* is reduced in a *ttg1* background indicating that *TTG1* is a positive regulator of *GL2* expression (Di Christina *et al.*, 1996; Yi Hung *et al.*, 1998).

The *WEREWOLF* (*WER*) gene has recently been identified and constitutes a third component of the root epidermal cell patterning process (Min Lee and Schiefelbein, 1999). As with *ttg1* and *gl2* mutations in *WER* result in root hair production in hairless cell positions. However, examination of epidermal cells in the meristematic zone showed that they all displayed the densely staining cytoplasm and reduced vacuole size characteristic of differentiating hair cells. This would suggest *WER* acts at an early stage of epidermal cell fate determination. Examination of *GL2* expression in the *wer* mutant background showed that not only was expression reduced but that its hairless cell position-dependent expression was abolished. This would indicate *WER* is required for the position-dependent expression of *GL2* (Min Lee and Schiefelbein, 1999). Cloning of the *WER* gene has revealed it to encode a polypeptide with a MYB-like DNA binding domain which are associated with transcriptional control. The transcript was found to be preferentially expressed in differentiating hairless cells and steady state levels were unaffected in both *ttg1* and *gl2* mutant backgrounds (Min Lee and Schiefelbein, 1999).

Unlike the *ttg1*, *gl2* and *wer* mutants, defects in the *CAPRICE* (*CPC*) gene result in roots with fewer than usual root hairs (Wada *et al.*, 1997). Double mutant analysis revealed that the *gl2* mutation was epistatic to *cpc* whilst the roots of *ttg1* :*cpc* plants had an intermediate phenotype indicating the genes possibly function in independent but opposing pathways. This was also the case with *cpc* :*wer* double mutants which displayed an intermediate phenotype (Min Lee and Schiefelbein, 1999). The *CPC* gene was found to encode a polypeptide with homology to the MYB-like DNA-binding domain but lacking the typical transcriptional activation domain. Overexpression of *CPC* resulted in transgenic plants in which almost all epidermal cells formed hairs, much like the *ttg1* and *gl2* mutants, indicating that it is a positive regulator of hair formation (Wada *et al.*, 1997).

Based on the available information, a model to explain the genetics of root epidermal cell patterning has been proposed (Min Lee and Schiefelbein, 1999) in which it is predicted that root hair differentiation is a default state. *TTG1* is predicted to be involved in the positive regulation of a bHLH protein which in turn interacts with either of the MYB-like *CPC* or *WER* polypeptides. The *WER*-bHLH complex is able to activate *GL2* expression resulting in a hairless cell. The lack of a

transcriptional activation domain in *CPC* would result in an inactive transcriptional complex with the bHLH protein. This would block *GL2* expression resulting in the default hair cell fate. An unknown mechanism would be required to restrict *WER* expression to hairless cells and conversely, *CPC* to hair cells.

The defined structure of the *Arabidopsis* root has made it a good model for the analysis of plant organ development. The importance of genetic screens for mutants displaying abnormal root development has been highlighted in the previous sections. Histological and clonal analysis has proved a valuable tool in showing that the root meristem initials are present by the heart stage of embryogenesis and the pattern of cell divisions that give rise to them (Dolan *et al.*, 1993; Scheres *et al.*, 1994). However, the identification and study of root mutants, their genetic interactions and the subsequent cloning of the genes involved has provided significant clues as to the processes involved in establishing this pattern. Studies of the *gnom* and *monopteros* mutants have shown how important the establishment of correct cell and embryo polarity at the beginning of embryogenesis is to determining a correct apical-basal axis and subsequently root development. This is also emphasised in the *fass* mutant which shows defective morphogenesis and yet cell polarity is maintained as is pattern formation. Studies of the *monopteros* and *bodenlos* mutants have shown that *MP* and *BDL* -dependent signalling from the apically adjacent cells in the embryo is required to specify hypophyseal cell fate since the defects in these mutants is initially in the apical daughter cell of the zygote. Also, the analysis of the *hobbit*, *short root* and *scarecrow* mutants raises the possibility that asymmetric cell divisions may play an important role in specifying different cell fates to daughter cells. Whether such division reflect a differential inheritance of cell fate determinants or rather the receipt of different positional information is open to debate (Gallagher and Smith, 1997).

The analysis of mutants displaying post-embryonic phenotypes has emphasised that the pattern laid down in the embryo is only a beginning and that root development is an ongoing process. The *ROOT MERISTEMLESS* genes are good examples of this since mutations in these genes do not appear to affect embryonic patterning and morphogenesis and yet prevent post-germinative cell proliferation indicating that the embryonic root meristem requires activation following dormancy. Furthermore, analysis of *rml1* and *rml2* along with *stunted plant1* indicates that the process of cell expansion in the root (and hypocotyl) is not coupled to cell division activity. Finally, the simple patterning of the root epidermis with hair and hairless cells has proved an effective model for genetic dissection.

Through mutational analysis a number of key genes have now been identified which are required for specifying cell fate in the epidermis. Perhaps unsurprisingly, genes such as *GLABRA2*, *WEREWOLF* and *CAPRICE* appear to encode putative transcription factors indicating that cell fate determination, at least in the epidermis, is dependent on the transcription of specific sets of genes. One question that can be asked is what upstream factors and signals are required for the control and spatial expression of such genes?

1.7 The Role of Plant Growth Regulators in Root Development

The identification and analysis of mutants has and is providing large amounts of information on the genes and processes that are required for root development. As more of these genes are cloned it has become apparent that a number of them are involved in regulating the distribution, synthesis and response to plant growth regulators. As such there is now increasing genetic evidence available to support the physiological information which indicates an important role for these compounds in plant development. This section will concentrate on the evidence supporting roles for the hormones auxin, ethylene and cytokinin in root development.

1.7.1 Auxin as a signal during embryogenesis

The plant hormone auxin has been shown to influence a number of processes including vascular development and apical dominance whilst at the cellular level it can affect cell division, elongation and differentiation (Davies, 1995; Hobbie, 1998). In developed seedlings and plants auxin is transported in a polar fashion from the shoot apex to the root, generally through vascular cells. This auxin polar transport is reliant on the activity of both influx and efflux carriers which import auxin from the surrounding medium and then pump it out of cells (reviewed in Palme and Galweiler, 1999). More recently, a number of studies have now indicated that auxins may play an important role in pattern formation and morphogenesis (Liu *et al.*, 1993; Fisher *et al.*, 1996; Hadfi *et al.*, 1998; Hardtke and Berleth, 1998; Sabatini *et al.*, 1999, Steinmann *et al.*, 1999).

One line of evidence that auxin is required for pattern formation in the embryo has come from treatment of isolated or cultured embryos with exogenous auxin or auxin transport inhibitors (Liu *et al.*, 1993; Hadfi *et al.*, 1998). Early

globular embryos of *Brassica juncea* treated in an *in vitro* culture system with various auxin transport inhibitors were found to develop into mature embryos with fused cotyledons, whereas treatment of heart-staged embryos in the same manner resulted in the formation of two normal cotyledons. The fused cotyledon phenotype was reminiscent of the less severe *gnom* mutant seedlings. The fact that heart-staged embryos formed normal cotyledons indicated that correct auxin polar transport was required in early globular embryos for the establishment of bilateral symmetry (Liu *et al.*, 1993). Treatment of isolated globular *Brassica juncea* embryos with various concentrations of the natural auxin, IAA, resulted in ball or egg-shaped embryos indicating an inhibition of axis formation and morphogenesis. Treatment of these embryos with the antiauxin p-chlorophenoxyisobutyric acid (PCIB) was found to inhibit cotyledon growth or inhibit hypocotyl and embryonic root development. These results indicated that changing the distribution or activity of auxin in the early embryo affects apical-basal pattern formation and meristem development (Hadfi *et al.*, 1998). The results would also suggest that auxin is probably produced very early in embryogenesis and, as the treatment with auxin transport inhibitors indicate, the establishment of correct auxin transport is a requirement to progress from radially to bilateral symmetry.

Characterisation and cloning of a number of embryo patterning genes is lending genetical evidence to support a role for auxin in embryogenesis. The embryos of *Brassica juncea* treated with either auxin, antiauxin or auxin transport inhibitors were very similar in phenotype to those of the *gnom* mutant (Mayer *et al.*, 1991; Mayer *et al.*, 1993). To determine whether mutations in the *GNOM* gene affect the canalisation of auxin flow during embryogenesis the cellular localisation of the auxin efflux carrier PIN1 (Galweiler *et al.*, 1998) was examined in developing wild-type and *gnom* mutant embryos (Steinmann *et al.*, 1999). In vascular cells of mature *Arabidopsis* the PIN1 protein is localised to the basal boundary of the cell. It was found that in wild-type embryos PIN1 was initially found on the inner cell boundaries but by the mid-globular stage, the four innermost cells were found to accumulate PIN1 on their basal boundary towards the developing root tip region. Progression through embryogenesis led to PIN1 accumulation being narrowed to vascular precursor cells along both the embryo axis and in the developing cotyledons. Examination of *gnom* embryos showed a different pattern of PIN1 accumulation, with none of the organisation of the wild-type. The innermost cells of the early embryo did not show the expected polar localisation and in older embryos, those cells that did show polar localisation at the basal boundary, were not aligned

with each other. Therefore, mutations in *GNOM* disrupt the ability to establish co-ordinated cell polarity in axis formation. The *GNOM* protein is a putative guanine-nucleotide exchange factor on ADP-ribosylation factor G protein (ARF GEF) (Busch *et al.*, 1996; Steinmann *et al.*, 1999). Subcellular localisation of *GNOM* indicated that a fraction of the protein was associated with multiple membrane compartments with the rest in the cytosol. Brefeldin A (BFA), an inhibitor of Golgi-mediated secretion which acts on ARF GEFs, was found to inhibit the GDP/GTP exchange activity of *GNOM*. Furthermore, treatment of cells with BFA resulted in a rapid reduction in the amount of cytosolic *GNOM* versus the membrane associated fraction whereas the partitioning of a control protein was unaffected. Therefore, the activity and partitioning of *GNOM* is sensitive to BFA. Since BFA is known to inhibit auxin efflux carrier activity (Delbarre *et al.*, 1998) its effect on PIN1 cellular localisation was examined in lateral roots. Ordinarily, PIN1 was localised to cell boundaries facing the root apex but BFA treatment resulted in distribution over the entire cell surface indicating that the polar localisation of PIN1 is BFA sensitive and thus may require the activity of *GNOM* or other BFA sensitive ARF GEFs (Steinmann *et al.* 1999). Given these results and previous observations (Mayer *et al.*, 1993) it has been proposed that the *GNOM* protein regulates vesicle trafficking required for the polar localisation of auxin transport carriers. The inability to establish correct polar auxin transport would explain the defects in axis formation observed in *gnom* mutant embryos (Steinmann *et al.* 1999).

A defect in canalising auxin polar transport is predicted to cause the phenotype displayed by *monopteros* mutants whereby axis formation and vascular development are affected. A link between auxin and the *MONOPTEROS* gene is also supported by the phenotype of adult plants which show defects in the differentiation and alignment of vascular cells and polar auxin transport. The *MONOPTEROS* gene has been found to encode a putative transcription factor that binds elements in auxin inducible promoters (Hardtke and Berleth, 1998). As yet it is unknown whether the *MONOPTEROS* polypeptide is required for the activation of downstream processes in response to the gradual canalisation of auxin flow or to actually direct canalisation itself. Support for the former comes from experiments in which the localisation of PIN1 was examined in *mp* embryos (Steinmann *et al.*, 1999). PIN1 localisation was found to be similar to the wild-type in early stage embryos with co-ordinated polar localisation to the basal region of the inner-most cells. Further experiments are required to resolve between these two possibilities but the *mp* mutant with its loss of basal pattern elements and early deviation from the

normal embryo cell division pattern indicates that the processes required for setting up correct auxin polar transport in the embryo are vital for basal patterning.

The *BODENLOS* gene also implicates auxin in apical-basal patterning. As discussed, mutations in *BDL* affect basal body formation in the embryo and adult plants show defective apical dominance and vascular development. The *bdl* mutation resulted in auxin insensitivity as determined by comparison with the *axr1* mutant. The *bdl:axr1* double mutants initially resembled *bdl* embryos until the globular stage after which differences could be observed. Seedlings of the double mutants resembled *mp* seedlings. Mutations in *AXR1* and also *AXR3*, another auxin sensitivity gene (Rouse *et al.*, 1998), do not affect apical-basal patterning unlike the *bdl* mutant. It may be that the *AXR1* gene product, which is believed to be involved in targeted protein degradation (reviewed in Leyser and Berleth, 1999), is not required at the early stages of embryogenesis which may explain why the double mutant embryos initially resemble *bdl* embryos before differences become apparent later. If the *BDL* gene is required for perception or response to auxin during very early embryogenesis, unlike *axr1* and *axr3*, then it would suggest that auxin is required for pattern formation during embryogenesis. The fact that cotyledonary defects observed in *bdl:mp* seedlings resemble the effects of auxin transport inhibitors in *Brassica juncea* embryos (Liu *et al.*, 1993) further implicates *BDL* and auxin in embryo patterning.

More recently another auxin resistant mutant has been identified which shows early defects in embryogenesis. The *axr6* mutant (Hobbie *et al.*, 2000) was initially isolated because of its auxin resistant root growth on auxin containing medium. Interestingly, analysis of the progeny of self-fertilisation produced three classes of seedling: wild-type auxin sensitive, mutant auxin resistant, and rootless. It was determined that the rootless phenotype was due to homozygosity for the mutant *axr6* gene and these seedlings often only had a single cotyledon with defective vascular patterns attached to a basal peg of largely undifferentiated cells. The fact that the heterozygous phenotype is dominant suggests that the *axr6* mutation is a gain of function. Analysis of developing embryos showed that the basal daughter cell, which normally divides transversely, divides periclinally in *axr6* embryos resulting in a suspensor that was two or more cells wide along its length. The division that normally gives rise to the hypophysis also did not occur which would account for the absence of a seedling root meristem. Furthermore, asynchronous and irregular cell division patterns resulted in embryos with defective patterning. Therefore, mutations in the *AXR6* gene disrupt the orientation and timing of cell

divisions during embryogenesis and when homozygous for the mutation result in loss of basal pattern elements. The auxin insensitive phenotype of the heterozygotes indicates, as with *bd1* mutants, that the perception of auxin during the earliest stages of embryogenesis is important for correct apical-basal patterning.

A final link between auxin and early development comes from further analysis of the *fass* mutant (Fisher *et al.*, 1996). As described previously mutations in the *FASS* gene are believed to uncouple pattern formation from morphogenesis because, whilst *fass* embryos have defective cell divisions such that no organ primordia can be distinguished, they still retain correct body pattern (Mayer *et al.*, 1991; Torres-Ruiz and Jurgens, 1994). In experiments in which the root growth of both wild-type and *fass* seedlings was determined following removal of the shoot it was found that isolated *fass* roots elongated approximately 2.5 times more than those of the wild-type. Since auxin is transported basipetally from the shoot to the root it was postulated that excess auxin was being produced in *fass* seedlings and that this was inhibiting the root growth prior to shoot excision. Measurement of free auxin levels in *fass* seedlings revealed there to be 2.5 times more than in wild-type seedlings. Measurements of the total amount of auxin which consists of free auxin, ester-linked and amide-linked auxin conjugates revealed that the wild-type actually had twice the amount of total auxin compared to *fass*. The difference was found to be in the reduced amount of amide-linked auxin conjugates in *fass* seedlings (Fisher *et al.*, 1996). This therefore indicates that the *FASS* gene product may be either an auxin-conjugating enzyme or a positive regulator of such an enzyme. This would indicate that the regulation of auxin levels, specifically the balance of free and conjugated forms, plays an important role in early plant development. Auxin is known to affect microtubule orientation and formation, which are likely to be important in determining the plane of cell division and direction of cell expansion (Blancaflor and Hasenstein, 1995) and the *ton* mutant, a likely allele of *fass*, has been shown to have disordered microtubule arrays (Traas *et al.*, 1995). This could explain the defective cell division during *fass* embryogenesis but questions the role of auxin in pattern formation. However, one possibility is that the role of auxin in pattern formation may not be dependent on its absolute levels but rather on establishing the correct gradient of distribution along the embryo axis. Thus, in *fass* embryos a reduction in free auxin may affect cell division planes but not the establishment of an auxin gradient. By contrast, mutations in genes such as *GNOM*, *MONOPTEROS* and *BODENLOS* which affect the establishment or perception of the putative auxin gradient would disrupt early apical-basal patterning.

Whilst the available genetical and experimental evidence supports a role for auxin in apical-basal patterning the actual presence and distribution of auxin during early embryogenesis has not been determined. Recent experiments have however added support to the possibility of an auxin gradient being established by the heart stage (Sabatini *et al.*, 1999). The promoters of many auxin inducible genes have been found to contain conserved auxin response elements (AREs) (reviewed in Abel *et al.*, 1996) which have been shown to bind auxin response factors (ARFs) (Ulmasov *et al.*, 1997a; 1999). To visualise the distribution of an auxin maximum in the embryo and root of *Arabidopsis* the ability of AREs in a promoter to confer auxin inducibility was utilised. A synthetic promoter was made by linking 7 copies of the auxin-responsive TGTCTC element to the minimal 35S CaMV promoter and this was used to drive expression of the *GUS* reporter gene (DR5::GUS; Ulmasov *et al.*, 1997b). In the wild-type, maximum GUS expression was first found to occur in the basal region of the heart-stage embryo, the site of the root primordia (Sabatini *et al.*, 1999). This would indicate that by this stage of embryogenesis, an apical-basal polar distribution of auxin has been achieved with the highest levels of auxin in the basal region. The fact that the genetic evidence seems to suggest an earlier stage for establishing this polar distribution may indicate that this reporter system is not sensitive enough to show auxin peaks earlier in development. Interestingly, no GUS expression was found in *mp* embryos at any stage of development though the reporter was still responsive to exogenously applied auxin indicating that the MP polypeptide was not required for expression. This provides support for the theory that the *mp* mutant is unable to establish correct polar auxin transport in the embryo.

1.7.2 Polar Auxin Transport in the Root

In the mature plant auxin is synthesised in the shoot apex and the major form, indole-3-acetic acid (IAA), is then transported away towards the basal tissues of the plant generally through the cells of the vasculature. Polar auxin transport is thought to play a role in a number of processes throughout the plant and in the root is believed to control lateral root development, root elongation and gravitropism (Estelle and Klee, 1994; Hobbie 1998). Transport of auxin is thought to require the action of specific protein transporters, influx carriers for uptake into the cell and efflux carriers for secretion out of cells. Mutant analysis has led to the identification of a number of candidate genes for these auxin carriers (Bennet *et al.*, 1996;

Galweiler *et al.*, 1998; Muller *et al.*, 1998; Luschig *et al.*, 1998; Marchant *et al.*, 1999).

The identification of chemical auxin transport inhibitors, such as 1-*N*-naphthylphthalamic acid (NPA), have been instrumental in understanding the importance of auxin transport (Katekar and Geissler, 1977). However, the analysis of putative auxin influx carriers has lagged behind that of the auxin efflux carriers because the inhibitors described to date target the efflux carriers (reviewed in Lomax *et al.*, 1995). Characterisation of the *auxin resistant 1* (*aux1*) mutant of *Arabidopsis* indicates that this may well encode a candidate auxin influx carrier (Maher and Martindale, 1980; Bennett *et al.*, 1996; Marchant *et al.*, 1999). The *aux1* mutant was initially isolated because of its agravitropic phenotype and altered growth response to the auxins IAA and 2,4-dichlorophenoxyacetic acid (Maher and Martindale, 1980). The *AUX1* gene was cloned and found to encode a putative membrane protein with similarity to a family of plant and fungal amino acid permeases (Bennett *et al.*, 1996). The fact that IAA is structurally similar to the amino acid tryptophan suggested that the AUX1 polypeptide may mediate the transport of auxin across the cell membrane. Furthermore, IAA is believed to be taken up in a protonated form along with a single proton (Rubery and Sheldrake, 1974; Raven, 1975) and plant amino acid permeases perform as proton-driven symporters (Bush, 1993).

It has been observed that the auxin influx carrier facilitates the uptake of IAA and 2,4-D but not the synthetic auxin 1-naphthaleneacetic acid (1-NAA), which enters the cell by diffusion (Delbarre *et al.*, 1996). In root elongation studies it was found that whilst the *aux1* mutant was resistant to IAA and 2,4-D compared to the wild-type, root growth was inhibited on media containing 1-NAA (Marchant *et al.*, 1999). The accumulation of 2,4-D, which is a substrate for the influx carrier alone (Delbarre *et al.*, 1996), was found to accumulate to much higher levels in wild-type roots compared to *aux1* and the agravitropic phenotype of *aux1* roots was rescued by growth on 1-NAA but not 2,4-D (Marchant *et al.*, 1999). The *AUX1* transcript was localised to the root apex (Bennett *et al.*, 1996) and promoter -GUS constructs indicated that expression was found in all tissues in the elongation zone and to a lesser extent in the lateral root cap, meristem initials and daughter cells (Marchant *et al.*, 1999). The experimental evidence would therefore suggest that AUX1 is a component of the auxin influx machinery and, because of the agravitropic phenotype of the *aux1* mutant, is required for root gravitropism.

Auxin transport in the root is believed to occur in two streams, one of which runs from the shoot to the root apex through cells in or adjacent to the stele (Lomax *et al.*, 1995). However, once auxin reaches the root tip it is then transported back towards the elongation and differentiation zones through the epidermal and cortical cell files and it is this flow that is believed to be crucial for root gravitropism (Evans, 1991). A putative efflux carrier component required for the gravitropic response has been recently identified independently by four separate groups (Luschnig *et al.*, 1998; Muller *et al.*, 1998; Utsono *et al.*, 1998; Chen *et al.*, 1998). The cloning of the *ETHYLENE INSENSITIVE ROOT1* (*EIR1*) gene, which is allelic to *AGRAVITROPIC1* (*AGR1*; Chen *et al.*, 1998) and *AtPIN2* (Muller *et al.*, 1998), was initially reported by Luschnig and colleagues. The roots of the *eir1* mutant are agravitropic and show greater resistance to both auxin transport inhibitors and ethylene than the wild-type. Furthermore, *eir1* roots were found to be longer than those of the wild-type with the difference likely to be due to increased cell elongation. Cloning of the *EIR1* gene revealed it encoded a polypeptide with 10 potential transmembrane domains with five at the amino terminus and five at the carboxyl terminus. These two transmembrane domains show homology to a number of bacterial transporters responsible for the transport of a variety of small molecules. Expression of the *EIR1* polypeptide in yeast was able to confer resistance to fluorinated indolic compounds whilst yeast containing a mutant form of *EIR1* were not resistant. The resistance to these compounds was probably due to *EIR1*-mediated secretion from the yeast cells. This suggested that *EIR1* may be responsible for the secretion of auxin from plant cells (Luschnig *et al.*, 1998). Analysis of the *agr1* mutant provided further support for a role for this protein in auxin transport. The root tips of *agr1* seedlings, when preloaded with radiolabelled IAA, were found to retain more than wild-type roots and *AGR1*-expressing yeast cells preloaded with radiolabelled IAA were able to secrete it faster than control cells (Chen *et al.*, 1998). Consistent with *EIR1/AGR1* being an efflux carrier in the root, both studies were able to show that the transcript was limited to the root in the meristematic and elongation zones (Luschnig *et al.*, 1998; Chen *et al.*, 1998).

Further information on the localisation of this putative efflux carrier came from experiments by Muller and colleagues. By using a probe derived from the *AtPIN1* gene, a putative auxin efflux carrier found in the vasculature of the inflorescence (Galweiler *et al.*, 1998), the related *AtPIN2* gene was isolated. A transposon knockout plant of the *AtPIN2* gene was isolated (*Atpin2::En701*) and was found to have agravitropic roots which were reduced in length compared to the

wild-type, unlike *eir1*. The roots of the *Atpin2::En701* seedlings were also found to be more sensitive than the wild-type to IAA and 1-NAA but not 2,4-D which is consistent with the substrate specificity of the auxin efflux carrier (Delbarre *et al.*, 1996). The AtPIN2 protein was localised to the membranes of root cortical and epidermal cell files, starting just distal to the quiescent centre, in the elongation zone. Localisation was to the basal end (furthest from the root apex) of these cells and also, in the case of cortical cells, in the side contacting an epidermal cell (Muller *et al.*, 1998). This is consistent with EIR1/AGR1/AtPIN2 being associated with auxin efflux activity in auxin flow away from the root tip in the cortical and epidermal cell layers.

The location of a putative auxin efflux carrier in the cortical and epidermal layers correlates with current theories on the role of auxin in the gravitropic response. Following perception of the gravity signal by the root cap, a signal is transduced via the meristem to the elongation zone where the side of the root orientated towards the stimulus accumulates auxin. This results in reduced elongation of these cells compared to the upper surface leading to root curvature towards the stimulus (Evans, 1991). In the *eir1/agr1/Atpin2* mutants, where presumably the second basipetal stream of auxin transport is affected, this redistribution of auxin would be inhibited, thus preventing a gravitropic response.

The lack of a gravitropic response has been used to screen for components of polar auxin transport in the root as described above. Another method has been the use of auxin transport inhibitors which have been shown to act by inhibiting the efflux carrier (reviewed in Lomax *et al.*, 1995). Auxin transport inhibitors such as NPA have been shown to bind a single high-affinity binding site, the NPA binding protein (NBP; Muday *et al.*, 1993), which is believed to be a separate protein to the efflux carrier (Morris *et al.*, 1991) and may regulate efflux activity. Wild-type seedlings grown in the presence of NPA or other transport inhibitors show three characteristic responses. At low concentrations lateral root growth is inhibited whilst at increasing concentrations root gravitropism and then elongation is inhibited. As many of the effects of auxin transport inhibitors are likely to result from the intracellular accumulation of auxin, the auxin resistant mutants are also likely to be resistant to these inhibitors. Auxin transport mutants should be distinguished from these mutants because they show normal auxin sensitivity. The *transport inhibitor response 3* (*tir3*) mutant was identified because its roots were able to elongate in the presence of NPA (Ruegger *et al.*, 1997). The *tir3* seedlings showed normal sensitivity to auxin treatment but auxin transport, measured in the inflorescence, was

found to occur at approximately 30% the levels of the wild-type. This decrease in auxin transport was found to correlate with a reduction in the NPA binding capacity of isolated microsomes compared to the wild-type. Furthermore, all organs displayed reduced elongation and roots showed a virtual absence of lateral root development. Lateral root initiation has been shown to be dependent on auxin transport from the shoot (Reed *et al.*, 1998) which would explain their absence in the *tir3* mutant. The analysis of the *tir3* mutant would suggest that the *TIR3* gene may encode the NBP or regulate its synthesis, stability or localisation. The results also support the theory that the NBP may function to regulate auxin transport by acting on the efflux carrier (Ruegger *et al.*, 1997).

A second mutant has been identified which shows an altered response to auxin transport inhibitors. Wild-type seedling roots, when allowed to grow to the bottom of a plate, continue to grow in a curling pattern which is abolished by the addition of NPA to the growth media. The *roots curl in NPA* (*rcn1*) mutant was isolated because its roots show an exaggerated curling pattern in the presence of NPA (Garbers *et al.*, 1996). In the absence of NPA, the roots and hypocotyl of *rcn1* seedlings were reduced in length compared to the wild-type but they showed normal auxin sensitivity. The mutant was found to have wild-type auxin efflux activity in the absence of NPA but showed greater sensitivity of efflux in the presence of NPA. Unlike *tir3* however, the *rcn1* mutation does not affect NPA uptake or binding and root elongation in the presence of NPA was similar to the wild-type. Cloning of the *RCN1* gene revealed it encoded the regulatory A subunit of protein phosphatase 2A (Slabas *et al.*, 1994). This suggests that a component of the auxin efflux regulatory machinery is controlled by its phosphorylation level. If RCN1 activity does regulate only a component, then it would explain the subtle phenotype of *rcn1*.

It has been demonstrated that the activities of the auxin influx and efflux carriers can be distinguished by their substrate specificities in tobacco suspension cells. The uptake of 2,4-D is mainly determined by influx carrier activity whilst 1-NAA mainly enters cells by diffusion and has its levels controlled by efflux carrier activity (Delbarre *et al.*, 1996). This has enabled the regulation of auxin influx and efflux carrier activity to be monitored in response to different conditions (Delbarre *et al.*, 1998). As has been discussed, it is proposed that auxin is transported into cells in a protonated form along with one or two protons (Rubery and Sheldrake, 1974; Raven, 1975). The activity of the two carriers was therefore examined following both increasing the external pH (pHe) and by intracellular (pHc)

acidification. Influx activity was found to decrease upon both increasing pHe and decreasing pHc whereas the efflux activity was only affected by decreasing pHc.

Treatment of cells with brefeldin A, which blocks Golgi mediated secretory pathways, was not found to affect influx carrier activity but efflux carrier activity was decreased. The inhibition of efflux activity by BFA was rapidly reversible upon removal of the BFA by washing. This suggests that efflux carrier activity is mediated by one or more short-lived plasma membrane bound proteins. This was supported by treatment of cells with the protein synthesis inhibitor cycloheximide (CHX) which, following a short lag period, inhibited the efflux activity but not the influx carrier.

Protein kinase inhibitors, such as staurosporine, were also found to rapidly inhibit efflux carrier activity but not influx activity. This would indicate that these inhibitors were interfering with the activity of protein kinases that control the phosphorylation of one or more proteins required for auxin efflux. If cells were pre-treated with inhibitors of protein phosphatases prior to treatment with staurosporine, the inhibitory effect of staurosporine still occurred. One possibility to explain why pre-treatment with phosphatase inhibitors fails to prevent the inhibition of efflux activity by staurosporine is that the phosphorylated proteins required for efflux activity are eliminated from the auxin transport system before being dephosphorylated (Delbarre *et al.*, 1998).

Taken together with the analysis of the *tir3* and *rcn1* mutants the emerging picture is that auxin transport activity can be regulated at multiple levels. The regulation appears to have greater focus on the activity of the efflux carrier rather than the influx carrier. The potential involvement of rapidly turned-over proteins in regulation of the efflux carrier as well as changes in the phosphorylation status of both these proteins and the NPA-binding protein implicate the involvement of signalling cascades in efflux carrier control. This experimental data correlates with the ability of roots (and the plant) to respond rapidly to environmental stimuli such as gravity, and highlights the importance of auxin transport in root development.

1.7.3 Auxin Distribution in the Root and its Possible Role in Patterning

Whilst studies of polar auxin transport indicate that auxin is redistributed once it reaches the root apex and is vital for tropic responses and lateral root development, they do not indicate what the distribution of auxin is and how this might root organisation. As described previously, a synthetic auxin response promoter linked to the *GUS* reporter gene (DR5::GUS; Ulmasov *et al.*, 1997;

Sabatini *et al.*, 1999) was used to determine regions of 'auxin maximum'. In the primary root this reporter showed maximal GUS activity in the columella initials, with lower activity in the quiescent centre and columella root cap. Treatment of roots with 2,4-D resulted in expression throughout the root but importantly, the columella and quiescent centre did not show increased sensitivity to this external auxin. This indicated that DR5::GUS activity reflected auxin levels independent of cell-type and not because of spatial differences in auxin sensitivity through the meristem (Sabatini *et al.*, 1999).

The expression of this perceived auxin peak in the root tip was examined in auxin response mutants. DR5::GUS activity in the *axr1* mutant (Leyser *et al.*, 1993), which shows reduced auxin responses, was found to be reduced but in the correct region. This was accompanied by a reduction in the number of columella root cap columns indicating a reduction in cell division in the root cap. DR5::GUS activity in the *axr3-1* mutant (Rouse *et al.*, 1998) was significantly reduced and coupled with this, columella cells did not form starch granules indicating incomplete specification. The columella initials were not observed to divide indicating that they are inactive. The *axr3-1* mutation therefore interferes with establishment of an auxin peak and cell fate in the primary root. The fact that these auxin response mutants, as well as *mp* discussed earlier, all display decreases in DR5::GUS activity coupled to defects in cell fate and division patterns, suggests that these processes require an auxin peak in the root tip (Sabatini *et al.*, 1999).

To determine the effect of defects in polar auxin transport on the distribution of this auxin maximum, DR5::GUS activity was monitored in auxin transport mutants. In *pin1-1* mutants DR5::GUS activity often showed peaks in the quiescent centre and this was associated with defective division of these cells and disorganisation of the columella. In the *eir1-1* background, expression was found in the lateral root cap and if roots were not aligned with gravity this expression accumulated in one side of the cap which reflects the defects in gravitropic response in this mutant. Unlike *pin1-1* no changes in cell organisation were observed and DR5::GUS activity was not altered in the *aux1-7* background. This indicates that components of the auxin efflux system are required for the correct spatial distribution of auxin and that, at least in *pin1-1*, this localisation is required for the correct orientated divisions of the quiescent centre. The fact that the DR5::GUS maximum was uncoupled from the columella initials in these mutants indicates this peak is not due to cell type specification and nor does it cause specification.

Furthermore, it indicates that cell specification is not simply determined by a specific auxin level (Sabatini *et al.*, 1999).

Whilst the local auxin concentration may not specify cell type, the auxin max in the root tip may be required for organising pattern elements and hence determine cell fate. Auxin transport inhibitors were used to alter the auxin distribution in order to determine the effect on cell fate. Several days after germination on NPA, DR5::GUS activity was found to occupy a region encompassing the original columella cells plus flanking cortical and epidermal cells. These cells divided horizontally in relation to the vascular bundle and began expressing columella initial markers. The cells on the outside expressed columella markers whilst those inside expressed a quiescent centre marker. Therefore, the lateral shift of the DR5::GUS peak resulted in former epidermal, cortical and endodermal cells acquiring columella, columella initial and quiescent centre cell identity. This suggests that the ectopic auxin accumulation resulting from transport inhibition is capable of organising pattern.

The results of the NPA experiments could also be achieved by 2,4-D application at concentrations between 10^{-4} and 10^{-7} M but lower concentrations induced neither DR5::GUS activity nor respecification of cell fate. The range of auxin concentration revealed that neither absolute auxin concentration nor an auxin gradient is sufficient to determine pattern. An additional factor was therefore required for determining patterning. One possibility was tissue prepattern in which the competency of cells to respond to auxin is different, whilst a second possibility was a signal arising from tissue contacting the respecified cells.

Laser ablation of the quiescent centre resulted in a new DR5::GUS peak in the vascular cells above the ablated cells and this was followed by respecification of vascular cells to form a new quiescent centre and columella. These ablation experiments along with auxin transport inhibition and auxin treatment indicate that in response to high levels of auxin, protoderm (epidermis), ground tissue (cortex and endodermis) and vascular cells can all be respecified to quiescent centre and columella cell types. This suggested tissue prepattern was unlikely to be the additional factor required for patterning in the root tip. The common factor in all the experiments was that the respecified cells were arranged in a polar fashion relative to the vascular bundle. Therefore, along with an auxin peak, information from the vascular bundle is likely to organise pattern and polarity in the root (Sabatini *et al.*, 1999).

1.7.4 Auxin and Root Growth

The analysis of mutants defective in auxin transport has shown that this process and therefore auxin is required for root elongation, gravitropism and lateral root development. Many of the responses that require auxin transport are attributed to the redistribution of auxin resulting in localised accumulation of this hormone. The response of roots to exogenously applied auxin is very much concentration dependent with low concentrations (10^{-10} to 10^{-9} M) inducing growth whilst higher concentrations ($\geq 10^{-6}$ M) inhibit. Though somewhat contradictory this highlights that the auxin dose-response is not a linear relationship and explains how changing the local concentration can result in different effects in the same tissue.

Regulation of auxin levels is therefore important for eliciting different responses in root development. Mutants affecting auxin homeostasis have been isolated and display defects in root development (Boerjan *et al.*, 1995; King *et al.*, 1995; Celenza *et al.*, 1995; Delarue *et al.*, 1998). The *superroot* (*sur1* ; Boerjan *et al.*, 1995), *rooty* (*rty* ; King *et al.*, 1995) and *alfl* (Celenza *et al.*, 1995) mutants were isolated independently and shown to be alleles of a single gene. Though initial growth of the mutant is similar to the wild-type, *rty* and *sur1* seedlings begin to show deviations from approximately 3 days post germination. Numerous adventitious roots begin to grow from the hypocotyl, lateral root primordia develop at high frequency, root hairs appear at higher density and root elongation is reduced. Along with defects in apical growth, the phenotype of the mutant resembles that of wild-type seedlings grown in the presence of micromolar amounts of auxin (King *et al.*, 1995). This indicated that the mutant overproduces auxin, a theory which was supported by the ability of mutant tissue explants to propagate in the absence of auxin (Boerjan *et al.*, 1995). Measurements of free and conjugated forms of auxin in the mutant showed that all were present at higher levels than the wild-type (King *et al.*, 1995; Boerjan *et al.*, 1995). In crosses of the *rty* mutant with both auxin resistant (*axr1-3*) and ethylene resistant (*etr1-1*) mutants, the *rty* phenotype was not completely blocked.

With regards to lateral root development the *etr1-1* cross was of particular interest because the double mutant showed no effect on *rty* dependent root proliferation (adventitious or lateral). This indicates that lateral (and adventitious) root development is dependent on auxin and not auxin-induced ethylene (see section on ethylene). High levels of auxin are therefore required to stimulate pericycle cells to divide in the first stages of lateral root development. This is supported by observations that auxin resistant mutants such as *axr1* and *aux1* and the auxin

transport mutant *tir3* all have fewer laterals than the wild-type. Also, the fact that lateral roots originate from division of pericycle cells bordering the vascular bundle correlates with theories that a signal from vascular cells along with an auxin peak organises root pattern (Sabatini *et al.*, 1999). The *alf4-1* mutant rarely produces lateral roots and cannot be rescued by levels of auxin that induce development in both wild-type and auxin resistant mutants (Celenza *et al.*, 1995). However, *alf4-1* root elongation is inhibited to the same degree as the wild-type by auxin. This indicates that there are two independent auxin signalling pathways involved in determining lateral root formation and primary root elongation (Celenza *et al.*, 1995).

As well as acting to control lateral root development, auxin has been implicated in the differentiation of root hair cells (Masucci and Schiefelbein, 1994; 1996). It was noted that the dominant *axr2* mutant which is resistant to auxin, ethylene and abscisic acid (Wilson *et al.*, 1990), was found to have fewer root hairs (Massuci and Schiefelbein, 1994). The *rhd6* mutant, which shows a reduction in the number of root hairs and a basal shift in the site of hair emergence on the epidermal cell, could be rescued by nanomolar concentrations of auxin (Massuci and Schiefelbein, 1994). The point at which auxin affects hair cell differentiation was examined by double mutant analysis (Massuci and Schiefelbein, 1996). Double mutants between *rhd6* and both *ttg* and *gl2* resulted in roots with a greater number of hairs than the *rhd6* mutant alone but significantly less than wild-type which suggests that *RHD6* is either negatively regulated by *TTG* and *GL2* pathway or acts in a separate pathway. Treatment of these double mutants with auxin resulted in roots with *ttg* and *gl2* like phenotypes. This shows that *TTG* and *GL2* are not required by auxin to rescue the *rhd6* phenotype indicating that auxin acts after *TTG* and *GL2* to influence root hair formation. Further support for a late role of auxin comes from its ability to induce root hairs on epidermal cells in the elongation zone of *rhd6* roots, a point in the root where epidermal cells have normally differentiated into hair-forming and hairless cells (Massuci and Schiefelbein, 1996).

Auxin is therefore able to influence many aspects of root development including elongation, cell division and cell differentiation as well as being involved in the organisation of pattern in the root tip. The ability of this hormone to act in so many different processes indicates the possibility of separate but interacting signal transduction pathways with potentially different auxin sensitivities. In concluding this section on the role of auxin in root development, the auxin response pathway will be discussed.

1.7.5 Auxin-Binding Protein – An Auxin Receptor?

Given the wide range of responses mediated by auxin, one of the most important areas of auxin biology has been to identify the receptor(s) that perceive this hormone and transduce the auxin stimulus into these responses. As this suggests, such a receptor must not only be able to bind auxin, but also be shown to transduce an auxin response. Whilst a number of proteins that bind auxin have been identified (Jones, 1994), the ability to show that they can transduce an auxin signal has been more difficult to prove.

One candidate that appears to fulfill some of the criteria for an auxin receptor is auxin-binding protein (ABP1). Initially isolated as a soluble auxin-binding protein from maize coleoptiles (Zm-ERabp1, Löbner and Klämbt, 1985a,b), genomic or cDNA clones of ABP1 have now been isolated from a number of other plant species including tobacco (Nt-ERabp1, Leblanc *et al.* 1997) and *Arabidopsis*, where it is encoded by a single gene (At-ERabp1, Palme *et al.* 1992). The auxin-binding proteins from these different species all share an N-terminal leader sequence and a C-terminal KDEL motif (Lys-Asp-Glu-Leu), which is involved in localisation to the endoplasmic reticulum (ER). Consistent with this feature, ABP1 has been shown to co-fractionate with the ER marker cytochrome c reductase, with estimates suggesting that at least 90% of the ABP1 is located in the ER lumen or on the ER membrane (Shimomura *et al.* 1988; Jones *et al.* 1989; Tillmann *et al.* 1989).

Auxin has been shown to rapidly induce proton secretion into the cell wall (Rayle and Cleland, 1977; Cleland *et al.* 1991), cause hyperpolarisation of the plasma membrane (Ephritikhine *et al.*, 1987) and rapidly induce gene transcription (Abel and Theologis, 1996). Such responses are consistent with auxin perception at the plasma membrane and cell wall as well as a cytoplasmic site of action, possibly the nucleus. Therefore, the predominant localisation of ABP1 to the ER is not consistent with the expected sites of auxin perception, casting doubts on the role of ABP1 as a legitimate auxin receptor. However, a number of studies have now shown that, whilst ABP1 has a KDEL ER-targeting motif and is predominantly localised to the ER, a small proportion of the protein is localised to other areas of the cell (Barbier-Brygoo *et al.*, 1989; Barbier-Brygoo *et al.*, 1991; Jones and Herman, 1993; Diekmann *et al.*, 1995).

Electrophysiological studies using tobacco protoplasts have been a valuable tool in studying the role of auxin and ABP1. The advantage provided by using protoplasts instead of whole tissue is that the plasma membrane is accessible to large macromolecules, such as antibodies. Auxin has been shown to modulate the

ion current across the plasma membrane of protoplasts, causing rapid hyperpolarisation (H^+ -ion efflux: Ephritikhine *et al.*, 1987; Barbier-Brygoo *et al.*, 1989; Barbier-Brygoo *et al.*, 1991). Antibodies raised to maize ABP1 were found to inhibit auxin-induced hyperpolarisation of tobacco protoplasts (Barbier-Brygoo *et al.*, 1989), whilst the sensitivity of the tobacco protoplasts to auxin was enhanced by the addition of maize ABP1 to the suspension media (Barbier-Brygoo *et al.*, 1991). Furthermore, it has been shown that a 15 amino acid C-terminal peptide, identical to the C-terminus of Nt-ERabp1, is able to elicit the same auxin-like hyperpolarisation as the full length protein when added to tobacco protoplasts. A peptide corresponding to the C-terminal 12 amino acids of Nt-ERabp1 did not elicit an auxin response, indicating that the full 15aa C-terminal domain is crucial for NtERabp1 function (Leblanc *et al.*, 1999).

The experimental work on tobacco protoplasts using maize ABP1 antibodies, NtERabp1 and synthetic peptides strongly supports the localisation of ABP1 to the plasma membrane as well as this being the site of auxin perception. The localisation of ABP1 to the plasma membrane of maize coleoptile tissue and protoplasts has been confirmed by a combination of microscopy and immunocytochemistry (Jones and Herman, 1993; Diekmann *et al.*, 1995). ABP1 was also localised to the cell wall and Golgi apparatus, and found to be secreted via the secretory system even though the protein retained its KDEL ER-retention signal. The secretion of ABP1 was further enhanced by starving cells of auxin (Jones and Herman, 1993). Therefore, whilst ABP1 is predominantly found in the ER lumen, it is also localised to the presumed sites of auxin perception. Interestingly, whilst the majority of the cellular pool of ABP1 is in the ER lumen, experimental evidence suggests that the physiological conditions of the ER are not compatible with binding of ABP1 to auxin (Tian *et al.*, 1995).

A body of indirect evidence indicates that ABP1 may function as an auxin receptor, at least at the plasma membrane. The use of transgenic plants has now provided more direct molecular genetic proof for the role of ABP1 as an auxin receptor (Jones *et al.*, 1998). The *Arabidopsis* ABP1 (At-ERabp1) cDNA was placed under the control of a tetracycline-derepressible promoter and this construct was introduced into tobacco plants expressing the tetracycline repressor. Expression of At-ERabp1 could therefore be specifically induced by feeding the plants a non-toxic tetracycline analog. The system that was used to examine the effect of inducible expression of At-ERabp1 was the auxin-induced epinastic growth response of excised tobacco leaf strips. It has been shown that the auxin

responsiveness of such leaf cells is developmentally regulated, correlating with the cell expansion phase of growth. Therefore, cells at the leaf tip are able to undergo ethylene-independent expansion following auxin treatment, whereas the cells at the basal lamina are not auxin-responsive (Keller and Van Volkenburgh, 1997; 1998). Strips of interveinal tissue from the basal region of the lamina were therefore chosen and exposed to both the tetracycline analogue and auxin. Strips from At-ERabp1 expressing plants did undergo epinastic growth whereas those from control plants (expressing the tetracycline repressor) were significantly less responsive. This growth was dependent on active auxin being present, with the inactive auxin analog 2-NAA being ineffective. Furthermore, when these transgenic plants were grown for longer periods under inducible conditions, isolated protoplasts had much greater volumes than from control treated plants. Such results show that ABP1 does mediate auxin-dependent cell expansion both on excised tissue and the whole plant (Jones *et al.*, 1998).

To further test the role of ABP1 as an auxin receptor, maize cells were transformed with a CaMV 35S:maize *ABP1* construct. Such cell lines were found to have significantly larger cells than control cell lines following auxin treatment. Importantly, this response was strongly dependent on auxin treatment with the distribution of cell sizes being approximately the same between control and ABP1 overexpressing lines in the absence of auxin. Taken together, the results of both the inducible expression of At-ERabp1 in whole plants and overexpression in maize cells strongly support the role of ABP1 as the auxin receptor that controls cell expansion (Jones *et al.*, 1998). It should be noted that the authors accept that given the complexity of auxin action it is likely that other, as yet, unidentified auxin receptors exist and are required to mediate other auxin responses.

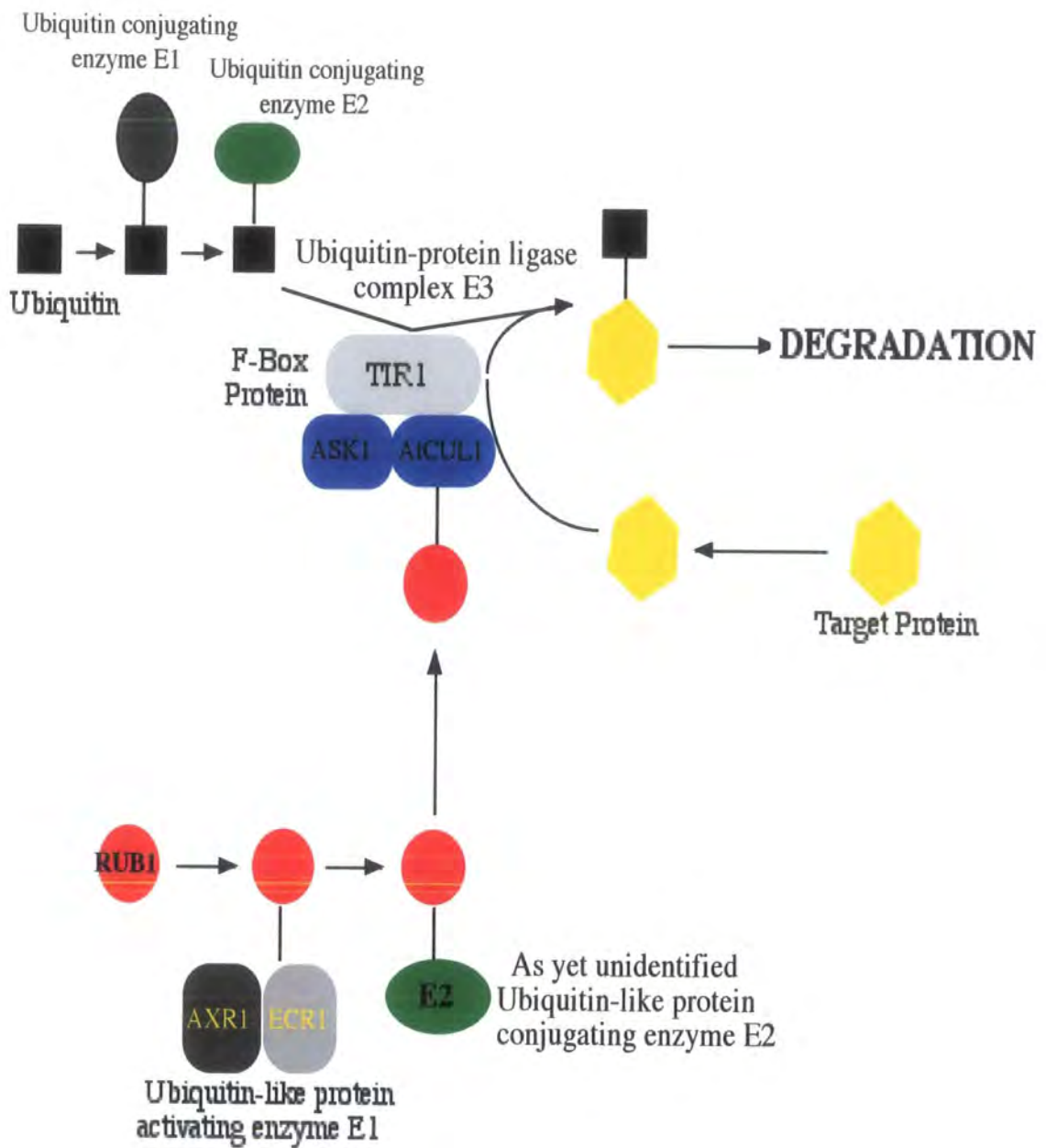
1.7.6 The Auxin Response Pathway

The *AXR1* gene was one of the first genes to be identified in *Arabidopsis* that is required for a normal auxin response. Mutations in this gene result in auxin resistant plants with diverse defects in leaf, flower and vascular development as well as lateral root formation and gravitropism (Lincoln *et al.*, 1990). The *AXR1* gene was cloned and found to encode a polypeptide with similarity to the N-terminus of the ubiquitin activating enzyme E1 (Leyser *et al.*, 1993). The E1 enzyme is required for activation of ubiquitin, a small acidic protein, which is then transferred to a second enzyme (E2) which then attaches the ubiquitin to proteins often with the help of a third ubiquitin-protein ligase (E3), targeting them for degradation. The E2 and

E3 enzymes often exist as multigene families and determine target protein specificity.

Cloning of *AXR1* implicated the ubiquitin pathway in auxin response. Activation of ubiquitin by E1 requires a C-terminal cysteine residue in E1 forming a thiolester linkage with the C-terminus of ubiquitin. However, this whole region of the protein is absent in AXR1 indicating that AXR1 cannot have E1 activity. Analysis of the yeast ubiquitin pathway provided the necessary clues to solve this apparent anomaly. In yeast E1 enzyme activity is carried out by two types of proteins, AXR1-like proteins and a second class of proteins homologous to the C-terminus of E1 which contain the active site cysteine (Johnson *et al.*, 1997; Lammer *et al.*, 1998; Liakopoulos *et al.*, 1998). Homology searches using the yeast Uba2p and Uba3p proteins identified an *Arabidopsis* EST encoding a 55 kD protein, ECR1, with homology to the C-terminus of E1 (del Pozo *et al.*, 1998). Several ubiquitin related (*RUB*, related to **u**biquitin) genes have been identified in *Arabidopsis* (Callis *et al.*, 1995). It was shown that by combining AXR1, ECR1, RUB1 and ATP the thiolester linkage could be formed between ECR1 and RUB1 (del Pozo *et al.*, 1998).

The link between auxin and the ubiquitin pathway was further strengthened by the cloning of the *TIR1* gene (Ruegger *et al.*, 1998). The *tir1* mutant was initially identified because of its resistance to auxin transport inhibitors (Ruegger *et al.*, 1997) but the primary defect was found to be in auxin response and not auxin transport (Ruegger *et al.*, 1998). Double mutant analysis with the *axr1-12* mutant indicated that the two genes function in the same or overlapping pathways. The *TIR1* gene was found to encode a polypeptide containing a recently identified motif, the F-box (Bai *et al.*, 1996), and a number of leucine-rich repeats. The TIR1 polypeptide showed greatest similarity to SKP2, a human S-phase kinase associated protein, and the yeast Grr1p protein (Bai *et al.*, 1996). These proteins have been shown to bind the SKP1 protein, an interaction requiring the F-box (Bai *et al.*, 1996; Li and Johnson 1997). The significance of this is that SKP1 and Grr1p are components of the E3 ubiquitin-protein ligase complex in yeast. This complex also contains the Cdc53 protein to which Rub1p is conjugated, an event which is thought to stabilise the E3 complex. Both SKP1 (ASK1) and Cdc53p (AtCUL1) orthologues have been identified in *Arabidopsis* (Porat *et al.*, 1998, Gray *et al.*, 1999) which suggests that an E3 ubiquitin-protein ligase complex functions in the auxin response pathway. To determine this, proteins that interact with TIR1 were identified by the yeast two-hybrid system and found to be *SKP1*-like genes, *ASK1* (Porat *et al.*, 1998) and



ASK2 (Gray *et al.*, 1999). Furthermore, the ASK1, ASK2 and AtCUL1 proteins could be coprecipitated with TIR1 in protein extracts, though the interactions of ASK1 and ASK2 were surprisingly not dependent on the F-box (Gray *et al.*, 1999). Further support for an E3 complex functioning in auxin response came from analysis of a mutant allele of *ASK1*. The *ask1-1* mutant was found to be male sterile due to chromosome nondisjunction (M. Yang and H. Ma, unpublished data) but this phenotype was also found to cosegregate with auxin resistance (Gray *et al.*, 1999). Overexpression of TIR1 was found to mimic the effect of growing plants in the presence of auxin indicating an increase in auxin response in these transgenic plants (Gray *et al.*, 1999)

The identification of E1 and E3 like complexes in *Arabidopsis* provides strong evidence that auxin response is mediated by a ubiquitin pathway (reviewed in Leyser and Berleth, 1999; see Figure 1.2). This however raises the question of where the auxin signal feeds into such a pathway? Among the targets of the yeast F-box protein-mediated ubiquitination pathway are proteins involved in cell-cycle progression. When these proteins are phosphorylated they can be targeted for Rub1p conjugation by the E3 complex (Skowyra *et al.*, 1997). The cell cycle in yeast is, amongst other factors, linked to nutrient availability, and cell-cycle progression does not occur in the absence of sufficient glucose. Glucose signalling is believed to affect association of Skp1p and Grr1p with the interaction of these proteins enhanced by sufficient glucose thus allowing the formation of a stable E3 complex and ubiquitination of targets (Skowyra *et al.*, 1997). Such a mechanism may be relevant to auxin action in plants. Auxin resembles the amino acid tryptophan and since nitrogen is more limiting to plant growth than carbon, it is possible that auxin regulates cell-cycle progression by stabilising the formation of the E3 complex (Leyser, 1998; Leyser and Berleth, 1999).

If auxin response is mediated by a ubiquitin pathway another question is what are the protein targets for degradation? One possibility are the early auxin genes which are transcriptionally activated within minutes of auxin application and are thought to mediate downstream auxin responses. There are four different families of early auxin induced genes identified in various species (reviewed in Abel and Theologis, 1996). These include the *SAUR* (Small Auxin UpRegulated) genes which are induced within 2-5 minutes of auxin treatment and, in soybean, code for small (0.5 kb) transcripts encoding small (9-10 kD), similar polypeptides and also the *AUX/IAA* family. The *AUX/IAA* genes have been found to consist of a family of at least 20 members in *Arabidopsis* (Abel *et al.*, 1995) and many can be

transcriptionally induced by the protein synthesis inhibitor cycloheximide indicating that they are repressed by short lived protein(s) (reviewed in Abel and Theologis, 1996). They encode short lived nuclear proteins with four conserved domains one of which resembles a $\beta\alpha\alpha$ DNA recognition motif found in some prokaryotic transcriptional repressors (Abel *et al.*, 1994). DNA binding requires dimerisation of the prokaryote repressors and it has also been shown that members of the AUX/IAA family can form homo- and heterodimers and that one member resembles ARF1 (IAA24, Kim *et al.*, 1997), the transcription factor that binds auxin response elements in promoters (Ulmasov *et al.*, 1997a). The large numbers of this family and the ability to form heterodimers indicates a huge repertoire of potential interactions and specificities. The role of this family in auxin response has recently been confirmed (Rouse *et al.*, 1998; Tian and Reed, 1999). Mutations in the *AXR3* gene are semidominant and result in increased auxin response (Leyser *et al.*, 1996). Cloning of the *AXR3* gene revealed that it encoded a member of the AUX/IAA family, *IAA17* (Rouse *et al.*, 1998). The semidominant *axr3* mutations all resulted in amino acid changes in the second conserved domain whilst intragenic revertants either resulted in additional amino acid changes or defects in splice site recognition. Likewise, dominant mutations in *shy2/iaa3* result in amino acid changes in domain II. As with *axr3* intragenic suppressors resulted in either aberrant splicing or premature truncation of the protein. Both gain and loss of function mutations in *shy2/iaa3* result in auxin defects such as root and lateral root growth (Tian and Reed, 1999). The increased auxin response in the *axr3* and *shy2* mutants may well result from increased stability of the respective proteins. This would correlate well with early auxin genes being the target for an auxin ubiquitin pathway. Following auxin sensing these early genes would be induced and mediate downstream activation of genes. They would then be rapidly targeted for degradation by the auxin ubiquitin pathway, thus introducing a feedback loop to control the amplitude of the response. Increased stability of an AUX/IAA protein would result in amplification of the auxin signal as in the *axr3* and *shy2* mutants. One interesting feature adds complication to the role of the AUX/IAA genes and suggests an alternative mode of action is that they appear able to repress transcription of genes containing the TGTCTC auxin response element when overexpressed in protoplasts along with an auxin inducible reporter (Ulmasov *et al.*, 1997b). It is possible that by overexpression other factors may be titrated away thus inhibiting the auxin response. It is however possible that the AUX/IAA proteins interact with ARF transcription factors prebound to auxin inducible promoters (Ulmasov *et al.*, 1999).

and inhibit transcription of these genes, perhaps even their own. Auxin-mediated degradation of these AUX/IAA proteins may therefore temporarily relieve the inhibitory effect before the negative feedback cycle reinstates the inhibition. The fact that many early auxin-induced genes are also induced by cycloheximide correlates with this model. Following treatment with cycloheximide AUX/IAA proteins would be rapidly turned over but could not be resynthesised and thus their inhibitory effect on transcription would be released. Such a system, in which transcription of auxin response genes is primed by ARFs already bound to promoters but held in check by AUX/IAA proteins, would allow for rapid responses to an auxin signal. How then could this alternative model explain how the mutations in domain II in *axr3* and *shy2* could give rise to increased auxin response? A clue is the fact that the intragenic suppressers generally either truncate the protein before the domain II mutation or result in splicing errors that either affect the reading frames of domains III and IV or result in loss of one of these domains. Domains III and IV are believed to be required for dimer formation, including ARF binding, and therefore their loss would prevent the mutant protein interacting with others. If the domain II mutations increased the stability of the protein it could inhibit ARF mediated transcription of some genes, possibly their own, by remaining bound to ARFs. It is therefore possible that by actually inhibiting its own transcription, it would remove its own inhibitory affect on downstream auxin response genes, amplifying the auxin signal.

Whilst AUX/IAA genes appear good candidates for auxin-mediated protein degradation another is the SAR1 protein. The *SAR1* gene was identified as a second site repressor of the *axr1* mutant phenotype resulting in plants with a near normal auxin response (SAR, Suppressor of Auxin Response; Cernac *et al.*, 1997). Analysis of *AXR : sar1-1* and *axr1-12 : sar1-1* plants showed that they were nearly identical indicating that the *sar1* not only suppresses but is epistatic to *axr1*. The analysis was consistent with the AXR1 protein acting on the *SAR1* gene or its product. The isolated *sar1-1* mutant was found to have reduced cell division in the root suggesting that it is a regulator of cell growth. AXR1 may therefore mediate the degradation of SAR1 in an auxin-dependent manner (Cernac *et al.*, 1997).

1.7.7 Ethylene and Root Development

The simple gas ethylene is able to affect a number of processes in plants including germination, senescence, leaf abscission, and fruit ripening (Abeles *et al.*, 1992). The biosynthetic pathway for ethylene has been determined and several of the genes encoding enzymes in this process have been cloned. Methionine is

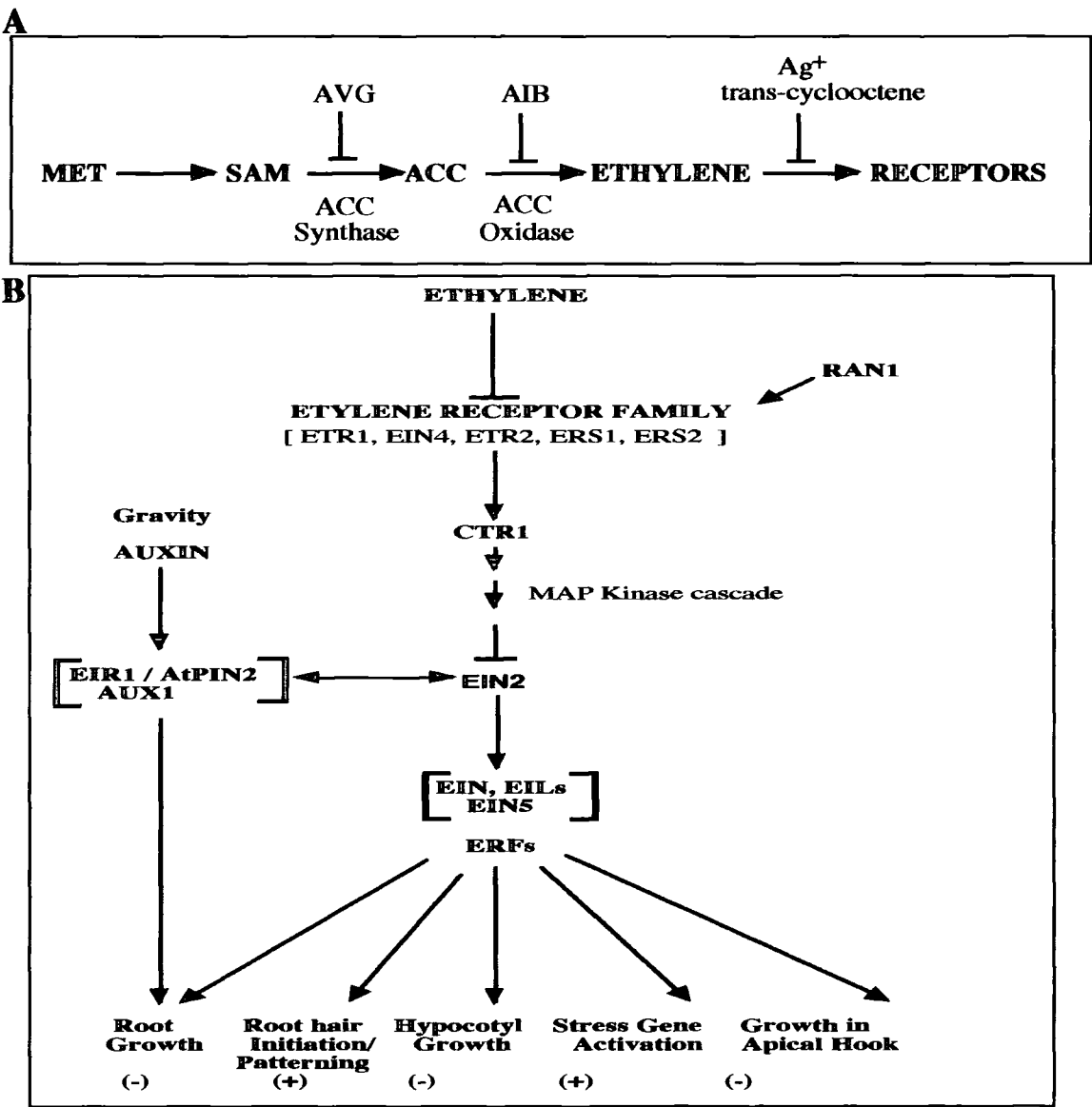
converted to S-adenylmethionine (SAM) which is converted to 1-aminocyclopropane-1-carboxylic acid (ACC), and finally to ethylene (Figure 1.3 a). The conversion of SAM to ACC is catalysed by ACC synthase, the key regulatory enzyme in the process (Kende, 1989; Sato and Theologis, 1989), which is coded for by a gene family in both *Arabidopsis* and tomato (Theologis, 1992). The conversion of ACC to ethylene is determined by ACC oxidase, which is constitutively present (Yang and Hoffman, 1984). Synthesis of ethylene can be blocked using aminovinylglycine (AVG) which inhibits ACC synthase, or the perception of ethylene can be blocked with silver ions which are believed to bind ethylene receptors. Ethylene is believed to have restricted movement in the plant and instead is thought that it is ACC that moves over large distances in the xylem (Bradford and Yang, 1980).

Ethylene has been implicated in a number of aspects of root development, particularly epidermal cell patterning (Masucci and Schiefelbein, 1994, 1996; Tanimoto *et al.*, 1995). As described previously, root hairs form on epidermal cells overlying two cortical cells resulting in files of hair and hairless epidermal cells. Treatment of wild-type roots with AVG resulted in roots virtually devoid of root hairs. This effect could be countered by including ACC in the media along with the AVG which showed the AVG effect was ethylene specific (Masucci and Schiefelbein, 1994). Similarly, growth of plants in the presence of silver ions also results in a reduction in the number of root hairs. The inclusion of ACC in growth media also has dramatic effects on root hair development by altering the fate of epidermal cells. At very high concentrations of ACC all epidermal cells, regardless of position, develop root hairs suggesting that ethylene is a positive regulator of root hair development (Tanimoto *et al.*, 1995). The role of ethylene in epidermal cell patterning has also been investigated in a number of mutants known to be defective in various aspects of ethylene signalling or production. The *ctr1* mutant was isolated because its phenotype resembles that of seedlings grown in the presence of ethylene and is believed to be a negative regulator of the ethylene response pathway (Kieber *et al.*, 1993). Analysis of root hairs in this mutant revealed that, as with ACC treatment, they formed in non-hair positions further supporting the theory that ethylene is a positive regulator of hair cell fate (Dolan *et al.*, 1994). Ethylene is believed to affect hair cell development at a late stage of development (Masucci and Schiefelbein, 1996). As with auxin, when double mutants between *rhd6* and either *ttg* or *gl2* were treated with ACC, the roots resembled those of the *ttg* and *gl2* mutants. This indicates that ACC, and most likely ethylene, does not act through a

Figure 1.3. The Ethylene Response Pathway

A) Ethylene synthesis. Arrows indicate enzymatic reactions whilst barred lines indicate the site of action of various inhibitors (aminoethoxyvinylglycine, AVG; α -aminoisobutyric acid, AIB).

B) Genetic pathway for the ethylene response pathway as determined by epistasis analysis of mutants (Roman *et al.*, 1995). For details of functions and gene symbols see text. Arrows indicate positive control whilst barred lines indicate negative control points. Brackets indicate uncertain gene order. Responses that are regulated positively by ethylene are indicated (+) whilst negatively regulated responses are indicated (-).



pathway that requires the TTG or GL2 proteins and is therefore likely to act downstream of these genes. Further supporting this conclusion was the fact that *ttg* and *gl2* mutants treated with AVG had reduced root hair formation. If ethylene acted before these genes then treatment with AVG would have no effect in these mutants (Masucci and Schiefelbein, 1996). It has been postulated that the effect of both ethylene and auxin on ectopic root hair production may not be due to switches in cell fate but rather by altering the control of cell expansion. Both hormones can influence cell expansion (Davies *et al.*, 1987; Abeles *et al.*, 1992) by reorientating microtubules (Shibaoka, 1994). Excess ethylene response in the *ctr1* mutant and large amounts of ACC may therefore cause a reorientation of expansion in all epidermal cells resulting in ectopic root hair production (Masucci and Schiefelbein, 1996).

The role of ethylene in radial expansion has already been discussed with regards to the *sabre* mutant which shows radial expansion of the cortical cell layer. This phenotype is partially rescued by growth in the presence of silver. In the same study it was found that growth of wild-type plants in the presence of ACC resulted in a reduction of root elongation as well as an increase in radial expansion in all cell layers (Aeschbacher *et al.*, 1995). Reduced elongation in the presence of ACC correlates with observations that the root length of some ethylene mutants such as *ctr1* is reduced compared to the wild-type. This relationship between ethylene and root elongation is not necessarily a simple one and introduces the subject of how ethylene interacts with other plant hormones, especially auxin, to regulate root development.

1.7.8 Ethylene and Auxin Interactions

The relationship between auxin and ethylene in root development is highlighted by the fact that a number of mutants have been isolated which show resistance to both. A good example is the potential auxin efflux carrier, *AtPIN2* (Muller *et al.*, 1998) which was found to be the same as *EIR1* mutations in which were identified as having ethylene-insensitive roots (Luschnig *et al.*, 1998). Another example is *axr2*, a dominant mutant that confers resistance to both auxin and ethylene (Wilson *et al.*, 1990).

Auxin is known to stimulate the production of ethylene (reviewed in Yang and Hoffman, 1984) and this correlates with the fact that the *ACS4* gene has been found to be an early auxin-induced gene (Abel *et al.*, 1995). Another *ACS* gene has been found to be expressed in root tips (Liang *et al.*, 1992; Rodrigues-Pousada *et*

al., 1993) which corresponds to an auxin peak in the root (Sabatini *et al.*, 1999). Induction of ethylene by auxin makes distinguishing between auxin and ethylene effects difficult. In order to determine the relative effect of both hormones transgenic plants were produced that overproduced auxin whilst inhibiting the production of ethylene to normal levels (Romano *et al.*, 1993). Whilst focusing on aerial phenotypes such plants were able to indicate that auxin is primarily responsible for apical dominance and leaf epinasty whilst ethylene is involved in inhibition of internode stem elongation (Romano *et al.*, 1993). The fact that the elongation of roots is inhibited by both auxin and ACC raises the possibility that their action, in this instance, is via a common mechanism.

One candidate for this common mechanism is the auxin transport machinery. Ethylene treatment has been shown to inhibit polar auxin transport (Morgan and Gausman, 1966; Burg and Burg, 1967). Analysis of auxin transport in ethylene treated pea epicotyls revealed that, whilst the transport velocity was similar to untreated tissue, transport was inhibited by up to 95% indicating that ethylene reduces transport capacity. Furthermore, NPA binding to microsomes was significantly reduced following ethylene treatment due to a reduction in the number of binding sites (Suttle, 1988). Since the NPA binding site is believed to be part of the auxin efflux carrier machinery and may regulate its activity (Ruegger *et al.*, 1997), this would suggest that ethylene inhibits auxin efflux by reducing the synthesis or localisation of the NPA-binding protein. Regulation of auxin transport by ethylene could explain the ability of ethylene to inhibit root elongation. By reducing auxin transport, ethylene could cause an accumulation of auxin in the root which would inhibit elongation. Alternatively, ethylene could prevent the second stream of auxin transport from the root tip to the elongation and differentiation zones resulting in insufficient auxin reaching these tissues and thus inhibiting elongation. The ability of auxin to induce ethylene and ethylene to inhibit polar auxin transport suggests a mechanism by which root elongation can be controlled by a feedback loop. It also explains the ethylene insensitive root of *eir1/Atpin2* since the auxin efflux component on which ethylene potentially exerts its effect is defective.

1.7.9 Ethylene and Cytokinin Interactions

Cytokinins were discovered as factors that acted with auxin to promote cell division in culture (Miller *et al.*, 1955). They have since been implicated in a number of processes in the plant including cell division, shoot initiation and growth (Binns,

1994). Cytokinins are known to modulate ethylene levels (Yang and Hoffman, 1984; Abeles *et al.*, 1992) and this is exemplified by the ability of cytokinin to produce certain effects in dark-grown *Arabidopsis* similar to those caused by ethylene (Lieberman, 1979).

Root elongation in light-grown seedlings has been shown to be inhibited by low levels of cytokinin (Su and Howell, 1992). In the dark the effect of cytokinin on seedling growth was very similar to the triple-response (see next section) produced by growth in ethylene suggesting the effects of cytokinin were coupled to ethylene (Cary *et al.*, 1995). Root and hypocotyl elongation was therefore examined in mutants resistant to ethylene. These mutants were found to be insensitive to normally inhibitory concentrations of cytokinin. Furthermore, growth in the presence of silver ions was also able to overcome the inhibitory effect of cytokinin in wild-type seedling roots and hypocotyls. Examination of ethylene levels on varying concentrations of cytokinin revealed that cytokinin was stimulating production of this gas and correlated well with the inhibition of root and hypocotyl elongation. This indicates that cytokinin-induced ethylene production could account for the inhibitory effects of cytokinin on root and hypocotyl elongation (Cary *et al.*, 1995).

Further indications of interactions between these two hormones has come from mutant analysis. The *ckr1* (Cytokinin Resistant, Su and Howell, 1992) mutant was isolated because of its ability to elongate roots on inhibitory concentrations of cytokinin. However, it has been shown to be allelic to the ethylene insensitive mutant *ein2* (Guzman and Ecker, 1990; Cary *et al.*, 1995). The ability of cytokinin to induce ethylene was used as the basis for a mutant screen to identify cytokinin-insensitive mutants (Vogel *et al.*, 1998a; 1998b). The *cin5* mutant was identified as a recessive mutation that is insensitive to low levels of cytokinin but showed normal responses to ethylene (Vogel *et al.*, 1998a). Cloning of the *CIN5* gene revealed that it was the *ACC Synthase 5* gene (Liang *et al.*, 1995) and that independent *cin5* mutant alleles were the result of amino acid substitutions in conserved regions (Vogel *et al.*, 1995a). At low concentrations of cytokinin, *cin5* mutants produced much less ethylene than wild-type plants but there was no difference when high cytokinin concentrations were used. This suggests that the *ACS5* gene is responsible for almost all ethylene production in response to low cytokinin and that at higher concentrations other factors must regulate ethylene production (Vogel *et al.*, 1998a). Examination of *ACS5* transcript levels following cytokinin treatment revealed only a modest transient increase in levels, not enough to account for the

prolonged increase in ethylene in response to the same amount of cytokinin. It was therefore concluded that some post-transcriptional modulation of *ACS5* was required to account for this anomaly. This was supported by examination of the *eto2* mutant which overproduces ethylene (Kieber *et al.*, 1993). The *eto2* mutant was found to be allelic to *cin5* and was caused by a frame-shift that results in a change to the C-terminal 12 amino acids of the protein. Transformation of *cin5* and wild-type plants with the *eto2* mutant version of the *ACS5* gene resulted in ethylene-overproducing plants. However, the steady-state levels of the *ACS5* message in *eto2* mutants was actually slightly lower than the wild-type. This suggests that the alteration of the C-terminus of *ACS5* in *eto2* is responsible for elevated ethylene levels and that this region of the protein regulates enzyme activity in response to cytokinin (Vogel *et al.*, 1998a).

Post-transcriptional regulation of *ACS* genes may be a common mechanism of increasing ethylene synthesis. The ethylene over-producing mutants *eto1* and *eto3* (Guzman and Ecker, 1990; Kieber *et al.*, 1993) were found to have elevated ACC synthase enzyme activity and yet had wild-type transcript levels for a number of members of this gene family. Also, the activity of ACC oxidase was not affected suggesting that, as with *ACS5* and cytokinin, post-transcriptional regulation of the *ACS* was responsible for the elevated ethylene levels of these mutants (Woeste *et al.*, 1999a). Further supporting evidence comes from the observations that the steady-state transcript levels of the active *ACS* gene family members is increased by treatment with cycloheximide (Liang *et al.*, 1992; Woeste *et al.*, 1999a). Combined with the fact that the transcript levels are normally very low (Woeste *et al.*, 1999a) this indicates that they are under the control of a short-lived protein repressor as with many of the early auxin-inducible genes.

The experimental evidence indicates that both auxin and cytokinin can induce ethylene levels, possibly by action on different members of the *ACS* gene family. It has been observed that the action of auxin and cytokinin on ethylene biosynthesis is synergistic such that the ethylene evolved is greater in the presence of both than the sum of both individually (Woeste *et al.*, 1999b). One hypothesis is that the synergism is due to cytokinin enhancement of auxin action (Lau and Yang, 1973). When ethylene induction was measured in the *cin5* mutant following treatment with both auxin and low levels of cytokinin it was found that the two hormones were still having a synergistic effect. Cytokinin may therefore increase the ability of auxin to induce ethylene. One possibility is that it acts post-

transcriptionally on the *ACS4* gene product in a manner similar to that of *ACS5* (Woeste *et al.*, 1999b).

1.7.10 Ethylene Signalling

The ethylene signalling pathway has been widely studied and a number of key components have now been identified (reviewed in Ecker, 1995; Kieber, 1997; McGrath and Ecker, 1998; Theologis, 1998; Woeste and Kieber, 1998). The basis of many of the screens for ethylene mutants has been the triple response.

Arabidopsis seedlings grown in the dark in the presence of ethylene display a shortened root and hypocotyl, a radially expanded hypocotyl and an exaggerated apical hook. This simple marker has led to the isolation of a number of ethylene mutants which fit broadly into the categories of either ethylene-insensitive or constitutive response. The latter consists of both ethylene overproducers and signalling mutants whilst both categories can also be tissue specific.

The first such mutant to be identified in *Arabidopsis* was *etr1*, a dominant mutation that resulted in ethylene resistance (Bleecker *et al.*, 1988). The *etr1* mutant was defective in a number of ethylene responses and failed to show increases in expression of ethylene-induced genes upon application of the hormone.

Furthermore, leaves of *etr1* bound only a small percentage of the ethylene bound by wild-type leaves. The *ETR1* gene was cloned and found to encode a protein similar to bacterial two-component histidine kinases (Chang *et al.*, 1993). In bacteria these proteins are involved in sensing and responding to environmental cues and consist of an N-terminal membrane spanning sensor domain and a C-terminal response domain. The fact that *etr1* plants bind less ethylene than wild-type whilst the *ETR1* protein has been shown to bind ethylene (Schaller and Bleecker, 1995) and as predicted (Burg and Burg, 1967) requires a copper cofactor (Rodriguez *et al.*, 1999), shows that *ETR1* is an ethylene receptor. A number of other ethylene receptors have now been cloned (*ERS1*, *ETR2*, *EIN4*, *ERS2*; Hua *et al.*, 1995; Sakai *et al.*, 1998; Hua *et al.*, 1998). The *ERS1* gene was cloned by cross-hybridisation to *ETR1* but unlike *ETR1* lacks the C-terminal regulator domain. However, expression of a mutant version of *ERS1*, equivalent to the *etr1-4* mutation, did confer dominant ethylene insensitivity on plants (Hua *et al.*, 1995). All the potential ethylene receptors identified in mutant screens resulted in this dominant ethylene insensitive phenotype. Loss of function alleles of each of these genes were isolated and the plants analysed and individually they each showed virtually normal ethylene responses (Hua and Meyerowitz, 1998). However, when the loss of function

mutants were combined the resultant plants showed constitutive ethylene responses suggesting that these proteins negatively regulate ethylene responses. This suggests that the receptors exist in two states, an active signalling state and an inactive state. In the absence of ethylene, the receptors are in an active state whilst in the presence of this hormone they switch to the inactive state. This explains how a gain of function mutation in just one of the receptors can lead to a dominant ethylene insensitive phenotype since the active state would be continuously operational (Hua and Meyerowitz, 1998).

As previously described, prior to identification of any ethylene receptors, it was predicted that such proteins would require a metal cofactor (Burg and Burg, 1967) and indeed purified ETR1 binds copper ions (Rodriguez *et al.*, 1999). It is believed that the inhibitory effect of silver ions on ethylene perception is determined by occupying this cofactor site in the receptors. The importance of a copper cofactor to ethylene perception was further emphasised by the cloning of the *RAN1* gene (Hirayama *et al.*, 1999). The *responsive-to-antagonist1* (*ran1*) mutant was identified because it displayed a triple response in the presence of the ethylene receptor antagonist *trans*-cyclooctene (TCO). Epistasis analysis revealed that *etr1* and *ein2*, an ethylene insensitive mutant, were both epistatic to *ran1*. Since *ETR1* encodes an ethylene receptor this indicated that *RAN1* functions very early in the ethylene pathway. The RAN1 protein was found to have similarity to a family of copper transporters, a function which was confirmed by the rescue of copper-transport defects in a yeast mutant expressing RAN1 (Hirayama *et al.*, 1999). It would seem likely that the role of RAN1 is therefore to supply copper ions to the ethylene receptors.

Cloning of *CTR1* was significant in that it was the first gene identified as being required for ethylene signalling (Kieber *et al.*, 1993). The *ctr1* mutant belongs to the class that shows a constitutive ethylene response and therefore phenotypically resembles plants grown in the continuous presence of ethylene and shows upregulation of a number of ethylene-induced genes. It was marked as a signalling mutant rather than an ethylene overproducer because it could not be rescued by growth in the presence of either silver ions or AVG. Furthermore, epistasis analysis indicated that it functions early in the ethylene pathway but after *ETR1*. Cloning of *CTR1* showed that it was constitutively expressed transcript unaffected by ethylene and encoded a protein with similarity to the Raf family of serine/threonine protein kinases (Kieber *et al.*, 1993). These proteins have been shown in mammalian systems to be activated by the small GTP binding protein Ras

and regulate the mitogen-activated protein kinase (MAPK) cascade. In this cascade MAP kinases are activated by phosphorylation by MAP kinase kinases (MAPKK) which in turn are activated by MAPKK kinases, a class of which Raf kinases are members (reviewed in Cobb *et al.*, 1994). The phenotype of the mutant indicates that the *CTR1* gene is likely to be a negative regulator of the ethylene signalling pathway, acting through a MAP kinase cascade (Kieber *et al.*, 1993). Furthermore, it has been shown that the ethylene receptors ETR1 and ERS1 can physically interact with CTR1 (Clark *et al.*, 1998) indicating that intermediates are not required between these proteins in order to control the ethylene signalling pathway.

Acting after *CTR1* in the ethylene signalling pathway is the *EIN2* gene (Guzman and Ecker, 1990; Alonso *et al.*, 1999). The *ein2* mutant is insensitive to both exogenously applied and endogenous ethylene (Roman *et al.*, 1995; Chen and Bleecker, 1995) and has been identified in screens for resistance to auxin transport inhibitors (Fujita and Syono, 1996) and cytokinins (Su and Howell, 1992). This suggests that EIN2 may be a component of a number of hormone signalling pathways, and is not specific to that of ethylene. The *EIN2* gene was cloned and found to be constitutively expressed and like *CTR1*, its levels were not affected by ethylene. The transcript encoded a large protein with an N-terminal membrane spanning domain and a C-terminal domain thought to be required for protein interactions. The N- and C-termini of the protein were predicted to lie on the same side of the membrane. Overexpression of the C-terminus of the EIN2 protein was able to confer constitutive ethylene response in an *ein2-5* background but overexpression of either the N-terminus or the whole protein did not have the same effect. It has been proposed that the N-terminus of the protein is a sensing domain that regulates the activity of the C-terminal activating domain. The similarity of the N-terminus to the Nramp family of proteins, several of which act as transporters of divalent cations, suggests that such a cation may be the signal to which the N-terminus responds (Alonso *et al.*, 1999).

Mutations in the *EIN3* gene, like *ein2*, result in insensitivity to exogenous and endogenous ethylene and has been ordered after *EIN2* in the ethylene signalling pathway (Roman *et al.*, 1995). Cloning of *EIN3* revealed it belongs to a small family of *EIN3-like* (*EIL*) genes of which there are three other members (Chao *et al.*, 1997). The EIN3 protein was determined to be localised to the nucleus and overexpression of both EIN3 and EIL proteins in both wild-type and *ein2-5* backgrounds resulted in constitutive ethylene responses. High level expression therefore activates ethylene responses even in the absence of an ability to perceive an

ethylene signal. The use of silver and AVG was not able to block this phenotype indicating that, as predicted by epistasis analysis, *EIN3* acts downstream in the ethylene pathway and is a positive regulator of ethylene response. The fact that, as with *CTR1* and *EIN2*, ethylene did not affect *EIN3* transcript levels indicates that it is regulated post-transcriptionally, possibly by phosphorylation as would be predicted by the cloning of *CTR1*.

A number of ethylene-induced genes from various plant species have been shown to have conserved ethylene response elements in their promoters (Meller *et al.*, 1993; Sessa *et al.*, 1995; Sato *et al.*, 1996). Ethylene-Responsive-Binding-Proteins (EREBPs) have been found to bind these elements (Ohme-Takagi and Shinshi, 1995) and a number of related genes have been identified in the *Arabidopsis* genome (Riechmann and Meyerowitz, 1998). An EREBP like gene, *Ethylene-Response-Factor1* (*ERF1*), was isolated and found to be transcriptionally upregulated by ethylene (Solano *et al.*, 1998). Furthermore, upregulation in response to ethylene required a functional *EIN3* gene suggesting that *ERF1* may be a target for *EIN3*. This was confirmed when *EIN3* was shown to specifically bind a 36 nucleotide region in the promoter of *ERF1*, an interaction that required the N-terminal region of *EIN3* and that promoter binding by *EIN3* involves homodimer formation. The evidence suggested that *ERF1* mediates ethylene responses in response to transcriptional activation requiring *EIN3*. The role of *ERF1* in ethylene response was confirmed by transgenic plants overexpressing this gene. These plants were found to exhibit a subset of ethylene responses such as inhibition of hypocotyl and root elongation that was independent of whether overexpression was in a wild-type or ethylene-insensitive background. It is likely that activation of *ERF1* and other related genes by *EIN3* and the *EIL* genes results in the activation of secondary target genes resulting in an ethylene response (Solano *et al.*, 1998). Therefore, the ethylene signal transduction pathway has, at least partially, been determined from the site of perception to the site of action (Figure 1.3 b).

1.8 The AtEM101 promoter trap line of Arabidopsis

This introduction has focused on a number of features concerned with our current understanding of the processes that govern plant root development. This has ranged from the genes that are required for the embryonic construction of the root initials and those genes required for post-embryonic development to the roles of plant hormones and their modes of action. One fact that is evident is that root growth and development is a continuing process and involves a complex interplay

between different gene activities, hormone signals and environmental cues. This current work will describe the molecular characterisation of the *POLARIS* locus of *Arabidopsis* and the potential role of the *POLARIS* gene in root development.

1.8.1 Isolation of Genes by Promoter Trapping

The isolation and study of mutants has been of significant importance in developing our current understanding of root development. Production of mutants on a large scale often involves the use of point mutation inducing chemicals such as ethylmethanesulfate (EMS). One problem with this approach is that often positional cloning methods are required to isolate the genes involved which, even with the current genome sequencing initiative, can be a long process. The use of insertional mutagens such as the T-DNA from *Agrobacterium tumefaciens* or alternative transposon methods offer the advantage that often the mutated gene is 'tagged' by the insertional mutagen making cloning easier. However, the initial work required to produce large numbers of independent mutant lines is more involved than with chemical methods. Both systems also have the drawback that they can offer no information on the expression pattern of the tagged genes until of course the gene is cloned. One fundamental flaw in both the chemical and insertional mutagen systems is that they require that mutation of a gene results in a characterisable phenotype, be it by biochemical or morphological methods. This creates a bias against a number of genes that belong to large gene families or have functional redundancy or that just have very subtle mutant phenotypes. Even when so called 'smart screens' are used where particular conditions are used, an example being use of the triple response to isolate ethylene mutants, the aforementioned classes of genes will most likely be overlooked.

The strategy of promoter trapping has been used successfully to study gene expression in *Drosophila*, mouse and *Caenorhabditis elegans* (Bellen *et al.*, 1989; Allen *et al.*, 1988; Hope, 1991). The method involves the integration of a reporter transgene (such as β -glucuronidase) into the genome of the organism being studied. The reporter possesses either a minimal promoter or no promoter at all and thus for expression to occur it must integrate downstream or proximal to the regulatory sequences of a native gene. The expression of the reporter should mimic that of the native gene and the reporter can therefore be used to examine the *in vivo* expression pattern and regulation of the tagged gene without the requirement for a mutant phenotype. This method therefore allows the analysis of the tagged genes which may show redundancy or subtle mutant phenotypes simply on the basis of the

reporter expression patterns. Promoter trapping also allows the analysis of previously difficult to target genes, a good example being genes expressed very early in embryogenesis. Mutational analysis of embryogenesis has often relied initially on identifying seedlings with aberrant phenotypes (Mayer *et al.*, 1991). The mutant gene giving rise to these seedling phenotypes could function at a number of stages of embryogenesis whereas analysis of reporter expression in a promoter trap line would indicate the exact stage at which expression was first evident.

The promoter trap used in this study is based on the T-DNA of *Agrobacterium tumefaciens* and contains a promoterless GUS reporter gene at the left border and the selectable marker gene *NPTII*, which confers resistance to the antibiotic kanamycin, at the right border (Topping *et al.*, 1991; Figure 1.4 a & b). Identification of lines with expression patterns of interest was determined by histochemical localisation of GUS enzyme activity (Topping *et al.*, 1991; Lindsey *et al.*, 1993; Topping *et al.*, 1994).

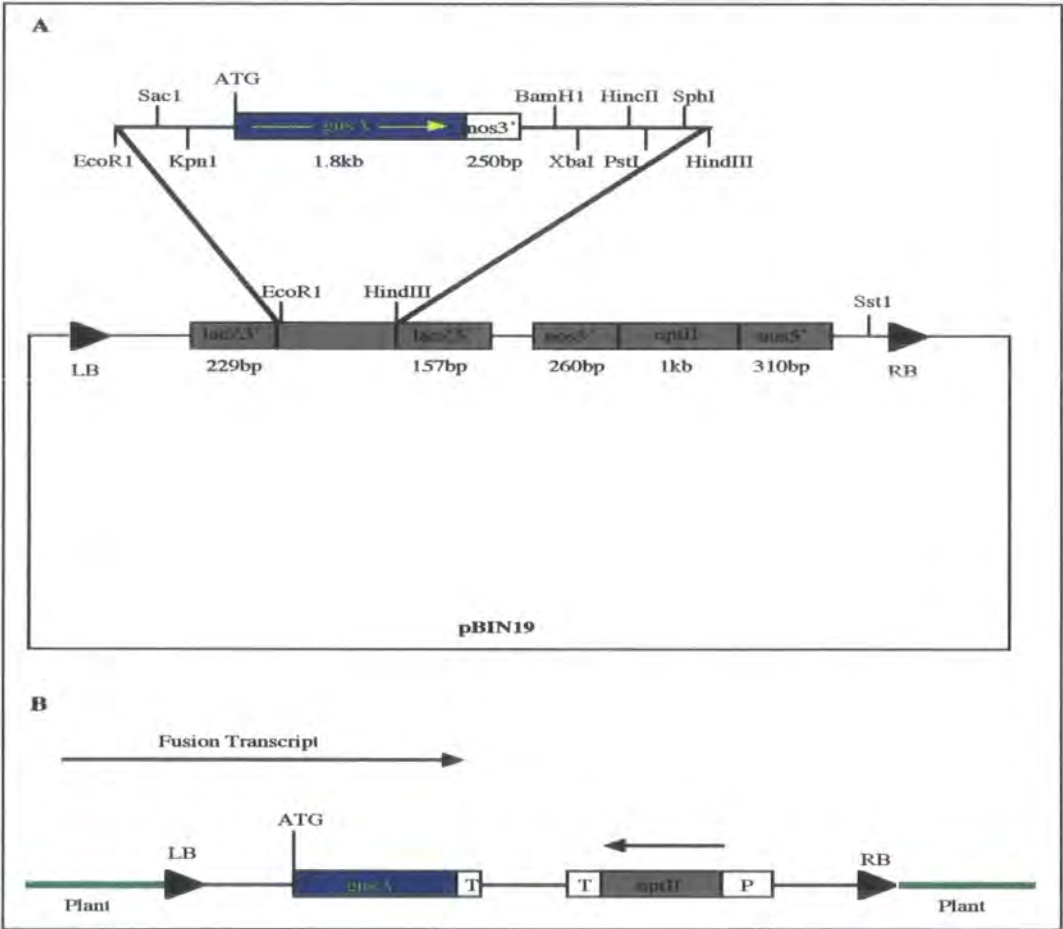
1.8.2 Identification and Characterisation of Line AtEM101

The AtEM101 line was identified in a screen of promoter trap transgenic lines exhibiting GUS enzyme activity in siliques and embryos of *Arabidopsis* (Topping *et al.*, 1994). GUS expression in line AtEM101 was first identified in heart-stage embryos in the basal region of the embryo that corresponds to the embryonic root primordium (Scheres *et al.*, 1994). No activity was found in the suspensor nor in the upper embryo at this early embryonic stage. As the embryo develops GUS activity is maintained in the embryonic root and by the late cotyledonary stage faint activity is observed in the cotyledons. In the young seedling GUS activity is found most strongly in the tips of both primary and lateral roots as well as weaker expression in the cotyledons and hypocotyl. In the mature plant expression was observed in the root tips and also the silique wall. Segregation analysis and Southern blotting indicated that the AtEM101 line contained a single T-DNA insert (Topping *et al.*, 1994). Plant DNA flanking the T-DNA insertion site was cloned and was used to isolate a lambda genomic clone of the wild-type locus. This was sub-cloned and the resultant 3.6 kb plasmid clone, which included the T-DNA insertion site, was fully sequenced (Topping *et al.*, 1994; J.F. Topping and I.M. Evans unpublished data).

The GUS expression in the root tips of the AtEM101 line occurs in all the cell types present (columella and lateral root cap, epidermis, meristem and immature vasculature) and occurs from the earliest stages of pericycle division in lateral root

Figure 1.4. Promoter Trap Vector pΔgusBIN19

- A)** The binary vector pΔgusBIN19 (Topping *et al.*, 1991) consists of the *gusA* coding region plus the *nos* transcriptional terminator inserted into the multiple cloning site of the plant binary vector pBIN19 (Bevan *et al.*, 1984). The 5' end of the *gusA* sequence is adjacent to the T-DNA left border (LB) and has its own ATG codon. Since translational stop codons are found in all reading frames of the T-DNA LB, insertion into a plant coding sequence is expected to result in transcriptional rather than translational fusions.
- B)** Schematic representation of the pΔgusBIN19 T-DNA promoter trap following integration into plant genomic DNA. Insertion downstream of a plant promoter is expected to result in the formation of a transcriptional gene fusion with *gusA*.



development (Topping *et al.*, 1994; Topping and Lindsey, 1997). Given that this expression pattern corresponds to the auxin peak in the root (Sabatini *et al.*, 1999) and that auxin plays a major role in root development (see section on auxin), the role of this hormone on GUS expression was examined (Topping and Lindsey, 1997). GUS enzyme activity in seedlings germinated on various concentrations of the synthetic auxin naphthalene acetic acid (NAA) was found to be significantly higher than in controls. Treatment with the cytokinin kinetin was observed to have the opposite effect. Interestingly, treatment of AtEM101 seedlings with the polar auxin transport inhibitor triiodobenzoic acid (TIBA) was not found to affect GUS expression in the primary root tip though, as previously reported treatment did result in a reduction in the number of lateral roots. Furthermore, extended cell division activity was not found to be required for expression since treatment with the cell-cycle inhibitor hydroxyurea (HU) did not significantly affect GUS activity or localisation.

GUS activity and localisation was also examined in the mutants *hydra* (Topping *et al.* 1997) and *gnom* (Mayer *et al.*, 1991, 1993; Shevell *et al.*, 1994) known to be defective in root development. Seedlings of the *hydra* mutant are dwarfed with supernumerary cotyledons, a short and expanded hypocotyl and a severely reduced or missing root system. The embryos lack the cellular organisation of the wild-type and lack the characteristic bilateral symmetry of the torpedo and cotyledonary stage embryos being globular in appearance with no apparent embryonic root (Topping *et al.* 1997). GUS expression in the *hydra* mutant was similar to the wild-type, being localised to the basal half of the embryo, even though there was no apparent embryonic root, and in *hydra* seedlings was in the basal region even in the absence of correct root organogenesis. Surprisingly, the same observations were made in the *gnom* mutant background which does not form a root meristem. The only deviation from the wild-type pattern of expression occurred in the most severe ball-shaped *gnom* embryos where GUS expression was diffuse and less localised. It was therefore proposed that GUS expression in the AtEM101 line marks polarity and that the tagged gene is part of a positional information pathway that marks root development and thus was named *POLARIS*. Given that the *POLARIS* marker is activated by auxin it was further proposed that auxin is a fundamental component of this positional information pathway (Topping and Lindsey, 1997).

1.8.3 Line AtEM101 has a Short Root Phenotype

One advantage of the promoter trap system utilised in this research is that it is based on the insertional mutagen, the T-DNA, a feature which allowed the rapid cloning of plant flanking DNA. To investigate root phenotype, AtEM101 seedlings, homozygous for the T-DNA, were back-crossed to wild-type and the F1 progeny were grown on vertical agar plates for 14 d in the light. Three classes of seedlings were identified. Approx. 25% (43/186) were GUS negative and exhibited a relatively long root, comparable with that of wild-type seedlings (mean length $75 \pm \text{SEM } 4$ mm; $n = 10$). 25% (41/186) were GUS positive and exhibited a significantly shorter root than the wild-type (mean length $38 \pm \text{SEM } 2$ mm, $n = 10$; i.e. ca. 51% at 14 d post-germination). The third class, which comprised ca. 50% of the seedlings (102/186), was GUS positive and exhibited an intermediate rate of root growth (mean length $53 \pm \text{SEM } 3$ mm; i.e. ca. 71% the length of wild-type roots at 14 d post-germination). These data show that a single T-DNA insertion had caused a semi-dominant mutation affecting root growth under the conditions studied (P. Chilley, unpublished data).

Short roots are observed in plants grown in the presence of the hormones auxin, cytokinin and ethylene indicating that line AtEM101 may be either overproducing one of these hormones or defective in signalling. When grown in the dark in the absence of exogenous hormones AtEM101 seedlings were found to have a phenotype similar to that of the triple response with an exaggerated apical hook, elongated hypocotyl and reduced root indicating that the AtEM101 line showed a potential defect in ethylene response (P. Chilley, unpublished data). Constitutive ethylene response mutants fall into two classes of either signalling mutants or ethylene overproducers. Growth in the presence of silver ions or AVG rescues the overproducing class but not the signalling class. The short root phenotype of AtEM101 seedlings was rescued by growth in the presence of silver ions indicating that it belongs to the ethylene overproducing class of constitutive response mutants (P. Chilley, unpublished data). Double mutants with *ctr1* (Kieber *et al.*, 1993) resulted in seedlings with a combinatorial phenotype of very short, hairy roots indicating that the *POLARIS* gene must act in either separate or interacting pathways to *CTR1* (P. Chilley, unpublished data). Crosses with other ethylene mutants has given similar results indicating that the *POLARIS* gene may be a novel ethylene response mutant. (P. Chilley, unpublished data).

1.8.4 Molecular Characterization of the *POLARIS* locus of *Arabidopsis thaliana*

This study aims to build on the previous characterisation of the AtEM101 line. Further analysis of the pattern of GUS expression in this line is presented along with histological analysis of the AtEM101 root which determines the likely nature of the short root defect. Characterisation of the wild-type genomic locus, into which the T-DNA inserted in line AtEM101, is detailed. This includes the cloning of the *POLARIS* gene, mutations in which result in the phenotype observed in the AtEM101 line, and a detailed analysis of the unusual structure and expression of this gene. Expression of a second, tightly linked gene is also presented. The potential role of the *POLARIS* gene in regulating root development in response to hormone signals is examined in transgenic plants overexpressing the gene. Finally, the role of the *POLARIS* gene in root development and hormone response is discussed and potential modes of action of this gene will be presented.

Chapter 2 Materials and Methods

Described in this chapter are the materials and methods which were used to obtain the results described in the following results chapters.

2.1 Materials

2.1.1 Chemicals

The chemicals used for this research were obtained from either Sigma Chemical Company Ltd. (Poole, UK), Fisher Scientific (Loughborough, UK), ICN Pharmaceuticals Ltd (Basingstoke, UK), Merck Ltd. (Poole, UK), Fisons Scientific Equipment (Loughborough, UK) or Bio-Rad Laboratories (Hemel Hempstead, UK) unless otherwise stated.

Oligodeoxynucleotide primers used in PCR reactions and manual DNA sequencing were obtained from MWG-Biotech (Ebersberg, Germany). X-Gluc and IPTG was from Melford Laboratories (Suffolk, UK). X-Gal was from Bioline (London, UK). SuperSignal® Ultra chemiluminescent substrate was from Pierce (Rockford, Illinois, USA). Vancomycin HCl was from Duchefa (Haarlem, The Netherlands).

2.1.2 Radiochemicals

Radiolabelled nucleotides were obtained from ICN Pharmaceuticals Ltd. [^{32}P]α-dCTP was supplied at a concentration of 10mCi/ml and a specific activity of 3000Ci/mmol. [^{32}P]α-UTP was supplied at a concentration of 10mCi/ml and a specific activity of 800Ci/mmol. [^{32}P]γ-ATP was supplied at a concentration of 170mCi/ml and a specific activity of >7000Ci/mmol.

2.1.3 Enzymes

Restriction endonucleases, T4 DNA ligase, RNase-free DNase, AMV reverse transcriptase, M-MLV reverse transcriptase, terminal transferase, RNasin ribonuclease inhibitor and polynucleotide kinase were obtained from Promega Ltd. (Southampton, UK). *Taq* DNA polymerase was from Bioline. The Expand™ High Fidelity PCR system and Proteinase K were from Boehringer Mannheim (Lewes, UK). Shrimp alkaline phosphatase was obtained from Sigma Chemical Company Ltd.

2.1.4 Kits

The Wizard plasmid purification kit, fmol DNA sequencing system and PolyAtract® mRNA isolation system were from Promega. The High Pure PCR Clean-Up kit was from Boehringer Mannheim. The Prime-It II random primer labelling kit was from Strategene Ltd (La Jolla, California, USA). The Topo-TA cloning kit was from Invitrogen (Groningen, The Netherlands). The RNeasy Plant RNA extraction kit was from Qiagen Ltd. (Surrey, UK). The GeneClean II kit was from BIO 101 Inc. (La Jolla, California, USA). The MAXIscript™ T7/T3 In Vitro Transcription kit and RPA III™ kit were from Ambion Inc. (Texas, USA). The Phytopure plant DNA extraction kit was from Nucleon Biosciences (Lanarkshire, UK).

2.1.5 Bacterial strains

The *E.coli* strains used were as follows: XL1-blue MRF⁺ (Jerpseth, *et al.* 1992), TOP10 (Grant, S.G.N., *et al.* 1990), HB101 (Lacks and Greenberg, 1977), Y1090 (Young and Davis, 1983), DH10B (Gibco BRL), and C600hfl (Huynh *et al.* 1985). XL1-blue MRF⁺ was used to prepare competent cells and as a plasmid host. The TOP10 strain was a host for pCR® 2.1-TOPO. Y1090 was used for plaque formation following infection with Lambda Ziplox whilst DH10B was required for automatic excision of pZL-1 from Lambda Ziplox. C600hfl was used for plaque formation following infection with Lambda gt10. HB101 was received with a special plasmid construct.

Agrobacterium tumefaciens LBA4404 (Ooms *et al.*, 1982; Hoekema *et al.*, 1983) and C58C3 (Dale *et al.*, 1989) were used for plant transformations. Both strains have been disabled so that they do not cause crown-gall disease but they still have the virulence factors required for T-DNA insertion into plant genomic DNA. LBA4404 has a rifampicin (Rf) resistance marker located chromosomally allowing selection with the presence of 100µg/ml rifampicin. Selection for the C58C3 strain was with 25µg/ml nalidixic acid. Both strains were grown in LB liquid or LB plates at a temperature of 28-30°C.

For long-term storage bacterial strains were frozen at either -20°C or -80°C in the form of glycerol stocks, made by adding 0.5ml of an overnight liquid culture to 0.5ml of sterilized 50% glycerol.

2.1.6 Plasmids

The following plasmids were used during this project: pBluescript SK- (Short *et al.*, 1988), pCR[®]2.1 TOPO (Invitrogen), pBIN19 (Bevan, 1984), pCIRCE (a derivative of pBIN19, Bevan 1998), pMOG1006 (MOGEN international n.v., Einsteinweg 97, NL- 2333 CB Leiden, Netherlands, constructed by T. W. Verwoerd, 1989), pRK2013 (Ditta *et al.*, 1980) pDH51 (Pietrzak, M., *et al.* 1986), smGFP (Davis, S.J., and Viersta, R.D., 1998), p λ EM1 and pGUS-1 (both kindly donated by Dr. J. Topping, University of Durham). The pBluescript SK- plasmid is a general purpose cloning vector. pCR[®]2.1 TOPO is used for cloning DNA fragments generated by PCR. pRK2013 provides mobilisation function. pDH51 contains the CaMV 35S promoter and terminator and was used in the overexpression of the *POLARIS* transcript. smGFP contains a GFP variant and was used as a template for PCR. p λ EM1 contains a 3.6kb wild type genomic clone of DNA sequence flanking the T-DNA in line EM101. pGUS-1 was used in the construction of promoter-GUS constructs and contains the β -Glucoronidase gene followed by the NOS terminator. pBIN19, pCIRCE and pMOG1006 are wide host range binary cloning vectors for *Agrobacterium* - mediated gene transfer into plant cells.

2.1.7 Bacterial culture media

All bacterial culture media was sterilized by autoclaving at 121°C for 20 minutes.

- LB: 10g/l bacto-tryptone, 5g/l bacto-yeast extract, 5g/l NaCl.
 - LB agar: prepared by adding 15g bacto-agar to one litre of LB prior to autoclaving.
 - SOC medium: 20g/l bacto-tryptone, 5g/l bacto-yeast extract, 5.84g/l NaCl, 10mM MgCl₂, 10mM MgSO₄, 2g/l glucose, pH 6.8-7.0. MgCl₂, MgSO₄ and glucose were added after autoclaving.
 - Lambda broth: 10g/l bacto-tryptone, 2.5g/l NaCl, 2g/l maltose, 10mM MgSO₄. MgSO₄ was added from a 1M stock after autoclaving.
 - Lambda plates: prepared by adding 10g bacto-agar to one litre of lambda broth
 - Lambda top agar: prepared by adding 7g bacto-agar to one litre of lambda broth.
- SOC medium: 20g/l bacto-tryptone, 5g/l bacto-yeast extract, 5.84g/l NaCl, 10mM MgCl₂, 10mM MgSO₄, 2g/l glucose, pH 6.8-7.0. MgCl₂, MgSO₄ and glucose were added after autoclaving.

2.1.8 Plant material

Arabidopsis thaliana var. C24 and Columbia were kindly supplied by Prof. Keith Lindsey (University of Durham) as was seed from the promoter trap line AtEM101 (C24 background).

2.1.9 Plant culture media

- 1/2 MS10: Half strength Murashige and Skoog medium (Sigma M5519), 10g/l sucrose, pH5.7 adjusted with 1M KOH, 8g/l agar, autoclaved at 121°C for 15 minutes.

2.1.10 cDNA libraries

Arabidopsis cDNA libraries were obtained from the *Arabidopsis* Biological Resource Centre, DNA stock centre, Ohio. cDNA library CD4-7 is a lambda Ziplox (Gibco BRL, Renfrenshire, Scotland, UK) derivative containing *Sall*-*NotI* cDNA inserts from the Columbia wild-type ranging from 400 - >2000 base pairs. Equal amounts of mRNA from tissue culture grown roots, 7 day etiolated seedlings, rosettes from staged plants of different ages and 2 light regimes, and 40 aerial tissue (stems, flowers and siliques) from the same plants as the rosettes, were used to make the library. The amplified library comes from 2×10^5 primary transformants.

cDNA library CD4-12 was prepared using mRNA from immature green siliques from var. Wassilewskija. *EcoRI* (*NotI*-*Sall*) adaptors (Gibco-BRL) were ligated to the cDNA, phosphorylated and ligated into *EcoRI* digested, dephosphorylated Lambda gt10 (Promega). Phage DNA was packaged with GigaPackII extracts (Stratagene) and transfected into *E.coli* strain C600hfl. The primary library contained 7.5×10^6 plaque forming units and a range of insert sizes from 0.45 - 2.1kb.

2.2 Plant transformation

2.2.1 Mobilisation of binary vectors into *Agrobacterium tumefaciens*

The binary vectors pBIN19, pCIRCE and pMOG1006 (containing various constructs) were mobilised from *E.coli* XL1-blue MRF' into *Agrobacterium tumefaciens* LBA4404 and C58C3 with the help of *E.coli* HB101 harbouring pRK2013 in a triparental mating as modified from Bevan (1984) and Hooykaas (1988). *A. tumefaciens* LBA4404 was grown in LB containing 100µg/ml rifampicin at 30°C with shaking (120rpm) for 48 hours. *A. tumefaciens* C58C3 was grown in LB containing 25µg/ml nalidixic acid at 30°C with shaking

(120rpm) for 48 hours. *E.coli* XL1-blue MRF' (constructs in pBIN19, pCIRCE and pMOG1006) and HB101 (pRK2013) were grown overnight in LB containing 50µg/ml kanamycin sulphate at 37°C with shaking (200rpm). 100µl from each of the three cultures was mixed in an Eppendorf tube, pelleted by centrifugation, resuspended in 10µl of 10mM MgSO₄ and pipetted onto a LB agar plate. Following overnight incubation at 30°C, during which time mobilisation was allowed to occur, the bacteria were streaked onto selective medium (LB agar containing 100µg/ml rifampicin and 50µg/ml kanamycin for *A. tumefaciens* LBA4404, or LB agar containing 25µg/ml nalidixic acid and 50µg/ml kanamycin for *A. tumefaciens* C58C3). After 48 hours incubation at 30°C, transconjugants had grown up and were restreaked out for clear single colonies which were then checked for the presence of the various constructs. Control experiments performed by Dr. W. Wei (University of Durham) showed that none of the strains used in this mating experiment could grow when streaked separately on the selective media.

2.2.2 Seed sterilisation and growth conditions

Arabidopsis seeds were surface sterilised by treatment with 70% ethanol for 1-2 minutes and 25% hypochlorite/0.05% Tween 20 for 30 minutes and washed in sterile water three times. Following seed transfer to sterile media, petri dishes were sealed with micropore tape (Industriacare Ltd., Shephed, UK) and stored in the dark at 4°C for four days. The plates were then transferred to a growth room with 16 hours light a day at 25°C. Photon flux density was 50-150µmol/m²/s. Plants in soil were grown in Levingtons multipurpose compost mixed 4:1 with silver sand (soil and sand from Klondyke Garden Centre, Chester-Le-Street, UK) in a greenhouse with 16 hours light per day.

2.2.3 *Arabidopsis* transformation: the root explant method

After Clarke *et al.* (1992).

Solutions and media

- Silver thiosulphate stock (1.25mg/ml): made by adding dropwise a solution of silver nitrate (2.5mg/ml) to an equal volume of a solution of sodium thiosulphate pentahydrate (14.6mg/ml) and then filter sterilised.
- 1/2 MS10: as described in section 2.1.9.
- B5 base: 1 x B5 salts (Sigma G5768), 20g/l glucose, 0.5g/l MES (2-(N-morpholino) ethane sulphonic acid), pH5.7.
- B5 agarose: as B5 base, but supplemented with 8g/l LMP agarose (GIBCO BRL).
- B5 agar: as B5 base, but supplemented with 8g/l agar.

- Callus inducing medium: B5 agar supplemented with 0.5mg/l 2,4-D (2,4-dichlorophenoxyacetic acid), 0.05mg/l kinetin and 5mg/l silver thiosulphate.
- Shoot overlay medium: B5 agarose supplemented with 5mg/l 2ip (N⁶-(2-isopentyl) adenine), 0.15mg/l IAA (indole-3-acetic acid), 850mg/l vancomycin and 50mg/l kanamycin sulphate (20mg/l hygromycin b was included when constructs in the binary vector pMOG1006 were used).
- Shoot inducing medium: B5 agar supplemented with 5mg/l 2ip (N⁶-(2-isopentyl) adenine), 0.15mg/l IAA (indole-3-acetic acid), 850mg/l vancomycin and 50mg/l kanamycin sulphate (20mg/l hygromycin b was included when constructs in the binary vector pMOG1006 were used).

Method

Arabidopsis thaliana C24 or EM101 (C24 background) seeds were surface sterilised and grown on 1/2MS10 medium supplemented with 5mg/l silver thiosulphate at 25°C. Roots were cut from 3 week old plants and incubated for 3 days on callus inducing medium prior to infection. *Agrobacterium tumefaciens* strain LBA4404 containing the desired binary vector construct was grown for 48 hours in LB supplemented with 100µg/ml rifampicin and 50µg/ml kanamycin sulphate. The culture was pelleted by centrifugation and resuspended in B5 base to an OD_{600nm} of 0.025-0.1 just prior to infection. The roots were then cut into pieces 2-5mm in length and transferred into 20ml of the diluted *Agrobacterium* culture and incubated for two minutes. The infected root pieces were filtered with a sterile mesh, blotted onto sterile filter paper and then incubated on the original callus inducing plates for a further 2-3 days. Following this incubation roots were washed in B5 base to remove any bacterial overgrowth and filtered with a sterile mesh and then blotted onto sterile filter paper. The root pieces were then mixed with pre-molten and cooled (30°C) shoot overlay medium and poured onto plates containing shoot inducing medium. After approximately 3 weeks of incubation at 25°C and dim light, transformed green callus began to grow from infected root pieces. After 4-8 weeks of selection on shoot inducing medium, expanded shoots were transferred to 1/2MS10 medium for seed set in 60ml polypots which were sealed with gas permeable, transparent SunCap film (C6920, Sigma Chemical Company Ltd.). Plants were allowed to set seed and left to dry in the polypots before seed was harvested. Seed was dried for 2 weeks at 25°C before being surface sterilised and plated onto 1/2MS10 medium supplemented with 35mg/ml kanamycin sulphate. For the retransformation of line EM101 seed was plated onto 1/2MS10 medium supplemented with 20mg/l hygromycin B and 35mg/ml kanamycin sulphate.

2.2.4 *Arabidopsis* transformation: the dipping method

After Clough and Bent (1998)

Solutions and media

- 5% sucrose (w/v)/0.05% Silwett L-77(v/v) (Lehle Seeds, Texas, USA).
- 1/2 MS10: supplemented with 35mg/l kanamycin sulphate (pBIN19 and pCIRCE based constructs) or 20mg/l hygromycin b (pMOG1006 based constructs) and 850mg/l vancomycin.

Method

Arabidopsis thaliana var. Columbia were grown in soil in 3.5' pots (10-15 plants per pot) with a plastic mesh placed over the soil. Plants were grown for 3-4 weeks until they were approximately 10-15cm tall and displaying a number of immature, unopen flower buds. 2-3 days prior to dipping open flowers and any young siliques were removed. *Agrobacterium tumefaciens* strain C58C3 was used for all binary vector constructs. The *Agrobacterium* were grown for 48 hours at 30°C in 200ml LB supplemented with 25mg/l nalidixic acid, 100mg/l streptomycin sulphate and 50mg/l kanamycin sulphate. The culture was pelleted by centrifugation and resuspended in 1litre of a freshly made solution of 5% sucrose. Once resuspended, Silwett L-77 was added to a final concentration of 0.05% (v/v). Plants were then dipped fully into the solution and gently agitated for 10-15 seconds before removal. Dipped plants were placed in transparent bags to maintain humidity and placed back in the greenhouse in a shaded position overnight. Occasionally a second dipping was repeated 6 days after the first. Following removal from the bags plants were allowed to set seed and dry out in the greenhouse. Seed was collected from individual pots of plants and allowed to dry for 2 weeks at 25°C. Seed was surface sterilised and germinated on 1/2MS10 with antibiotic selection. Antibiotic resistant plants were transferred to soil and seed from these plants was tested for segregation on selective plates.

2.3 GUS enzyme analysis

2.3.1 Histochemical GUS analysis

After Stomp (1990)

Solutions

- X-Gluc stock: 20mM X-Gluc (5-Bromo-4-Chloro-3-Indolyl- β -D-Glucuronide) in N,N-dimethylformamide, stored at -20°C.
- X-Gluc buffer: 100mM NaH₂PO₄, 10mM EDTA, 0.1% (v/v) Triton X-100, 0.5mM potassium ferricyanide(K₃[Fe(CN)₆]) and 0.5mM potassium ferrocyanide (K₄[Fe(CN)₆]), pH7.0.

- X-Gluc staining solution: prepared by mixing 1 volume of X-Gluc stock with 19 volumes of X-Gluc buffer to give a final concentration of 1mM X-Gluc.
- Chloralhydrate solution: 8g chloralhydrate, 3ml water, 1ml glycerol.

Method

Localisation of GUS enzyme activity was determined by staining plant tissue for up to 24 hours in 1mM X-Gluc staining solution at 37°C. Stained tissues were then cleared of chlorophyll by soaking in 70% ethanol. Photographs were taken on Ektachrome 160 tungsten-balanced film (Kodak) on an Olympus SZH10 research stereo microscope fitted with an Olympus SC35 type 12 camera.

Analysis of staining in root tips after short staining periods (1-30 minutes) was carried out by clearing roots in chloralhydrate solution for 10 minutes. Excised roots were then mounted on microscope slides under a coverslip with a drop of chloralhydrate solution. Root tips were then examined for staining using DIC (differential interference contrast/ Normarski) optics on a Nikon Optiphot-2 microscope fitted with a Nikon FX-35 camera containing Ektachrome 160 tungsten-balanced film (Kodak).

2.4 Histological Examination of Roots

2.4.1 Fresh Transverse Root Sections

After Benfey *et al.* (1993)

Seedlings were grown on 1/2MS10 media for 4-7 days and then gently removed. A 4% agarose solution was boiled to dissolve the agarose and allowed to cool to approximately 50°C before being poured onto the surface of a petri dish. Roots were dragged through the molten agarose so that the root became embedded in an agarose coating and the agarose was then allowed to harden. Transverse sections of the root were then cut with a hand-held razor blade, mounted in 10% glycerol on a microscope slide under a cover slide, and observed using DIC/Normarski optics on a Nikon Optiphot-2 microscope fitted with a Nikon FX-35 camera containing Ektachrome 160 tungsten-balanced film (Kodak).

2.4.2 Examination of Root Tips

- Chloralhydrate solution: 8g chloralhydrate, 3ml water, 1ml glycerol.
- Lugol Solution (Sigma).

Method

The roots of 4 day old seedlings were excised and mounted on microscope slides in chloralhydrate solution and left to clear for 20-30 minutes. The

meristem and root cap were then viewed with Normarski optics on a Nikon Optiphot-2 microscope fitted with a Nikon FX-35 camera containing Ektachrome 160 tungsten-balanced film (Kodak).

For the examination of starch granules in the columella, roots were soaked in Lugol's solution for 6 minutes and then rinsed briefly in water before being transferred to chloralhydrate solution for 10 minutes. Roots were mounted in chloralhydrate solution and starch staining viewed with DIC/Normarski optics on a Nikon Optiphot-2 microscope fitted with a Nikon FX-35 camera containing Ektachrome 160 tungsten-balanced film (Kodak).

2.4.3 Cell Measurements

After Di Laurenzio *et al.* (1996)

- Acidified Methanol: 10ml methanol, 2ml conc. HCL, 38ml water.
- Clearing Solution: 1:1 mixture of 14% hydroxylamine in 60% ethanol and 14% NaOH in 60% ethanol.

Method

Tissue was incubated for 15 minutes in acidified methanol at 55°C and then transferred to clearing solution for 15 minutes at room temperature. Tissue was then re-hydrated through 40%, 20% and 10% ethanol for 10 minutes each, followed by 30 minutes in 25% glycerol in 5% ethanol. Roots were excised and mounted in 50% glycerol on microscope slides under coverslips and viewed using DIC/Normarski optics on a Nikon Optiphot-2 microscope fitted with a Nikon FX-35 camera containing Ektachrome 160 tungsten-balanced film (Kodak). For cell measurements slides of root sections were projected onto a screen and measured with a ruler. Calibrations were made using a stage micrometer observed at the same magnification.

2.5 Extraction and purification of nucleic acids

2.5.1 Miniprep of plasmid DNA using the Wizard™ minipreps DNA purification system

Plasmid DNA from small culture volumes (1-10ml) was isolated using the Wizard™ minipreps DNA purification system from Promega. The resulting plasmid DNA was suitable for DNA sequencing and all cloning purposes. The bacteria containing the plasmid of interest were grown overnight at 37°C with vigorous shaking in LB containing the appropriate antibiotic in a 15ml Falcon tube. 1.5mls of culture was transferred to an Eppendorf tube and the bacterial cells were pelleted by centrifugation at 13,400xg for 2 minutes. The supernatant was discarded and the pellet resuspended in 200µl of resuspension solution

containing RNase A to degrade cellular RNA. 200µl of lysis buffer was added and the tube inverted several times following which 200µl of precipitation buffer was added resulting in the formation of a white precipitate containing cellular debris and genomic DNA. Following centrifugation at 13,400xg for 5 minutes to pellet the precipitate, the cleared lysate was mixed with 1ml of Wizard™ minipreps DNA purification resin. A Wizard™ minicolumn was assembled with a 3ml syringe barrel and attached to a Vac-Man™ laboratory vacuum manifold (Promega) attached to a vacuum line. Then lysate and resin was pipetted into the syringe barrel and drawn through the Wizard™ minicolumn by vacuum. 2ml of wash solution was pipetted into the barrel and drawn through the Wizard™ minicolumn by vacuum. The apparatus was disassembled and the Wizard™ minicolumn dried by centrifugation at 10,000xg for 2 minutes. Plasmid DNA was eluted by the addition of 50µl of sterile, distilled water to the Wizard™ minicolumn. Following 1 minutes elution time the Wizard™ minicolumn was placed in an Eppendorf tube and centrifuged at 13,400xg for 20 seconds. The flowthrough collected in the Eppendorf contained the purified plasmid DNA.

2.5.2 Maxipreps of plasmid DNA

After Maniatis *et al.* (1982)

Solutions

- Solution I: 50mM glucose, 25mM Tris-HCl pH8, 10mM EDTA. Stored at room temperature after autoclaving. 5mg/ml lysozyme added just prior to use
- Solution II: 0.2N NaOH, 1% (w/v) SDS. Made fresh.
- Solution III: to 60ml 5M potassium acetate add 11.5ml glacial acetic acid and 28.5ml sterile, distilled water. The resulting solution is 3M with respect to potassium and 5M with respect to acetate. Stored at 4°C.

Method

To prepare large amounts of plasmid DNA 200-500ml of LB containing the appropriate antibiotic was inoculated with the bacteria harbouring the plasmid of interest. After overnight growth at 37°C with vigorous shaking, cells were pelleted by centrifugation at 6000rpm for 10 minutes. The supernatant was discarded and the bacterial pellet resuspended in 10ml of solution I and left at room temperature for 5 minutes. 20ml of solution II was added and mixed by inversion several times. The tube was placed on ice for 10 minutes to allow complete lysis of the bacteria. 15ml of ice cold solution III was added and mixed by inversion. A white precipitate formed consisting of cell debris and genomic DNA. The solution was centrifuged for 20 minutes at 9500rpm to pellet the precipitate following which the cleared lysate was removed. 0.6 volumes of

isopropanol was added to the cleared lysate and left to stand at room temperature for 15 minutes before centrifugation at 9500rpm for 20 minutes to pellet the plasmid DNA precipitate. Supernatant was removed and the plasmid pellet was washed with 70% ethanol. The dried pellet was then resuspended in 200 μ l of sterile distilled water.

2.5.3 Plant DNA extraction using the Phytopure kit

The Phytopure kit was from Nucleon Biosciences and was used to prepare plant genomic DNA for Southern blotting analysis and PCR amplification.

1 gram (wet weight) of plant tissue was ground to a fine powder in liquid nitrogen using a mortar and pestle and transferred to a 50ml polypropylene tube. 4.6ml of reagent 1 was added and mixed by inversion. DNase-free RNase was added to a concentration of 400 μ g/ml to digest cellular RNA. The mixture was placed in a shaking water bath at 65°C for 10 minutes then placed on ice for 20 minutes. 2ml of ice cold chloroform was added and mixed by inversion. 200 μ l of Nucleon Phytopure DNA extraction resin suspension was added which binds polysaccharides and other impurities. The mixture was shaken gently for 10 minutes at room temperature. The mixture was centrifuged at 1300xg for 10 minutes and the DNA containing upper phase was removed. To this one volume of cold isopropanol was added and mixed by inversion. The solution was centrifuged for 5 minutes at 4000xg to pellet the DNA. The DNA pellet was washed with 70% ethanol and centrifuged for 5 minutes at 4000xg. The ethanol was removed and the pellet allowed to air dry. The DNA pellet was resuspended in 200 μ l of sterile, distilled water and stored in 20 μ l aliquots at -80°C.

2.5.4 A quick DNA extraction method for PCR

Solutions

- Extraction buffer: 200mM Tris-HCl pH 7.5, 250mM NaCl, 25mM EDTA, 0.5% (w/v) SDS.

Method

A small leaf or leaf disk was placed in an Eppendorf along with a small amount of quartz sand and 400 μ l of extraction buffer. The tissue was macerated with a hand held grinder for approximately 15 seconds and then vortexed vigorously. The sample was centrifuged at 13400xg for 5 minutes to pellet cell debris. The cleared supernatant was removed to a new Eppendorf and DNA precipitated with an equal volume of isopropanol. Following centrifugation at 13400xg for 5 minutes the DNA pellet was washed with 70% ethanol. After centrifugation the DNA pellet was allowed to dry and then resuspended in 50 μ l sterile distilled water. 2.5 μ l of this DNA prep was used in subsequent 50 μ l PCR reactions.

2.5.5 RNA extractions using Guanidine hydrochloride

After Logemann *et al.* (1987)

Solutions

- Extraction buffer: 8M Guanidine hydrochloride, 20mM EDTA, 20mM MES, 50mM β -Mercaptoethanol.
- Sterile, distilled water treated with 0.05% (v/v) DEPC (diethylpyrocarbonate). Briefly, DEPC was added and stirred overnight before autoclaving for 25 minutes to remove traces of DEPC.
- 3M Sodium acetate pH5.2 (DEPC treated).
- 1M acetic acid.

Method

This method was used to isolate RNA from medium to large amounts of tissue and also tissue high in polysaccharides, especially siliques. Prior to RNA extraction, plant tissue was quick frozen in liquid nitrogen and then stored at -80°C . 0.5-10g of tissue was ground in liquid nitrogen using a mortar and pestle. More liquid nitrogen was added and 2 volumes of extraction buffer was added and ground in with the sample. The powder was transferred to a 50ml tube and allowed to thaw on ice. The sample was further disrupted by homogenisation with a polytron homogeniser. Cell debris was pelleted by centrifugation at 9500rpm for 10 minutes at 4°C and the resulting supernatant was filtered through Miracloth (Calbiochem, La Jolla, California, USA). An equal volume of 25:24:1 phenol:chloroform:isoamyl-alcohol was added and the mixture firmly mixed by inversion several times, then incubated on ice for 5 minutes. Following centrifugation at 9500rpm for 30 minutes at 4°C the RNA containing upper phase was removed to a new tube. 0.2 volumes of ice cold 1M acetic acid was added and mixed by inversion followed by the addition of 0.7 volumes of ice cold absolute ethanol. The RNA was allowed to precipitate overnight at -20°C before pelleting by centrifugation at 9500rpm at 4°C . The RNA pellet was washed twice with 10ml 3M sodium acetate pH5.2 by centrifugation at 9500rpm for 10 minutes at room temperature to remove contaminating polysaccharides. Finally the RNA pellet was washed with 70% ethanol and after drying, resuspended in 100 μl of DEPC treated water.

2.5.6 RNA extraction using the Qiagen RNeasy kit

The RNeasy kit from Qiagen was used to prepare total RNA from small amounts of tissue (50-100mg). Tissue was frozen in liquid nitrogen prior to RNA extraction. The sample was ground under liquid nitrogen to a fine powder in a mortar and pestle and transferred to an Eppendorf containing 450 μl of

buffer RLT (10 μ l of β -mercaptoethanol added per 1ml of buffer RLT) and vortexed vigorously. The sample was transferred to the QIAshredder spin column sitting in a 2ml collection tube and centrifuged for 2 minutes at 13400xg. The flow-through was removed to a new Eppendorf and 0.5 volumes of ethanol was added and mixed by pipetting. The sample was transferred to an RNeasy mini spin column sitting in a 2ml collection tube and centrifuged for 15 seconds at 13400xg. The flow-through was discarded and 700 μ l of buffer RW1 was added to the column and the tube centrifuged for 15 seconds at 13400xg. The flow-through was discarded and the column placed in a new 2ml collection tube. Two washes were performed with 500 μ l buffer RPE by centrifugation at 13400xg for 15 seconds and then 2 minutes. The column was transferred to an Eppendorf and 50 μ l of RNase-free water was applied to the column followed by centrifugation at 13400xg for 1 minute to elute the RNA. This step was repeated once more.

2.5.7 Purification of DNA from agarose gels using the GeneClean II kit

The GeneClean II kit was used to purify DNA fragments from agarose (Helena BioSciences, Sunderland, UK) gels following restriction enzyme digestion or PCR. DNA fragments were separated on 0.7-1.5% agarose gels in TAE. The gel slice containing the fragment of interest was cut from the gel and placed in 3 volumes (w/v) of NaI stock solution in an Eppendorf and incubated at 50-55°C for 5 minutes or until the gel slice had dissolved. 5-10 μ l of glassmilk suspension was added and mixed by gentle inversion. The tube was incubated on ice for 5-10 minutes with mixing every 1-2 minutes to allow binding of DNA. Following centrifugation at 13400xg for 10 seconds the supernatant was removed and the glassmilk pellet was washed 3 times by resuspending in 200 μ l of NEW wash and centrifugation at 13400xg for 10 seconds. After the final wash the supernatant was removed and the pellet was resuspended in 5-10 μ l sterile water and heated at 50-55°C for 2 minutes. The tube was then centrifuged for 30 seconds and the DNA containing supernatant was removed to a new tube. The elution step was then repeated.

2.5.8 Purification of DNA using the *High Pure* PCR Product Purification kit

The *High Pure* PCR Product Purification kit was obtained from Boehringer Mannheim and was used to purify DNA and cDNA from PCR reactions, restriction enzymes and reverse transcriptase. It was also used to remove

oligonucleotide primers (less than 100bp) from DNA. The DNA containing solution was mixed with binding buffer (100µl buffer per 20µl DNA solution) and pipetted into a *High Pure* filter tube in a 2ml collection tube and centrifuged at 13400xg for 30 seconds. The flow-through was discarded and 500µl wash buffer added to the filter tube followed by centrifugation at 13400xg for 30 seconds. The wash step was repeated but with 200µl of wash buffer. The filter tube was placed in an Eppendorf and 50µl of elution buffer (or 10mM Tris-HCl pH 8-8.3 for certain applications) added. DNA was eluted by centrifugation at 13400xg for 30 seconds.

2.5.9 Purification of mRNA from total RNA

The polyadenylated (poly(A)⁺) fraction of RNA was purified from plant total RNA using the PolyAtract® system from Promega. Up to 1mg of total RNA was made up to a volume of 500µl in sterile, DEPC treated water in an Eppendorf and heated at 65°C for 10 minutes to disrupt RNA secondary structure. To the RNA 3µl of biotinylated-Oligo (dT) probe and 13µl of 20x SSC was added and mixed before allowing the tube to slowly cool to room temperature (approximately 10 minutes) during which time annealing of the biotinylated-Oligo (dT) probe to the poly(A) tail of mRNA occurred. Streptavidin-Paramagnetic particles (SA-PMP) in an Eppendorf were washed 3 times with 300µl of 0.5x SSC and captured using a magnetic stand. After the final wash the SA-PMP were resuspended in 100µl of 0.5x SSC. The annealing reaction mix was then added to the washed SA-PMP and incubated for 10 minutes at room temperature allowing streptavidin binding to the biotin. The SA-PMP were captured using the magnetic stand and the supernatant removed. The SA-PMP were then washed 4 times with 300µl of 0.1x SSC by resuspension and then capture of the SA-PMP. After the final wash all the supernatant was removed and the SA-PMP were resuspended in 100µl of sterile, DEPC treated water. The SA-PMP were captured using the magnetic strand and the mRNA containing supernatant was removed to another tube. The elution step was repeated with 150µl of sterile, DEPC treated water. To concentrate the mRNA, 1/10 volume of 3M sodium acetate pH 5.2 and 1µl of 10mg/ml glycogen (Boehringer Mannheim) was added and mixed followed by 2.5 volumes of ethanol. After overnight storage at -20°C the precipitate was pelleted by centrifugation at 18000xg for 20 minutes at 4°C. After washing with 70% ethanol the pellet was dried and resuspended in 10-20µl sterile, DEPC treated water.

2.6 Electrophoresis

2.6.1 DNA agarose gel electrophoresis

After Sambrook *et al.* (1989).

Solutions

- 1x TAE buffer: 40mM Tris-acetate pH 8.0, 1mM EDTA
- 10x loading buffer: 0.25% (w/v) bromophenol blue, 0.25% (w/v) xylene cyanol FF, 0.25% acridine orange (w/v), 25% Ficoll (type 400) in water.
- DNA markers: 100bp ladder (Promega) or Hyperladder I and Hyperladder IV (Bioline) were used according to the manufacturers instructions.

Method

Gels of 0.7% to 2% (w/v) agarose were prepared in 1x TAE buffer depending on the size of the DNA fragments to be separated. Gels were melted in a microwave, allowed to cool to approximately 50°C before 0.1µg/ml of ethidium bromide was added and mixed. The molten agarose was immediately poured into a gel tray and allowed to solidify at room temperature for 20-40 minutes. DNA samples were mixed with 1/10 volume of 10x loading buffer and loaded into gel wells by pipetting. DNA markers were run alongside sample DNA to enable approximate sizing of fragments. Electrophoresis was performed at 5-10V/cm in 1x TAE buffer. DNA was visualised on a UV transilluminator (Gel Doc 1000 system with Molecular Analyst version 2.1.1 software, Biorad) and photographed. If a Southern blot was to be performed a ruler was placed alongside the gel to enable DNA fragment sizes following hybridisation.

2.6.2 RNA formaldehyde gel electrophoresis

Method based on those by Sambrook *et al.* (1989) and Farrel (1993).

Solutions

- 10x MOPS buffer: 0.2M MOPS pH 7.0, 50mM sodium acetate pH 7.0, 1mM EDTA pH 8.0, prepared with DEPC treated water.
- FSB (Formamide sample buffer): prepared by mixing 100µl 10x MOPS buffer, 100µl DEPC treated water, 100µl of 100% formamide, 120µl of 37% formaldehyde.
- 10x loading buffer: purchased from Promega.
- RNA markers : purchased from Promega.

Method

Gels of 1% were prepared by melting an appropriate amount of agarose in DEPC treated water. After cooling to approximately 70°C, 10x MOPS buffer

was added to give a final concentration of 1x, and formaldehyde (37%) added to give a final 3% concentration. The molten gel was immediately poured into a gel tray and left to solidify for 1-2 hours at room temperature. The gel was electrophoresed in 1x MOPS for 1 hour at 3-6V/cm prior to loading of samples. RNA samples (up to 50µg) in a maximum volume of 25µl water were mixed with an equal volume of FSB, incubated for 10 minutes at 65°C and placed immediately on ice. After the addition of 1/10 volume of loading buffer samples were loaded on to the gel and electrophoresed as stated. For northern analysis samples were run alongside RNA markers (5µg). Gels were photographed after staining alongside a transparent ruler before blotting.

2.6.3 Staining of RNA formaldehyde gels

Ausubel *et al.* (1995).

Solutions

- 0.5M Ammonium acetate

Method

After electrophoresis the RNA gel was placed in a container and submerged in enough 0.5M ammonium acetate to cover it. The gel was shaken gently for 20 minutes and the solution then replaced with fresh solution for a further 20 minutes. The solution was then replaced with fresh 0.5M ammonium acetate containing 0.5µg/ml ethidium bromide and shaken gently for 40 minutes to stain RNA. The gel was then de-stained in fresh 0.5M ammonium acetate for 20 minutes to 2 hours and photographed.

2.6.4 DNA sequencing gels

Solutions

- 10x TBE buffer: 108g Tris base, 5.8g EDTA, 55g Boric acid, sterile, distilled water to 1 litre.
- 40% (19:1) Acrylamide:Bis-acrylamide solution (Sigma)

Method

A Bio-RAD sequencing gel kit with glass plates of 20cm x 50cm was used according to the manufacturer's instructions. The top plate was siliconised with Repellcote (BDH, Poole, UK). 80ml of a 6% (w/v) gel solution was prepared by mixing 12ml 40% (19:1) Acrylamide:Bisacrylamide solution, 8ml 10x TBE buffer, 33.6g of ultra-pure urea and 32ml sterile, distilled water and then filtered through 2 sheets of Whatman filter paper no.1. 10ml of this solution was mixed with 40µl TEMED and 40µl ammonium persulphate (250mg/ml) and immediately used to seal the base. The remaining 70 ml was mixed with 30µl TEMED and 480µl ammonium persulphate (250mg/ml) and immediately

poured between the glass plates using a 60ml syringe. A 'shark tooth' comb was inserted (flat surface in contact with the gel) and the gel allowed to polymerise at room temperature. The gel was pre-run in 1x TBE buffer at 55W until a gel temperature of 50°C was achieved. The 'shark tooth' comb was then inverted such that the teeth just penetrated the surface of the gel. Electrophoresis was re-started until a temperature of 50°C was again achieved. The wells were rinsed of urea and the samples loaded following heating to 70-75°C for 2-3 minutes. Electrophoresis was continued at 55W to maintain a constant gel temperature.

Following electrophoresis, the plates were dismantled and the gel fixed in 5% (v/v) methanol : 5% (v/v) acetic acid for 20 minutes before transfer to Whatman 3MM paper. This was covered in Saran wrap and the gel dried down onto the paper using a Bio-Rad gel slab vacuum drier (model 483). Autoradiography was carried out for 1-7 days.

2.6.5 Mini denaturing polyacrylamide gels

For RNase protection assays samples were electrophoresed in denaturing polyacrylamide gels. However, instead of a sequencing gel apparatus, the Mini-PROTEAN® II Electrophoresis Cell (Bio-Rad) was used, as per manufacturer's instructions, with glass plates of 10cm x 8cm. To 10ml of gel solution was added 15µl TEMED and 100µl ammonium persulphate (250mg/ml). The solution was immediately pipetted between the glass plates and a comb inserted. Once the gel had polymerized the comb was removed and the gel clamp assembly was fitted into the inner cooling core and placed in the buffer chamber. 1x TBE buffer was poured into the upper and lower buffer chambers and the gel was pre-run at 150V. Samples were heated to 90°C and loaded onto the gel following rinsing of urea from the wells. Electrophoresis was continued at 150V following which the gel plates were separated and the gel transferred to Whatman 3MM paper. The gel was wrapped in Saran wrap and autoradiography was carried out for 1-7 days without drying the gel.

2.7 Nucleic acid hybridisation

Southern and northern analyses were carried out using Zeta-Probe GT membranes (Bio-Rad) according to the manufacturer's instructions.

2.7.1 Southern blotting

This technique involves the transfer of DNA fragments from agarose gels to a nylon membrane following which the membrane is incubated with a probe of known DNA sequence in order to detect homologous sequences. After electrophoresis gels were treated with 2-3 volumes of depurinating solution

(0.25M Hcl) for 15 minutes. The gel was then transferred to 2-3 volumes of denaturing solution (0.5N NaOH, 1.5M NaCl) and incubated with gentle shaking for 30 minutes. The gel was then incubated in 2-3 volumes of neutralising solution (3M NaCl, 0.5M Tris-Hcl, pH7.4) for 30 minutes. The gel was rinsed briefly in sterile water and DNA was blotted in a tray containing 0.4M NaOH. A glass plate was placed on a platform in the tray and covered with 3 pieces of Whatman 3MM paper so that they overhung the glass plate and rested in the 0.4M NaOH thus forming a wick through which the 0.4M NaOH could move. The gel was placed on the paper and a piece of pre-wetted (in sterile water) Zeta-Probe GT membrane placed on the gel avoiding trapping air bubbles. Clingfilm was placed around the edges of the gel so that liquid movement could only occur through the membrane. 4 pieces of Whatman 3MM paper were placed on top of the membrane followed by 2 layers of absorbant nappy inners on top of which was placed a tray and a small weight (250-400 grams). The DNA was allowed to transfer to the membrane by capillary action overnight. The blotting apparatus was then dismantled and the membrane rinsed briefly in 2x SSC (1x SSC: 150mM NaCl, 15mM trisodium citrate) and vacuum dried at 80°C for 35 minutes to fix the DNA to the membrane.

2.7.2 Northern blotting

This technique involves the transfer of RNA to a nylon membrane in order to detect a transcribed sequence using a known fragment of DNA as a probe. Following electrophoresis, RNA formaldehyde gels were gently shaken in sterile water for 2x 20 minutes to remove traces of formaldehyde which can interfere with transfer. A blotting apparatus the same as described in section 2.7.1 was used except instead of 0.4M NaOH, the blotting solution was 10x SSC. Therefore, the gel was placed on the paper and a piece of pre-wetted (in sterile water) Zeta-Probe GT membrane placed on the gel avoiding trapping air bubbles. Clingfilm was placed around the edges of the gel so that liquid movement could only occur through the membrane. 4 pieces of Whatman 3MM paper were placed on top of the membrane followed by 2 layers of absorbant nappy inners on top of which was placed a tray and a small weight (250-400 grams). The RNA was allowed to transfer to the membrane by capillary action overnight. The blotting apparatus was then dismantled and the membrane rinsed briefly in 2x SSC and vacuum dried at 80°C for 35 minutes to fix the RNA to the membrane.

2.7.3 Colony hybridisation

Solutions

- Denaturing solution: 0.5M NaOH, 1.5M NaCl.
- Neutralisation solution: 0.5M Tris-HCl pH8.0, 1.5M NaCl.
- 2x SSC:

Method

Following ligation of DNA fragments into a plasmid vector and transformation into bacteria, the bacterial plates were incubated at 4°C for 2 hours. Zeta-Probe GT membrane was cut into discs and gently lowered onto the bacterial plate. The membrane was quickly orientated by making asymmetric pin marks through the membrane and then peeled from the plate. The membrane was then placed bacterial surface up on a sheet of Whatman paper soaked in denaturing solution for 3 minutes. The membrane was then quickly transferred to a sheet of Whatman paper soaked in neutralisation solution for 3 minutes after which it was briefly washed in 2x SSC. Nucleic acid was fixed to the membrane by vacuum drying at 80°C for 35 minutes prior to hybridisation.

2.7.4 Radio-labelling of probes with [³²P]α-dCTP

In the case of Southern and northern blotting and for plaque or colony hybridisations, double-stranded DNA probes were used. Plasmid DNA containing the DNA probe template of interest was digested with the appropriate restriction enzyme and the resulting fragments were separated on an agarose gel. The DNA fragment of interest was purified from the gel using the GeneClean II kit.

DNA fragments were radioactively labelled using the Prime®-It II random primer kit (Stratagene Ltd.). In an Eppendorf tube 25 - 50ng of DNA template was mixed with 10μl of random oligonucleotide primers and made up to a volume of 34μl with sterile, distilled water. The mixture was denatured at 100°C for 5 minutes, centrifuged briefly and allowed to cool to room temperature. To this was added 10μl of 5x buffer (dCTP labelling buffer), 5μl of [³²P]α-dCTP and 1μl Exo(-) Klenow (5U/μl) following which the mixture was incubated at 37°C for 30 minutes. The reaction was stopped by adding 2μl stop mix. The radio-labelled probe was separated from unincorporated [³²P]α-dCTP using a NucTrap probe purification column (Stratagene Ltd.). Firstly the column was pre-wet with 70μl of 1x STE buffer (100mM NaCl, 20mM Tris-HCl pH7.5, 10mM EDTA). The liquid was pipetted onto the column and a 10ml luer-lock syringe was attached and the plunger slowly depressed forcing the liquid through the column. The labelling reaction was then applied to the column and

forced into the column using the syringe. A further 70µl of 1x STE buffer was applied to the column and the radio-labelled probe was eluted from the column into an Eppendorf using the syringe.

The probe was boiled for 5 minutes, snap cooled on ice and then added to the hybridisation mixture.

2.7.5 End-labelling with [³²P]γ-ATP

DNA markers for RNase protection assays and oligonucleotides for primer extension were end-labelled with [³²P]γ-ATP. To 10pmol oligonucleotide was added 0.5µl [³²P]γ-ATP, 1µl polynucleotide kinase (PNK) 10x buffer (supplied with enzyme, Promega Ltd.), 1µl (10units) PNK and water to 10µl. The reaction was incubated at 37°C for 30 minutes before inactivation of the PNK by heating at 90°C for 3 minutes. Labelled oligonucleotide was separated from unincorporated label using a NucTrap probe purification column (Stratagene Ltd.) as described in section 2.6.4.

Labelling of the 100bp ladder and φX174 DNA/Hinf I dephosphorylated markers (Promega Ltd.) was as follows: 5µl of the DNA markers was mixed with 1µl PNK 10x buffer, 1µl [³²P]γ-ATP (diluted to 10µCi/µl), 1µl (10 units) PNK and 2µl of water. The reaction was incubated at 37°C for 30 minutes following which PNK was inactivated by the addition of 1µl 0.5M EDTA. The reaction mix was then diluted to 40µl with gel loading buffer II (Ambion) and 2-5µl of this was then heated to 90°C for 3 minutes before loading onto a denaturing polyacrylamide gel. Markers could be visualised following overnight exposure of the gel to X-ray film.

2.7.6 Pre-hybridisation and hybridisation

Solutions

- 50x Denhardts solution: 5g Ficoll (type 400), 5g polyvinylpyrrolidone, 10g Bovine serum albumin, water to 500ml, filter sterilise.
- 20x SSPE: 3.6M NaCl, 0.2M Na₂HPO₄·7H₂O, 0.02M EDTA.
- Pre-hybridisation solution: 50% formamide (v/v), 5x Denhardts solution, 0.1% SDS (w/v), 5x SSPE, 2.5mg polyadenylic acid, 2.5mg sonicated herring sperm DNA, sterile water to 25ml.
- Hybridisation solution: 50% formamide (v/v), 2x Denhardts solution, 0.1% SDS (w/v), 5x SSPE, 1mg polyadenylic acid, 2mg sonicated herring sperm DNA, sterile water to 10ml.

Method

The pre-hybridisation step is designed to block sites on the membrane to which the probe may bind non-specifically. Membranes were placed in hybridisation bottles (Techne) with the bound nucleic acid facing the solution. 25ml of pre-hybridisation solution was added minus the herring sperm DNA which was boiled for 10 minutes, snap cooled on ice and then added once the solution had reached the desired temperature. The bottle was placed inside a Techne hybridisation oven (model HB-1D) at 42°C and after the addition of herring sperm DNA was allowed to pre-hybridise with rotation for 4 hours to overnight. Afterwards pre-hybridisation solution was replaced with hybridisation solution with the herring sperm DNA being added last. Radiolabelled probe was then added to the hybridisation mix and left between 24-48 hours.

2.7.7 Washing conditions

Solutions

- Wash solution 1: 2x SSC, 0.1% SDS.
- Wash solution 2: 1x SSC, 0.1% SDS.
- Wash solutions 3 & 4: 0.1x SSC, 0.1% SDS.

Method

After hybridisation, the solution was drained off and the membrane washed twice for 10 minutes at room temperature with 50ml wash 1. This was followed by two washes with wash 2 for 10 minutes at room temperature with 50ml per wash. Wash 3 was performed as before except at a temperature of 42°C. Finally wash 4 was performed as previous washes except at a temperature of 65°C. The stringency of wash 3 was 76% whilst wash 4 was to 100% stringency. Following the final wash, the membrane was removed and blotted dry before being wrapped in Saran wrap and exposed.

2.7.8 Ribonuclease protection assays

This technique involves the synthesis of a radiolabelled antisense RNA probe complementary to a region of the RNA message you wish to detect. The RNA probe is hybridised to a RNA mixture containing the message of interest before being treated with ribonucleases which degrade all the non-hybridised single stranded RNA. The message of interest forms a duplex with the antisense RNA probe and is protected in the complementary region from ribonuclease attack. The results are then analysed by denaturing polyacrylamide gel electrophoresis and autoradiography.

Method

To perform ribonuclease protection assays the RPA III™ kit from Ambion was used. 50µg of total RNA or 5µg poly(A)⁺ RNA was mixed with 4 x 10⁵ cpm of

labelled RNA probe in an Eppendorf. To the RNA was added 1/10 volume of 5M ammonium acetate and after mixing 2.5 volumes of absolute ethanol were added and mixed. Samples were stored at -20°C for 1 hour and then RNA pelleted by centrifugation at 14000 rpm at 4°C for 30 minutes. The supernatant was discarded and the RNA pellet was allowed to air dry for 5 minutes. RNA pellets were then resuspended in 10µl of hybridisation buffer by vigorous pipetting and vortexing. The samples were then heated to 95°C for 4 minutes to disrupt RNA secondary structure before being moved to 45°C for overnight hybridisation. The next day, the RNase Digestion III buffer was thawed and mixed well before removal of 150µl x the number of samples. To this was added a 1:100 dilution of the RNase A/ RNase T1 enzyme mix. The sample tubes were then removed from the incubator and centrifuged briefly. 150µl of the RNase digestion buffer with RNase was added to each sample, mixed and then transferred to 37°C to allow complete digestion of unhybridised RNA. Following this incubation, 225µl of the RNase inactivation/precipitation buffer was added to each sample and mixed. Samples were then incubated at -20°C for 2 hours before the reaction products were pelleted by centrifugation at 14000rpm for 30minutes at 4°C. The supernatant was removed and pellets allowed to air dry for 5 minutes before resuspension in 10µl of gel loading buffer II. The samples were then heated at 95°C for 3 minutes before being loaded onto a mini denaturing polyacrylamide gel and run alongside [³²P]γ-ATP end-labelled φX174 DNA/Hinf I markers (Promega Ltd.). After electrophoresis the gel was transferred to Whatman paper and exposed to X-ray film for periods of 1-7 days without drying.

2.7.9 Radiolabelling of RNA probes

To produce RNA probes for RNase protection assays the MAXIscript™ T7/T3 In Vitro Transcription kit was used. Templates for the transcription reaction were prepared by cloning of a suitable DNA fragment into the pCR2.1 TOPO vector (Invitrogen) which contains a promoter for the phage T7 RNA polymerase. The DNA fragment was orientated such that it would produce an antisense transcript when transcription occurred from the T7 promoter. The vector was linearized at a position 3 prime to the insert and T7 promoter with a suitable restriction enzyme so that run-off transcripts of a defined length were produced. Following digestion, one half volume of Proteinase K (100µg/ml in 2mM CaCl₂, 10mM Tris-HCl pH 8.0) was added to the reaction and incubated at 50°C for 30 minutes. The sample was extracted once with phenol/chloroform and to the upper aqueous was added 1/10 volume 5M ammonium acetate and 2 volumes of ethanol. The sample was left to precipitate at -20°C for 1 hour and

the DNA was pelleted by centrifugation at 13400xg for 10 minutes. The supernatant was removed and the pellet air dried following which it was resuspended in 10-20µl RNase-free water. The transcription reaction was performed as follows. To 1µg of template DNA in an Eppendorf was added 2µl 10x transcription buffer, 1µl each of 10mM ATP, CTP, and GTP followed by 50µCi [³²P]α-UTP. The reaction was mixed and then 2µl of T7 RNA polymerase + ribonuclease inhibitor was added and mixed. The transcription reaction was allowed to proceed for 1 hour at 37°C before 1µl of RNase-free DNase (2u/µl) was added to remove the DNA template. Samples were left at 37°C for 15 minutes before the addition of an equal volume of gel loading buffer II. The sample was heated at 95°C for 4 minutes before being loaded onto a mini denaturing polyacrylamide gel. Following electrophoresis the front glass plate of the gel assembly was removed and the gel was exposed to X-ray film for 15 seconds. Following developing of the X-ray film the gel was aligned with the film and the position of the radiolabelled transcript in the gel was determined. This band of gel was cut out and macerated in 350µl of Probe elution buffer (RPA III™ kit, Ambion) and incubated with occasional vortexing at 37°C for 4-6 hours during which time the probe diffused from the gel slice. After this time 5µl of the solution was pipetted into 4ml scintillation fluid in a scintillation vial and the counts per minute (cpm) determined by a liquid scintillation analyzer (model 1600 TR, Packard, Berks, UK).

2.7.10 Primer extension

After Praekelt, and Meacock (1990)

This technique is designed to determine the exact base at which transcription of a particular message starts. To 100µg of total RNA in 10µl was added 1.5pmol (10ng) of end-labelled oligonucleotide. 4µl of 5x AMV reverse transcriptase buffer (supplied with enzyme, Promega Ltd.) and 1µl (40 units) RNasin was added and the volume made up to 20µl. The mix was heated at 65°C for 3 minutes to denature RNA secondary structure and then transferred to 42°C for 1 hour to allow primer annealing. Primer extension was carried out by adding 16µl dNTP mix (12.5mM each), 6µl 5x AMV RT buffer, 2µl (20 units) AMV reverse transcriptase (Promega Ltd.) and 6µl water and incubating at 42°C for 2 hours. The reaction was stopped by the addition of 1µl 10% (w/v) SDS and 5µl 0.5M EDTA. RNA was hydrolysed by adding 20µl 1M NaOH and boiling for 5 minutes. The solution was neutralised by the addition of 20µl 1M HCl and 1µl of glycogen (10mg/ml, Boehringer Mannheim) was added to aid recovery of cDNA. cDNA was precipitated by the addition of 300µl of ethanol and centrifugation at 13400xg for 15 minutes. The pellet was resuspended in 5µl gel

loading buffer II (Ambion) and loaded onto a DNA sequencing gel alongside a sequencing reaction. Electrophoresis, gel drying and autoradiography was performed as described in sections 2.5.4 and 2.6.11.

2.7.11 Autoradiography

Autoradiography was carried out using X-ray film (Amersham Hyperfilm-MP) in a cassette fitted with an intensifying screen. Cassettes were left at -70°C for periods ranging from overnight to 4 weeks depending on the abundance of the target nucleic acid in the sample. X-ray film was developed using a Compact X4 automatic developer (X-ograph imaging systems, Malmesbury, UK).

2.7.12 Probe stripping

If a membrane was to be reprobed it first had to be stripped. The membrane was not allowed to dry between hybridisations, and was stripped as soon as possible after autoradiography. The membrane was washed twice in a large volume of 0.1x SSC/ 0.5% SDS (w/v) for 20 minutes at 95°C. The membrane was checked by exposure overnight to ensure probe had been successfully stripped prior to pre-hybridisation.

2.8 cDNA library screening

2.8.1 Plating lambda phage libraries to generate plaques

After Ausubel *et al.* (1995).

Solutions:

- Lambda broth.
- Lambda plates.
- Lambda top agar.
- SM buffer (λ suspension media): 5.8g/l NaCl, 2g/l $\text{MgSO}_4 \cdot 7\text{H}_2\text{O}$, 50mM Tris-HCl (pH 7.5), 0.1g/l gelatin.

Method

The *E.coli* host strain (Y1090 for lambda Ziplox and C600Hfl for lambda gt10) was grown overnight in 5ml lambda broth at 37°C with vigorous shaking. For cDNA library screening lambda plates were prepared in 22.5cm x 22.5cm square Petri dishes. For each plate, 100 μ l of phage stock (up to 500,000 pfu diluted if necessary in SM buffer) was mixed with 3.6ml of *E.coli* culture and incubated at room temperature for 20 minutes followed by 10 minutes at 37°C. To this was added 40ml of molten lambda top agar supplemented with 10mM MgSO_4 at 50°C. This was mixed then poured quickly onto the lambda plate and

spread by tilting of the Petri dish. Following incubation overnight at 37°C plaques were visible as clear areas in the bacterial lawn.

2.8.2 Plaque lifts for hybridisation with DNA probes

Method based on that of Sambrook *et al.* (1989).

Solutions

- Denaturing solution: 0.5M NaOH, 1.5M NaCl.
- Neutralisation solution: 0.5M Tris-HCl pH8.0, 1.5M NaCl.

Method

After the generation of lambda plaques plates were incubated at 4°C for 2 hours to harden the top agar. A sheet of Zeta-Probe® GT membrane was cut to size (approximately 20cm x 20cm) and was placed on the surface of the plate for 2 minutes. The orientation of the membrane on the plate was marked by piercing through the corners of the membrane and marking the position of the needle holes on the back of the plate. The membrane was then carefully removed from the plate and a duplicate lift performed as detailed except that the membrane was left in place for 4 minutes. The membrane was then placed, phage side up, on a sheet of Whatman 3MM paper soaked in denaturing solution for 5 minutes following which it was transferred to a new sheet of Whatman 3MM paper soaked in neutralisation solution for 5 minutes. The membrane was allowed to air dry before being baked at 80°C for 30 minutes. Hybridisation with double-stranded DNA probe was performed as described in section 2.7.6.

2.8.3 Removal and storage of positive plaques

Following autoradiography, the position of the membrane was marked on the X-ray film and, using the pin marks, the film was then orientated to the plate. Positive plaques were removed from the plate by using the wide end of a Gilson pipette tip. The plug was then placed in an Eppendorf containing 1ml of SM buffer and stored at 4°C.

2.9 DNA cloning into plasmid vectors

2.9.1 Digestion of vector and insert DNA with restriction endonucleases

Restriction enzymes and 10x reaction buffers were obtained from Promega Ltd. Reactions were carried out according to the manufacturers instructions. Typically, a digestion reaction contained 1-5µg of DNA, 3µl of 10x reaction buffer, 1µl restriction enzyme (10units/µl) and made up to 30µl with sterile, distilled water.

Reactions were left at the required temperature for a period of 1 - 4 hours. Following digestion reactions vector DNA was dephosphorylated prior to ligation. Insert DNA was either purified by using the High Pure PCR clean up kit (Boehringer Mannheim) or was purified from gel slices using the GeneClean II kit.

2.9.2 Dephosphorylation of vector DNA

Following restriction digestion, vector DNA was treated with shrimp alkaline phosphatase (Sigma Chemical Company) to dephosphorylate the 5' ends prior to ligation to prevent re-ligation of vector ends. This was only performed if the vector DNA had been treated with just one restriction enzyme. After digestion, to 1-5µg of vector DNA with the relevant restriction enzyme in a total volume of 30µl was added 1 unit of shrimp alkaline phosphatase. The reaction was incubated at 37°C for 30 minutes followed by 10 minutes at 70°C to inactivate the phosphatase. Linearized vector DNA was purified from agarose gel slices as detailed in section 2.5.7.

2.9.3 T-tailing of vector DNA

After Finney *et al.* (1995)

T-tailing of the vector involves the addition of a thymidine nucleotide to the 3' end of DNA strands following vector linearization. This facilitates the cloning of PCR products since *Taq* DNA polymerase adds a 5' adenosine nucleotide. pBluescript SK(-) (5µg) was cut with the restriction enzyme *Sma*I and purified from an agarose gel slice as detailed in section 2.5.7. The DNA (10µl) was mixed with 10µl Mg⁺⁺ free 10x PCR buffer (supplied with *Taq* DNA polymerase from Bioline), 3µl 50mM MgCl₂, 20µl 5mM dTTP, 1µl *Taq* DNA polymerase (5 units) and made up to 100µl with sterile, distilled water. The reaction was incubated at 75°C for 2 hours and was used in ligation reactions without further purification.

2.9.4 Ligation of DNA fragments

The enzyme T4 DNA ligase catalyses the formation of a covalent phosphodiester bond between a 5'-phosphoryl group and an adjacent 3'-hydroxyl group. In a typical ligation reaction 50-100ng of vector DNA (cut with a suitable restriction enzyme(s) or T-tailed) was mixed with an equal molar amount of insert DNA. To this was added 2µl of 5x ligation buffer (supplied with enzyme from Promega Ltd.) and 1µl (3 units) of T4 DNA ligase and the volume made up to 10µl with sterile, distilled water. The contents were mixed

and incubated at 14°C overnight before transformation of competent *E.coli* cells.

2.9.5 Ligation of PCR fragments into pCR@2.1-TOPO

DNA fragments generated by PCR were generally cloned into the pCR@2.1-TOPO vector from Invitrogen. The vector is supplied linearized with 3' thymidine overhangs for efficient ligation of PCR products. It also utilises the ligation activity of the topoisomerase enzyme resulting in fast, high efficiency ligation. To 1µl of the pCR@2.1-TOPO vector was added 1-2µl of fresh, unpurified PCR product and the reaction made up to 5µl. The reactants were mixed and left at room temperature for 5 minutes to allow ligation to proceed. The tube was then placed on ice until ready for transformation into TOP10 competent cells (Invitrogen).

2.9.6 Transformation of *E.coli* with plasmid DNA by electroporation

After Ausubel *et al.*, (1994)

E. coli XL1-blue MRF' were used for the preparation of electrocompetent cells. A single colony of XL1-blue MRF' from a fresh LB plate was inoculated into 500ml of sterile LB media and was grown overnight at 37°C with vigorous shaking. The culture was poured into two centrifuge bottles (250ml each) and chilled on ice for 10 minutes before cells were pelleted by centrifugation at 6000 rpm for 10 minutes at 4°C. The supernatant was removed and the cells resuspended in 250ml (per bottle) of ice cold sterile, distilled water. The centrifugation step was repeated and the supernatant removed. The cells were resuspended by gentle swirling in the small amount of remaining water before the addition of another 250ml of ice cold sterile, distilled water. Following centrifugation as before, the supernatant was removed and the cells resuspended in 20ml of ice cold filter-sterilised 10% glycerol. Another centrifugation step was performed as before, the supernatant removed and the cells resuspended in an equal volume (approximately 1-2ml) of ice cold filter-sterilised 10% glycerol. 50µl aliquots were pipetted into ice cold Eppendorfs and flash frozen in liquid nitrogen before being stored at -80°C until required. For electroporation, a 50µl cell aliquot was defrosted on ice and pipetted into an ice cold electroporation cuvette (0.2cm electrode gap, Bio-Rad). 2µl of a ligation mix was pipetted into the cells and mixed by gentle swirling. Electroporation was carried out using Gene Pulser and Pulser Controller apparatus from Bio-Rad. The Gene Pulser was set to 2.5kV and 25µFD and the Pulser Controller to 200 ohms.

Immediately after electroporation, 500µl of SOC medium was added and the cells were transferred to an Eppendorf tube. Following incubation at 37°C for 1 hour with gentle shaking, 100-200µl of the cells were spread onto LB plates containing an appropriate antibiotic for selection of recombinants and grown overnight at 37°C. If blue/white colour selection of recombinants was required, 37.5µg/ml X-Gal and 37.5µg/ml IPTG was added to the molten LB agar prior to pouring. Due to disruption of the *lacZ* gene, recombinants would appear white instead of blue for non-recombinants.

2.9.7 Transformation of TOP10 One Shot™ competent cells

TOP10 One Shot™ competent cells were supplied with the TOPO TA Cloning® kit (Invitrogen) along with the ligation ready pCR®2.1-TOPO vector. Following the ligation of PCR products a tube of TOP10 One Shot™ competent cells was defrosted on ice. 2µl 0.5M β-mercaptoethanol was added to the cells and mixed by gentle stirring with a pipette tip. This was followed by the addition of 2µl of the ligation mix which was again mixed by gentle stirring. The tube was incubated on ice for 30 minutes before heat shocking at 42°C for 30 seconds. The tube was returned to ice for 2 minutes following which 250µl of SOC medium was added. The tube was then incubated for 30 minutes (ampicillin selection) to 1 hour (kanamycin selection) at 37°C with gentle shaking. 50-100µl of cells was then spread onto LB plates containing either 100µg/ml ampicillin or 50µg/ml kanamycin sulphate and 37.5µg/ml X-Gal. Recombinants appeared as white colonies following overnight growth at 37°C.

2.10.1 DNA sequencing

DNA sequencing was performed by the DNA sequencing lab at the University of Durham using an ABI 373 DNA sequencer and dye terminator labeling reactions (Perkin Elmer Applied Biosystems). Samples were normally supplied in plasmid form prepared using the Wizard™ minipreps DNA purification system from Promega at a concentration of 0.2µg/µl. Primers for sequencing were supplied at a concentration of 3.2pmoles/µl.

2.10.2 Manual DNA sequencing

Manual DNA sequencing was performed using the fmol® DNA sequencing system (Promega Ltd.) using an end labelled primer. Labelling of primers was performed as described in section 2.7.5 but the purification step using the NucTrap columns was omitted. The template for sequencing was supercoiled plasmid DNA. For the reaction, four 0.5ml microcentrifuge tubes were labelled

A, G, T and C. Into each tube was added 2µl of the appropriate d/ddNTP mix and a drop of mineral oil was used to overlay the reaction. A mastermix was then prepared containing 100ng plasmid template, 5µl fmol® sequencing 5x buffer, 1.5µl labelled primer (1.5pmol) and made up to 16µl with water. 1µl of sequencing grade *Taq* DNA polymerase (5u/µl) was added to the mastermix and 4µl of this mastermix was then pipetted onto the wall of the 4 reaction tubes and mixed with the d/ddNTP mix by brief centrifugation. The tubes were then added to a thermal cycle heating block at 94°C and thermal cycling commenced. A typical profile would be 30 cycles of 94°C for 30 seconds, 60°C for 30 seconds and 72°C for 1 minute. Following cycling 3µl fmol® sequencing stop solution was added to each reaction. The tubes were then heated at 70°C for 2 minutes before loading 2-3µl onto a DNA sequencing gel.

2.11 Polymerase Chain Reaction

2.11.1 Standard PCR

For standard PCR reactions, *Taq* DNA polymerase was obtained from Bioline and was supplied with Mg⁺⁺ free 10x reaction buffer and 50mM MgCl₂ stock solutions. Oligodeoxynucleotide primers were obtained from MWG-Biotech as lyophilised pellets and resuspended to the desired concentration in sterile, distilled water. The template for amplification was either genomic DNA, a cloned fragment of DNA in a plasmid or lambda, cDNA or a bacterial colony. A standard PCR reaction contained 10-100ng of DNA sample, 0.2µM of each primer, 1.5µl 50mM MgCl₂ (1.5mM final concentration), 5µl Mg⁺⁺ free 10x reaction buffer, 1mM dNTP mix and 2.5 units of *Taq* DNA polymerase made up to 50µl with sterile, distilled in a 0.5ml Eppendorf. Reactions were overlayed with 40µl of mineral oil and placed in a DNA Thermal Cycler (Perkin Elmer, Foster City, CA, USA) once the block temperature had reached 90°C. A typical amplification was carried out using the following conditions: 1 cycle of 2 minutes denaturation at 94°C then 30 cycles of 30 seconds denaturation at 94°C, 30 seconds annealing at 55°C and 1 minutes extension at 72°C. A final extension of 7 minutes at 72°C was performed after the amplification steps. 10-20µl of the reaction was run on a 0.7-2% (w/v) agarose gel to check the products. Cloning of PCR fragments was carried out as described in sections 2.8.4 and 2.8.5.

2.11.2 PCR using Expand™ High Fidelity PCR system

The Expand™ High Fidelity PCR system consists of a mix of both *Taq* and *Pwo* DNA polymerases. Due to the 3'-5' exonuclease proofreading activity of *Pwo* DNA polymerase the Expand™ High Fidelity PCR system results in a 3-fold increase in the fidelity of DNA synthesis (8.5×10^{-6} error rate). This system was therefore used when a high degree of sequence fidelity was required, for example, the cloning of DNA fragments for subsequent transformation into plants. The system was supplied with 10x reaction buffer containing 15mM $MgCl_2$. A typical reaction contained 10-100ng of DNA target, 0.2 μ M of each primer, 5 μ l 10x reaction buffer, 1mM dNTP mix and 2.5units enzyme mix made up to 50 μ l with sterile, distilled water in a 0.5ml Eppendorf and overlaid with 40 μ l of mineral oil. The tube was placed in a pre-heated block at 90°C. A typical amplification was carried out using the following conditions: denaturation at 94°C for 2 minutes then 30 cycles of denaturation at 94°C for 30 seconds, primer annealing at 60°C for 30 seconds and extension at 72°C for 2 minutes. This was followed by a final extension at 72°C for 7 minutes. If the expected product was greater than 3kb in length then the extension step was carried out at 68°C instead of 72°C with a general rule of 1minute extension per kilobase of target. 5-10 μ l of product was then analysed on a 0.7-1% (w/v) agarose gel. Cloning of PCR fragments was carried out as described in sections 2.8.4 and 2.8.5.

2.12 Cloning of cDNA ends by RACE

RACE (Rapid Amplification of cDNA Ends) is a useful technique if only a limited amount of sequence data is available for a specific transcript. It allows the isolation of transcript sequence data both upstream and downstream of the known sequence without any initial knowledge of these regions. The method involves the addition of an anchor sequence to either the 5' or 3' end of a cDNA following reverse transcription. A primer to this anchor sequence can then be used in subsequent PCR reactions along with a gene specific primer.

2.12.1 Cloning of cDNA 3' ends (3' RACE)

3' RACE involves identification of transcript sequence downstream of a known region. In this study, 3' RACE was used to clone cDNA's when cDNA library screening failed and also provided information on likely polyadenylation sites.

2.12.2 cDNA synthesis

Oligonucleotide

- Oligo d(T)₁₅ anchor: CCAAGCTTCTGCAGGAGCTCTTTTTTTTTTTTTTTT

Method

Poly(A)⁺ RNA was isolated from total plant RNA (Columbia ecotype) as described in section 2.4.7 and 1µg of this was mixed with 1µl of Oligo d(T)₁₅ anchor primer (10µM stock) in a total volume of 10µl. This primer anneals to the poly(A) tails of mRNA and includes an anchor sequence for subsequent PCR. The sample was heated at 65°C for 10 minutes and rapidly cooled on ice. To this was added in order: 4µl of 5x AMV buffer (supplied with AMV reverse transcriptase, Promega Ltd.), 2µl dNTP mix (12.5mM stock), 1µl RNasin (Promega Ltd.) and 2µl (20 units) AMV reverse transcriptase in a total volume of 20µl. After mixing and brief centrifugation the sample was incubated at 42°C for 45 minutes and 50°C for 25 minutes. The reverse transcriptase was inactivated by heating at 95°C for 3 minutes.

2.12.3 Cloning *POLARIS* and *GENE X* cDNA clones by 3' RACE

Oligonucleotides

- RACE Anchor primer: CCAAGCTTCTGCAGGAGCTC
- 3.0 prom: GGAACACGAAATCCGAAGAGCGAG
- EM1 RT3: GGAAGTTTCCGACAAGAACAG
- RT 35/55:

Method

For PCR amplification a mastermix was assembled as described in section 2.11.1. The template for amplification was 2µl of the first strand cDNA from section 2.12.2. For amplification of the *POLARIS* cDNA, 0.2µM of both the 3.0 prom primer and the RACE Anchor primer were used. The tube was placed in a pre-heated block at 90°C and the following cycle used: 94°C for 2 minutes followed by 35 cycles of 94°C denaturation for 30 seconds, 60°C primer annealing for 30 seconds and 72°C extension for 45 seconds. A final extension at 72°C for 7 minutes was performed. Products were analysed on a 1% (w/v) agarose gel and were blotted to Zeta-Probe® GT membrane and probed with a 560bp *Pst*I-*Eco*RI DNA probe kindly donated by Dr. J. Topping (University of Durham). This fragment was sub-cloned from λEM1, a 20kb genomic DNA fragment isolated from a wild-type *Arabidopsis* genomic library, isolated by Dr. J. Topping using a fragment of T-DNA flanking DNA from line AtEM101 as a probe. The amplification products were then cloned and colony hybridisation

performed using the 560bp *PstI-EcoRI* DNA probe. Colonies that hybridised were grown overnight at 37°C and plasmid DNA isolated and inserts sequenced. For amplification of the *GENE X* cDNA, 0.2µM of both the EM1 RT3 primer and the RACE Anchor primer were used. The tube was placed in a pre-heated block at 90°C and the following cycle used: 94°C for 2 minutes followed by 35 cycles of 94°C denaturation for 30 seconds, 55°C primer annealing for 30 seconds and 72°C extension for 1 minute. A final extension at 72°C for 7 minutes was performed. Products were analysed on a 1% (w/v) agarose gel and cloned as described in sections 2.8.5 and 2.8.7. 50 white bacterial colonies were screened by colony PCR (section 2.11.1) using the primers EM1 RT3 and RT 35/55 which amplify a region of approximately 125bp. One positive colony was then grown overnight at 37°C and plasmid DNA isolated and the insert sequenced.

2.12.4 Cloning of cDNA 5' ends (5' RACE)

5' RACE identifies sequence upstream of a known region. 5' RACE was used to clone the 5' ends of both the GUS-fusion transcript and the *POLARIS* transcript.

2.12.5 cDNA synthesis

Oligonucleotides

- GUS PA: CCAGGTGTTTCGGCGTG GTGTAGAGC
- RACE 2: GGTTCATTCATGTTTCAGTGAG

Method

For initial 5'RACE experiments on the GUS-fusion transcript, poly(A)⁺ RNA was isolated from total plant RNA from the AtEM101 line and 1µg of this was mixed with 1µl of the GUS PA primer (10µM stock) in a total volume of 10µl. cDNA synthesis was then performed as described in section 2.12.2.

For later 5'RACE experiments to determine the transcript initiation site of both the *POLARIS* transcript and the GUS-fusion transcript, cDNA synthesis was carried out as described in section 2.12.6 but with the following alterations. cDNA synthesis was carried out using the RACE 2 primer (10µM stock) with either 5µg of poly(A)⁺ RNA from the Columbia ecotype (for the *POLARIS* transcript) or 20µg total RNA from the AtEM101 line (for the GUS-fusion transcript).

2.12.6 Purification of cDNA

The first strand cDNA was purified away from remaining RNA and primer using the *High Pure* PCR Product Purification kit from Boehringer Mannheim

as described in section 2.5.8. The only modification was that instead of using the elution buffer provided in the kit, 50µl of 10mM Tris-HCl pH8.0-8.3 was used for the elution.

2.12.7 Tailing of cDNA

A homopolymeric A-tail was added to the 3' end (ie. 5' end of transcript) of the synthesised cDNA using the enzyme terminal transferase (Promega Ltd.).

17.5µl of the purified cDNA from section 2.12.6 was pipetted into an Eppendorf. To this was added 5µl of 5x TdT reaction buffer and 2.5µl 2mM dATP. The sample was heated at 94°C for 3 minutes to denature secondary structure and cooled rapidly on ice. Following brief centrifugation to collect the sample, 1µl (10 units) of terminal transferase was added to the tube and mixed. The reaction was incubated on ice for 30 minutes followed by 10 minutes at 37°C. After the reaction the terminal transferase was inactivated by heating at 70°C for 10 minutes. The sample was used in PCR without further purification.

2.12.8 Cloning of the *POLARIS* and GUS-fusion transcripts 5' ends

Oligonucleotides

- GUS PB: GGC GTGACATCGGCTTCAAATGGCG
- P40.N2: TTCACGGGTTGGGGTTTCTACAGG
- EXT-S1: GTGTGCCTCACGTGCTCTTCTC
- POL5'EXT: CTCACTACTACCCAAACTAAAACAC
- Oligo d(T)₁₅ anchor: CCAAGCTTCTGCAGGAGCTCTTTTTTTTTTTTTTTT
- RACE Anchor primer: CCAAGCTTCTGCAGGAGCTC
- POL5'TEST: GGAGACTAAAGCGAACATATAAAACC

Method

For primary PCR, 5µl of the tailing reaction from section 2.12.7 was used in a standard 50µl PCR reaction. For initial analysis of the GUS-fusion transcript, primary PCR was performed using the GUS PB primer (10µM stock) and the Oligo d(T)₁₅ anchor primer (10µM stock). Amplification conditions were as follows: initial denaturation at 94°C for 2 minutes followed by 35 cycles of 94°C for 30 seconds, 60°C for 30 seconds and 72°C for 1 minute. This was followed by a final extension at 72°C for 7 minutes. For later analysis of the GUS-fusion and *POLARIS* transcripts, primary PCR was performed using the EXT-S1 primer (10µM stock) and the Oligo d(T)₁₅ anchor primer (10µM stock). Amplification conditions were as follows: initial denaturation at 94°C for 2 minutes followed by 35 cycles of 94°C for 30 seconds, 55°C for 30 seconds

and 72°C for 1 minute. This was followed by a final extension at 72°C for 7 minutes.

An aliquot of the primary PCR reactions was taken and diluted 1:20. 1µl of this was then used as a template for secondary PCR in a standard 50µl reaction. For initial analysis of the GUS-fusion transcript, secondary PCR was performed using the P40.N2 primer (10µM stock) and the RACE Anchor primer (10µM stock). Amplification conditions were as follows: initial denaturation at 94°C for 2 minutes followed by 35 cycles of 94°C for 30 seconds, 60°C for 30 seconds and 72°C for 1 minute. This was followed by a final extension at 72°C for 7 minutes. Products were analysed on a 1% (w/v) agarose gel and cloned into the pCR2.1 TOPO cloning vector (Invitrogen). Plasmid DNA from 10 white colonies was checked by restriction enzyme digestion and the 3 longest clones (RAC60, RAC70 and RAC90) were sequenced. All 3 clones aligned with T-DNA sequence but only RAC90 extended into the plant flanking DNA by approximately 140bp.

For later analysis of the GUS-fusion and *POLARIS* transcripts, secondary PCR was performed using the POL5'EXT primer (10µM stock) and the RACE Anchor primer (10µM stock). Amplification conditions were as follows: initial denaturation at 94°C for 2 minutes followed by 35 cycles of 94°C for 30 seconds, 55°C for 30 seconds and 72°C for 1 minute. This was followed by a final extension at 72°C for 7 minutes. Products were analysed on a 1% (w/v) agarose gel and cloned into the pCR2.1 TOPO cloning vector (Invitrogen). White colonies were screened by colony PCR using the primers POL5'EXT and POL5'TEST which amplify a 100bp product. Plasmid DNA was isolated from positives and analysed by restriction digests. 8 colonies for the GUS-fusion transcript were sequenced and 3 for the *POLARIS* transcript. All aligned with each other and fell into two distinct categories with one set of sequences being approximately 100bp longer than the other set.

2.13 RNA-Specific PCR (RS-PCR)

RNA-specific PCR is a modification of the 3' RACE method and is particularly useful for analysing the expression of transcripts which lack introns. Such transcripts present a problem since conventional RT-PCR with 2 gene specific primers amplifies an identical sized product from both mRNA and genomic DNA. Any genomic DNA contamination in your RNA sample therefore presents problems. The method uses an RNA-specific anchor primer, unlike in 3' RACE where an oligo(dT) anchor primer is used, to prime cDNA synthesis

of your specific transcript. PCR amplification of this message can then be performed using one gene specific primer and the anchor primer.

2.13.1 DNase treatment of RNA

After Sanyal *et al.* (1997)

Total RNA was isolated from plants (Columbia ecotype). 10µg of total RNA was mixed with 2µl of 5x RT buffer (supplied with AMV reverse transcriptase, Promega Ltd.). To this was added 2units of RQ1-DNase (RNase free, Promega Ltd.) and the volume made up to 10µl. The reaction was incubated at room temperature for 15 minutes. DNase was inactivated by the addition of 1µl of 25mM EDTA pH 8.0 and heating at 65°C for 10 minutes. 5.5µl of this RNA (5µg) was then used in reverse transcription.

2.13.2 cDNA synthesis

Oligonucleotide

• POL-RS-PCR: CTTATACGGAT ATCCTGGCAA TTCGGACTTG
ATAGGGTGAT CAATGGA (underlined region is complementary to the 3' end of the *POLARIS* transcript).

Method

To 5.5µl of the DNased RNA was added 1µl of POL-RS-PCR primer (10µM stock). The sample was heated at 70°C for 10 minutes to denature RNA and allow primer annealing. The sample was then placed on ice and to this was added in the following order: 3µl of 5x AMV buffer, 2µl dNTP (12.5mM), 1µl (40 units) RNasin and 2µl (20 units) AMV reverse transcriptase. The sample was made up to 20µl with sterile water and incubated at 42°C for 45 minutes and then 50°C for 20 minutes. A negative control for each sample was also performed in which AMV reverse transcriptase was omitted from the cDNA synthesis reaction. cDNA was then purified away from the POL-RS-PCR primer using the *High Pure* PCR Product Purification kit from Boehringer Mannheim.

2.13.3 Amplification of *POLARIS* cDNA

Oligonucleotides

• RS-PCR-Anchor: CTTATACGGAT ATCCTGGCAA TTCGGACTT
• POL5'TEST: GGAGACTAAAGCGAACATATAAAACC

Method

5µl of the purified cDNA was used as template for PCR amplification. 1µl of the primers RS-PCR-Anchor and POL5'TEST (both 10µM stocks) was used with amplification cycles of : 94°C for 2 minutes then 50 cycles of 94°C for 30

seconds, 60°C for 30 seconds and 72°C for 1 minute. A final extension for 7 minutes at 72°C was then performed and 20µl of the products analysed on a 1% (w/v) agarose gel. A fragment of 443bp was the expected product. The reactions in which AMV reverse transcriptase had been omitted were not expected to produce a product.

2.14 Analysis of proteins

2.14.1 Protein extraction

Solutions

- Tween 20/Tris-buffered saline (TTBS): 0.1% (v/v) Tween 20, 100mM Tris-HCl, pH7.5, 0.9% (w/v) NaCl.

Method

Plant material was frozen in liquid nitrogen and ground to a fine powder with a mortar and pestle. The powder was mixed with an equal volume (w/v) of TTBS and vortexed vigorously before pelleting cell debris by centrifugation at 9400rpm for 10 minutes. The supernatant was taken, mixed with an equal volume of tricine sample buffer and electrophoresed through tris-tricine protein gels.

2.14.2 Precipitation of proteins

Solutions

- 100% Trichloroacetic acid solution: Sterile, distilled water is added to 100g TCA to a final volume of 100ml.

Method

Following protein extraction, TCA (100% solution) was added to the sample to a final concentration of 10% (v/v). The sample was incubated on ice or at -20°C for 1 hour and then centrifuged at 13400xg for 15 minutes. The supernatant was discarded and the pellet washed by adding the original volume of ice cold ethanol or acetone followed by centrifugation for 5 minutes. The supernatant was discarded and the pellet air dried before resuspension in TBST or 2x tricine sample buffer.

2.14.3 Electrophoresis of proteins using the tris-tricine buffer system

After Schagger and von Jagow (1987)

Solutions

- 30% acrylamide/0.8% bisacrylamide (37.5:1) solution (Bio-Rad).

- Tris-HCl/SDS, pH 8.45: 3M Tris base, pH8.45, filtered through a 0.45µM filter. SDS added to 0.3% (w/v).
- 4x Tris-HCl/SDS, pH6.8: 0.5M Tris base, pH6.8, filtered through a 0.45µM filter. SDS added to 0.4% (w/v).
- Separating gel: 9.8ml 30% acrylamide/0.8% bisacrylamide solution, 10ml Tris-HCl/SDS, pH8.45, 7.03ml sterile, distilled, water, 3.17ml glycerol.
- Stacking gel: 1.62ml 30% acrylamide/0.8% bisacrylamide solution, 3.1ml Tris-HCl/SDS, pH8.45, 7.78ml sterile, distilled water.
- Cathode buffer: 12.11g Tris base, 19.92g tricine, 1g SDS diluted to 1 litre with sterile, distilled water.
- Anode buffer (10x stock): 121.1g Tris base dissolved in 400ml sterile, distilled water and pH adjusted to pH8.9. Made up to 500ml.
- 2x tricine sample buffer: 2ml 4x Tris-HCl/SDS, pH6.8, 2.4ml glycerol, 0.8g SDS, 0.31g DTT, 2mg Coomassie blue R-250, sterile water to 10ml.

Method

Protein gel electrophoresis was performed using the Mini-PROTEAN®II Electrophoresis cell equipment from Bio-Rad as per manufacturers instructions. Separating and stacking gel solutions were degassed under vacuum for 10 minutes. To the separating gel solution was added 15µl TEMED and 100µl 10% (w/v) ammonium persulphate. The solution was mixed by swirling then pipetted between the glass plates until the solution was approximately 1cm below the comb. The gel was overlaid with 1ml of water saturated butanol and left to polymerise for 20 minutes. The butanol was then poured off and the surface of the gel rinsed with sterile water. To the stacking gel was added 10µl TEMED and 50µl 10% (w/v) ammonium persulphate. The gel was then pipetted onto the separating gel and a comb inserted. Following polymerisation the comb was removed and the wells washed with cathode buffer. The gel sandwich was assembled into the electrophoretic cell and the upper buffer chamber filled with cathode buffer. The lower buffer chamber was filled with 1x anode buffer. Protein samples were mixed 1:1 with 2x tricine sample buffer and heated at 100°C for 3 minutes before loading onto the gel. Electrophoresis was carried out initially at 30V until samples entered the separating gel and then at 150V until the tracking dye reached the bottom of the gel. The apparatus was disassembled and the gel either stained or blotted.

2.14.4 Staining of protein gels

Solutions

- Fixing solution: 5% (v/v) glutaraldehyde
- Staining solution: 10% (v/v) acetic acid, 0.025% (w/v) Coomassie blue R-250.
- Destain: 10% (v/v) acetic acid.

Method

Following electrophoresis, protein gels were placed in fixing solution for 1 hour which prevents the diffusion of small polypeptides from the gel. The gel was then rinsed 4 times with water for 5 minutes each before being transferred to staining solution for 1 hour with gentle shaking. Following this it was destained from 1 hour to overnight. Proteins were visualised as blue stained bands in the gel.

2.14.5 Blotting of protein gels

After Towbin *et al.* (1979).

Proteins were blotted to Immun-Blot™ PVDF membrane (Bio-Rad) before localisation of proteins by antibodies.

Solutions

- Transfer buffer: 3.03g Tris base, 14.41g glycine, 150ml methanol to 1 litre with sterile, distilled water.

Method

Following electrophoresis the gel was equilibrated in transfer buffer for 30 minutes. Two pieces of PVDF membrane was cut to the size of the gel and wet for 2-3 seconds in methanol before equilibrating in transfer buffer for 15 minutes. The transfer sandwich was assembled in a tray filled with transfer buffer so that the transfer cassette was covered. A pre-wet sponge pad was placed on the bottom half of the cassette and on top of this was placed a wet filter paper cut to the size of the gel. The first PVDF membrane was placed on the filter paper. The gel was placed on top of this and any air bubbles removed following which the second membrane was lowered onto the gel avoiding air bubbles. Another wetted filter paper was placed on top of the membrane followed by another sponge pad. The transfer cassette was closed and inserted into the Mini Trans-Blot® Electrophoretic Transfer Cell (Bio-Rad). The transfer chamber was filled with transfer buffer and a Bio-Ice cooling unit inserted along with a magnetic stirrer to maintain a transfer temperature below 40°C. Transfer was performed at 100V for between 30 minutes and 1 hour. Following transfer the membranes was rinsed in water briefly before being stained, either

permanently or reversibly, to check protein transfer before protein detection was carried out.

Ordinarily, transfer of proteins in such a system would be towards the anode since many proteins have an isoelectric point below the pH of the transfer buffer, in this case ~pH 8.3, such that at this pH they have a net negative charge.

However, proteins with very high isoelectric points (very basic proteins) will still have a net positive charge at pH 8.3 and thus will have a tendency to migrate towards the cathode. The POLARIS polypeptide is predicted to be very basic and for this reason a membrane was placed on the cathode side of the blotting sandwich as well as the anode side. Preliminary blotting experiments with the N-terminal (of POLARIS) polypeptide used for antibody production indicated that transfer in this system was towards the cathode for this particular polypeptide.

2.14.6 Staining of PVDF membrane for total protein Solutions

- Staining solution: 40% (v/v) methanol, 5% (v/v) glacial acetic acid, 0.02% Coomassie blue R-250.
- Destaining solution: 40% (v/v) methanol, 5% (v/v) glacial acetic acid.

Method

For permanent staining of proteins on the PVDF membrane following blotting the membrane was rinsed several times in water before being placed in staining solution for 1-2 minutes. The membrane was removed and shaken in several changes of destaining solution. Proteins successfully bound to the membrane were stained blue. This method is incompatible with protein detection by antibodies unlike reversible staining.

2.14.7 Reversible staining of membranes for total protein Solutions

- Staining solution: 0.5g Ponceau S was dissolved in 1ml glacial acetic acid, then made up to 100ml with water.
- Tris-buffered saline (TBS): 100mM Tris-HCl, pH7.5, 0.9% (w/v) NaCl.

Method

In order to check that protein transfer to the membrane had been successful, the membrane was stained with a reversible protein stain. Following electrophoretic transfer the membrane was briefly rinsed in water then placed in staining solution for 30 minutes with gentle agitation. The membrane was destained by several washes with water and transferred proteins were visualised as red bands on the membrane. To remove the stain prior to protein detection, the membrane was rinsed several times in TBS.

2.14.8 Protein detection by chemiluminescence

Following the separation of proteins by SDS-PAGE and their transfer to a support membrane, a specific protein can be detected by immunological techniques. A primary antibody is raised to the polypeptide of interest and following blocking of non-specific protein sites, the membrane is incubated with this antibody. A secondary antibody against the first is then used to detect the primary antibody. The secondary antibody is conjugated to the enzyme hydrogen peroxide, which acts on a chemiluminescent substrate. The light emitted by the product can then be detected by exposure of the membrane to X-ray film.

Solutions

- 10x TBS, pH7.6: to 800ml add 24.2g Tris base and 80g NaCl. Adjust pH to 7.6 then make up to 1 litre.
- Blocking buffer: 1x TBS, 5% (w/v) dried skimmed milk powder, 0.1% (v/v) Tween 20.
- Antisera buffer: 1X TBS, 5% (w/v) dried skimmed milk powder, 0.01% (v/v) Tween 20.
- Wash buffer: 1x TBS, 0.05% (v/v) Tween 20.
- Secondary antibody: Goat anti-rabbit IgG (H+L)-HRP conjugate (Promega Ltd.)
- SuperSignal® Ultra chemiluminescent substrate (Pierce).

Method

The membrane was placed in blocking buffer with gentle shaking for 1 hour at room temperature or overnight at 4°C. A 1:10,000 dilution of the primary antibody was made in antisera buffer and the membrane was then incubated in this for 1 hour at room temperature with gentle shaking. The membrane was rinsed in antisera buffer three times for 5 minutes each before incubation with the secondary antibody at a 1:50,000 dilution in antisera buffer. The membrane was washed twice in wash buffer for 5 minutes each and a final wash for 15 minutes before being briefly rinsed in water. Equal volumes of the SuperSignal® Ultra chemiluminescent substrate components were mixed and poured over the membrane (0.125ml/cm² membrane) and incubated for 5 minutes with gentle agitation. Excess liquid was then blotted from the membrane in Saran wrap. The membrane was exposed to Hyperfilm-ECL (Amersham) for periods ranging from 10 seconds to overnight before developing.

2.14.9 Antibody production

Antibody production was carried out by Quality Controlled Biochemicals, Inc., Hopkinton, USA. Briefly, an N-terminal peptide was synthesised and this was conjugated to a carrier protein, keyhole limpet hemocyanin. This was injected into two rabbits and following booster injections serum was taken and polyclonal antibody was isolated by affinity chromatography using the synthesised peptide linked to an agarose gel column. Affinity purified antibody was supplied at a concentration of 1.74mg/ml. Pre-immune serum was also supplied.

2.15 Plasmid Construction

This section details constructs mentioned in subsequent result or discussion chapters but for which results are not shown.

2.15.1 Construction of *POLARIS*- GFP fusions

Oligonucleotides

- PolProm: GCGAGCTCAAGCTTGAGGGAAAGAGAGGAAG
- NH-PolR: CGGGATCCATGGATTTTAAAAAGTTTAAAC
- NH-GFPF: CGGGATCCAGTAAAGGAGAAGAAGAACTTTTC
- NH-GFPRv: CGGAATTCCTTATTTGTATAGTTCATCC
- 5'UTR-Rv: GCTCTAGATCATGTTTCAGTGAGACAC
- C-GFPF: GCTCTAGAATGAGTAAAGGAGAAGAAC
- C-GFPRv: CGGGATCCTTTGTATAGTTCATCCATGC
- C-POLF: CGGGATCCATGAAACCCAGACTTTGT
- C-POLRv: CGGAATTCTCATCAATGGATTTTAAAAAG
- NOS FOR: CAGGTACCCCGATCGTTCAAACATTTGGC
- NOS REV: CAGGTACCCCAATTCCCGATCTAGTAAC

Method

By creating translational fusions between the putative *POLARIS* polypeptide and green fluorescent protein (GFP) driven by the *Polaris* promoter it was hoped to localise the site of *POLARIS* action more accurately than with the GUS enzyme. Since it was not known whether the N or C- termini were required for localisation (if localisation does occur) both N and C-terminal GFP fusions were produced. The construct in which the *POLARIS* polypeptide was located at the N-terminus was called pN-POL:GFP whilst the C-terminal fusion was named C-GFP:POL. Both constructs were inserted into the plant transformation vector pCIRCE into which a portion of the NOS terminator had been cloned. The modified vector was named pCIRCE-NOS.

2.15.2 Construction of pCIRCE-NOS: The NOS terminator is a transcriptional terminator from the Ti plasmid of *Agrobacterium tumefaciens* and in pCIRCE and pBIN19 it is located downstream of the *NPT II* gene. Using the primers NOS FOR and NOS REV, a 338bp region of the NOS terminator was amplified from pCIRCE using the Expand™ High Fidelity PCR system and 30 cycles that included primer annealing at 60°C and 30 seconds extension at 72°C. The primers incorporate a site for *KpnI* and following amplification the PCR product was digested with this enzyme and ligated into digested and dephosphorylated pCIRCE. Only plasmids in which the NOS terminator had inserted such that the NOS FOR primer site was adjacent to the *BamHI* site were used. Orientation was determined by colony PCR on recombinants using the M13 for and NOS FOR primers with a positive result generating a ~350bp product. Subsequent cloning of *POLARIS* : GFP fusion cassettes was such that this NOS terminator was at the 3' end of the cassettes.

2.15.3 Construction of pN-POL:GFP: The *POLARIS* open reading frame and upstream sequence was amplified from pλEM1 using the Expand™ High Fidelity PCR system and the primers PolProm and NH-PolR (10μM stocks) with 30 cycles of 60°C annealing and 1 minute extension at 72°C. The product was digested with *SacI* and *BamHI*, sites incorporated into the primers, and cloned into digested pBluescript SK-. Primer NH-POLR anneals to the 3' end of the *POLARIS* open reading frame but does not include the TGA stop codon. The GFP sequence was amplified from smGFP using the Expand™ High Fidelity PCR system and the primers NH-GFPF and NH-GFPRv (10μM stocks) with 30 cycles of 60°C annealing and 1 minute extension at 72°C. The fragment was digested with *BamHI* and *EcoRI*, sites incorporated into the primers, and cloned into digested pBluescript SK- downstream of the *POLARIS* open reading frame. A successful ligation resulted in a translational fusion between *POLARIS* and GFP. The whole cassette was then excised as an *HindIII* fragment (these sites are incorporated within the PolProm and pBluescript SK-) and ligated into digested pCIRCE-NOS. The orientation of the fragment in pCIRCE-NOS was such that transcription of the POL:GFP fusion proceeded from LB to RB.

2.15.4 Construction of pC:GFP:POL: The *Polaris* 5'UTR and promoter was amplified from pλEM1 using the Expand™ High Fidelity PCR system and the primers PolProm and 5'UTR-Rv (10μM stocks) with 30 cycles of 60°C annealing and 1 minute extension at 72°C. Following digestion with *SacI* and *XbaI* (sites incorporated within PolProm and 5'UTR-Rv respectively) the

fragment was ligated into digested pBluescript SK-. The *POLARIS* open reading frame was then amplified from p λ EM1 using the Expand™ High Fidelity PCR system and the primers C-POLF and C-POLRv with 30 cycles of 58°C annealing and 30 seconds extension at 72°C. The product was digested with *Bam*H1 and *Eco*R1 (sites incorporated within the respective primers) and ligated downstream of the *POLARIS* 5'UTR and promoter in pBluescript SK-. GFP was amplified from smGFP with the primers C-GFPF and C-GFPRv with 30 cycles of 60°C annealing and 1 minute extension at 72°C. Following the insertion of the *POLARIS* 5'UTR and promoter into pBluescript SK- it was found that whilst the *Xba*1 site had been reconstructed (as determined by DNA sequencing), the plasmid would no longer cut with this enzyme. The GFP was supposed to be inserted as a *Xba*1 and *Bam*H1 fragment but due to this problem the GFP fragment was first cloned into the pCR®2.1 TOPO vector. It was then excised as a *Bam*H1 fragment using the vectors site and ligated into pBluescript SK- downstream of the *POLARIS* 5'UTR and promoter. The removal of the GFP stop codon in the C-GFPRv primer results in a fusion of GFP with *POLARIS* at the C-terminus. The whole cassette was excised as an *Hind*III fragment and ligated into digested pCIRCE. The orientation of the fragment in pCIRCE-NOS was such that transcription of the GFP: POL fusion proceeded from LB to RB.

Chapter 3 The Promoter trap line AtEM101

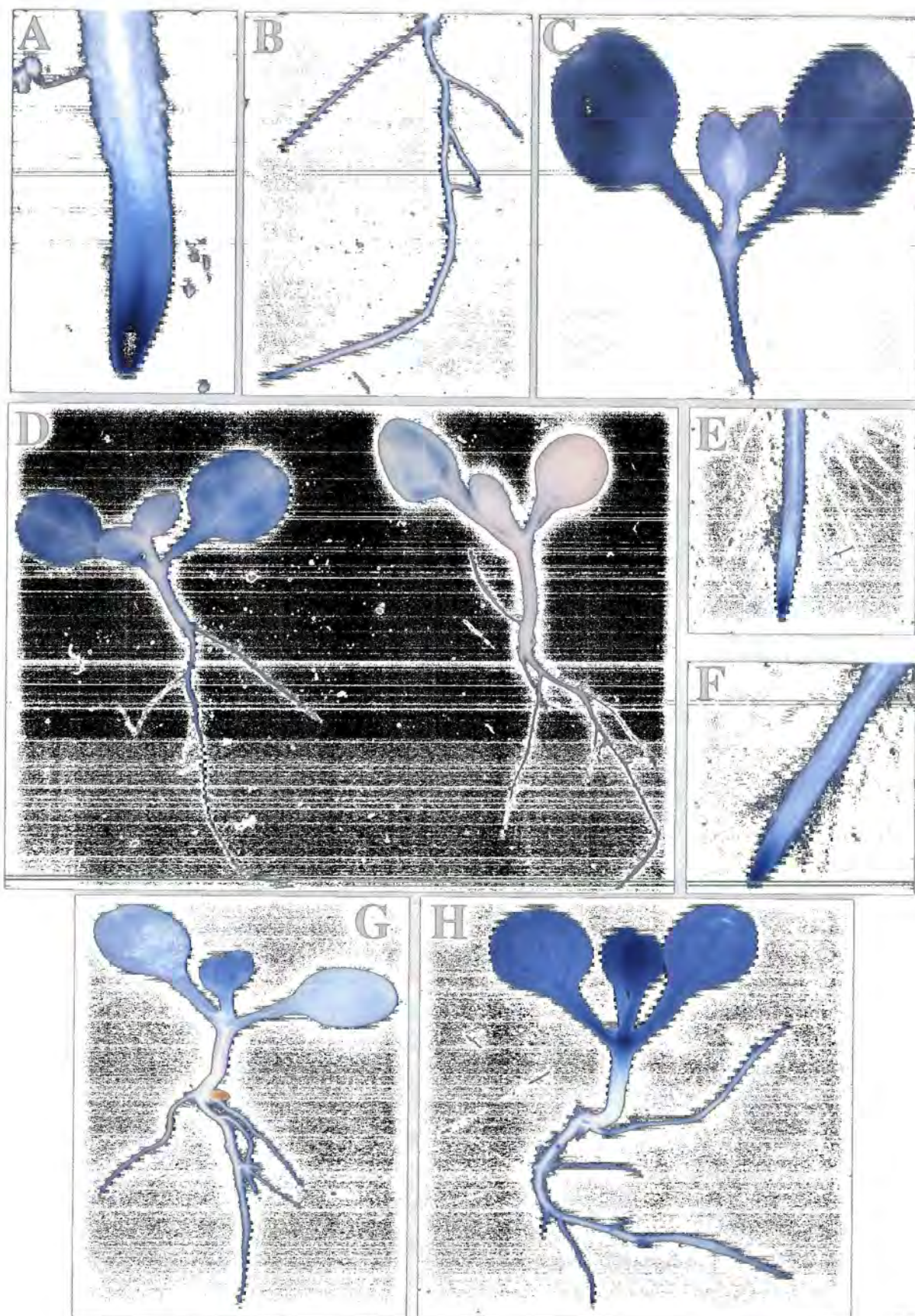
Line AtEM101 was isolated from a transgenic population transformed with the promoter trap vector pAgusBin19 (Lindsey *et al.*, 1993; Topping *et al.*, 1991). Histochemical localization of GUS activity has been reported previously (Topping *et al.*, 1994; Topping and Lindsey, 1997) with expression found most strongly in the basal half of embryos from the heart stage onwards and the tips of both primary and lateral roots. Low levels of GUS activity were reported in the seedling hypocotyl, the silique wall, and also the cotyledons, but not in true leaves. This line has also been shown to have a short root mutant phenotype which is potentially a result of a defect in ethylene production or synthesis (P. Chilley, unpublished data). Further characterization of the *Arabidopsis thaliana* promoter trap line AtEM101 is described in this chapter. For all results described, in this and subsequent chapters, work was carried out on AtEM101 seedlings homozygous for the single promoter trap T-DNA insert, unless otherwise stated.

3.1 GUS expression pattern of line AtEM101

To examine the pattern of GUS activity in this line more closely, organs and whole seedlings or plants were subjected to various times of histochemical staining. Also, the steady state levels of the GUS transcript in various organs were examined by northern analysis to determine if they correlated with the histochemical analysis.

The pattern of histochemical GUS staining in AtEM101 seedlings 7 days post-germination was determined by staining for both 6 and 24 hours followed by destaining in 70% ethanol. After 1 hours staining, GUS could be seen in the tips of both primary and lateral roots and after 6 hours extremely weakly in the cotyledons (Figure 3.1 a & d). Following a longer 24 hour stain, GUS staining was now clearly visible in the cotyledons, hypocotyl, and petioles of both the cotyledons and first leaves with weaker staining present in the expanded first leaves (Figure 3.1 c & d). Staining in the cotyledons and first leaves was very diffuse in what appeared to be all cell types and seemed to be more concentrated at the base of the organ, next to the petiole. A noticeable exception to the staining pattern was the vascular elements of all of these organs. The longer staining time did not result in GUS staining in any other part of the root other than the tips (Figure 3.1 b).

The GUS staining of the root tips correlates loosely with the site of an auxin peak in the root (Sabatini *et al.*, 1999). The longer staining times described resulted in strong staining throughout all cell types of the tip and did not indicate the initial site of



expression. Shorter staining times were therefore used in an attempt to identify if GUS expression originated at the site of the auxin peak. GUS staining was first observed in the central columella cells with expression then being observed throughout the columella root cap, in the lateral root cap, quiescent centre and young vasculature (Figure 3.2 a & b). By 30 minutes strong staining is observed in all the aforementioned cell types but is absent in the files of epidermal, cortical and endodermal cells (Figure 3.2 c). The initial GUS expression in the AtEM101 root tip is therefore very similar to that of DR5::GUS lines and corresponds to the sites of an auxin peak in the root tip.

To determine whether the staining pattern seen reflected steady state GUS transcript levels, northern analysis was performed using a radiolabelled *gusA* probe prepared from the 1.9kb *XbaI-SstI* fragment of pΔGUS (Topping *et al.*, 1991). The highest levels of GUS transcript were found in the tips of AtEM101 seedlings and the uppers of 7 day seedlings (uppers constitute the hypocotyl, cotyledons and first leaves) with lower levels found in roots where the tips had been removed, and also siliques (Figure 3.3). The fact that there appear to be comparable transcript levels in the root tips and seedling uppers is not wholly consistent with the histochemical staining pattern. As shown in the root tips, whilst expression is strong, it is limited to only a proportion of the cells present whilst in the uppers a larger proportion of cells express GUS, albeit at a lower level. Alternatively, there may be root tip specific translational enhancers resulting in higher protein production. GUS expression in roots in which the tips have been removed is explained by the fact that it is likely that a number of initiating lateral roots and lateral root primordia were not removed. However, in general it can be concluded that the histochemical staining pattern is a good indicator of transcript levels.

Though most of the emphasis on gene expression will be on the embryo and seedling, a study of GUS expression in older tissue was also performed. Three week old soil grown plants were stained for 24 hours and then destained in 70% ethanol. Rosette leaves were found to display variable staining though, most commonly appeared on the outside edge of the leaf (Figure 3.4 a). Staining of cauline leaves again showed variability but was often found to be strong at the node with occasional weaker staining along the mid-vein (Figure 3.4 b & c). The stem also showed variability of staining with GUS expression sometimes seen extending both up and down from a node and occasionally at internodes (Figure 3.4 c). As reported previously, silique walls were seen to stain strongly even from very early stages of development, though none of the floral organs appeared to show staining (Figure 3.4 d). As expected GUS expression was found in the root tips of these older plants though unlike, with 7 day seedlings, staining was often found to extend back further into the expansion zone (Figure 3.4 e).

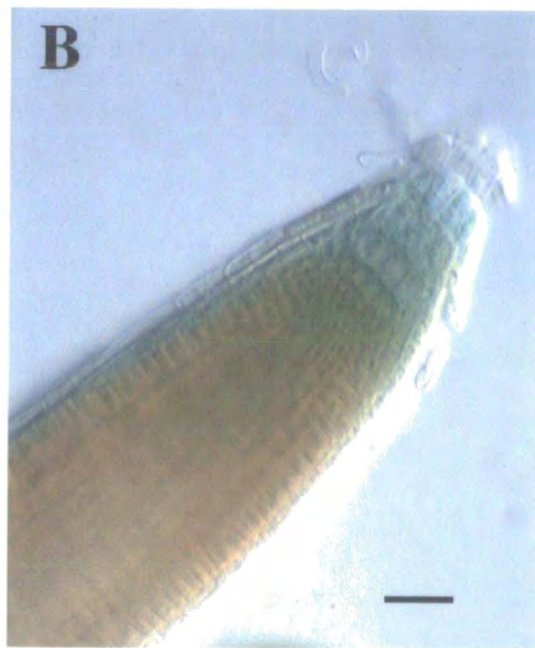
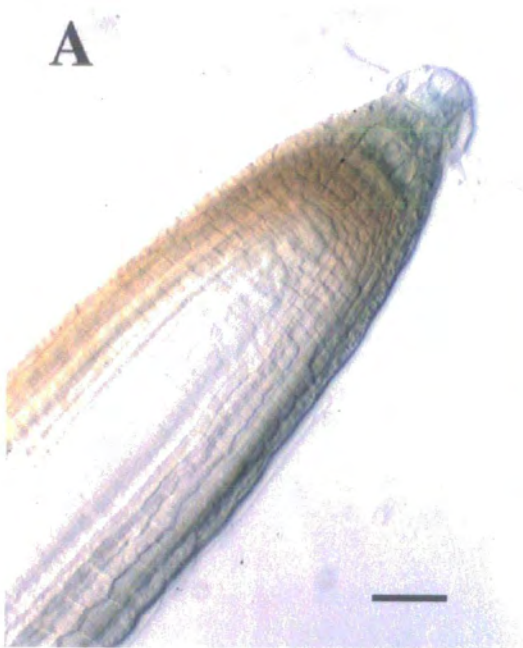
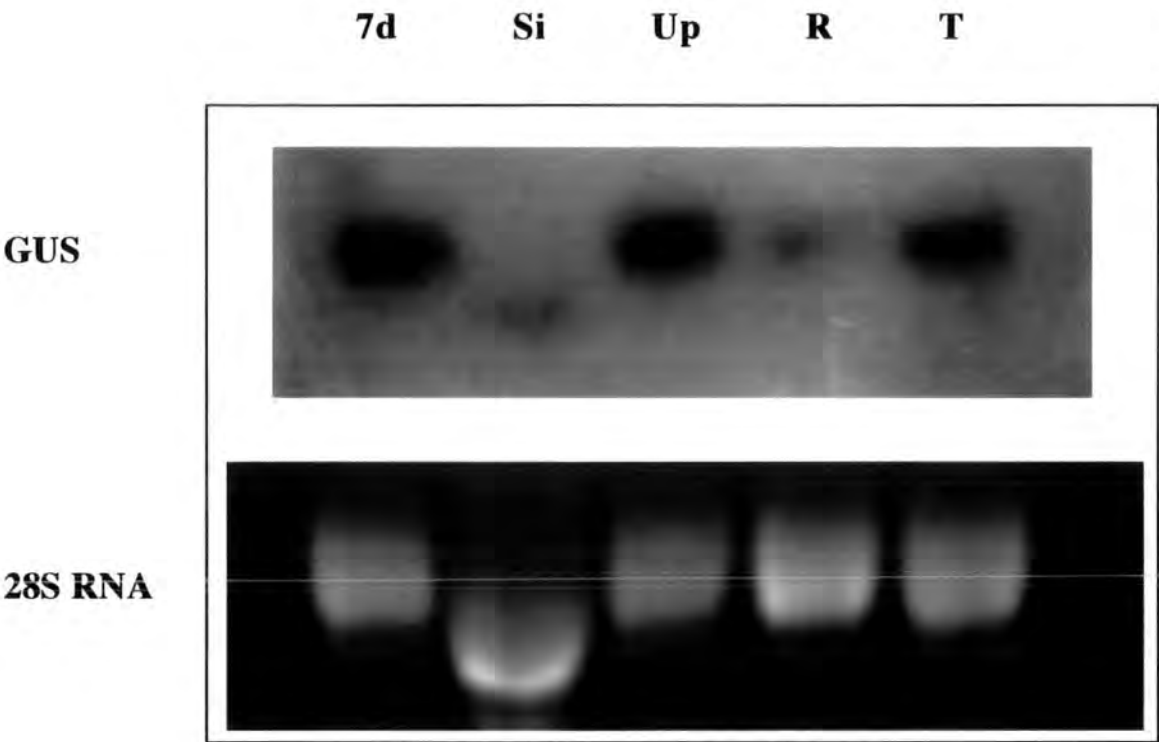
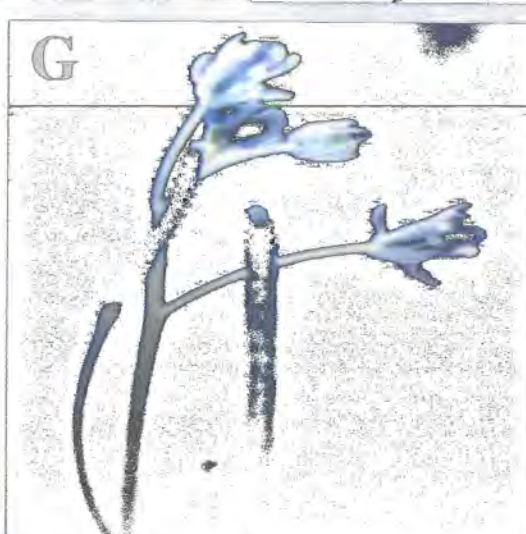
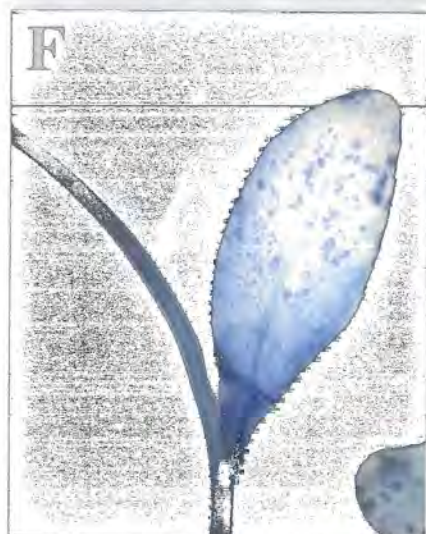
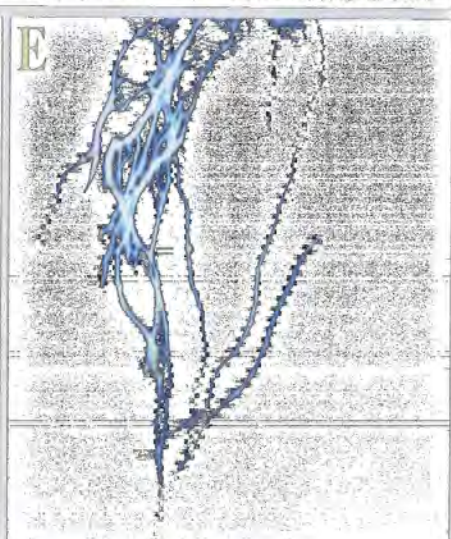
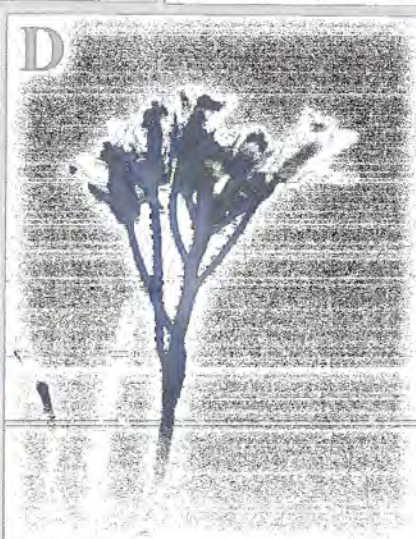
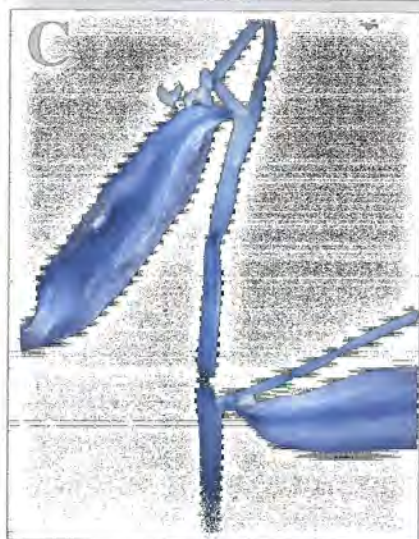
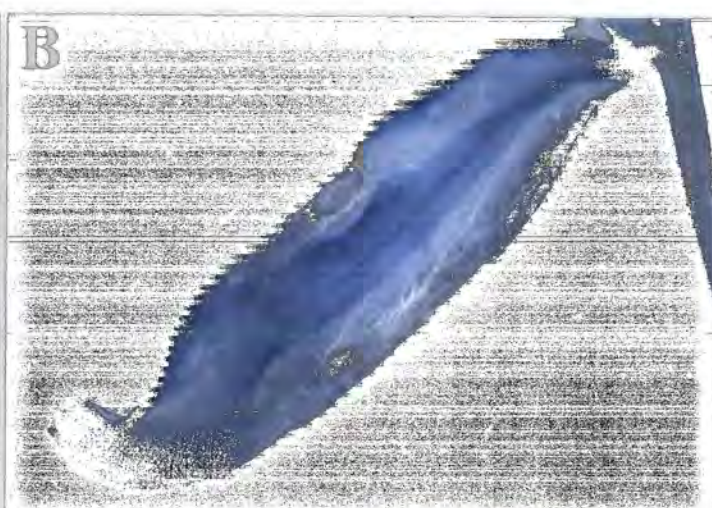
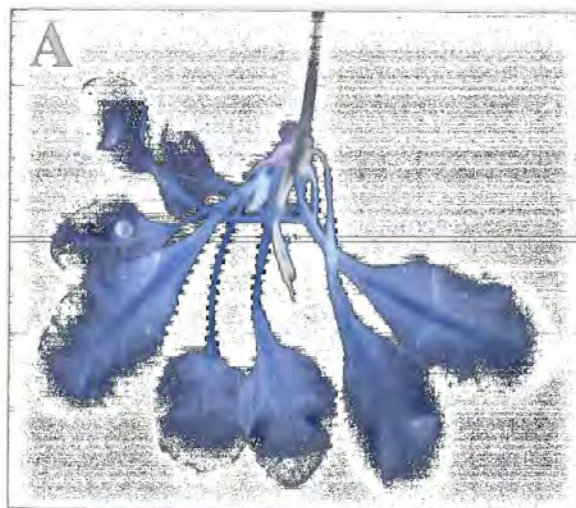


Figure 3.3. Analysis of GUS-fusion transcript levels in organs of the AtEM101 line

RNA gel analysis was performed with 10 µg of total RNA and hybridised with a randomly labelled GUS probe. Organs used were whole 7 day seedlings (7d), green siliques (Si), the aerial parts of 7 day seedlings (Up), the root minus their tips of 7 day seedlings (R), and the root tips of 7 day seedlings (T). The upper panel shows GUS-fusion transcript levels whilst the lower panel shows the ethidium bromide stained 28S RNA.





3.2 Analysis of the GUS-fusion transcript

One of the premises of promoter trapping is that upon integration of the T-DNA downstream of a native gene promoter, transcription can proceed through the T-DNA left border to produce a fusion transcript with the promoterless *gusA* gene. Identification of such a fusion transcript therefore provides good evidence that the T-DNA has inserted within a true plant gene.

3.2.1 Transcription initiates outside the T-DNA

To determine if the *gusA* transcript was expressed as a fusion to a plant gene northern blot analysis was performed on 20µg of total RNA extracted from 7 day old AtEM101 seedlings. The blot was initially hybridised to a *gusA* probe and following autoradiography the blot was stripped, re-exposed to ensure complete probe removal and then re-probed with a 560bp *Pst* 1-*EcoR* 1 genomic fragment containing ~160bp of T-DNA left border plant flanking sequence (both probes were kindly donated by Dr. J. Topping, University of Durham). Both probes detected a transcript of approximately 3kb (Figure 3.5) which did not appear in RNA from wild-type plants. The T-DNA left border and *gusA* coding sequence are approximately 2.7 kb in length and so this result strongly indicates that not only is transcription likely to initiate outside the T-DNA but that there is approximately 300bp of plant sequence at the 5' end of the fusion transcript. This result also indicated that it was likely that the T-DNA had inserted into a plant gene.

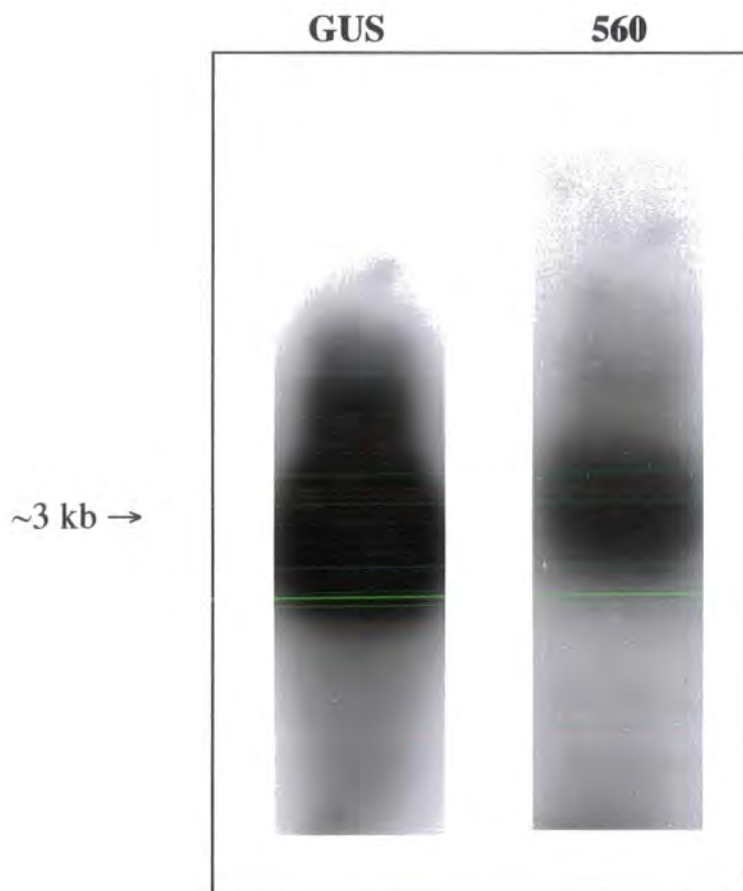
3.2.2 Initiation of transcription of the fusion transcript

A 3.6 kb genomic clone of the locus into which the T-DNA promoter trap is inserted had been cloned and sequenced (pλEM1; Dr. J. Topping and Dr. I.M Evans, University of Durham, see Figure 4.1 b). Analysis of approximately 250bp of plant flanking DNA immediately upstream of the T-DNA did not reveal any likely TATA boxes which usually proceed a transcript initiation site. In order therefore to further understand the structure of the GUS-fusion transcript and to facilitate cloning of the wild type gene the fusion-transcript initiation site was determined by 5' RACE using oligonucleotide primers designed to the *gusA* coding sequence and the T-DNA left border. Since the 5'RACE reactions did not result in one specific product (Figure 3.6 a), a shotgun cloning approach was taken and several independent clones of different sizes were isolated and sequenced (see sections 2.12.4 to 2.12.8). Several of these were found to align with the *gusA* and T-DNA LB sequences indicating that the RACE reaction had recognised the GUS-fusion transcript. The longest RACE product, clone RAC90, from



Figure 3.5. Transcription of the GUS Transcript Initiates Outside of the T-DNA LB

RNA blot gel analysis was performed with 20 μ g of total RNA from the AtEM101 line run alongside RNA molecular markers (Promega). The blot was initially hybridised with a randomly labelled GUS probe and exposed. The blot was then stripped and re-probed with the 560bp *Pst*I-*Eco*RI genomic DNA probe that contains T-DNA flanking sequence. Both probes hybridised to the same ~3kb transcript.



this initial 5'RACE experiment confirmed the results of the northern analysis, that the GUS-fusion transcript does initiate outside the T-DNA LB. This clone extended 190bp upstream of the T-DNA insertion site into the plant flanking DNA, to position 3020 of the 3.6kb genomic clone (Figure 4.1 b, CGAGGGGA, 3020 is underlined). The RACE clone sequence (Figure 3.6 b) also showed that splicing occurs between the plant flanking DNA and the left border resulting in the removal of a 112bp intron (Figure 3.6 b & c). Therefore the RAC90 clone extends from position 3020 to 3163 (TCAGGCG, 3163 is underlined) of the 3.6kb genomic clone (Figure 4.1 b). Analysis of the sequence using the NetPlantGene program (Hebsgaard *et al.*, 1996) showed that both the acceptor and donor splice sites shared high homology to predicted splice sites in *Arabidopsis thaliana*.

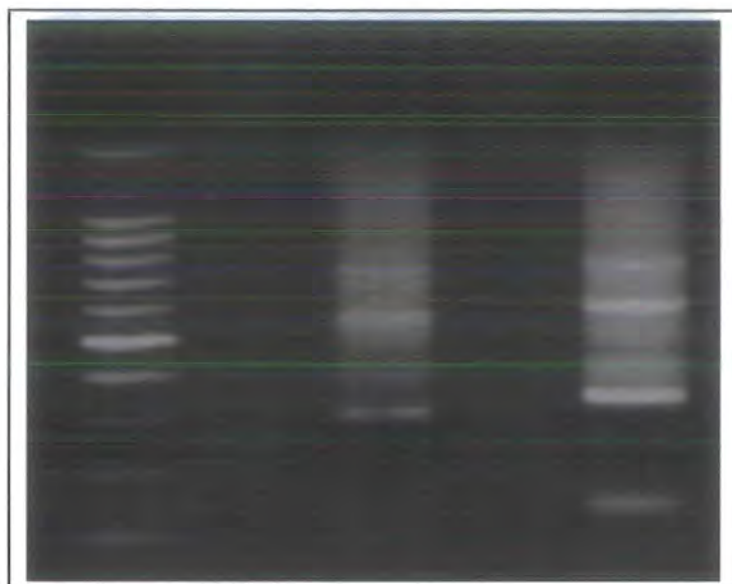
At this point it was not known whether the RAC90 clone represented the start of transcription or just a truncated reverse transcription product. The fact that there was not a likely TATA box within a 50bp region upstream of the end of this clone indicated that the latter might be the case, though the possibility remained that the promoter driving GUS expression did not require a TATA box. Later 5' RACE experiments described in section 4.2.2 were able to confirm that the RAC90 clone represents a truncated product and that the major transcript initiation site is approximately 380bp upstream of the T-DNA insertion site. The 5' RACE experiments were therefore able to confirm that transcription was initiating outside of the T-DNA and gave good evidence for the presence of a wild-type gene.

3.3 Auxin treatment rapidly upregulates GUS transcript levels

The plant hormone auxin has been implicated as playing a positive role in root development (Boerjan *et al.*, 1995; King *et al.*, 1995; Celenza *et al.*, 1995; Delarue *et al.*, 1998; Sabitini *et al.*, 1999). Auxin synthesised in the shoot is transported down into the root and it has been shown that IAA applied to the base of maize roots accumulates in the root tip (Kerk and Feldman, 1995). This accumulation of auxin in the root tip correlates with GUS expression indicating that this hormone may play a role in the regulation of the GUS-fusion transcript. When seeds of the AtEM101 line were germinated on medium containing the synthetic auxin 1-NAA, it was found that GUS activity in extracts of 6 days post-germination seedlings was 4-fold higher than in untreated seedlings. In contrast AtEM101 seedling germinated on media containing kinetin, a cytokinin, showed a 70% reduction in GUS activity (Topping and Lindsey, 1997). These results show that auxin is likely to be a positive regulator of the GUS-fusion transcript but do not indicate whether the effect seen is a primary auxin response

A **M** **P40.N2** **Nested1**

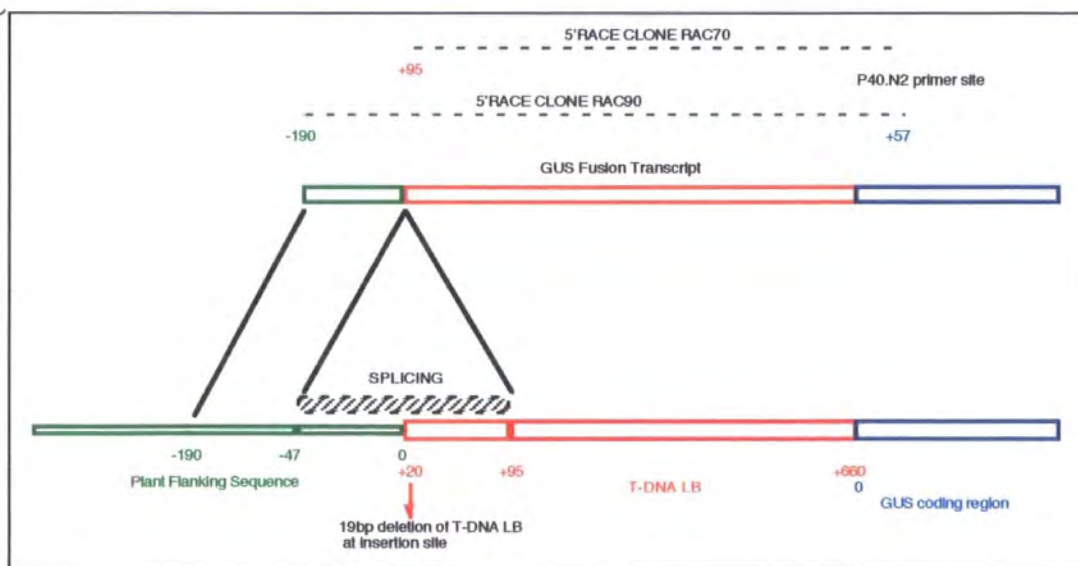
1.5kb →
1kb →
500bp →



B

1	TTTTTTTTTTT	TTTTTTTTTGG	GAGCGAAGAC	AGTCCACGTA	GCTGCAGAGA
51	GAAAGAGAAG	AGCACGTGAG	GCACACGTTC	CTTGTGTAAG	ACTTGTGTGTG
101	GTGATGTTGG	CGCAGTGTCT	CACTGAAACA	TGAATGAAAC	CCAGACTTTG
151	TTTAAATTTT	AGACCACTGA	GACGGGCAAC	AGCTGATTGC	CCTTCACCGC
201	CTGGCCCTGA	GAGAGTTGCA	GCAAGCGGTC	CACGCTGGTT	TGCCCCAGCA
251	GGCGAAAATC	CTGTTTGATG	GTGGTTCCGA	AATCGGCAAA	ATCCCTTATA
301	AATCAAAAGA	ATAGCCCGAG	ATAGGGTTGA	GTGTTGTTCC	AGTTTGGAAC
351	AAGAGTCCAC	TATTAAAGAA	CGTGGACTCC	AACGTCAAAG	GGCGAAAAAC
401	CGTCTATCAG	GGCGATGGCC	CACTACGTGA	ACCATCACCC	AAATCAAGTT
451	TTTTGGGGTC	GAGGTGCCGT	AAAGCACTAA	ATCGGAACCC	TAAAGGGAGC
501	CCCCGATTTA	GAGCTTGACG	GGGAAAGCCG	GCGAACGTGG	CGAGAAAGGA
551	AGGGAAGAAA	GCGAAAGGAG	CGGGCGCCAT	TCAGGCTGCG	CAACTGTTGG
601	GAAGGGCGAT	CGGTGCGGGC	CTCTTCGCTA	TTACGCCAGC	TGGCGAAAGG
651	GGGATGTGCT	GCAAGGCGAT	TAAGTTGGGT	AACGCCAGGG	TTTTCCCAGT
701	CACGACGTTG	TAAAACGACG	GCCAGTGAAT	TCCCGGGTGG	TCAGTCCCTT
751	ATGTTACGTC	CTGTAGAAAC	CCCAACCCGT	GAA	

C



as typified by the SAUR genes, some of which show transcriptional upregulation within 5 minutes of auxin treatment (Abel and Theologis, 1996), or a slower secondary response.

In order to determine this, AtEM101 seedlings were grown on media lacking auxin and 7 days post-germination were transferred onto media containing 10 μ M 1-NAA for time periods ranging from 30 minutes to 24 hours. In parallel, AtEM101 seedlings were also transferred onto media containing 10 μ M kinetin. RNA extracted from these seedlings was then analysed by northern blotting to determine if changes had occurred in the steady state levels of the GUS-fusion transcript (Figure 3.7). Auxin treatment resulted in a large induction of transcript levels over the 24 hour period, with a maximum of 6.9 times normal levels 24 hours post-transfer. The response itself was rapid with significant increases within 30 minutes of transfer (almost 3 times normal levels). Though earlier periods were not tested it would seem reasonable to suggest that this is likely to be a primary auxin response, indicating that the GUS-fusion transcript is transcriptionally controlled to react to changes in auxin levels and may represent a novel member of the early-auxin genes. A number of these genes are known to be upregulated in response to treatment with the protein synthesis inhibitor cycloheximide (CHX; Abel and Theologis, 1996). In order to determine if GUS-fusion transcript levels were upregulated in response to CHX, 7 day old seedlings were transferred to media containing 50 μ M CHX for 2 hours. Northern analysis did not indicate a large-scale induction in response to this compound (data not shown).

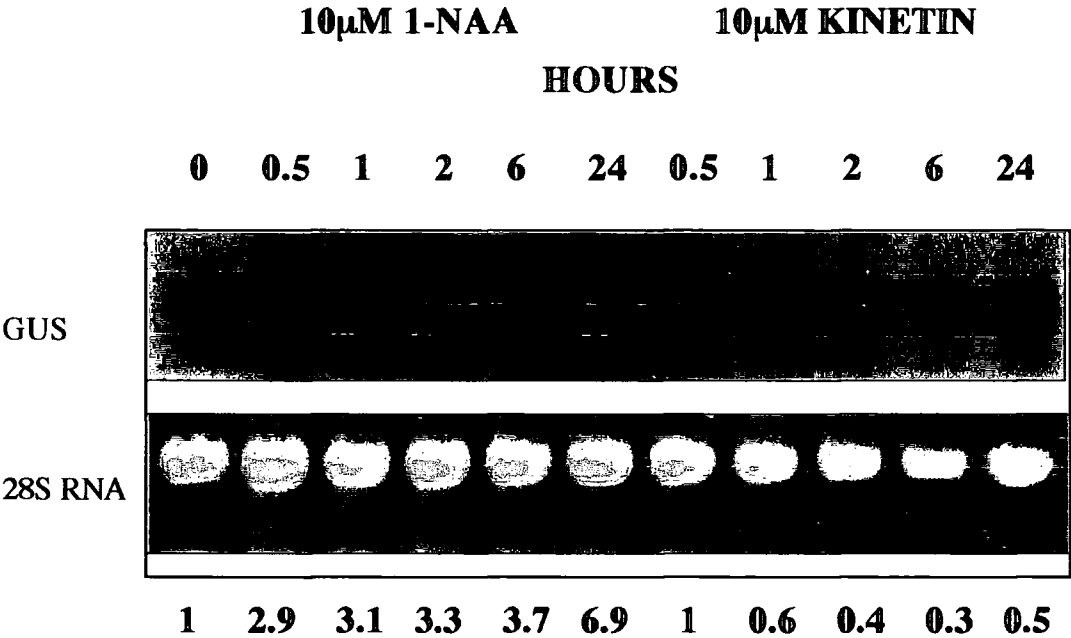
It had been shown previously that treatment with cytokinin resulted in reduced GUS activity in AtEM101 seedlings (Topping and Lindsey, 1997). This data is supported by the RNA analysis which indicates that GUS-fusion transcript levels are reduced up to 3.3 times following transfer to media containing 10 μ M kinetin (Figure 3.7). The response to kinetin treatment was not as rapid as the changes seen following 1-NAA treatment which may reflect a requirement for other intermediates to be generated to block expression of GUS. Another possibility is that the GUS-fusion transcript is relatively stable and that the kinetin response is as rapid as that of auxin and is not reflected truly by steady state RNA levels.

3.3.1 The effect of inactive auxin analogues on GUS-fusion transcript levels

In order to determine whether the increase in GUS-fusion transcript levels observed following treatment with 10 μ M 1-NAA is specifically an auxin response the effect of the

Figure 3.7. Analysis of GUS-Fusion Transcript Levels in Line AtEM101 Following Treatment with Auxin or Cytokinin

Seedlings were grown for 7 days on 1/2MS10 media and then transferred to new media supplemented with either 10 μ M 1-NAA or 10 μ M Kinetin for the times indicated (hours). RNA gel blot analysis was performed with 10 μ g of total RNA and hybridised with a randomly labelled GUS probe. The upper panel shows levels of the GUS-fusion transcript and the lower panel shows ethidium bromide staining of 28S RNA. Numbers below the lower panel show the ratio of GUS-fusion transcript at that time point to the untreated control.



inactive auxin analogues was examined. AtEM101 seedlings were grown for 6 days in the absence of auxin before being transferred to media containing 10 μ M of either the active auxins 1-NAA or 2,4-D or their inactive analogues 2-NAA or 2,3-D for 24 hours. RNA extracted from these seedlings was then analysed by northern blotting. As expected, treatment with the active auxins resulted in significant increases in the levels of the GUS-fusion transcript compared to levels from the untreated sample (Figure 3.8). Interestingly, 2,4-D appears to elicit a stronger response than 1-NAA, a result that supports histochemical staining observations (Paul Chilley, unpublished results). By comparison, treatment with the inactive auxin analogues resulted in no observable increase in transcript levels compared to those from untreated seedlings.

This result strongly suggests that the observed increases in GUS-fusion transcript levels are an auxin response and combined with the speed of the response (ca. three-fold increase within 30 minutes), indicate that a primary auxin response gene may have been tagged by the promoter trap.

3.3.2 Line AtEM101 Shows Normal Auxin Sensitivity

Loss of function mutations in some primary auxin response genes such as *SHY2/IAA3* result in short roots that show reduced sensitivity to exogenous auxin application (Tian and Reed, 1999). Roots of AtEM101 were therefore tested for their ability to elongate on inhibitory concentrations of the synthetic auxins 1-NAA and 2,4-D in a vertical plate assay. After 3 days growth on normal media AtEM101 and C24 seedlings were transferred to vertical plates containing 10nM or 1 μ M of either 1-NAA or 2,4-D or normal media as a control. After a further 3 days the degree of elongation was determined compared to the controls (Table 3.1). On 10nM auxin no difference was observed in the sensitivity of AtEM101 roots compared to C24 roots, with 2,4-D having the greatest inhibitory effect. On the higher auxin concentration root elongation was virtually completely inhibited in both AtEM101 and C24 making accurate comparisons impossible. The results on the lower auxin concentration indicate however that the sensitivity of AtEM101 roots is very similar to the wild-type. Expression of the auxin-induced gene *SAUR-AC1* (Gil *et al.*, 1994) did not appear to be affected in the AtEM101 line again suggesting normal auxin sensitivity (data not shown).

Figure 3.8. GUS-Fusion Transcript Levels Following Treatment with Active and Inactive Auxin Analogues

RNA gel blot analysis was performed with 20µg of total RNA from 7 day AtEM101 seedlings treated for 24 hours with either the active auxins 1-NAA and 2,4-D or the inactive analogues 2-NAA and 2,3-D. The upper panel shows GUS-fusion transcript levels compared to those of an untreated control (Unt.) following hybridisation with a randomly labelled GUS probe. The lower panel shows ethidium bromide staining of the 28S RNA prior to transfer.

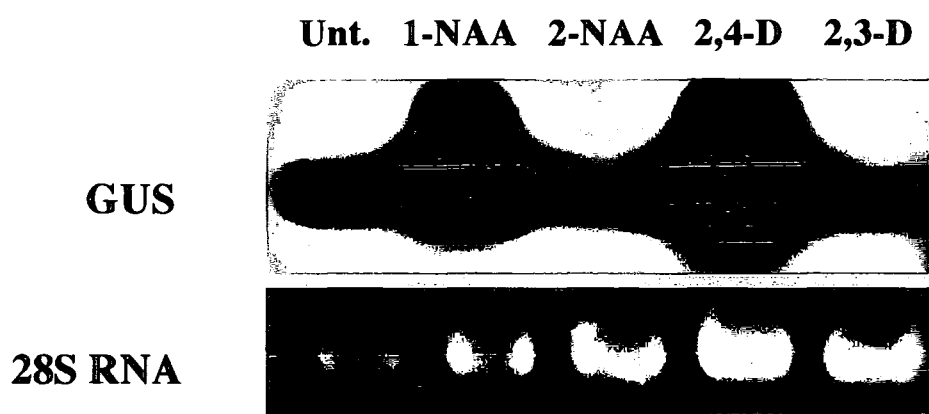


Table 3.1 Root Growth of AtEM101 and C24 on Auxin, BA and ACC

For auxin experiments, seedlings were germinated on 1/2MS10 media on vertical plates in the light. 3 days post-germination, seedlings were transferred to 1/2MS10 vertical plates supplemented with the indicated concentrations of either 1-NAA or 2,4-D. After 3 days root elongation was measured for 10 seedlings per treatment. Data was normalised using the elongation of roots on 1/2MS10 as a control (% of control). For BA and ACC experiments, seedlings were germinated on media containing the indicated concentrations, in the dark. Roots were measured 7 d.p.g and normalised using root length of seedlings grown on 1/2MS10 as a control. A probability smaller than 0.05 indicates that there is a statistical difference between the two sets of samples. SEM, standard error of the mean. ND, not determined.

	C24 n=10		AtEM101 n=10		Probability
	Mean Root Length +/- SEM (mm)	% of Control	Mean Root Length +/- SEM (mm)	% of Control	
Auxin Control 1/2 MS10	25.9 +/- 2.2	100	14.7 +/- 1.6	100	ND
2,4-D 10nM	14.7 +/- 1.5	56.8	7.7 +/- 0.6	52.4	0.9
2,4-D 1uM	2.0 +/- 0.0	7.7	2.0 +/- 0.0	13.6	ND
1-NAA 10nM	20.8 +/- 2.9	80.3	11.6 +/- 0.9	78.9	0.44
1-NAA 1uM	2.9 +/- 0.1	11.2	2.7 +/- 0.2	18.4	ND
ACC/BA Control 1/2 MS10	18 +/- 0.7	100	11.6 +/- 0.4	100	ND
BA 100pM	17.9 +/- 0.7	99.4	9.2 +/- 0.4	79.3	0.012
BA 1nM	17.3 +/- 0.8	96.1	9.4 +/- 0.4	81.0	0.06
BA 10nM	16.9 +/- 0.8	93.9	8.3 +/- 0.4	71.6	0.0015
BA 100nM	9.6 +/- 0.2	53.3	4.9 +/- 0.3	42.2	0.016
BA 1uM	9.0 +/- 0.3	50.0	3.3 +/- 0.3	28.4	4.5X10 ⁻⁶
ACC 10pM	14.6 +/- 0.8	81.1	8.9 +/- 0.3	76.7	0.59
ACC 100pM	11.3 +/- 0.5	62.8	7.4 +/- 0.4	63.8	0.75
ACC 1nM	7.2 +/- 0.2	40.0	4.8 +/- 0.3	41.3	0.66
ACC 10nM	3.5 +/- 0.2	19.4	1.9 +/- 0.2	16.4	0.24

3.4 Line AtEM101 may show enhanced ethylene synthesis and is hypersensitive to cytokinins but not ACC

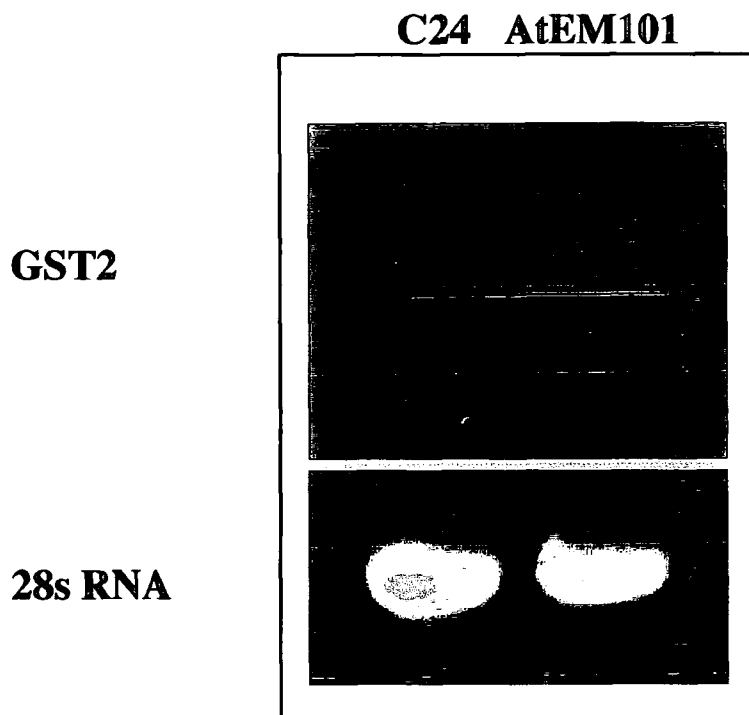
When homozygous for the T-DNA insertion the roots of the AtEM101 line are shorter and appear to have a larger number of root hairs which extend closer to the root tip than roots of wild-type C24 plants. Also, AtEM101 seedlings germinated in the dark appear to have an exaggerated apical hook (Paul Chilley, unpublished data). Such features are consistent with seedlings grown in the presence of the gaseous hormone ethylene and homozygous AtEM101 plants share similarities with the ethylene *eto* and *ctr1* mutants (Guzman and Ecker, 1990; Kieber *et al.*, 1993). The phenotype of the AtEM101 line would therefore suggest that these plants show either enhanced synthesis or perception of ethylene (Paul Chilley, unpublished data).

To examine whether AtEM101 plants show enhancement of ethylene-dependent processes at the molecular level the expression of the ethylene induced GST2 gene (Zhou and Goldsborough, 1993), a glutathione-S-transferase, was determined in AtEM101 plants compared to wild-type C24 plants by northern analysis (Figure 3.9). In untreated plants it was found that the steady state levels of the GST2 mRNA were significantly increased in AtEM101 seedlings compared to the wild-type. This result therefore supports the hypothesis that the AtEM101 mutant shows enhanced synthesis or perception of ethylene.

The sensitivity of AtEM101 roots to the cytokinin, BA, and the ethylene precursor, ACC, was also examined. ACC, which is converted to ethylene by the enzyme ACC oxidase, was chosen instead of ethylene for these experiments because of the ease of application. Seed was germinated in the dark on media containing various concentration of either BA or ACC. The roots of both AtEM101 and C24 seedlings (n=10), which were grown on the same plates, were then measured 7 d.p.g and compared to those of seedlings grown on unsupplemented 1/2MS10 media (Table 3.1). In the case of C24 root growth, concentrations of BA below 10nM were not found to have an appreciable effect on root growth whereas 100pM BA was found to result in AtEM101 roots that were only 79% of the length of the controls. Over the range of concentrations used, AtEM101 roots were found to be more sensitive to BA than those of C24. The results of growing AtEM101 and C24 seedlings in the presence of ACC do not follow the same pattern as those of BA (Table 3.1). Over the range of ACC concentrations used (10pM to 10nM), AtEM101 and C24 roots appeared to have similar sensitivities. Together, however these results indicate that AtEM101 roots are hypersensitive to cytokinins over a wide range of concentrations, but not to the ethylene precursor ACC.

**Figure 3.9. Expression of an Ethylene-induced GST in AtEM101
Determined by RNA Gel Blot Hybridisation**

RNA gel blot analysis was performed with 20µg of total RNA from 7 day seedlings and hybridised with randomly labelled *GST2* cDNA. The bottom panel shows the ethidium bromide stained 28S RNA.

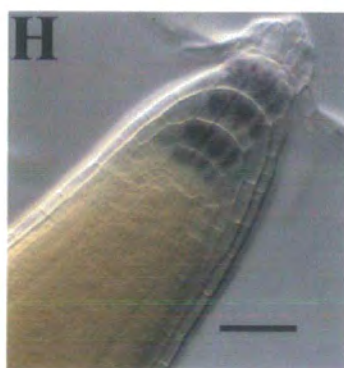
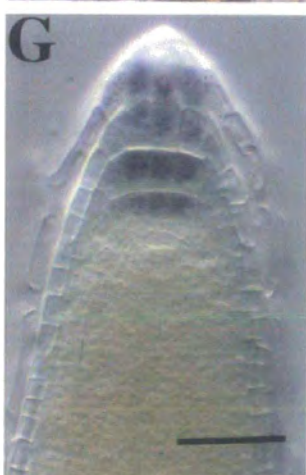
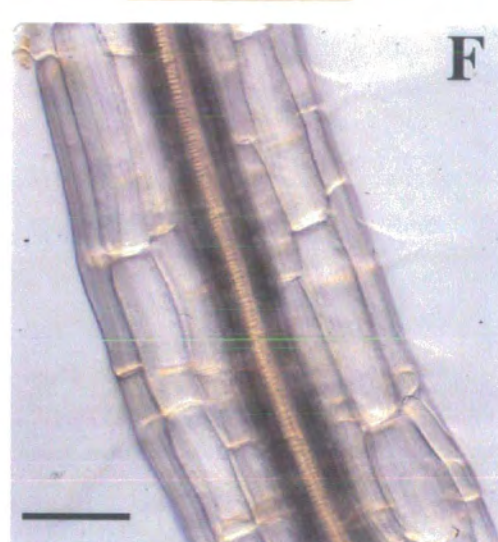
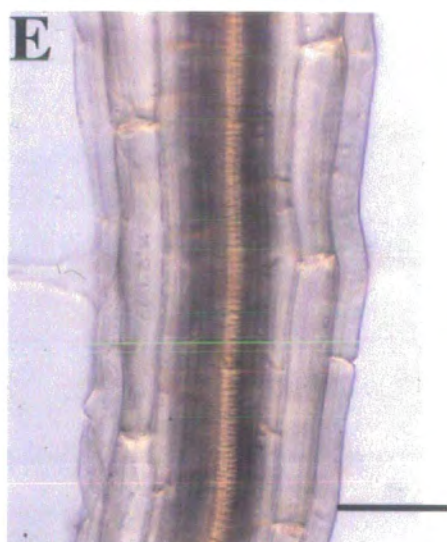
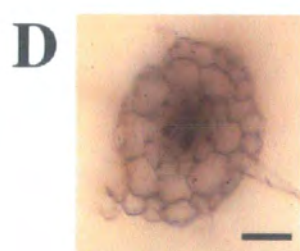
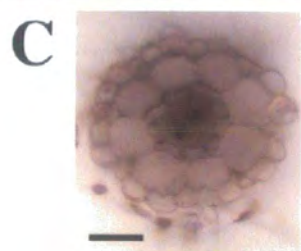
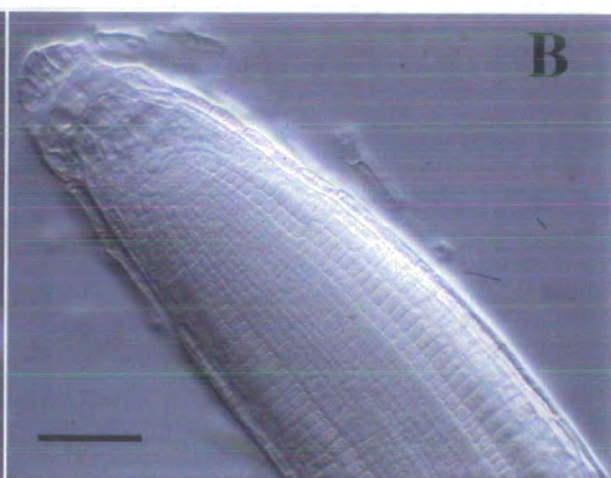
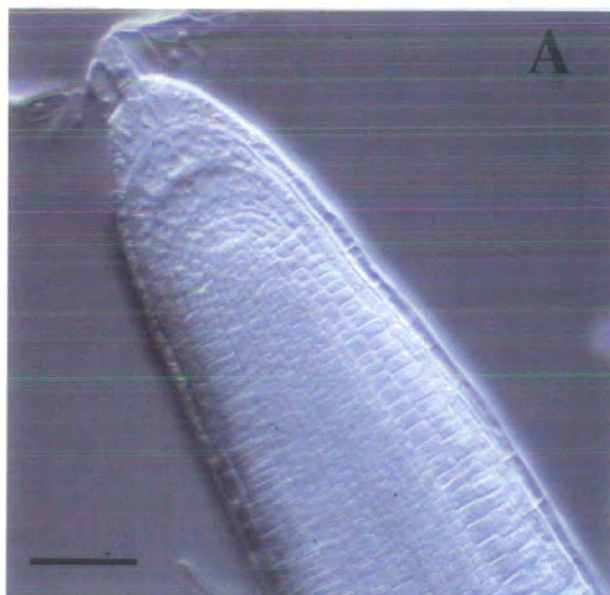


3.5 Histological Examination of AtEM101 Roots

A number of short root mutants have been identified in screens for genes controlling root development (Benfey *et al.* 1993; Cheng *et al.*, 1995; Hauser *et al.*, 1995; Scheres *et al.*, 1995). Some of these mutants, such as *short root*, have been found to be defective in radial patterning whilst other mutants such as *sabre* show abnormal cell expansion. Fresh transverse sections through the maturation zone of both AtEM101 seedling roots were examined for any defects in radial patterning. The pattern of AtEM101 roots was the same as wild-type C24 roots with a variable number of epidermal cells surrounding eight cortical cells, eight endodermal cells and the vascular bundle. None of these cell layers showed any sign of excessive expansion in the AtEM101 line (Figure 3.10 c & d). Root hairs were observed to develop in the usual position overlying two cortical cells, indicating that epidermal cell patterning was also unaffected in line AtEM101 (Figure 3.10 d).

Examination of the meristematic region of AtEM101 roots indicated that the meristem showed the correct pattern and organisation though the columella appeared slightly wider than those of C24 roots (Figure 3.10 a & b), an observation confirmed by cell measurements (M. Souter, unpublished data). The columella cells accumulate starch granules, a feature which can be used to confirm the specification of these cells. Examination of AtEM101 and C24 root tips by Lugol staining indicated however that there was no change in starch granule distribution (Figure 3.10 g & h).

The short root of AtEM101 is therefore not the result of abnormal cell patterning. One possibility to explain the phenotype was a reduction in meristem activity whilst a second is that expansion is reduced, resulting in shorter cells. To test the latter possibility cortical cells from above the maturation zone of both C24 and AtEM101 4 day old seedlings were measured. From 68 independent measurements it was found that the average length of cortical cells from AtEM101 roots was 98.8 μ m compared to 123.2 μ m for C24 (Figure 3.10 e & f; Table 3.2). No significant difference was seen in the width of these cells (21.7 μ m for AtEM101 versus 22.5 μ m for C24) though measurements across the whole root, 100 μ m from the tip, indicated that the AtEM101 root is more radially expanded than that of C24 (M. Souter, unpublished data). This difference in cell length was evident in all the cell layers and was not specific to the cortex indicating the reduced root length of AtEM101 roots is due to a reduction in the directional expansion of cells. As with the examination of the radial sections, the examination of optical sections of the root indicated that root hairs developed in cell files overlying two cortical cells. The apparent hairy root phenotype of AtEM101 (P. Chilley, unpublished data) is



therefore due to reduced epidermal cell length compacting hair files together and not defective patterning.

Table 3.2. Comparison of Cortical Cell Measurements Between AtEM101 and C24

Cell measurements were performed as described in Materials and Methods section 2.4.3. N=68 for both C24 and AtEM101. For a difference to be statistically significant the probability was required to be smaller than 0.05. NA, not available.

Cortical Cell	C24	AtEM101	Different (Probability)
Cell Length (uM)	123.2	98.8	YES (3.14×10^{-6})
Standard Dev. N=68	9.8	7.7	NA
Cell Width (uM)	22.5	21.7	NO (0.09)
Standard Dev. N=68	0.82	0.77	NA
Length/Width	5.5	4.6	NA

3.6 Summary

Presented in this chapter is a characterisation of the promoter trap line AtEM101. Expanding on previous results it has been shown that in 7 day old seedlings GUS expression is localised predominantly in the root tips, petioles, cotyledons, and faintly in the hypocotyl. The expression in the root tip corresponds to the site of an auxin peak in the root. In older plants GUS expression is found at the nodes and siliques with variable staining of both rosette and cauline leaves as well as the stem.

Transcription of GUS initiates outside of the left border as determined by both RNA blot analysis and 5' RACE. It has been shown that levels of this GUS-fusion transcript increase rapidly after treatment with auxin, the speed of transcriptional induction indicating a possible primary auxin response and inactive auxin analogues do not affect transcript levels. Cytokinins also appear to have a regulatory role in

determining the expression of GUS. Whilst AtEM101 may mark an auxin primary response gene, the roots of this line show normal auxin sensitivity.

It has also been demonstrated at the molecular level that the line AtEM101 has much higher transcript levels of the ethylene-induced *GST2* gene. This result supports unpublished observations on the AtEM101 mutant phenotype suggesting that this mutant shows either enhanced synthesis or perception of ethylene. The roots of the AtEM101 line were also more sensitive to the growth inhibitory effects of cytokinins but not to the ethylene precursor ACC.

Histological analysis of the AtEM101 root indicates that the short root phenotype is correlated with reduced cell expansion. No defects are observed in the meristem structure and organisation nor in the radial pattern of the root. The apparent hairy phenotype of AtEM101 roots is not due to defective epidermal patterning but rather a reduction in epidermal cell lengths.

Chapter 4 Cloning and characterisation of the *POLARIS* gene

The previous chapter described the promoter trap line AtEM101. The short root phenotype of this line has been shown to co-segregate with the T-DNA indicating that the T-DNA is probably interrupting the expression of a gene in this line. Both northern experiments and 5'RACE experiments on the GUS promoter trap indicate that transcription initiates outside of the T-DNA strongly supporting the presence of a gene in the region of the T-DNA. This chapter therefore details the characterisation of the wild-type genomic locus into which the T-DNA in line AtEM101 has inserted. This includes the cloning of two genes one of which, named *POLARIS*, is tagged by the T-DNA in line AtEM101. The structure of this gene, its expression pattern and the nature of its putative polypeptide will be presented.

4.1 Genomic organisation of the *POLARIS* locus

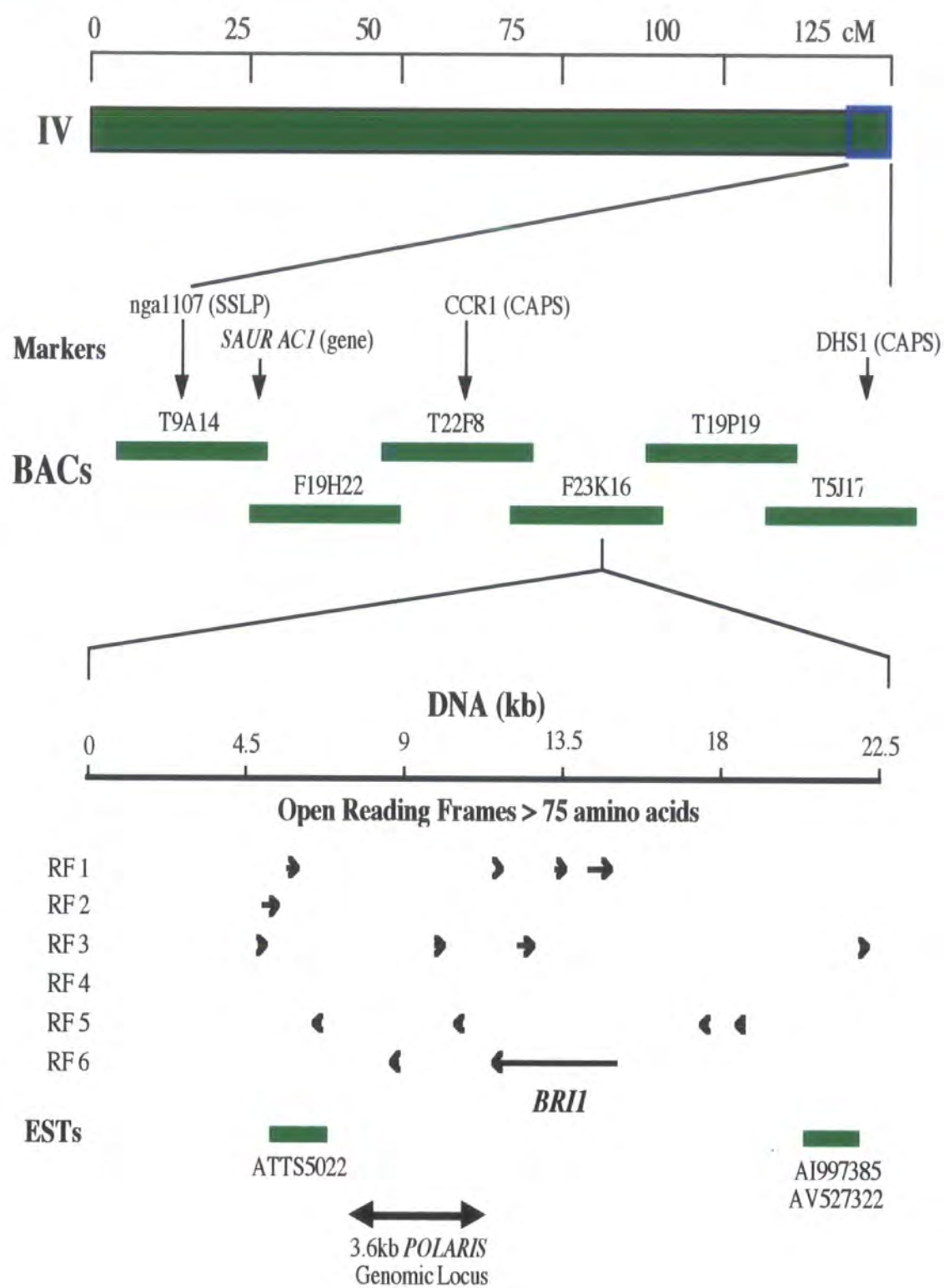
The AtEM101 line contains a single T-DNA per haploid genome, as determined by Southern analysis, and plant flanking DNA was amplified by IPCR (Topping *et al.*, 1994). Screening of an *Arabidopsis* λ GEM 11 library with radiolabelled plant flanking DNA resulted in the identification of a genomic clone and a 3.6kb *EcoR* 1 fragment which hybridised with the plant flanking DNA was sub-cloned into pBluescript KS+ (Dr. J. Topping, unpublished results) and sequenced (Dr. I.M. Evans, unpublished results). The sequence is shown in figure 4.1 b. Alignment of the IPCR product with both the genomic sequence and pAgusBIN19 revealed that the T-DNA insertion had resulted in a 19bp deletion of the Left Border with no apparent rearrangement of the plant DNA (Dr. J. Topping, unpublished results). The T-DNA had inserted at position 3208 of the 3.6kb clone (Figure 4.1 b). Sequence analysis of the sense strand of the 3.6kb clone revealed only a small number of open reading frames with the largest coding for a 92 amino acid novel polypeptide which ended approximately 450bp upstream of the T-DNA insertion site (Figure 4.1b). The T-DNA itself had inserted within a small open reading frame of 36 amino acids (Figure 4.1 b & c).

In order to identify a cDNA, a *Pst* 1-*EcoR* 1 fragment which corresponds to positions 3047-3606 and contains 161bp of LB flanking sequence, was radiolabelled and used to screen cDNA libraries (obtained from *Arabidopsis* Biological Resource Centre). 1×10^6 plaques of both whole plant and silique cDNA libraries were screened but attempts to identify a cDNA were unsuccessful. This indicated that the transcript was

Figure 4.1. Genomic Organisation and Clone Sequence

- A) Organisation of the *Arabidopsis* genome. The *POLARIS* genomic locus is located at the bottom of chromosome IV. This region is boxed in blue and expanded to show the BAC contigs and the position of various markers. Database searches locate the *POLARIS* genomic locus on BAC F23K16. Shown at the bottom of A) is an analysis of open reading frames (starting ATG), larger than 75 amino acids, within approximately 10kb upstream and downstream of the *POLARIS* gene. Also shown are the positions of two ESTs, ATTS5022 and AI997385 (also AV527322), as well as the position of the *BRI1* gene and the 3.6kb *POLARIS* genomic locus.
- B) The sequence was kindly made available by Dr. J. Topping and Dr. I.M. Evans. Shown in red is the putative 92aa *GENE X* ORF (position 2422-2700), with the position of the EM1 RT3 primer (2535-2555) shown in bold. The full-length *POLARIS* gene is shown in blue (position 2735-3340). The putative 36aa ORF is shown in bold whilst the T-DNA integration site, between bases 3208 and 3209, is underlined. For more detailed sequence diagrams of *POLARIS* and *GENE X* see Figures 4.8 and 4.9.
- C) Open reading frames. All ORFs beginning with an ATG (Met) codon and ending in a STOP codon are shown. The T-DNA has inserted into a 36aa ORF (blue arrow →).
- D) NetGene2 output indicating splice sites and putative exons. This programme predicts both acceptor and donor splice sites based on homology to consensus sequences for these sites in *Arabidopsis*. The likelihood that such a site is actually used is expressed as a confidence value with 1.00 being highly probable. Putative exons are predicted on the GC content of a particular region of sequence. Exons, in general, have a higher G-C content than introns which are much more A-T rich. Putative exons are shown in the coding panels with a large positive value (0-1) of the trace (red line) indicating the position and length of an exon.

A

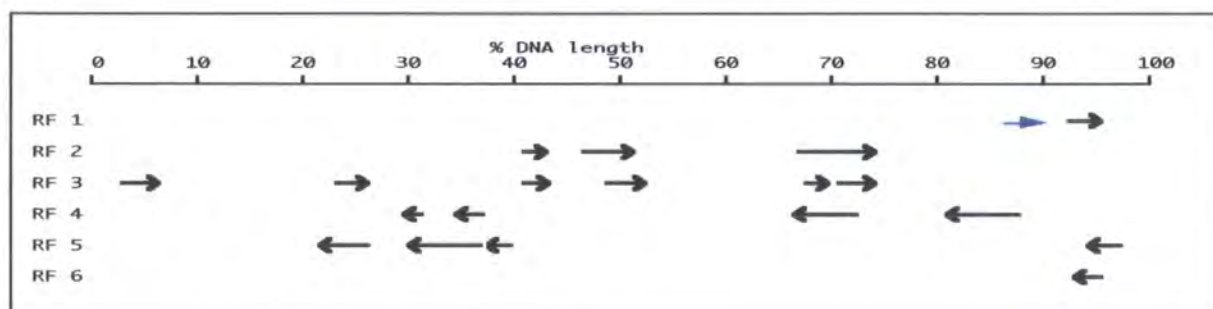


B

1 GAATTCGGAT CCCTGTAATT GGTGGGCTTT TAAATGTATC TTATTTTAAA
51 CGGAGTCAAC AGAAAATTAT ATTGTAATGA GTTCCAAAAA ACAGCTTATT
101 GAGTCTATGT TTCAAATTGA TGGGCCTTAT AATGGGCTTC TTTAAATTTT
151 ACAC TTGTTC AATAAAGACA GATTACCATA ATGAGCCTAT AGACGAGGAA
201 AAT TCTATTG GGTTTAATGA TAGACCCAAG TCCACGAATA TAGCGATCAC
251 GTGACAAACC AAGAAATTCG ACAAATGGAT AAGCGCGTTT AAGCACGTGA
301 GCGTCTCGAC TCTCTCGATT CCCAAAAGTG TAATGTAAAA CCTTAAATAG
351 TGTAATACGT TGATCAACTT AGATTACGAA ACCTTATTAC GAAAAGAAAA
401 CAAA ACTATT AAAGAAATAG AAATCATAAG TTACGAGGAC ATGAAAAGTT
451 GTGACCCGCT TGCTCCGCCG AGTCCGAGGG AGACTCCAC GTGATTCCCT
501 CGTGGACCGC ACGTTCGCTA CCTTAATCCA AGGTCTTAAA TAATCATTTT
551 CATAACTACTG TATACTATGT ATCAATGTAA TTTAGTTAAT TTATCTCAAA
601 AATTGACACG ATAGCCAATT GTGTTGTTAC TCAAAGTATT TGCCATCATC
651 AAATTTCTTA TTTTTTTTCT TCTATTATAT ACTGATTTAC GACATTACAT
701 ATATATTTTAT GGACAACTG ATTCCATTTG CTAATTAGCT ATTATCAAAA
751 GCAAATTTTC CAATTATTTT ACAAGGCTCT GTTAAAGCAG TTCAAACCAT
801 TGGAAAAAGT TAAGATAACG TAATCCTGAC GCCCAAACAT TAATTATGGC
851 TTTAAAGAAA AAAAACTTG TTGAAAGGAG ACTGGGAATT AAAAACGAGA
901 AAGCTGGGAG AAGCTGCGAG GAGATGAATA TAATATTTGA AACTTCATTA
951 TACATTACCA AAATCTGAGC CGTCGCTTTT TGTTTCTTTG TCTCTTCGTC
1001 GTGAAAAGAA GGAAGATTCC TAGGTGAGAT GAATCCAACA ATTTCTTTGA
1051 TTAAATTAGT TTAACACTAT ATCTTTATTT TAGTTAAGGT ATTTTTTTGT
1101 AAGTTGTAAA GAGAGCCAAA CATATGGAGA CTAAATAACA TATATTGACA
1151 AAAAAAATA TATATGCAGA GAAAGTATTA TTCATAGACA TAATTTCGATT
1201 TAAGACTATG ATAATATATA TACAATACAT ATTAGAATAA GCTCTAGCAT
1251 GCAATTTGAC AGTAACTCGG TAAGAACAAC TTTGACCGCT TGTTATCATG
1301 TGAAATAATA ATATCTTGTT GATAGTCGTT ACGTACATTT TTACAAAACA
1351 TTATAAATCA CAGGTAAACA AAAAATATGC AGAAATATTG TTATCCTTTG
1401 AGTCAATAGA GAACGTATTT ACATAGTTTT TTCCACGACG ACACATTTAA
1451 CTAATCAACG TCGTTTTTCAG AAGTCTTAGC TGTATATGAA TGGCAGAGAG
1501 CTCACACGCG TGGAAATGGG TTTGTCTACA TGTTTACGTA CAAAACAAAT
1551 TCTTAATTAT TTTCTTTGTT TG TAGCTTTG TG TAGTTCTG ACATCGTCGA
1601 AACCTCAGTT TCTAAACAAT TTATTTGACA AACAAGCTTT AGCCCGTGCG
1651 GGAAGTTTTG TACGTGAGAA AGAAGCCTCG AGAATGAATA AA ACTACGAT
1701 AAGATTGATT CAACTTCAGA TTTCCAACCC CATAACTAGG TATATATACA
1751 TATATAAATT GATTAATGAT TATGTATTTA CGTACACATC GCAATCCTCC
1801 ACTTATATGC CTTACAGAAA AATATCTAAA TGCATGGACC GTCTTGCACT
1851 TGACCCATAT TTACATATTT AGAGCAATTT TATATGTACA TAATCAGATA
1901 CATGACGACG TT TAAACGTG AATTATTGGT TTGATTGAAA GAAAAGATC
1951 CTAAAATGAT AGAATGGTTT TGTAATTATG TATTTTTAGT ACAAATTGCT

2001 TAATTCCTTT GAATCGTAAC CCTTTATGTG TTCAAGTACG CCCTAATTTT
 2051 ATCAAAATTT ATGATAGGAA ACAAATTTCT ACCACCGTGT TATGTTTTTA
 2101 CTAATTTTTT TTTGTAGTTC CTATTAATTT TGTCATTTGC AACTCAGAAT
 2151 TTTTGTATTA TAGTATAAGT ATAATTTTTA TGGATAGTGG CTTTTTTTGC
 2201 ATTGTGCGTA TTCCTGTATT TAATTTTATG TGACTTGATT TCTTGATATC
 2251 AGACAAAGAG CAATGAAACC CACGTACGTA CCCAATAATT CCGCGTAACG
 2301 AATAGTATTA TTGACAAGTT GTCAAAATAA TATATAAAAT TTCTTAAGGC
 2351 ATATGAAAAA AACAAAATGT ATTAAGAATA TTTATTAGGA AGATAATAAA
 2401 TTAATTAAGA GAAGTGTATG **GATGAGAAGG AAACACACGT GGGAGAGAGA**
 2451 **TGAGAGAGGG AAAGAGAGGA AGAGGTCAAT TCGGCGGAGA CAGGAAAGGG**
 2501 **ACGGCGGCCC ACGGCGGAAG GAGACGTTGT TAGGGGAAGT TTCCGACAAG**
 2551 **AACAGCTTGC ATGCACGGTG GCCCACGTGC TCCGTACCCA CCACCGTCGC**
 2601 **GCGTGTTCCG CTTGATAGCT ACTCATCTCT TCTTTTCCTT CTTCACAGT**
 2651 **TTCAGCGCGT TTGTTTATAC GCGCCTATGT CAGTGTCTTG TCTAGGATGA**
 2701 ATAATAGTGT ATTGGTATGT ATGTGCACGT ATCCGTATCG CATTTGTTTC
 2751 AAGTTTTTTT TTCTATAATG TTTCTTCGAA ATCCATGATC ATATAGTATA
 2801 TAAGAAGCAT GTATTTATAA TGTTCACCTT AATATATTAG TATTGGAGAC
 2851 TAAAGCGAAC ATATAAAACC CAAATAAACC TTTCTTTAAG TTTTATTAAA
 2901 AGTCTAAACA CTTGATTTGT GTTTTAGTTT GGGTAGTAGT GAGAAAAGAA
 2951 AAATAAATAA TCAAAAAGAT TAAAGAAGAA AGAATTTGAA AGCAAGGAAC
 3001 ACGAAATCCG AAGAGCGAGG GGAGCGAAGA CAGTCCACGT AGCTGCAGAG
 3051 AGAAAGAGAA GAGCACGTGA GGCACACGTT CTTGTGTAA GACTTGTTGT
 3101 GGTGATGTTG GCGCAGTGTC TCACTGAAAC ATGAATGAAA **CCCAGACTTT**
 3151 **GTTTTAATTT CAGGCGAAGG TCCATTTCTC CATGTTATAT ATCAATCTCT**
 3201 **TATTTATTAG TAGCAAAATT GTTTAAACTT TTTAAATCC ATTGATCACC**
 3251 CTATCATTTT CAATATCTAC ATACAATCTT ATGTCTCGAT AAAGGTTTAT
 3301 CTTTATCTTA TTATGCAATA CATATCCCTC CCATTTCTAT ATTGCAAATT
 3351 ATGACATCAA AAAACCATTC TTTTGATTCT ACTTGGGCCA ATAACAAAAT
 3401 CAATAGTAAT GGAAAAAATA ACGTAGATGG ATATAAATAT AGTCCAACGG
 3451 TTCAATTTCA TCAGTAATAA GTATATAGCA AAAAAAAAAA CGTTTAACTC
 3501 AGCATAGTTC AAAAGGGACC ACATTGGTCA TGTAATATA ACATCCATAA
 3551 AAACAAATTT AAGTCTCATC TATTCTCACT TTCCCATTCC CGTGCAGTGT
 3601 GAATTC

C



D

Donor splice sites, direct strand

pos	5'→3'	phase	strand	confidence	5'	exon	intron	3'
297		1	+	0.74	GT	TTAAGCAC	^GTGAGCGTCT	
335		0	+	0.74	AA	AGTGTAAT	^GTAAAACCTT	
513		0	+	0.90	TG	GACCGCAC	^GTTTCGTACC	
533		1	+	0.88	TT	AATCCAAG	^GTCTTAAATA	
1024		0	+	0.97	AG	ATTCCTAG	^GTGAGATGAA	
1270		0	+	0.93	CA	GTAACCTCG	^GTAAGAACAA	H
1740		2	+	0.94	CC	ATAACTAG	^GTATATATAC	H
2274		1	+	1.00	TG	AAACCCAC	^GTACGTACCC	H
2715		0	+	0.88	TA	GTGTATTG	^GTATGTATGT	
3087		0	+	0.74	CG	TCCTTGT	^GTAAGACTTG	
3170		0	+	0.87	TC	AGGCGAAG	^GTCCATTCTT	

Acceptor splice sites, direct strand

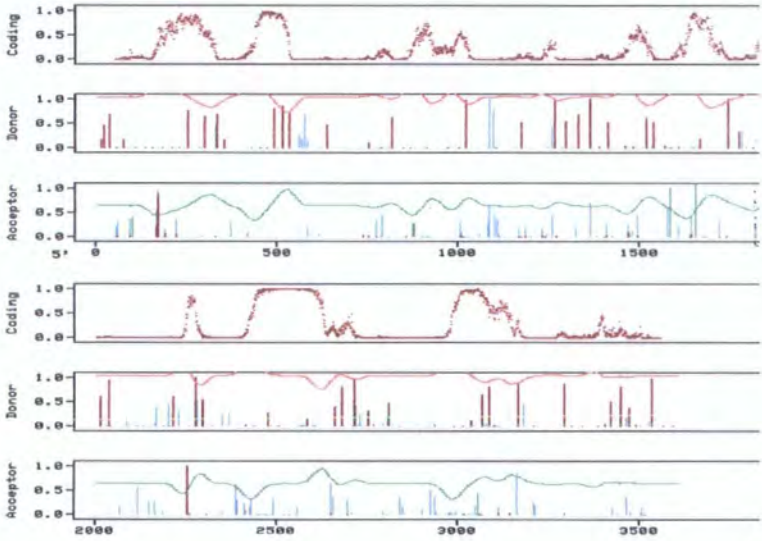
pos	5'→3'	phase	strand	confidence	5'	intron	exon	3'
171		1	+	0.93	AT	AAAGACAG	^ATTACCATAA	
2252		1	+	0.93	TT	GATATCAG	^ACAAAGAGCA	

CUTOFF values used for confidence:

Highly confident donor sites (H): 95.0 %
Nearly all true donor sites: 50.0 %

Highly confident acceptor sites (H): 95.0 %
Nearly all true acceptor sites: 20.0 %

Direct strand (+ strand)



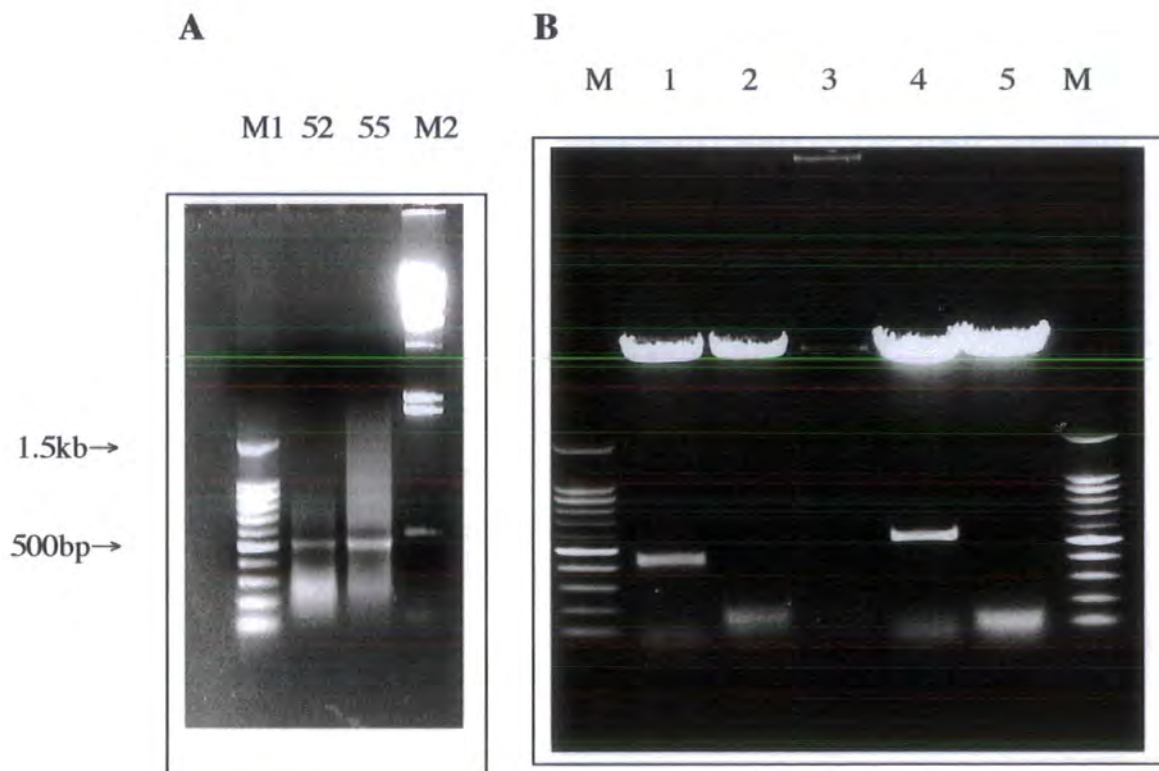
either very low abundance and was not represented in the cDNA library, or that the probe did not contain enough homologous sequence to the putative cDNA.

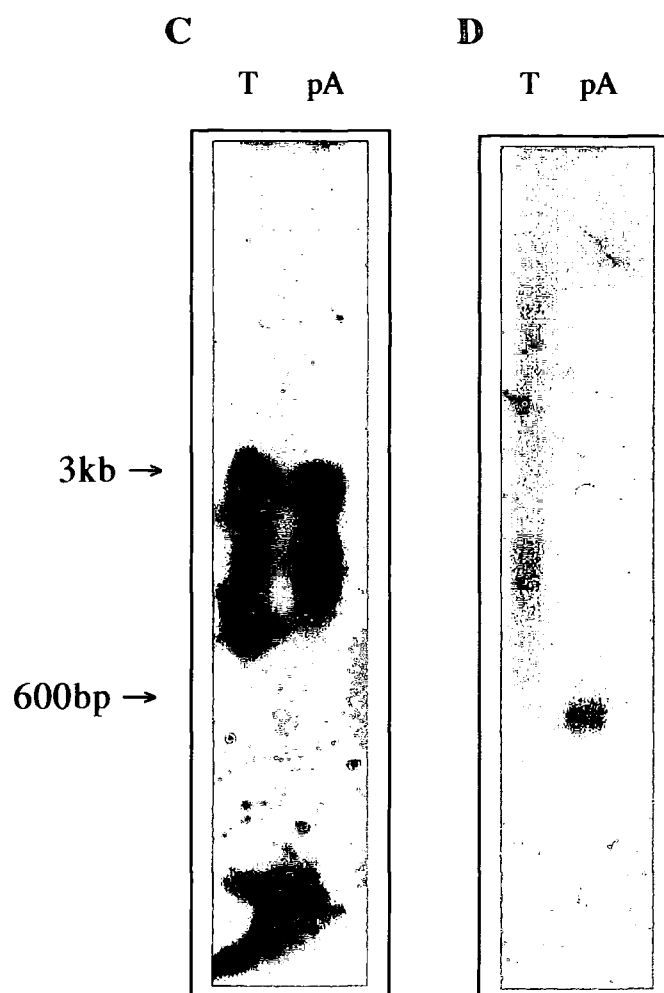
Prior to the 5' RACE experiments on the transgenic line, described in the previous chapter, a second approach to try to identify a cDNA was utilised. The genomic sequence was subjected to analysis by the NetPlantGene programme (Hebsgaard *et al.*, 1996) which predicts splice sites and also putative exon sequence. The output indicated that in the 700bp of sequence upstream of the T-DNA insertion site there were two possible exon-like regions (Figure 4.1 d). The putative exon farthest from the T-DNA displayed partial overlap with the 92 amino acid open reading frame (Figure 4.1 b) whilst the second exon did not have an open reading frame associated with it. The region into which the T-DNA had inserted was immediately downstream of this second putative exon. A possibility therefore was that the T-DNA had either inserted into the intron of a gene, an untranslated region or an intragenic region.

The most likely candidate for a transcribed region was the region encoding the putative 92 amino acid polypeptide. To determine if this region was transcribed and whether the T-DNA may have inserted within the putative gene an oligonucleotide primer (EM1 RT3:GGAAGTTTCCGACAAGAACAG, Figure 4.1b) was designed for 3' RACE. This method allows the isolation of the 3' ends of transcripts when only a small region of 5' sequence is known. RNA was extracted from wild-type 7 day seedlings (Columbia ecotype) and 3' RACE performed as described in sections 2.10.2 and 2.10.3 and the results of the PCR reaction can be seen in figure 4.2a. The major product of approximately 500bp was cloned and sequenced (Figure 4.2 b). Alignment with the 3.6kb genomic clone revealed that the amplified cDNA was completely contiguous along its entire length of 316 or 317bp from the EM1 RT3 primer site to a polyadenylation site at position 2851 or 2852 (GACTA, Figures 4.1b, 4.9). The remainder of the clone was poly(A) indicating that the oligo d(T)₁₅ anchor primer had, as should be expected, annealed to the transcripts poly(A) tail and that the clone was not a result of genomic DNA contamination. The fact that the polyadenylation site for this transcript is approximately 360bp upstream of the T-DNA (Figure 4.1 b) indicated that it was unlikely that this transcript represented the tagged gene. However, to ensure this was the case, northern analysis was performed using polyA⁺ RNA isolated from 7 day old AtEM101 seedlings with the radiolabelled 3'RACE clone as a probe. As a control a duplicate lane was hybridised to a GUS probe. If the transcript was associated with the T-DNA it was expected to hybridise to the GUS-fusion transcript which previously had been shown to initiate outside the T-DNA left border (Section 3.2.1). The result shown (Figure 4.2 c & d) indicates that the novel cDNA does not cross-hybridise with the

Figure 4.2. Cloning of *GENE X* by 3' RACE and Analysis of Expression in the AtEM101 line

- (A) 3' RACE reaction using the oligod(T)RACEAMP and RT3 primers at 52°C and 55°C annealing temperatures (M1-100bp ladder, Promega; M2- λ HindIII, Gibco BRL)
- (B) Plasmid preps and *EcoRI* digests. Plasmids in lanes 1 and 4 contain inserts and were sequenced with plasmid 1 proving to be *GENE X* (M-100bp ladder, Promega).
- (C) RNA gel blot analysis was performed on 20 μ g of total RNA (T) and 2 μ g of poly(A) RNA (pA) from the AtEM101 line and probed with a randomly labelled GUS probe.
- (D) RNA gel blot analysis was performed on 20 μ g of total RNA (T) and 2 μ g of poly(A) RNA (pA) from the AtEM101 line and probed with a randomly labelled *GENE X* probe.





GUS-fusion transcript and that it is in fact a small, low abundance transcript of approximately 500bp. This result indicated that this novel gene, named *GENE X*, was likely not to be the gene interrupted by the T-DNA.

Given this result no further molecular characterisation of this novel gene was performed. However sequence analysis revealed that *GENE X* could encode two possible polypeptides, one of 92 amino acids as stated and also a second of 44 amino acids, the ATG codon of which was 140bp downstream of the larger polypeptides ATG. Given the size of the transcript at approximately 500bp the transcriptional start site would be around position 2360 on the genomic clone given that there is no splicing of the message. This is supported by the presence of a TATA box (TATATAA) at approximately position 2331, 90bp upstream of the translational start of the 92 amino acid polypeptide.

Since the polyadenylation site of *GENE X* was only 356bp upstream of the T-DNA insertion site there was the possibility that the T-DNA had inserted in the promoter of a downstream gene and not in coding sequence. To determine if this might be the case, a further 1kb of the lambda genomic clone was sequenced (Dr. I. M. Evans, unpublished results). Database searches (Arabidopsis thaliana database, BLAST search) identified the sequence as that of the *BRI 1* gene, a putative receptor kinase involved in brassinosteroid signalling. This gene had been mapped to the bottom of chromosome 4 between the SSLP marker nga1107 and the CAPS marker DHS1 (Li and Chory, 1997; Figure 4.1 a). The *BRI 1* gene was located on the non-transcribed strand and ended virtually at the *EcoR* 1 site that completes the 3.6kb genomic clone. Therefore the *BRI 1* gene was in the wrong orientation to activate the T-DNA promoter trap and was approximately 400bp downstream of the T-DNA insertion site suggesting that it was unlikely that *BRI 1* was the tagged gene in the AtEM101 line.

Analysis of approximately 4.6kb of genomic sequence had therefore revealed that the T-DNA in the AtEM101 line had inserted into a 755bp region between two genes, *GENE X* and *BRI 1* on chromosome 4, neither of which were transcriptionally linked to the T-DNA. Screening of cDNA libraries with a probe spanning the T-DNA insertion site but not containing any portion of the *GENE X* or *BRI 1* genes had not identified a transcribed sequence. The possibility remained that the T-DNA had inserted not into a gene but into intragenic region and had been spuriously activated, possibly due to its close proximity to the two aforementioned genes. Database searches using a 22.5kb fragment of the BAC clone F23K16, containing approximately 10kb of DNA both upstream and downstream of the T-DNA insertion site revealed only two other ESTs

(ATTS5022 and AI997385), neither of which fell within the 3.6kb genomic locus (Figure 4.1 a).

4.2 Cloning of the *POLARIS* gene

It had been determined that the initiation of transcription of the GUS-fusion transcript occurred outside of the T-DNA left border (Chapter 3.2.1) indicating the presence of possible promoter-like elements between *GENE X* and the T-DNA. Analysis of the genomic sequence between the T-DNA insertion site and the polyadenylation site of *GENE X* revealed a putative TATA box (consensus sequence TATA^A/_TA^A/_T), of sequence TATATAT, only 25bp upstream of the insertion site. However, a GUS-fusion transcript initiating downstream of this element would not hybridise to the probe used in the conditions of hybridisation. Therefore, to determine the transcriptional start site, 5' RACE was performed on the GUS-fusion transcript as described in Chapter 3.2.2. The results of this experiment revealed transcription was initiating at least 190bp upstream of the T-DNA insertion site.

4.2.1 Isolation of a partial cDNA by 3' RACE

To resolve whether transcriptional initiation outside of the left border was due to the close proximity of *GENE X* and *BRI 1* or whether it was due to the T-DNA inserting within another gene, 3' RACE was performed. Two oligonucleotide primers, 3.0 Prom and 3.1 Prom, which anneal approximately 200bp and 100bp respectively upstream of the T-DNA, were designed based upon the GUS 5' RACE results. Figure 4.3 indicates the position of these primers and also other primers mentioned in this chapter. For the 5' RACE 1µg of poly(A)⁺ RNA from 7 day seedlings (Columbia ecotype) was reverse transcribed with the Oligo d(T)₁₅ anchor primer. PCR amplification of the cDNA was then performed with either primer 3.0 Prom or 3.1 Prom in combination with the RACE anchor primer. An aliquot of the amplification products were resolved by agarose gel electrophoresis and blotted to membrane following which they were hybridised to the ³²P labelled 560bp *Pst* 1-*EcoR* 1 probe. This probe spans the T-DNA insertion site but does not contain the 3.0 prom primer site. Two bands of approximately 400bp and 300bp corresponding to the reaction products of the 3.0 Prom and 3.1 Prom primers respectively hybridised strongly to the probe though neither of these bands represented major products of the 3'RACE reactions (Figure 4.4 a & b). The products of the 3.0 Prom reaction, which represented the longest product, were cloned directly and the resulting recombinant colonies were transferred to membrane and hybridised with the

Figure 4.3. Primer Sites

A schematic diagram of the *POLARIS* locus is presented with the positions of various primers, described in the text, indicated by arrows. Numbers refer to the position of the 5' nucleotide of the primer. Larger arrows within the grey rectangle represent the putative *GENEX* and *POLARIS* open reading frames. The asterisk indicates a *Pst*I site. The dashed arrow shows the antisense RNA probe used during the RNase protection assay experiments

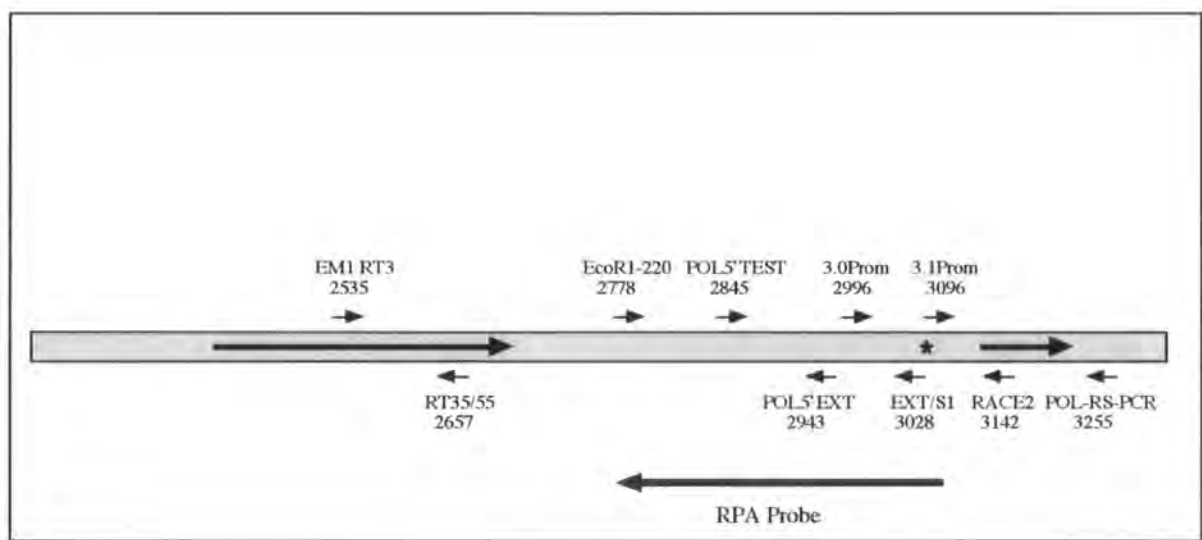


Figure 4.4. Cloning of a Partial *POLARIS* cDNA by 3' RACE

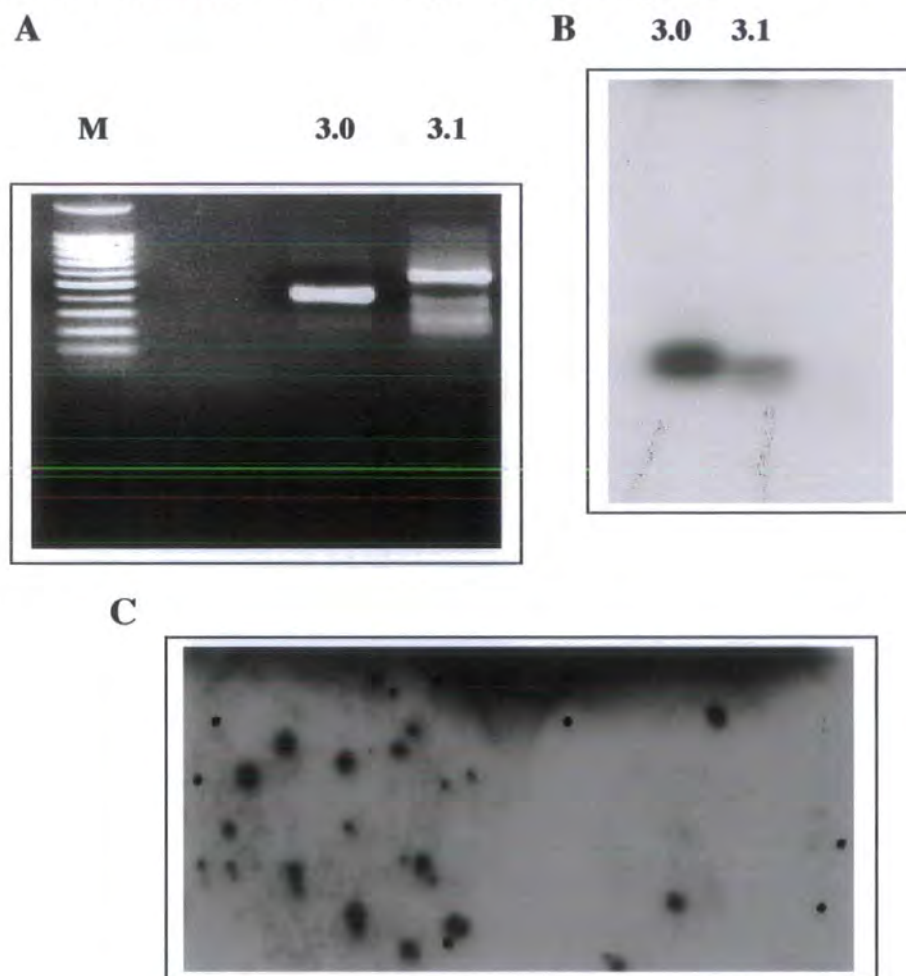
(A) 3' RACE performed with the oligod(T)RACEAMP primer and either the 3.0prom or 3.1prom primers (M-100bp ladder, Promega). Products were analysed on a 1% ethidium bromide stained agarose gel

(B) Southern analysis of the 3' RACE products. The Gel from (A) was blotted and probed with the randomly labelled 560bp *Pst*I-*Eco*RI fragment.

(C) Colony hybridisation. The 3.0prom 3' RACE reaction was shotgun cloned into the pCR2.1 vector and transformed into bacteria. Colony lifts were performed and membranes hybridised with the randomly labelled 560bp *Pst*I-*Eco*RI fragment.

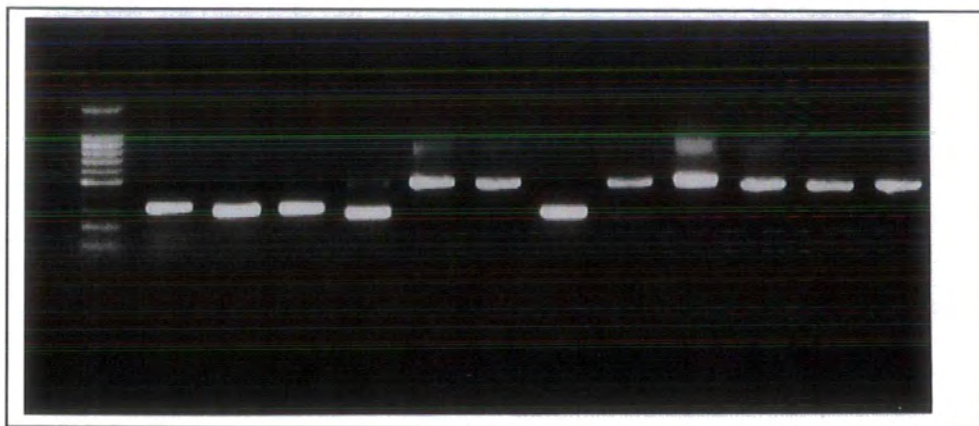
(D) Colony PCR. Inserts of positive colonies from (C) were amplified with the M13 forward and M13 reverse primers and analysed on a 1% ethidium bromide stained agarose gel (M-100bp ladder, Promega).

(E) Southern blot analysis of the colony PCR gel from (D). The membrane was hybridised with the randomly labelled 560bp *Pst*I-*Eco*RI fragment.



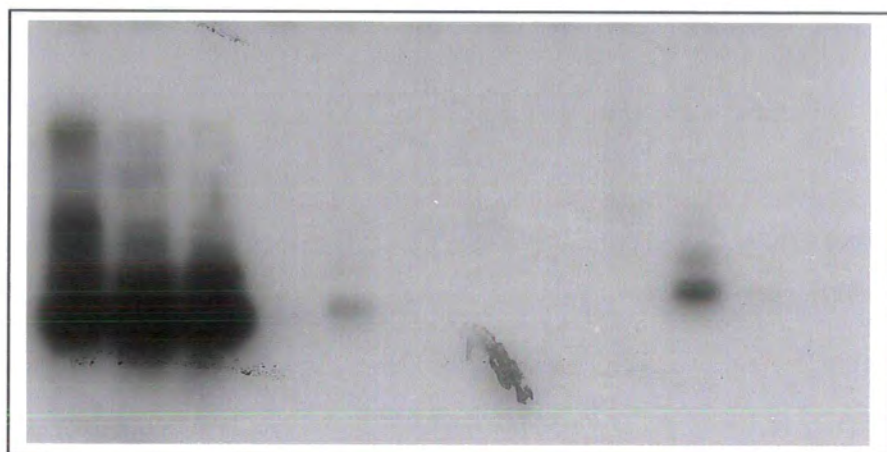
D

M 1 2 3 4 5 6 7 8 9 10 11 12



E

1 2 3 4 5 6 7 8 9 10 11 12



560bp *Pst* 1-*EcoR* 1 probe (Figure 4.4 c). Colonies that tested positive were grown in liquid culture and plasmids isolated. Inserts were excised by enzyme digestion and again blotted to membrane followed by hybridisation to the same probe (Figure 4.4 d & e). Inserts that hybridised to the probe were sequenced and the sequence compared to that of the 3.6kb genomic clone. One clone aligned completely with the genomic sequence from the 3.0 Prom primer site to a polyadenylation site 55bp downstream of the T-DNA and represented a partial cDNA of approximately 270bp.

The isolation, by 3' RACE, of this cDNA indicated that the T-DNA in the AtEM101 line had inserted within a gene which was named *POLARIS*. Database searches with this partial cDNA did not identify any sequences with a high degree of similarity indicating that *POLARIS* is a novel gene.

To determine the number of copies of the *POLARIS* gene in the *Arabidopsis* genome Southern analysis was performed. Figure 4.7 b shows the result of hybridisation of the partial *POLARIS* cDNA at high stringency to genomic DNA from wild-type plants that had been digested with the indicated restriction endonucleases and then size fractionated by agarose gel electrophoresis followed by transfer to membrane. The result would suggest that the *POLARIS* gene is found at a single locus in the genome.

4.2.2 Determining the transcriptional initiation site

The 3' RACE experiment described in the previous section was based on the results of the 5' RACE experiments performed on RNA isolated from the AtEM101 line. However, it was not known whether the 5' RACE product obtained extended to the transcriptional start site. In order to identify the initiation site of the *POLARIS* gene two experimental approaches were taken. Firstly, the start site was roughly mapped by RNase protection assays following which it was fine mapped by repeating the 5' RACE experiments with a new set of oligonucleotide primers (Figure 4.3).

For the RNase protection assays (RPA) an antisense probe was generated by amplification of a 299bp region of the genomic locus using the oligonucleotides *EcoR* 1-220 and EXT/S1 (Figure 4.3) followed by cloning into the pCR2.1 TOPO vector (Invitrogen). The EXT/S1 primer site was approximately 80bp downstream of the 3.0 Prom primer site used in the cloning of *POLARIS* by 3' RACE, whilst the *EcoR* 1-220 primer site was approximately 75bp upstream of the *GENE X* polyadenylation site. The fragment was orientated such that it would produce an antisense RNA to the *POLARIS* transcript following transcription from the vector's T7 promoter. The full length probe includes vector sequence from the T7 promoter site to the multiple cloning site, as well as

further vector sequence from the cloning site to the *Bam*HI site where the vector was linearised for *in vitro* transcription. Therefore, the full-length probe is 413bp (lane Y-, Figure 4.5.), with only 299bp complementary to the *POLARIS* genomic sequence. The [³²P]α-UTP labelled antisense probe was annealed to either 50µg total RNA isolated from AtEM101 7 day seedlings or 5µg poly(A)⁺ RNA isolated from 7 day wild-type seedlings (Columbia ecotype). The products of the RPA were resolved by denaturing polyacrylamide gel electrophoresis followed by autoradiography. As can be seen in figure 4.5 RNA from both the transgenic line and wild-type plants resulted in a major protected fragment of approximately 250bp whilst a less intense band of 299bp, corresponding to the full complementary region of the probe was also seen. This result indicates that as should be expected, transcription initiates from the same site in both the transgenic line and wild-type. More surprisingly it also suggested that the start site was within the transcribed region of *GENE X*. The fact that there were two protected fragments indicated two possibilities. One was that the full length protected fragment was due to hybridisation with contaminating genomic DNA in the RNA sample. The second explanation was that there could be two start sites with the one that results in the 250bp protected fragment used more frequently by the transcriptional machinery.

To resolve this question, 5' RACE experiments were repeated on RNA from both the wild-type and transgenic line. Synthesis of cDNA was performed using the primer RACE 2 (Figure 4.3) with either 2µg poly(A)⁺ RNA from 7 day wild-type seedlings (Columbia ecotype) or 20µg total RNA isolated from 7 day AtEM101 seedlings. Following tailing of the cDNA, primary PCR was performed using the oligo d(T)₁₅ anchor and EXT/S1 primer pair. Secondary PCR was performed using the RACE anchor and POL 5'EXT primer pair (Figure 4.6). The secondary PCR products were cloned directly and recombinant bacterial colonies screened by PCR using the primer pair, POL 5'EXT and POL 5' TEST, which generate a 100bp product. The POL 5' TEST primer anneals across the *GENE X* polyadenylation site which, from the RPA results, corresponds approximately to one of the putative start sites. Plasmids were isolated from colonies that tested positive by this screening approach and were sequenced. The RACE products fell into two distinct groups of approximately 120bp and 200bp with little indication of intermediate length products. The size of the 5' RACE products correlated well with the RPA results. Alignment of the longest clones in the two groups with genomic sequence indicated two putative start sites approximately 95bp apart with both upstream of the *GENE X* poly(A) site. Start site 1, which is approximately 23bp upstream of the poly(A) site, has the sequence CCACTTAATA

Figure 4.5. RNase Protection Assay on AtEM101 and Wild-type RNA

RPA was performed using a radiolabelled antisense *POLARIS* transcript. This was hybridised with 20µg AtEM101 total RNA (E), 100µg Columbia total RNA (Ct) or 5µg Columbia poly(A) RNA (Cp). Following RNase treatment products were separated on a urea polyacrylamide gel which was then exposed to x-ray film. As controls, yeast RNA was hybridised with the *POLARIS* probe and then either subjected to RNase treatment (Y+) or left untreated (Y-). Radiolabelled ϕ X174 *Hinf*I DNA markers (M) were used for determining product size. AtEM101 and Columbia poly(A) lanes show the two protected fragments which correspond to transcription start sites 1 and 2 (TS1+2). The intensity of the bands give an indication of the relative use of each start site

M Y- Y+ E Ct Cp

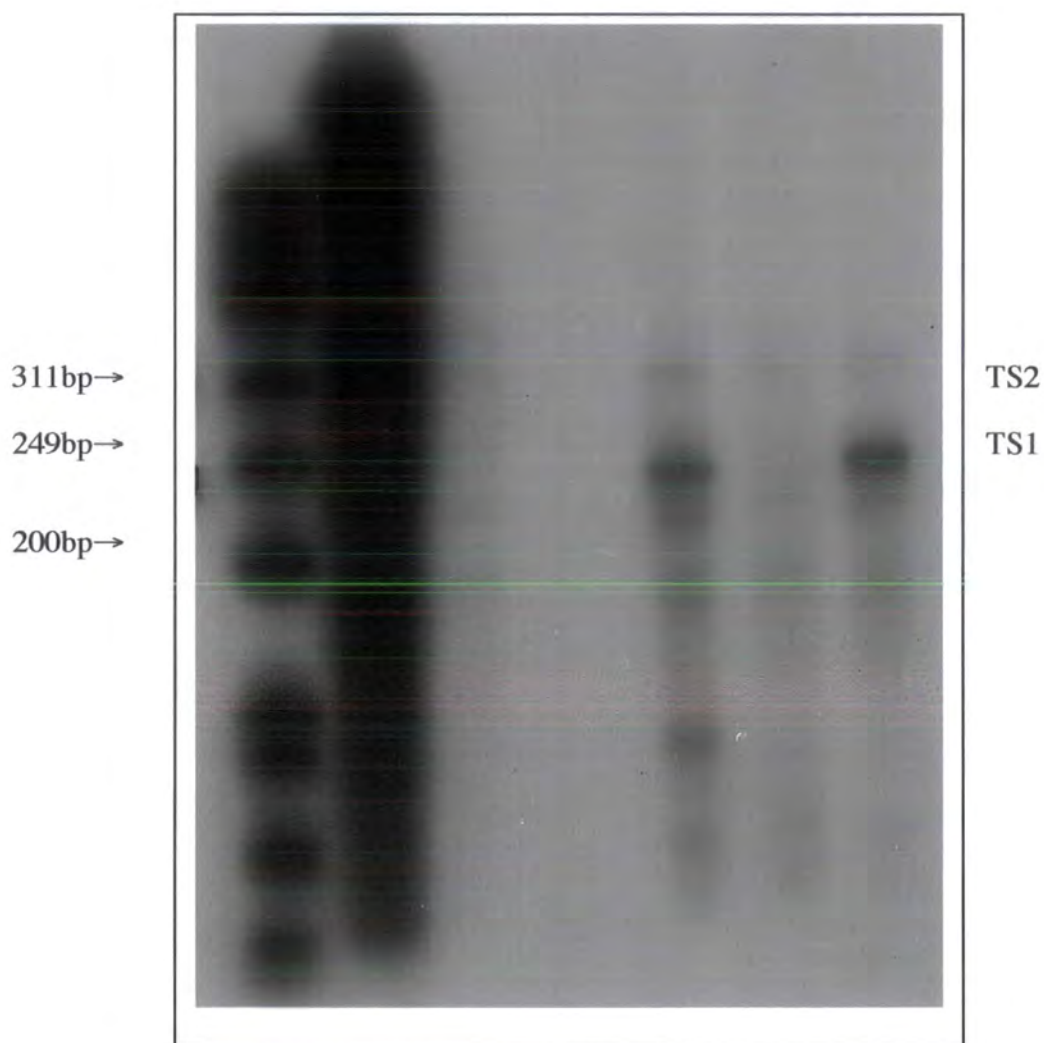
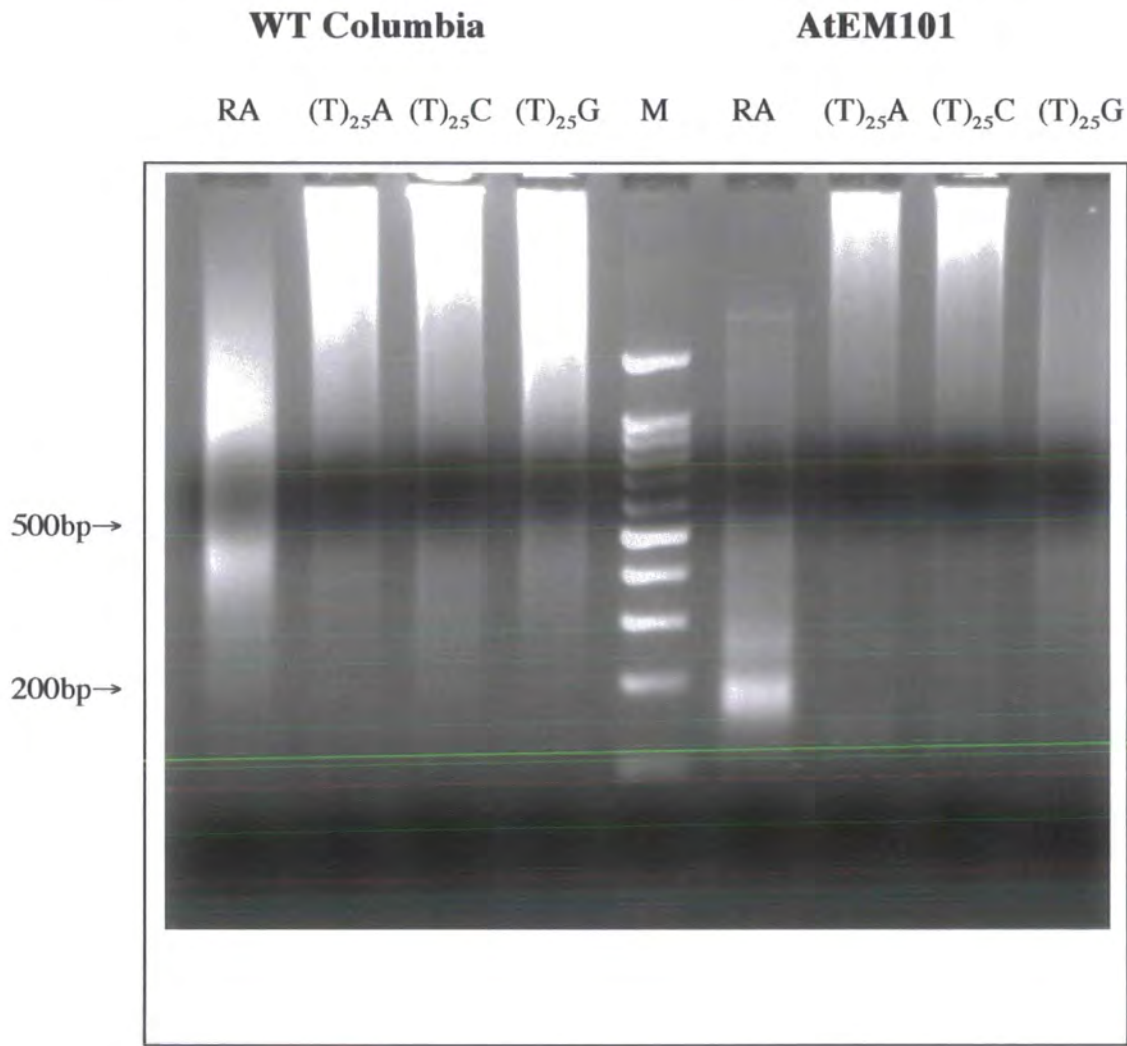


Figure 4.6. Isolation of the Transcript Start Site of *POLARIS* by 5'RACE

5' RACE was repeated using either 2µg of wild-type poly(A) RNA or 20µg of AtEM101 total RNA. Second round PCR was performed on a 1:20 dilution of the first round PCR reactions using the POL 5'EXT primer and either the RACE Anchor primer (RA), (T)₂₅A, (T)₂₅C or (T)₂₅G primers. Products were analysed on a 1% ethidium bromide stained gel alongside DNA molecular markers (M-100bp ladder, Promega).



with the RACE results unable to resolve which of the three highlighted bases is likely to represent the initiation site. Start site 2, which is approximately 117bp upstream of the poly(A) site, has the sequence ATCCGTAT (Figures 4.8 and 4.9 a & b). Two RACE clones had an additional G residue indicating that the reverse transcriptase had proceeded through the methylated G cap. The RPA results indicate that the start site generating the shorter transcript, start site 1, is used more frequently than start site 2. The possibility remains that strong RNA secondary structure is responsible for the results seen in both the RACE and RPA experiment. However, analysis of the sequence upstream of the putative start sites reveals that start site 1 has a very good predicted TATA box, TATATAA, at positions -32 to -26. In comparison, start site 2 has a poorer TATA like sequence, AATAATA, at positions -35 to -29. This could be considered support for two initiation sites rather than RNA secondary structure and could explain why site 1 appears to be used more frequently.

4.2.3 Structure of the *POLARIS* gene

Cloning of the *POLARIS* gene by both 5' and 3' RACE allows for an accurate sizing of the transcript at between 427bp or 606bp. Northern analysis using the 3' RACE clone as a probe supported this sizing and also indicated very low steady state levels of the transcript (Figure 4.7 c). Unlike the GUS-fusion transcript there was no evidence that there was any splicing of the wild-type transcript. Database searches with the transcript sequence did not identify any genes sharing strong homology. The cDNA did however identify a BAC clone mapped to chromosome 4 confirming the previous assumptions based on the location of the T-DNA near *BRI* 1 (BAC clone F23K16, GenBank ATF23K16, Figure 4.1 a).

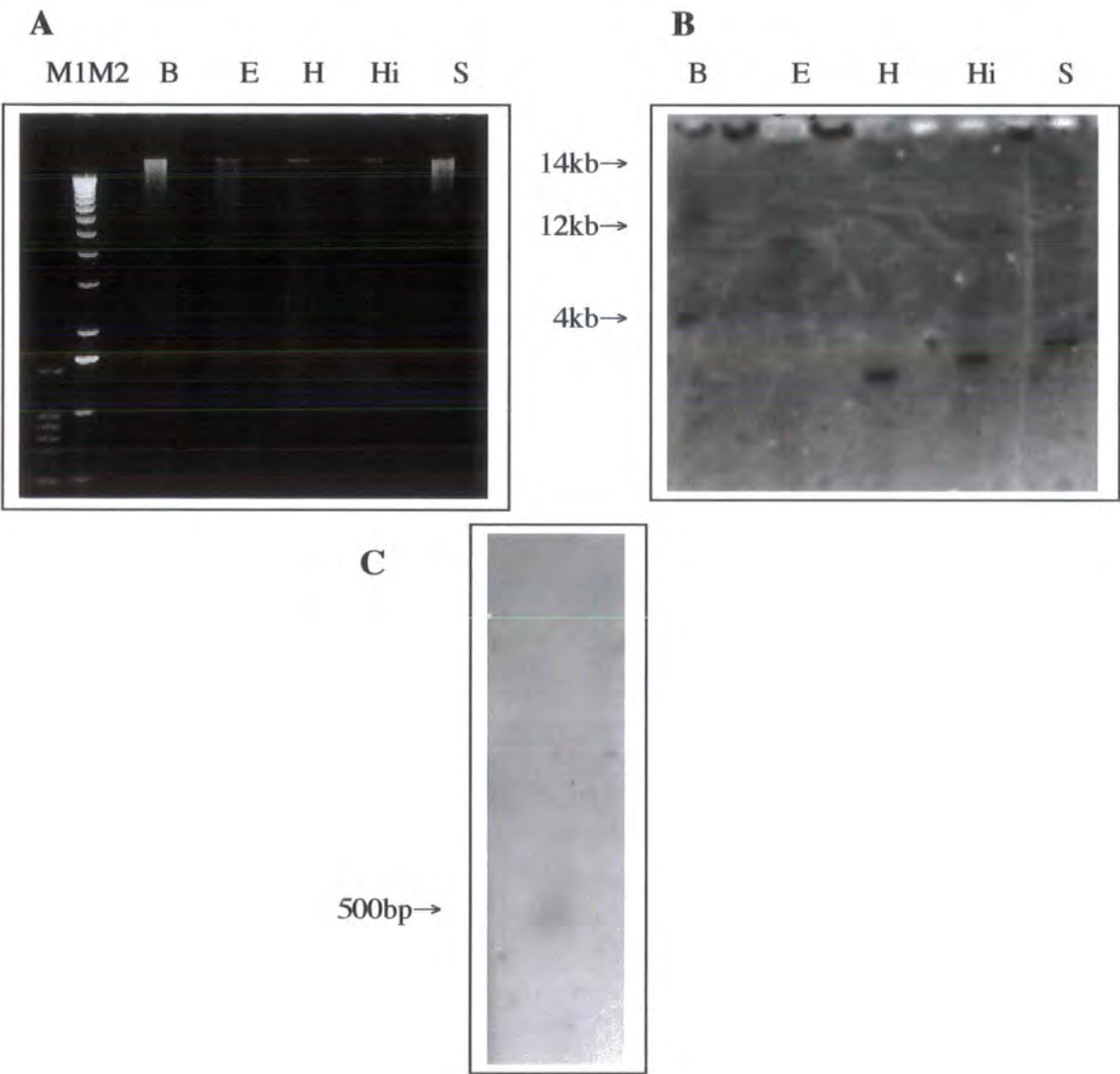
The structure of the *POLARIS* gene was further complicated when, following further 3' RACE experiments, it was found that the 3' end of the transcript is variable. Four separate polyadenylation sites were identified following the random sequencing of separate 3' RACE clones. Three of these, which included that of the poly(A) site first identified, were within a 14bp region of each other. The last poly(A) site is situated a further 70bp downstream as shown in Figure 4.8 (see also Figure 4.9). Many mammalian genes have a poly(A) signal with a consensus sequence AAUAAA 10-30bp upstream of the transcripts 3' end. This sequence is either missing from many plant genes studied (Kuhlemeier, 1992) or less conserved with a consensus AAUNNN (Gallie and Bailey-Serres, 1997). However, analysis of upstream sequence did identify putative signals. Approximately 25-30bp upstream of the grouped poly(A) sites was the sequence TTATAA with the same element also appearing 10bp further upstream. The

Figure 4.7. Southern and northern analysis of *POLARIS*

A) 1.5µg of DNA (Columbia ecotype) was digested with *Bam*HI (B), *Eco*RI (E), *Hinc*II (H), *Hind*III (Hi) or *Sac*I (S) and separated on a 1% ethidium bromide stained agarose gel alongside DNA molecular markers (M1-100bp ladder, M2-1kb ladder; Promega) and blotted to membrane.

B) The membrane was hybridised with the randomly labelled *POLARIS* 3'RACE cDNA.

C) RNA gel analysis was performed with 2µg of poly(A) RNA (Columbia ecotype) and probed with the randomly labelled *POLARIS* 3'RACE cDNA.



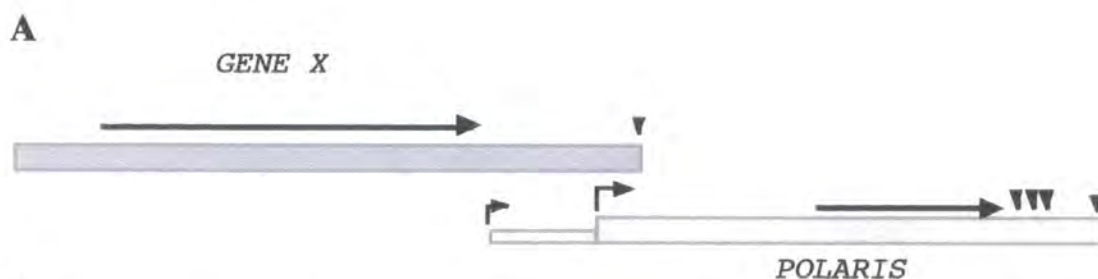
```

1   GTATCGCATTTGTTTCAAGTTTTTTTTTCTATAATGTTTCTTCGAAATCC
51  ATGATCATATAGTATATAAGAAGCATGTATTTATAATGTTCCACTTAATA
101 TATTAGTATTGGAGACTAAAGCGAACATATAAAACCCAAATAAACCTTTC
151 TTTAAGTTTTATTAAAAGTCTAAACACTTGATTTGTGTTTTAGTTTGGGT
201 AGTAGTGAGAAAAGAAAAATAAATAATCAAAAAGATTAAAGAAGAAAGAA
251 TTTGAAAGCAAGGAACACGAAATCCGAAGAGCGAGGGGAGCGAAGACAGT
301 CCACGTAGCTGCAGAGAGAAAGAGAAGAGCACGTGAGGCACACGTCCTT
351 GTGTAAGACTTGTTGTGGTGATGTTGGCGCAGTGTCTCACTGAAACATGA
401 ATGAAACCCAGACTTTGTTTTAATTTTCAGGCGAAGGTCCATTTCTCCATG
    M K P R L C F N F R R R S I S P C
    *
451 TTATATATCAATCTCTTATTTATTAGTAGCAAAATTGTTTAAACTTTTAA
    Y I S I S Y L L V A K L F K L F K
    ↓       ↓       ↓
501 AAATCCATTGATCACCTATCATTTTCAATATCTACATACAATCTTATGT
    I H
551 CTCGATAAAGGTTTATCTTTATCTTATTATGCAATACATATCCCTCCCAT
    ↓
601 TTCTATATTGCAAA

```

Figure 4.8. The *POLARIS* Transcript

Nucleotide and deduced amino acid sequence of the *POLARIS* transcript. The bold arrowhead indicates the main transcript initiation site and smaller arrows indicate poly(A) sites. Underlined is the 9 amino acid upstream ORF that precedes the 36 amino acid ORF. The asterisk marks the T-DNA insertion site.



B

CAAAATGTATTAAGAATATTTATTAGGAAGATAATAAATTAATTAAGAGA
 AGTGTATGGATGAGAAGGAAACACACGTGGGAGAGAGATGAGAGAGGGAA
 AGAGAGGAAGAGGTCAATTCGGCGGAGACAGGAAAGGGACGGCGGCCAC
 GGCGGAAGGAGACGTTGTTAGGGGAAGTTTCCGACAAGAACAGCTTGCA
 GCACGGTGGCCACGTGCTCCGTACCCACCACCGTCGCGCGTGTTCGCT
 TGATAGCTACTCATCTCTTCTTTTCTTCTTCCACAGTTTCAGCGCGTTT
 GTTTATACGCGCCTATGTCAGTGTCTTGTCTAGGATGAATAATAGTGTAT
 TGGTATGTATGTGCACGTATCCGTATCGCATTTGTTTCAAGTTTTTTTTT
 |||||
 GTATCGCATTTGTTTCAAGTTTTTTTTT

CTATAATGTTTCTTCGAAATCCATGATCATATAGTATATAAGAAGCATGT
 |||||
 CTATAATGTTTCTTCGAAATCCATGATCATATAGTATATAAGAAGCATGT

ATTTATAATGTTCCACTTAATATATTAGTATTGGAGACTA
 |||||
 ATTTATAATGTTCCACTTAATATATTAGTATTGGAGACTAAAGCGAACAT
 ATAAAACCCAAATAAACCTTTCTTTAAGTTTTATTAAAGTCTAAACACT
 TGATTTGTGTTTTAGTTTGGGTAGTAGTGAGAAAAGAAAAATAAATAATC
 AAAAAGATTAAAGAAGAAAGAATTTGAAAGCAAGGAACACGAAATCCGAA
 GAGCGAGGGGAGCGAAGACAGTCCACGTAGCTGCAGAGAGAAAGAGAAGA
 GCACGTGAGGCACACGTTCTTGTGTAAGACTTGTTGTGGTGATGTTGGC
 GCAGTGTCTCACTGAAACATGAATGAAACCCAGACTTTGTTTTAATTTCA
 GGCGAAGGTCCATTTCTCCATGTTATATATCAATCTCTTATTTATTAGTA
 GCAAAATTGTTTAACTTTTTTAAATCCATTGATCACCTATCATTTCAT
 ATATCTACATACAATCTTATGTCTCGATAAAGGTTTATCTTTATCTTATT
 ATGCAATACATATCCCTCCCATTTCTATATTGCAAA

Figure 4.9. Overlap Between the *GENE X* and *POLARIS* Transcripts

(A) Schematic representation of the overlap between the *GENE X* and *POLARIS* transcripts. Shaded boxes represent the transcripts with large arrows indicating the position of the largest open reading frames. ▽ indicates polyadenylation sites whilst ▶ indicates the transcript start sites of *POLARIS*.

(B) Nucleotide sequence of the two transcripts showing the regions of overlap. *GENE X* sequence is in black and *POLARIS* in blue. The transcript initiation site of *GENE X* is unknown and sequence ~25bp downstream of a likely TATA box is shown. Sequence in bold represents start site 1 of *POLARIS* and poly(A) sites are underlined.

fourth poly(A) site was preceded 24b upstream by the sequence AATACA. The different 3' ends of the transcript may reflect some role for this 3' sequence in controlling the stability of the transcript. The fact that the GUS-fusion transcript, which shares 5' sequence but not 3' sequence with the wild-type transcript, is a moderately abundant message supports this possibility.

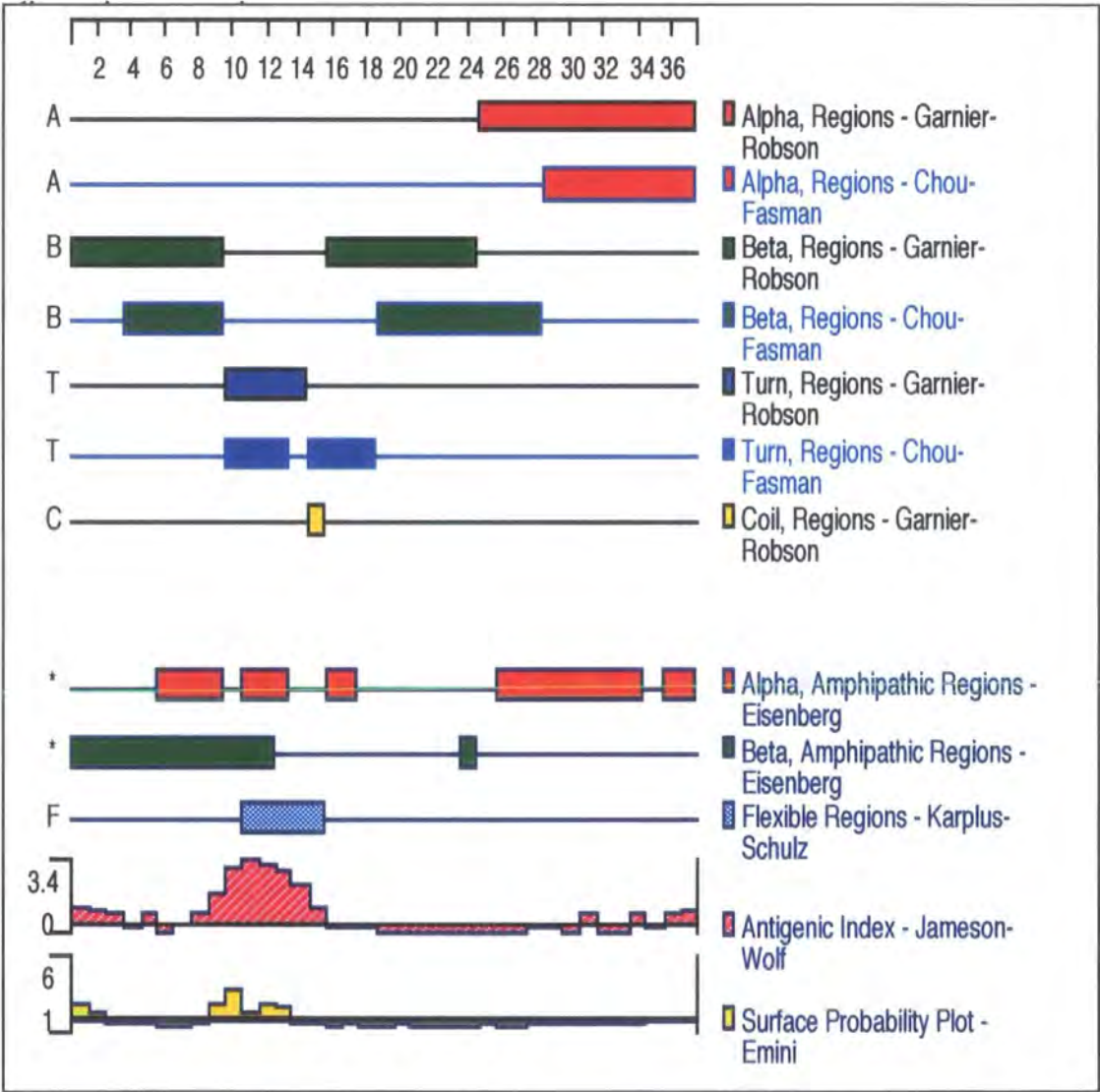
4.3 The *POLARIS* gene putatively encodes a small polypeptide

The *POLARIS* gene therefore encodes a small, low abundance mRNA with variability of both the 5' and 3' ends. Analysis of the sequence for major open reading frames revealed only one of 36 amino acids with a predicted molecular mass of 4.6kD. In the AtEM101 line, the T-DNA had inserted within the 36aa ORF in the 25th codon (leucine). Therefore, the transgenic line is likely to represent a complete knockout of the putative *POLARIS* polypeptide.

Using the Protean programme, which is part of DNASTAR'S LASERGENE software, the putative polypeptide secondary structure was determined (Figure 4.10) The N-terminal 24 amino acids of this putative polypeptide are predicted to form two β -sheets whilst the remaining 12 amino acids are likely to form an α -helix. Situated between the two β -sheets are three basic arginine residues (positions 10 to 12) which may form a turn region and a possible cleavage site. Within each of the β -sheets is a cysteine residue (positions 6 and 17) which present a potential for disulphide bond formation between the two β -sheets. The second β -sheet contains the repeat SIS separated by four residues. The proximity of these serine residues to the basic arginine residues of the β -turn may signify a cAMP- and cGMP-dependent protein kinase phosphorylation site (determined using the ScanProsite programme; <http://www.expasy.ch/tools/scnpsit1.html>). The C-terminal α -helix also contains the repeat of KLFLFK. The lysine residues along with the terminal histidine residue represent the only charged residues in this helical region. The three amino acid spacing between each of the lysine residues indicates that they would all lie on the same face of the α -helix creating an amphipathic helix with both hydrophobic and charged faces. The fact that the predicted helical region is leucine rich indicates the potential for a leucine zipper motif in which leucines are repeated every seventh residue such that they are stacked above each other on the same face of the helix. Indeed two of the leucines form a heptad (leucines 25 and 32) which may be significant given the small size of the polypeptide. Classically this motif mediates protein interactions with other proteins having the same motif indicating a potentially important role for this helix in the function

Figure 4.10. Secondary Structure Predictions of the Putative POLARIS Polypeptide

Polypeptide secondary structure predictions were performed using the Protean programme, which is part of DNASTAR'S LASERGENE software. A variety of predictions are shown which generally correlate well in suggesting that the POLARIS polypeptide consists of two N-terminal β -sheets and a C-terminal α -helix. For further



of the *POLARIS* polypeptide. Bipartite protein structures, as predicted for the *POLARIS* polypeptide, are often found in transcription factors. However, the fact that the β -sheets are not rich in basic residues, except for arginines 10-12, probably indicates that this region is not involved in DNA/RNA binding.

Database searches (*Arabidopsis thaliana* Database, BLAST and FASTA) revealed that this putative polypeptide shared sequence similarity to domains in several plant proteins. The highest sequence homology was to the N-terminus of a putative RNA-binding glycine-rich protein (38% identity and 51% similarity) and a polypeptide with similarity to 11-s seed storage proteins (45% identity and 51% similarity). The small size means that it is unlikely however that such sequence similarities indicate much about the potential function of the putative *POLARIS* polypeptide.

4.3.1 The 5' UTR of *POLARIS* contains small upstream ORFs

An unusual feature of the *POLARIS* transcript is that a large proportion is untranslated region. The 36 amino acid ORF is preceded by a very long 5' UTR of between 305bp and 399bp depending on the start site used. Conversely it is followed by a very short 3' UTR of between 11bp and 95bp depending on the poly(A) site selected.

Analysis of the sequence of the long 5' UTR revealed some unusual features. The region of 5' UTR between start sites 2 and 1 was found to contain three very small ORFs of 6, 3 and 3 amino acids respectively, the first of which starts 34bp downstream of the putative start site (2). Given that this start site is used less frequently and the small size of these ORFs there may be little significance of these small upstream ORFs. However, the 5' UTR extending from start site 1 of 305bp was also found to contain two small ORFs of 9 and 8 amino acids, the positions of these relative to the 36 residue ORF suggests that they may play an important regulatory role in *POLARIS* translation. The 9 amino acid ORF initiates 30bp downstream of start site 1 and is in frame with the 36 amino acid ORF, indeed the TGA stop codon immediately precedes the ATG of *POLARIS* (Figure 4.8). The 8 amino acid ORF overlaps with *POLARIS* with its ATG 4bp upstream of the *POLARIS* ATG. By analysis of a large number of vertebrate 5'UTRs Kozak (1987) was able to determine that a -3 purine (A or G) and G in the +4 position relative to the ATG codon is important in determining the efficiency by which an ATG codon is chosen for translation initiation. None of the three main ORFs (9, 8 and 36) are in particularly favourable contexts though the 9 and 8 amino acid ORFs have a G and A residue in the -3 position respectively. The small size of these two potential polypeptides indicates that it is unlikely that they represent true gene products. Their presence in the 5' UTR may not be coincidental since only 5-10% of eukaryote

messages contain upstream ATGs (Kozak, 1987). Their position closer to the 5' end of the transcript means that they are more likely to be translated than the larger 36 residue ORF. They may therefore play an important role in controlling both the translation of the *POLARIS* polypeptide and also the transcript stability.

4.3.2 The putative *POLARIS* polypeptide is undetectable using a polyclonal antibody

Though the *POLARIS* transcript contains an ORF that encodes a polypeptide of 36 amino acids there remains a possibility that this is not translated and that *POLARIS* is potentially an active RNA molecule. A polyclonal antibody was therefore raised to a synthetic peptide representing the N-terminal 18 amino acids of the putative polypeptide (see Materials and Methods). Tests showed that pre-serum obtained before inoculation with the peptide did not recognise the peptide whereas serum taken following inoculation did (data not shown).

Total protein was extracted from wild-type Columbia seedlings 7 d.p.g and varying amounts (1 µg to 30 µg) were separated on tris-tricine polyacrylamide gels alongside peptide molecular markers before transfer to membrane and incubation with primary and secondary antibodies. However, following chemiluminescent detection, no polypeptide of the predicted 4.6kD was detected though there was non-specific binding to some larger polypeptides. Immunoprecipitation experiments using this antibody also proved unsuccessful.

There are a number of possibilities as to why a polypeptide of the predicted size was not detected. The *POLARIS* transcript is low abundance and therefore it is likely therefore that if the 36 amino acid ORF is translated it will be present in very small amounts, possibly below the detectable limits of the system used. There is also the possibility that much of the N-terminus of this predicted polypeptide is cleaved off following translation and thus the antibody may not recognise the cleavage product. However, the inability to detect such a polypeptide still leaves the possibility that *POLARIS* is an active RNA molecule.

4.4 Expression pattern of the *POLARIS* gene

If the premise of the promoter -trapping strategy is correct the pattern of GUS expression seen in the AtEM101 line should match that of the *POLARIS* gene. Northern analysis had already revealed that the *POLARIS* transcript is much less abundant than the GUS-fusion transcript. Further experiments revealed that the *POLARIS* transcript

was almost impossible to detect without large amounts of poly(A⁺) RNA being used for northern analysis. A PCR-based technique was therefore used to determine the expression pattern of *POLARIS*. However, due to the small size of the transcript and its lack of introns, conventional RT-PCR was complicated by the presence of contaminating genomic DNA even following DNase treatment. To analyse expression of *POLARIS*, the technique of RNA-specific PCR (RS-PCR) which is a modification of the 3' RACE method where an RNA specific anchor primer is used for the reverse transcription step instead of an oligo (dT) anchor primer. 10µg of total RNA was treated with DNase and then half of this treated RNA was converted to cDNA using AMV reverse transcriptase and the POL-RS-PCR primer (Figure 4.3). A negative control was performed using the remaining RNA in which the cDNA synthesis step was repeated but without the addition of AMV reverse transcriptase. Amplification of the cDNA was performed with the POL 5' TEST and RS-PCR-Anchor primers following purification of the cDNA away from residual POL-RS-PCR primer.

The expression of *POLARIS* was examined in the same tissues as used for analysis of GUS-fusion transcript levels in the AtEM101 line. As can be seen in figure 4.11 transcript levels appear to be highest in 7 day seedling uppers, green siliques and root tips. Roots from which the tips were removed show little expression. Reactions from which AMV reverse transcriptase was omitted did not give rise to any detectable products. It would appear from this result therefore that the expression pattern of *POLARIS* in wild-type plants is consistent with the data obtained from the study of the AtEM101 line.

It has been shown that auxin treatment causes significant increases in the steady-state levels of the GUS-fusion transcript in line AtEM101. Furthermore, treatment with the ethylene precursor ACC had been shown to reduce the amount of GUS detectable by histochemical staining (Paul Chilley, unpublished results). 6 day old seedlings (Columbia ecotype) were therefore transferred to media containing either 10µM 1-NAA or 100µM ACC for 24 hours following which RNA was extracted. RS-PCR was performed on these samples as described with RNA from untreated 7 day seedlings used as a control. As can be seen in figure 4.12 the treatment with the synthetic auxin 1-NAA did not significantly alter transcript levels, however, treatment with ACC resulted in a significant reduction in levels. The result of 1-NAA treatment is not consistent with the AtEM101 line though the effect of ACC on levels of the *POLARIS* transcript is consistent with observations of reduction in GUS levels following ACC treatment of AtEM101 seedlings (P. Chilley, unpublished results). This difference may be due to the relative stability's of the GUS-fusion transcript and the *POLARIS* message. The

Figure 4.11. Analysis of the *POLARIS* transcript in various organs by RS-PCR

RNA from wild-type Columbia 7 day seedlings (7d), green siliques (Si), 7 day seedling aerial parts (Up), 7 day root minus their tips (R), and 7 day root tips (T) was reverse transcribed and RS-PCR was performed. As a control RS-PCR was performed on RNA without a reverse transcription step (-RT). Products were run alongside DNA standards (M-100bp ladder, Promega)

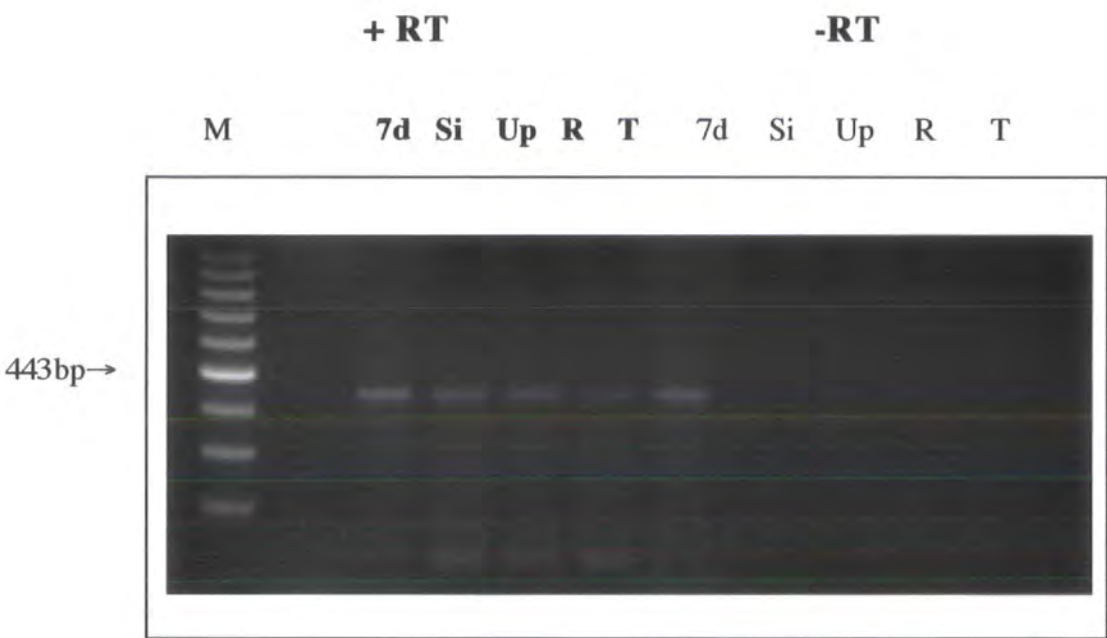
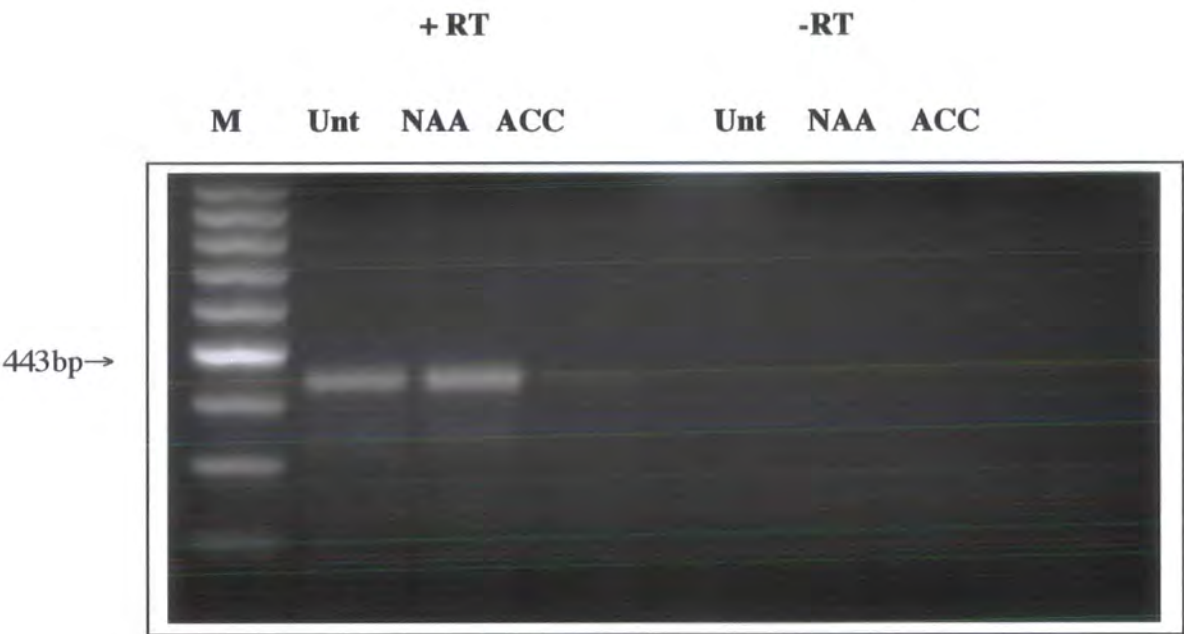


Figure 4.12. RS-PCR of the *POLARIS* transcript following treatment with auxin or ACC

6day old Columbia seedlings were transferred to media containing either 10μM NAA or 100μM ACC for 24 hours. RS-PCR of *POLARIS* was performed using RNA extracted from these seedlings and an untreated control (Unt). Controls in which reverse transcriptase was omitted from the reaction were also performed (-RT). Products were analysed on a 1% ethidium bromide stained agarose gel alongside DNA molecular markers (M-100bp ladder, Promega).



apparent relative instability of the *POLARIS* message means that increases in the rate of transcription would not necessarily result in significant increases in the steady-state levels of the transcript. To confirm these possibilities would require nuclear run-off experiments or more quantitative PCR methods.

4.5 Summary

Described in this chapter is a characterisation of the *POLARIS* locus. The T-DNA in the AtEM101 line was found to have inserted between two genes, *BRI 1* and the novel *GENE X*. Though there was only 750bp between these two genes it was found that another gene, *POLARIS*, was present and was interrupted by the T-DNA in the AtEM101 line. This gene is single copy in the genome and has an unusual organisation with its 5' end overlapping with the 3' end of *GENE X*. Experimental evidence suggests that there are two transcriptional initiation sites to the *POLARIS* gene as well as variable 3' ends. The transcript itself encodes a putative 36 amino acid polypeptide though this is preceded by some small upstream open reading frames. The polypeptide is predicted to form a bipartite structure with two N-terminal β -sheets and an amphipathic C-terminal α -helix which may be involved in protein-protein interactions. The AtEM101 line is expected to be deficient in this polypeptide as the T-DNA inserts within the open reading frame. For this reason, the AtEM101 line can be considered to be a mutant of the *POLARIS* gene and will therefore be referred to in later chapters as *pls*. The expression of the *POLARIS* transcript is likely to match that of the GUS expression since RS-PCR results suggest it is expressed most strongly in the root tips and aerial parts of 7 day seedlings. There is also evidence that the transcript downregulated by ACC treatment, though 1-NAA treatment does not appear to significantly alter levels.

Chapter 5 Cloning and Characterisation of the *POLARIS* Promoter and Preliminary Analysis of the *GENE X* Promoter

Having described the cloning of the *POLARIS* gene and its unusual organisation, apparently overlapping with a second upstream *GENE X*, this chapter will detail the cloning of the *POLARIS* promoter and the examination of transgenic *Arabidopsis* plants transformed with the GUS gene under the control of this promoter. The use of both a short and a longer promoter fragment is used to determine the potential position of various tissue specific and hormone responsive elements in the *POLARIS* promoter. Also described is the putative expression pattern of *GENE X* which is upstream and overlapping with *POLARIS*. The genome organisation of this locus with potentially two separately controlled overlapping genes is particularly unusual in eukaryotes. By examining the expression pattern of various promoter GUS constructs the aim was to determine whether these two genes are under the control of separate promoters or whether they show coordinate regulation from the same promoter. Though previous results indicate that *GENE X* is expressed in the AtEM101/*pls* line this does not discount the possibility that both genes can share common promoter elements and expression patterns.

5.1 Cloning of the *POLARIS* promoter

The *POLARIS* locus shows unusual genome organisation with overlap between the 5' end of *POLARIS* and the 3' end of *GENE X*. Ordinarily, in eukaryotes, two genes are separated by an intergenic region of variable length though overlapping genes do exist with either different transcription start sites or translation of different reading frames (Kozak, 1986; Small *et al.*, 1998). The results presented so far indicate that *GENE X* is an independent transcriptional unit to *POLARIS*. However, one possibility is that they encode separate messages controlled by the same promoter.

To test these possibilities two promoter GUS constructs were introduced into wild-type *Arabidopsis* plants. The two constructs differed in the amount of upstream sequence that was included but shared a common 3' end which consisted of the putative *POLARIS* polypeptide, minus its TGA STOP codon, fused to the GUS protein coding sequence creating a true N-terminal translational fusion between *POLARIS* and GUS. The shorter promoter construct, p584POL:GUS, included approximately 370bp of sequence upstream of transcriptional start site 1 (section 4.2.2) and was designed such

that it did not contain the ATG codon of the 92 amino acid reading frame that is the putative product of *GENE X*. The longer promoter construct, p1635POL:GUS, includes an additional 820bp of upstream sequence which presumably includes the transcriptional start site of *GENE X*. The position of the primers used for cloning the two promoter constructs is shown in Figure 5.1 i.

For construction of p584POL:GUS the *POLARIS* polypeptide sequence and upstream sequence was amplified from pλEM1 (section 3.2.2) using the Expand™ High Fidelity PCR system (section 2.11.2) and the primers NH-PolR and PolProm (10μM stocks). 30 cycles were performed with primer annealing at 60°C for 30 seconds and 1 minute extension at 72°C (Figure 5.1 a). The PolProm primer contains recognition sites for the enzymes *Sac* 1 and *Hind* III whilst NH-POLR contains a *Bam*H 1 site. The PCR fragment was cut with *Sac* 1 and *Bam*H 1 and ligated into pBluescript SK- cut with these two enzymes. Following sequencing the construct was excised as a *Hind* III-*Bam*H 1 fragment and ligated into these sites of pGUS-1 (Figure 5.1 c & d). This resulted in the in-frame cloning of the *POLARIS* polypeptide sequence in front of the GUS gene. The whole cassette was then transferred to the plant transformation vector pCIRCE as an *Hind* III-*Eco*R 1 fragment (Figure 5.1 f & g).

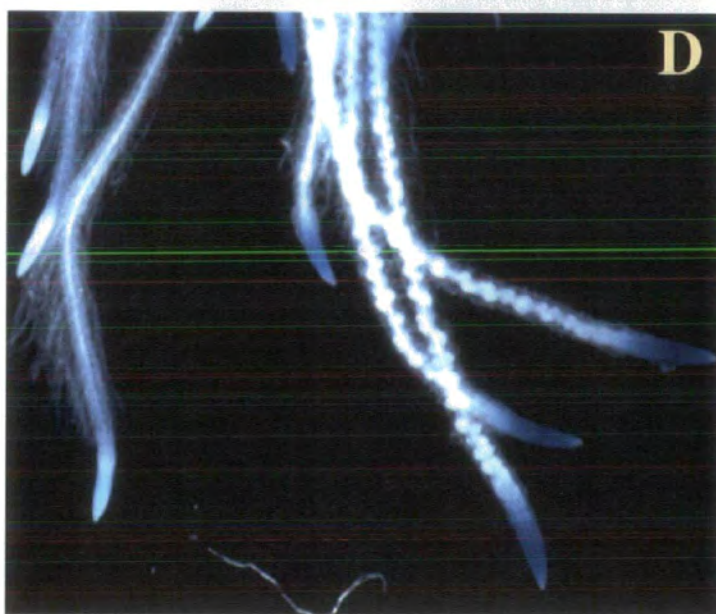
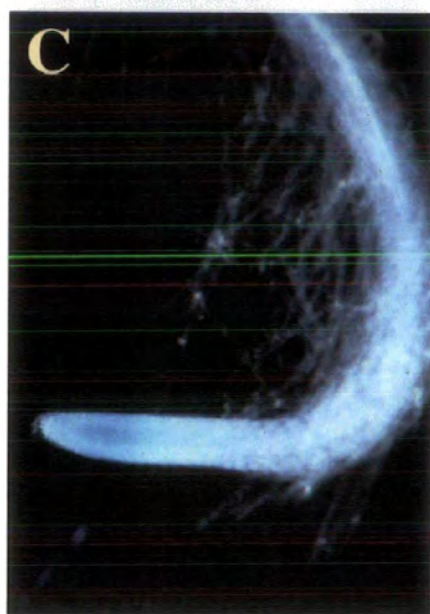
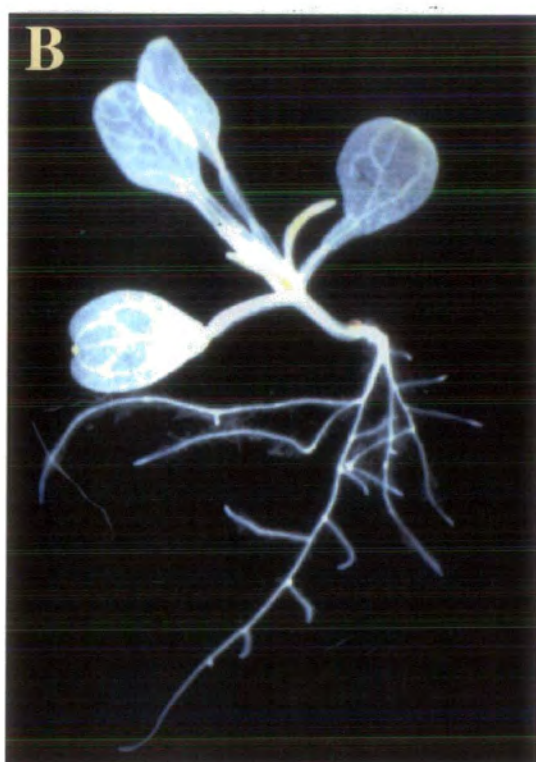
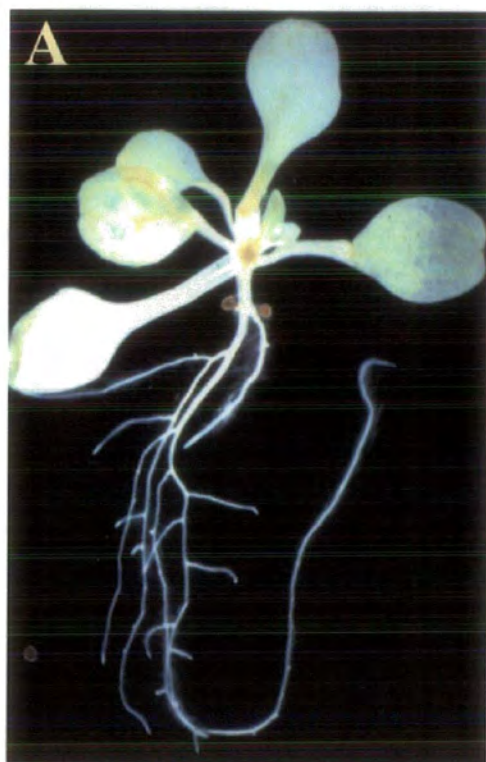
For construction of p1635POL:GUS the *POLARIS* polypeptide sequence and upstream sequence was amplified from pλEM1 using the Expand™ High Fidelity PCR system (section 2.11.2) and the primers NH-POLR and PROM1635 (10μM stocks). 30 cycles were performed with primer annealing at 60°C for 30 seconds and 2 minutes extension at 72°C (Figure 5.1 b). The fragment was cloned into the pCR®2.1-TOPO vector from Invitrogen. The PROM 1635 primer contains a *Hind* III recognition site, which supposedly occurs within the upstream sequence at this point. This however was found to be a sequence error and since the Expand™ enzyme mix has proof reading capabilities, the primer *Hind* III site was corrected during PCR. Therefore, when the construct was transferred to pGUS-1 as an *Hind* III-*Bam*H 1 fragment, the *Hind* III site used was from the pCR®2.1-TOPO vector's cloning site (Figure 5.1 c & e). As with p584POL:GUS, this resulted in the in-frame cloning of the the *POLARIS* polypeptide sequence in front of the GUS gene. The whole cassette was then transferred to the plant transformation vector pCIRCE as an *Hind* III-*Eco*R 1 fragment (Figure 5.1 f & h).

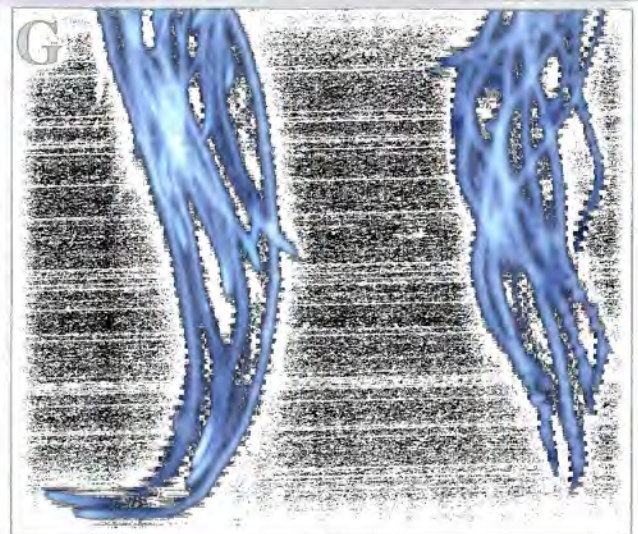
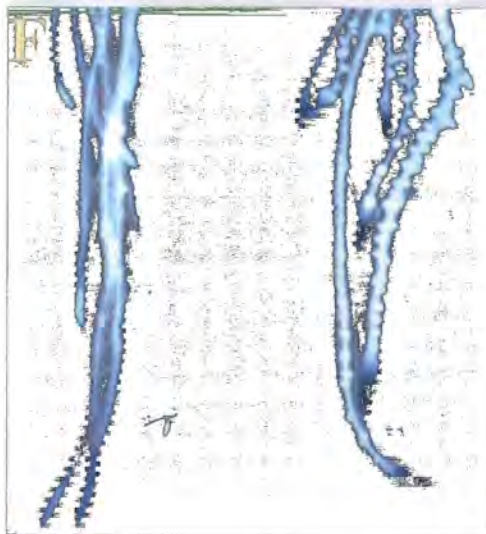
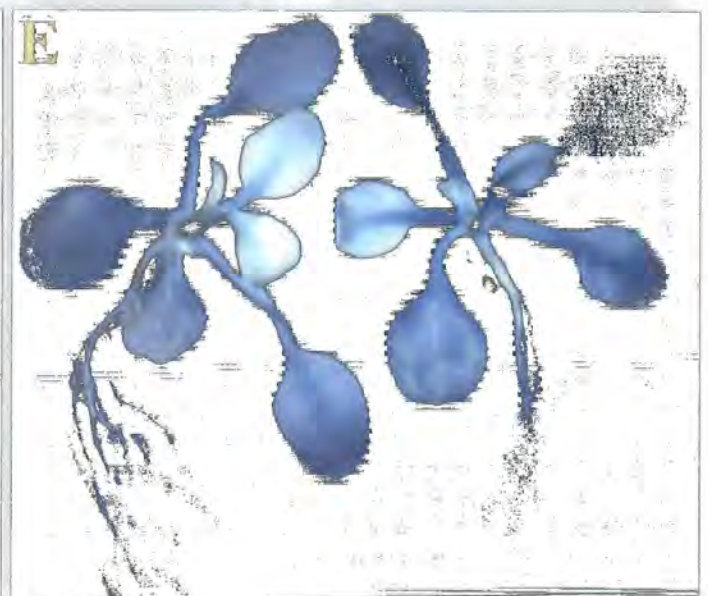
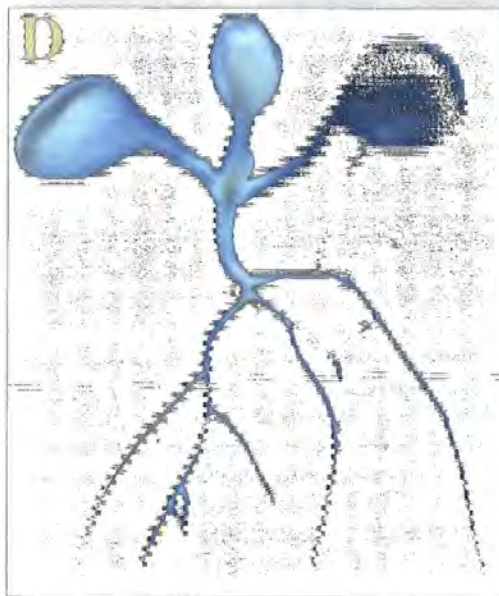
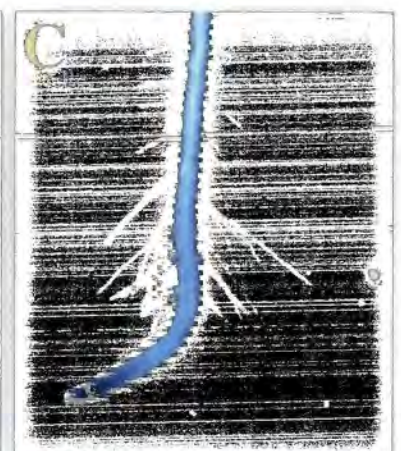
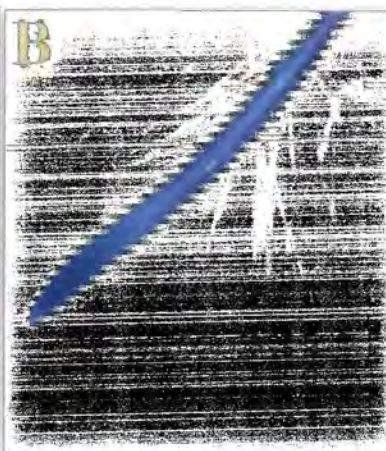
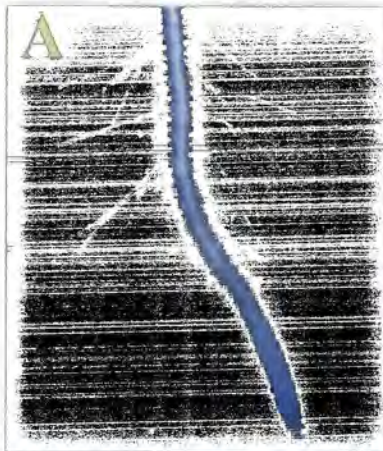
Following transfer of the two promoter-GUS cassettes into the plant binary vector pCIRCE, the vectors were then introduced into *Agrobacterium tumefaciens* strain C58C3 by tri-parental mating (section 2.2.1). For plant transformation the Columbia (Col-O) ecotype was used and transformed using the floral-dip method (Clough and

Bent, 1998; section 2.2.4). Following transformation, dipped plants were allowed to grow to maturity and seed was collected. Primary T1 transformants were selected on 1/2MS10 medium containing kanamycin, selection for which is conferred by the introduced promoter-GUS containing T-DNA. After several days growth on selective medium non-transformed seedlings were bleached whereas transformants had healthy green uppers. These transformants were then transferred to unsupplemented 1/2MS10 medium for several days. To reduce the number of lines analysed, these T1 transformants were screened by removing the root tips from individual seedlings and staining them histochemically for GUS. T1 seedlings, for both constructs, which showed GUS staining were transferred to new 1/2MS10 medium plates and allowed to recover for one week before being transplanted to soil. The T1 transformants were allowed to self fertilise and the T2 seed was collected from each independent transformant and used for subsequent analysis.

For the p584POL:GUS construct six independent T2 lines were generated and 7day old seedlings grown on 1/2MS10 medium were analysed histochemically for GUS staining. Each line showed staining of a proportion of root tips but in a pattern more restricted than that seen in the *pls* line. In *pls* GUS expression is found in the columella root cap, epidermis, meristem and immature vascular tissue of the primary root (Topping and Lindsey, 1997; and this study, section 3.1). The p584POL:GUS lines all lacked staining in the root cap and also the meristem with the strongest staining seen in the central stele (Figure 5.2 c). Also, even after longer staining times up to 24 hours, GUS expression was not seen in the cotyledons or hypocotyl of these lines (Figure 5.2 a & b).

For the p1635POL:GUS construct ten independent T2 lines were generated and analysed. 7 day old seedlings of each line showed staining of the root tip. If shorter staining times of ~1 hour were used the staining pattern reflected that of the p584POL:GUS lines with GUS generally limited to the stele except in lines 22 and 28 where expression was more diffuse throughout the tip region (data not shown). Longer staining times resulted in more uniform staining throughout the whole root tip as in *pls* (Figure 5.3 a, b & c). Compared to the p584POL:GUS lines the intensity of staining was also stronger in the p1635POL:GUS lines. Interestingly, the cotyledons and hypocotyl of the p1635POL:GUS seedlings did show staining that mimicked the *pls* line (Figure 5.3 d & e).





5.2 Auxin response of the *POLARIS* promoter

Examination of the *pls* line has shown that the *POLARIS* gene is rapidly upregulated by auxin and may be a primary response gene (section 3.3). If this is indeed the case it would be expected that there are auxin response elements (AREs) in the *POLARIS* promoter. A number of these elements have been identified in the promoters of other auxin inducible genes such as the sequence TGTCTC found in the soybean *GH3* and SAUR 15A promoters (Li *et al.*, 1994; McClure *et al.*, 1989; Liu *et al.*, 1994).

Sequence analysis of the two promoter constructs did not identify any elements with full identity to any known AREs. However, the p584POL:GUS promoter did contain a number of TGTCTC-like elements. Two overlapping elements were identified starting at position -146 (TGTCTTGTCTA) relative to the putative transcriptional start site (1). These were just upstream of the sequence AATAAT (position -130) which has similarity to the sequence AATAAG found just downstream of the TGTCTC element in two AREs in the soybean *GH3* promoter (Liu *et al.*, 1994). Furthermore, at positions -85 and -61 are putative TGTCTC-like elements with sequence TGTTTC separated by a T-rich tract. The region of the p1635POL:GUS promoter construct that did not overlap with 584POL:GUS did not contain any TGTCTC-like elements.

Preliminary experiments were performed to determine the region of the *POLARIS* promoter that confers auxin inducibility. Both promoter constructs were analysed in an experiment in which 5 day old T2 seedlings were transferred onto medium containing 10 μ M NAA for 2 days. These seedlings were then compared to control seedlings grown on medium lacking NAA for a visible increase in histochemical GUS staining. Each of the 5 independent 584POL:GUS lines and 5 of the 1635POL:GUS lines were analysed. Since the T2 seed was heterozygous, a number of individual seedlings for each line, both control and NAA-treated, were stained to account for variability.

After 5 hours, staining each of the 584POL:GUS lines grown in the presence of NAA showed a detectable increase in GUS staining intensity, compared to the controls (Figure 5.2 d). GUS was still localised to the root tips following the NAA treatment but was seen in a higher proportion of mature lateral root tips as well as appearing to be more diffusely localised in the tips themselves. Following a longer 24 hour staining period a small number of NAA treated seedlings showed weak GUS staining in the cotyledons or young leaves (data not shown). No untreated seedlings were found to show this pattern. Each of the 1635POL:GUS lines tested showed an increase in the intensity of GUS staining following NAA treatment (Figure 5.3 f & g). It was also observed that both after 5 and 24 hour staining periods, the intensity of staining in the cotyledons and young leaves was also increased, compared to the controls.

These preliminary histochemical results are consistent with the presence of AREs in the 584POL:GUS region of the promoter. The auxin response is also not restricted to the root tips and occurs in the other organs of the seedling which normally express *POLARIS*. The fact that a small number of NAA treated 584POL:GUS seedlings showed staining of the cotyledons/young leaves indicates that this promoter fragment must contain at least some of the elements required for directing expression in these organs.

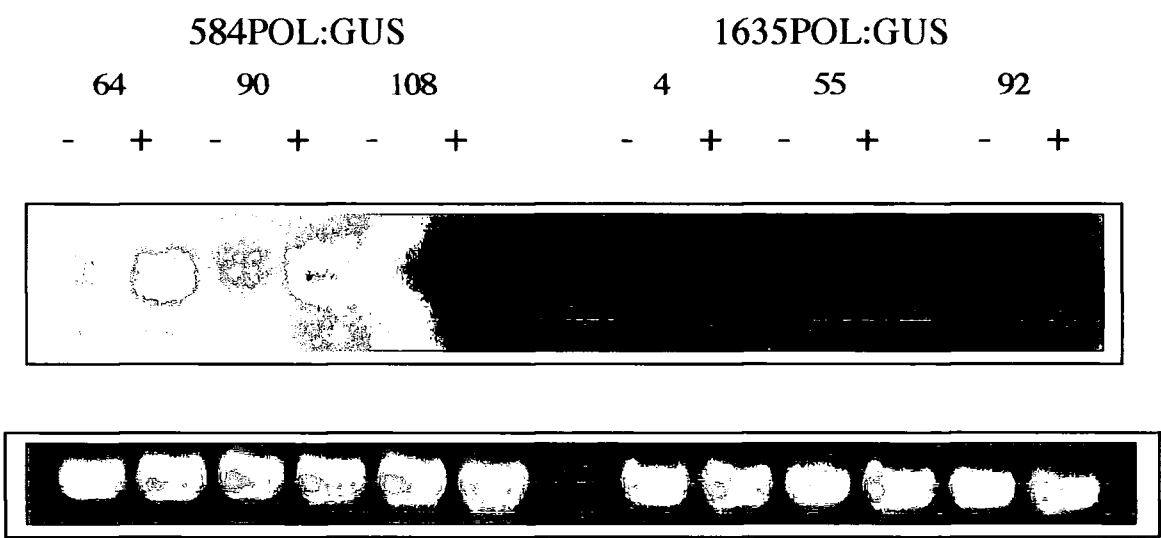
5.2.1 Examination of the auxin response by northern blot analysis

In order to confirm the results of the histochemical analysis, RNA blot analysis was performed. RNA was extracted from seedlings (three independent T2 lines for both the 584POL:GUS and 1635POL:GUS lines) which had been grown for 7 days on 1/2MS10 medium (untreated) or for 6 days on 1/2MS10 medium followed by transfer to media containing 10 μ M NAA for 24 hours. For each line and treatment, 20 μ g of total RNA was electrophoretically separated on a RNA denaturing gel and transferred to membrane before being hybridised with a radiolabelled GUS probe. Figure 5.4 shows that both the 584POL:GUS lines and the 1635POL:GUS lines show an increase in GUS transcript levels following auxin treatment, confirming that the shorter promoter fragment contains AREs. The magnitude of the response was determined using a densitometer for both the 584POL:GUS and 1635POL:GUS lines. There was approximately a 2.5 fold increase in transcript levels for both sets of lines following auxin treatment compared to the untreated controls. This indicates that the auxin response is determined by the region of the promoter found in the 584POL:GUS construct. It does not rule out the presence of further AREs upstream of the region found in the 1635POL:GUS construct. Auxin treated GUS transcript levels were higher in the 1635POL:GUS lines for both untreated and auxin treated samples which reflects the histochemical staining data. Sizing of the transcript against known RNA markers indicated a transcript of ~2.6kb which correlates well with the expected size for a true fusion to *POLARIS* (400bp for *POLARIS*, 1.8kb for GUS and 250bp for the NOS terminator).

The results of this RNA analysis correspond well to the histochemical staining data. This indicates that the auxin inducibility of the *POLARIS* promoter is most likely regulated by the region contained within the 584POL:GUS promoter construct which is within a 370bp region upstream of transcriptional start site 1 (section 4.2.2).

Figure 5.4. Auxin response of the 584POL:GUS and 1635POL:GUS Promoters

Seedlings from six independent lines containing either the 584POL:GUS or 1635POL:GUS promoter GUS constructs (3 for each) were grown on 1/2MS10 medium for 6 days then either transferred to 1/2MS10 medium controls (-) or medium containing 10µM NAA (+) for 24 hours. RNA was extracted from these seedlings and RNA blot analysis was performed with 20µg of total RNA and hybridised with a randomly labelled GUS probe (upper panel). The lower panel shows ethidium bromide staining of the 28S RNA.



5.3 Expression pattern of the putative *GENE X* promoter

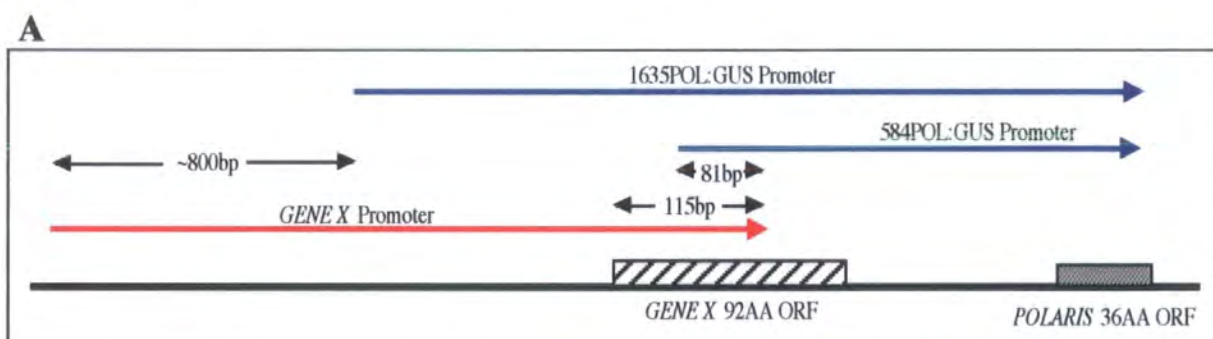
The previous results suggest that the *POLARIS* promoter overlaps the *GENE X* transcript and would indicate that these are two separate genes. Differences between the two *POLARIS* promoter constructs demonstrate that some of the tissue specific domains are upstream of the *GENE X* 92aa ORF. To gain further insight into the expression pattern of *GENE X*, 1.5kb of putative upstream sequence was linked to the GUS reporter gene and GUS expression was examined histochemically in transgenic seedlings. The region linked to GUS initiated 115bp downstream of the putative start of the 92aa *GENE X* ORF and overlaps with the 5' most 81bp of the p584POL:GUS construct (Figure 5.5 a). Due to poor primer site availability this overlap was unavoidable, however it was assumed that because the overlap occurred in the *GENE X* ORF that this region would probably not contribute to the promoter activity of *GENE X*.

For *GENE X* promoter-GUS constructs, 1.5kb of upstream sequence was amplified from p λ EM1 using the Expand™ High Fidelity PCR system (section 2.11.2) and the primers GENEX FOR and GENEX REV (10 μ M stocks). 30 cycles were performed with primer annealing at 60°C for 30 seconds and 2 minutes extension at 72°C (Figure 5.5 b). The fragment was cloned into the pCR@2.1-TOPO vector from Invitrogen and confirmed to be correct by sequencing. The GENEX FOR and GENEX REV primers both contain *Bam*HI restriction sites. The promoter fragment was therefore excised from pCR@2.1-TOPO by digestion with this enzyme and ligated into *Bam*HI digested pGUS. Since insertion of the *GENE X* promoter into pGUS could occur in both forward and inverse orientations, plasmids with inserts in the correct orientation were selected by colony PCR using the GENEX FOR and GUSPA primers. Plasmids isolated from colonies testing positive for the correctly orientated *GENE X* promoter-GUS cassette were sequenced to confirm correct orientation and the promoter-GUS cassette was then transferred to the binary vector pCIRCE as an *Xba*I-*Eco*RI fragment (Figure 5.5 c & d). The binary vector was then introduced into *Agrobacterium tumefaciens* strain C58C3 by tri-parental mating (section 2.2.1). For plant transformation the Columbia (Col-O) ecotype was used and transformed using the floral-dip method (Clough and Bent, 1998; section 2.2.4). Following transformation, dipped plants were allowed to grow to maturity and seed was collected. T1 transformants were selected on 1/2MS10 medium containing kanamycin, selection for which is conferred by the introduced promoter-GUS containing T-DNA.

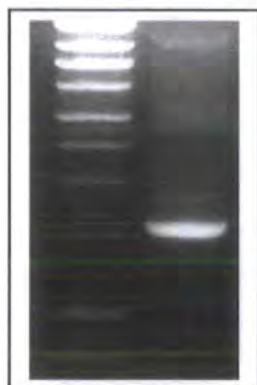
Ten independent T1 transgenic lines were generated by this method and these transformants were then transferred to unsupplemented 1/2MS10 medium for several

Figure 5.5. Isolation and Cloning of the *GENE X* Promoter

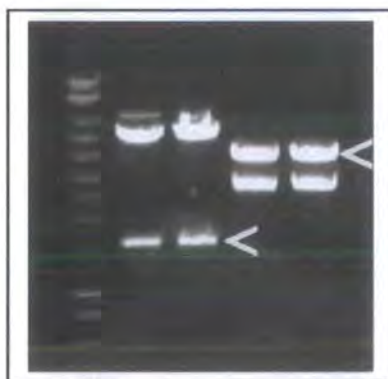
- A)** Schematic diagram showing the relative positions of the *POLARIS* and *GENE X* promoter fragments.
- B)** A ~1.5kb genomic fragment was amplified from the pλEM1 clone using the primers GENEXfor and GENEXrev primers. The product was visualised on a 1% ethidium bromide stained gel alongside DNA molecular markers (Hyperladder I, Bioline).
- C)** Following ligation into the vector pGUS, plasmids were isolated from two colonies which tested positive for the *GENEX* promoter by colony PCR with the GENEXfor and GUSPA primers. Plasmids were digested with *Bam*HI to release the 1.5kb promoter (lanes 2 & 3, arrow) or *Xba*I/*Eco*RI to release the 4kb promoter-GUS cassette (lanes 4 & 5, arrow). Lane 1, Hyperladder I (Bioline).
- D)** Following ligation of the 4kb *Xba*I/*Eco*RI promoter-GUS cassette into the binary vector pCIRCE, plasmid was isolated from a colony determined by colony PCR with the GENEXfor and GUSPA primers to contain the correct insert. The plasmid was digested with *Xba*I and *Eco*RI and the expected bands of ~10kb (pCIRCE) and 4kb (promoter-GUS cassette) were present (lane 1). Lane 2, Hyperladder I (Bioline).



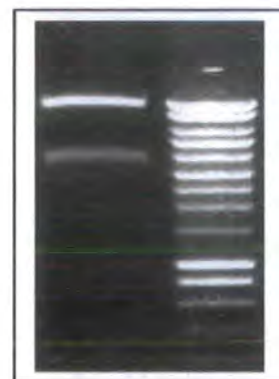
B



C



D

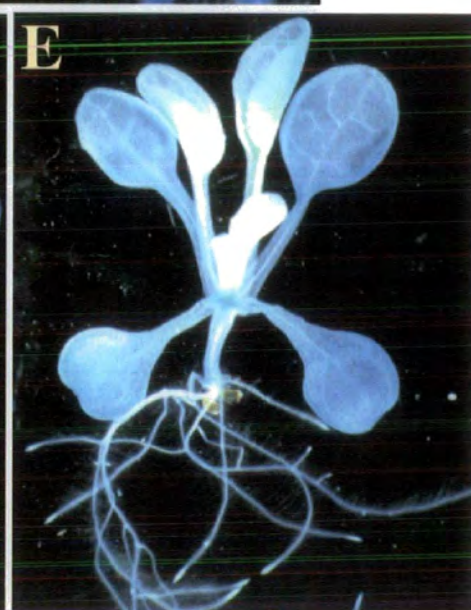
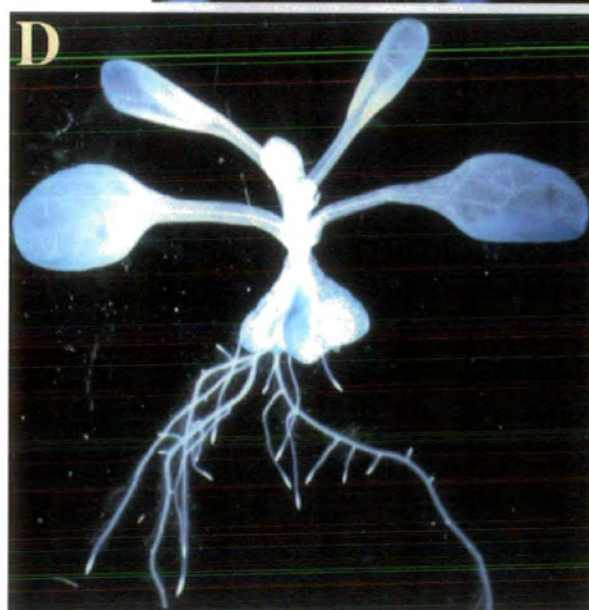
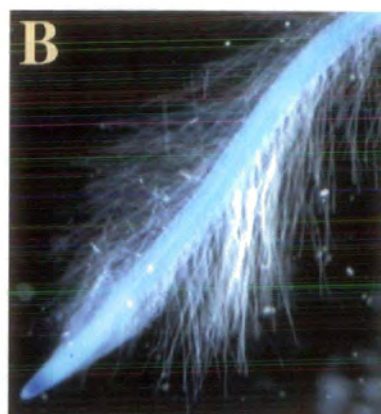
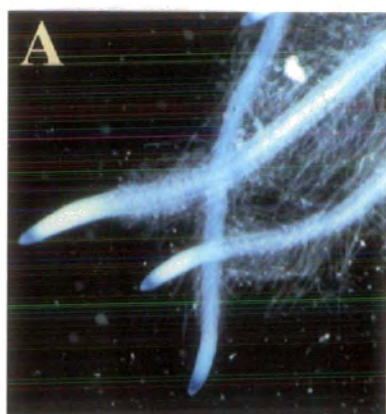


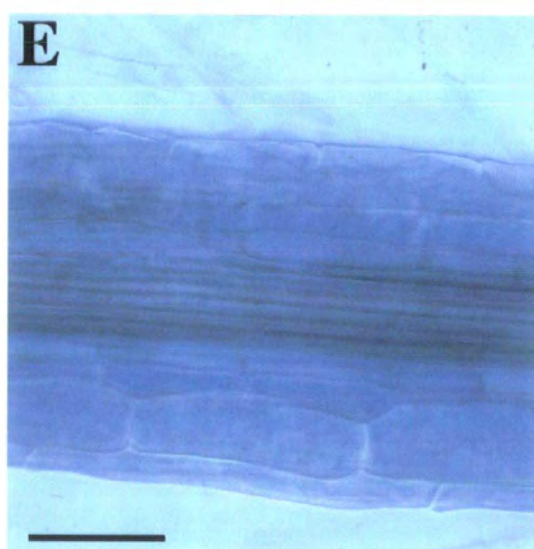
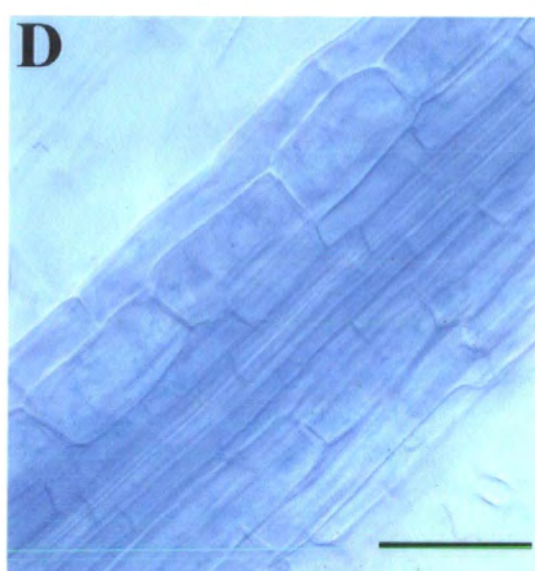
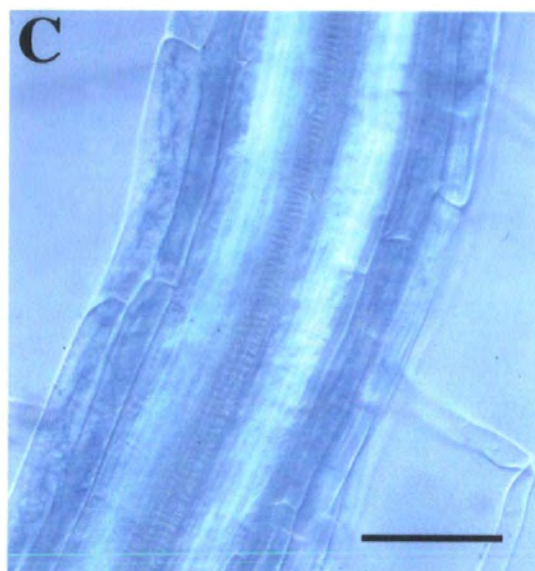
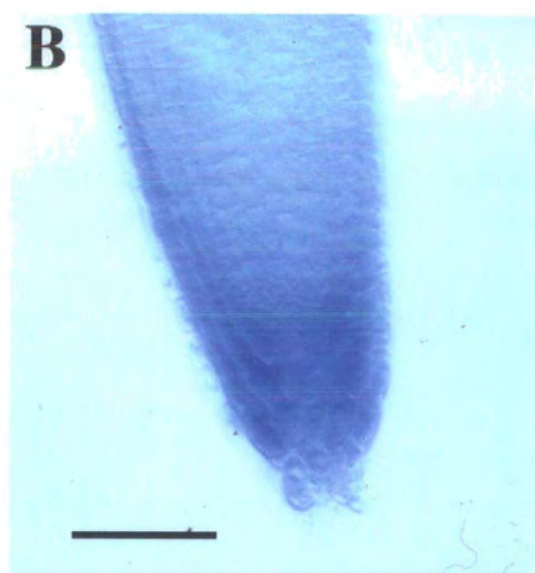
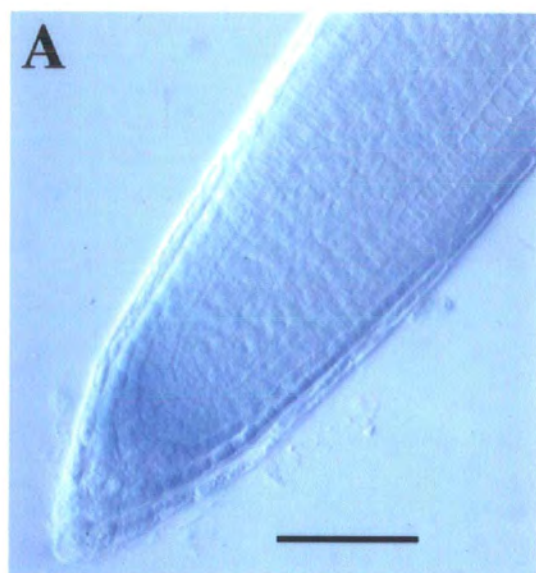
days. These T1 seedlings were examined histochemically for GUS expression after 6 hours staining. Though variability was observed in the different lines the consensus staining pattern was that of diffuse staining in the cotyledons and young leaves with weaker staining of the petioles and hypocotyl (Figure 5.6 d & e). The roots of these 10 transgenic lines showed expression at the tips and in a number of the lines, throughout the rest of the root, though staining appeared to be absent from the meristematic and expansion zones (Figure 5.6 a, b & c). Examination of the staining in the root tip using Normarski optics revealed that it was restricted mostly to the columella cells of the root cap with staining also present in the lateral root cap. No staining was observed in the quiescent centre or meristem nor in the young vasculature (Figure 5.7 a & b). Expression throughout the rest of the root was variable in its specificity. Analysis of optical longitudinal sections indicated that, depending on the independent T1 transgenic line, expression was seen most strongly in the cortex, endodermis and even the vascular bundle (Figure 5.7 c, d & e). The consensus was strong expression in the cortex and endodermis with weaker expression in the vasculature and very little if any staining of the epidermis.

5.4 Summary

This chapter has detailed the cloning and partial functional characterisation of the *POLARIS* and *GENE X* promoters. For the *POLARIS* gene it has been shown that weak root tip expression and auxin response is determined by a 370bp region upstream of start site 1 (section 4.2.2). This sequence overlaps fully with part of the putative *GENE X* transcript, though not with the start of the 92aa ORF. This indicates that this gene forms part of the *POLARIS* promoter. Other components of the *POLARIS* promoter that direct expression in the cotyledons, young leaves and hypocotyl as well as enhancing root tip expression appear to lie in a region 800bp upstream of this short p584POL promoter fragment.

Since the organisation of *POLARIS* and *GENE X* is very unusual for eukaryotes the question remained as to whether these genes share the same promoter and thus show co-ordinate regulation. The expression pattern of *GENE X* was therefore examined by fusing a 1.5kb fragment, predicted to contain at least part of the *GENE X* promoter, to GUS. This sequence included the start of the 92aa ORF and showed a short overlap with the p584POL:GUS construct. This promoter resulted in GUS expression being observed in the cotyledons, young leaves, petioles and hypocotyl. In the root, GUS was observed in the columella and lateral root caps, as well as the rest of the root behind the expansion zone.





The expression pattern of *GENE X*, as predicted by GUS histochemistry of putative promoter GUS transgenic lines, does show overlap with that of the *pls* line and thus *POLARIS*. However, the GUS expression patterns of both *pls* and the *GENE X* promoter lines are subtly different in their cell and tissue specificities. This indicates that *POLARIS* and *GENE X* are two separately regulated genes which may share, in part, common promoter elements. The fact that the coding region of *GENE X* forms part of the promoter for *POLARIS* is unusual but examples of overlapping genes have been identified in other organisms (ie. *Entamoeba histolytica* , Gangopadhyay *et al.*, 1997).

Chapter 6 Complementation of the *pls* mutant phenotype and analysis of plants overexpressing *POLARIS*

The *pls* line has been determined to have a mutant phenotype characterised by shorter roots due to reduced cell elongation. The phenotype segregates with the single T-DNA and appears to be semi-dominant, since heterozygotes for the mutation display an intermediate phenotype between the homozygote mutants and the wild-type (Paul Chilley, unpublished results). Though the *POLARIS* gene is interrupted by the presence of the T-DNA in *pls*, the possibility remains that the expression of another closely linked gene could be affected in the *pls* line and is therefore responsible for the mutant phenotype. Indeed two other genes, *BRI1* (Li and Chory, 1997) and *GENE X* (this study), are tightly linked to the T-DNA. This chapter will therefore describe the results of reintroducing a wild-type copy of the *POLARIS* gene back into the *pls* mutant line to determine whether it is the knockout of *POLARIS* in *pls* that is responsible for the mutant phenotype.

The observations that *pls* shows an apparent increase in ethylene synthesis (P. Chilley, unpublished data; this study) suggests that the *POLARIS* gene may potentially have an important role in regulating the levels or the perception of this hormone in the root. Furthermore, *pls* roots are hypersensitive to cytokinins and ACC indicating a role for *POLARIS* in determining sensitivity to these compounds. To investigate the possible role of *POLARIS*, transgenic plants expressing a truncated version of the *POLARIS* transcript under the control of the constitutive CaMV 35S promoter were therefore examined. The results of this analysis will also be presented.

6.1 Complementation of the *pls* mutant phenotype by retransformation with the *POLARIS* gene

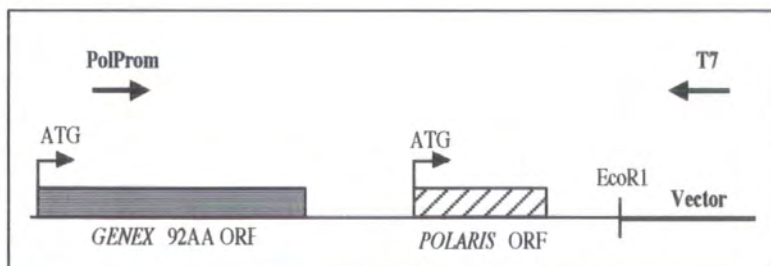
To prove that the mutant phenotype of the *pls* line is due to disruption of the *POLARIS* gene requires introduction of a functional copy of the *POLARIS* gene back into the *pls* line such that a wild-type phenotype is restored. The unusual genomic organisation of the *POLARIS* locus, with the unknown *GENE X* positioned immediately upstream of *POLARIS*, presented a problem. The results of the promoter cloning (section 5.1) showed that the longer 1635POL:GUS construct reproduced the GUS expression pattern seen in *pls* whereas the shorter 584POL:GUS construct only reliably

showed GUS expression, at lower levels, in the root tip. However, the 1635POL:GUS construct is likely to contain the whole *GENE X* coding sequence and therefore to use this promoter would involve introducing the two genes back into *pls*, with the additional problem being that *GENE X* and *POLARIS* show overlap in their expression patterns. Therefore, although the 584POL:GUS construct contains only part of the *POLARIS* promoter, it was decided to use this promoter.

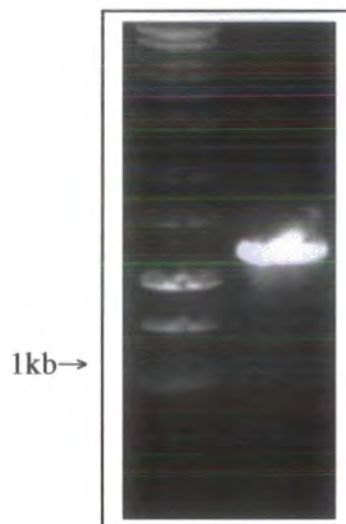
Since *pls* already contains the single T-DNA promoter trap, that confers kanamycin resistance, a different selectable marker was required for retransformation. The binary vector, pMOG1006, that confers resistance to hygromycin, was therefore used. For the experiment, a 1.15kb genomic fragment which contained the whole *POLARIS* transcript and originated at the PolProm primer site (start of the 584POL. promoter) and ended at an *EcoR* I site approximately 350bp downstream of the end of the transcript, was used (Figure 6.1 a). The 1.15kb DNA fragment was amplified from pλEM1 (section 3.2.2), using the Expand™ High Fidelity PCR system (section 2.11.2), with the primers PolProm and T7. The T7 primer site flanks the pBluescript SK+ multiple cloning site (the 3.6kb genomic clone was inserted into the vector's *EcoR* I site, Dr. J. Topping, University of Durham). 30 cycles were performed with primer annealing at 55°C for 30 seconds and 90 seconds extension at 72°C (Figure 6.1 b). The fragment was cloned into the pCR®2.1-TOPO vector from Invitrogen and confirmed to be correct by DNA sequencing. The fragment was excised from pCR®2.1-TOPO as an *EcoR* I - *Hind*III fragment and transferred to pMOG1006, using the *Hind*III site within the PolProm primer. Correct insertion of the genomic fragment into pMOG1006 was determined by restriction enzyme analysis (Figure 6.1 c & d).

Following cloning of the *POLARIS* locus into pMOG1006, the binary vector was introduced into *Agrobacterium tumefaciens* strain C58C3 by tri-parental mating (section 2.2.1). For the plant transformation, *pls* plants homozygous for the promoter trap T-DNA were used, and transformed using the floral-dip method (Clough and Bent, 1998; section 2.2.4). Following transformation, dipped plants were allowed to grow to maturity and seed was collected. Primary T1 transformants were selected on 1/2MS10 medium containing hygromycin, selection for which was conferred by the new pMOG1006 derived T-DNA. The putative transformants were then transferred to 1/2MS10 medium without selection for several days prior to transfer to soil. The individual T1 plants were allowed to self-fertilise and seed from these primary transformants was germinated on non-selective 1/2MS10 medium. Following DNA extractions the presence of the new T-DNA was confirmed by PCR analysis using

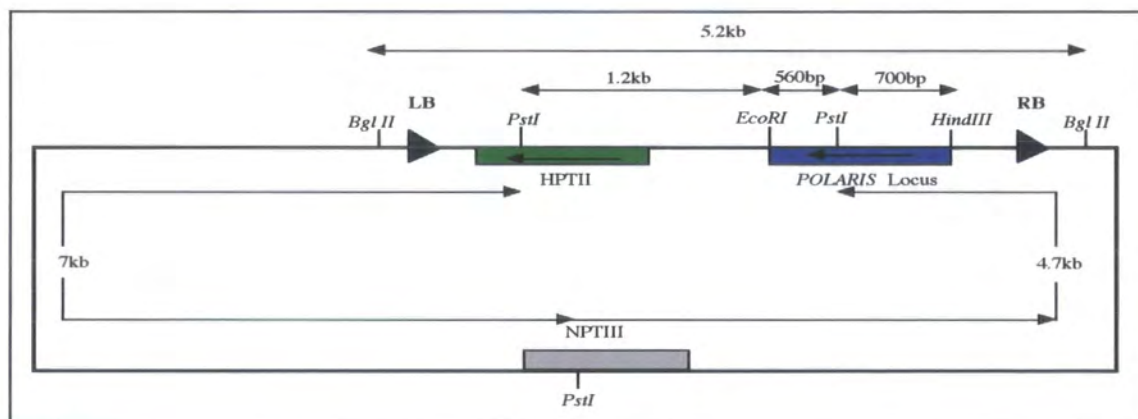
A



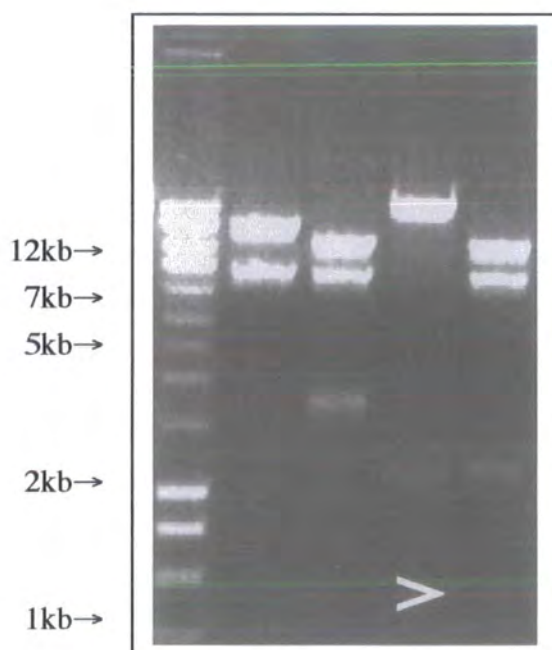
B



C



D



primers to the hygromycin resistance marker (Figure 6.2 a). Those seedlings that tested positive by this method were again transferred to soil and were allowed to self-fertilise.

T2 progeny of these hygromycin resistant progeny were grown on non-selective 1/2MS10 medium for 7 days along with controls of both *pls* and C24 seedlings. To identify potential complementing lines the primary roots of the re-transformed lines were compared to those of *pls* and C24 and those lines with significantly longer roots (than *pls* seedlings) were grown and T3 seed collected. To ensure that no wild-type contaminants had accidentally been included, T2 seedlings from each potential complementing line were histochemically stained for GUS activity. All lines examined showed GUS staining in the root tips (data not shown).

T3 seed from selfing of independent T2 progeny was grown on 1/2MS10 medium for either 6 or 9 days. The roots of 10 individual seedlings for each line were then measured and the mean length of these roots was compared to those of *pls* and C24 seedlings of the same age. The mean root length of 6 day old *pls* seedlings was 12.85mm compared to 21.2mm for wild-type C24 roots. Each of the complementing T3 lines had mean root lengths longer than the *pls* mutant, ranging from 14.75mm for line 26A to 18.5mm for line 25C, though not as long as roots of wild-type C24 (Figure 6.3 a, appendix II). The roots of a second set of T3 complementing transgenics were also compared to those of *pls* and C24 seedlings, 9 days post-germination. *pls* roots had a mean length of 14.7mm compared to 25.05mm for the wild-type C24. The mean root length of the T3 complementing transgenics ranged from 16.2mm for line 77A to 21.65mm for line 87A, with each independent line again having longer roots than those of the *pls* mutant (Figure 6.3 b, appendix II).

Though the new T-DNA had been shown to be present in each of these lines, it had not been determined whether the new copy of *POLARIS* was being expressed. In order to determine this, RNA was extracted from the seedlings of potential complementing transgenics as well as from *pls* and C24 controls, and tested for the presence of the *POLARIS* transcript by RS-PCR. As expected, the *POLARIS* transcript was not detected in *pls* RNA but was found in RNA from C24 and potential complementing lines (Figure 6.2 b). Therefore the increased root lengths in these lines correlated with the presence of the new T-DNA and the expression of the introduced copy of *POLARIS*.

It has been shown that the expression of an ethylene-induced *GST2* gene is upregulated in the *pls* line compared to wild-type C24 (section 3.4). Along with an increase in root length, the potential complementing transgenics were also examined for the expression of this gene by northern blotting, the premise being that complementation of the mutant phenotype would result in downregulation of this gene. Though loading is

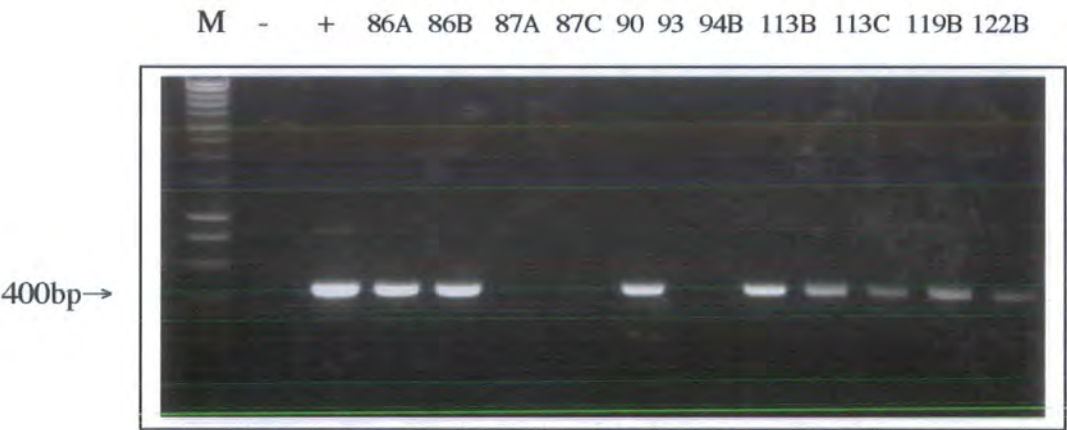
Figure 6.2. Complementation of the AtEM101 Mutant Phenotype

A) PCR analysis performed on genomic DNA extracted from independent AtEM101 lines transformed with the *POLARIS* gene. A 400bp fragment of the hygromycin resistance gene (HPT II) found on the new T-DNA was amplified. As controls PCR was performed with the transformation vector pMOG1006 (+) or the original AtEM101 line (-).

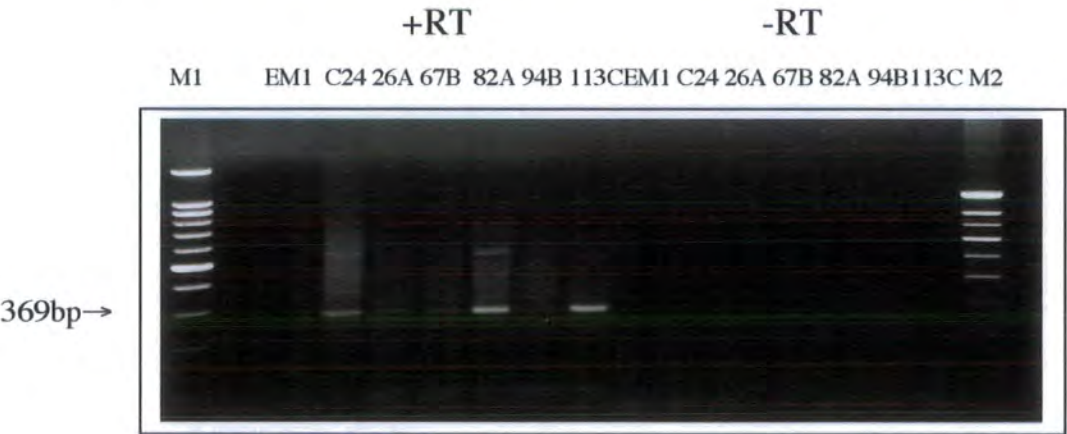
B) RS-PCR performed on independent AtEM101 lines transformed with the *POLARIS* gene to determine if *POLARIS* is expressed. Included are wild-type C24 and AtEM101 controls. Controls were also performed in which reverse transcriptase was omitted from the reaction (-RT). Products were analysed on a 1% ethidium bromide stained gel alongside DNA molecular markers (M1-100bp ladder, Promega; M2-hyperladder IV).

C) RNA gel blot analysis performed using 10µg of total RNA extracted from independent AtEM101 lines transformed with the *POLARIS* gene. As controls RNA from both the wild-type C24 and the original AtEM101 line were included. The blot was probed with a randomly labelled GST2 cDNA. The lower panel shows ethidium bromide staining of the 28S RNA.

A



B

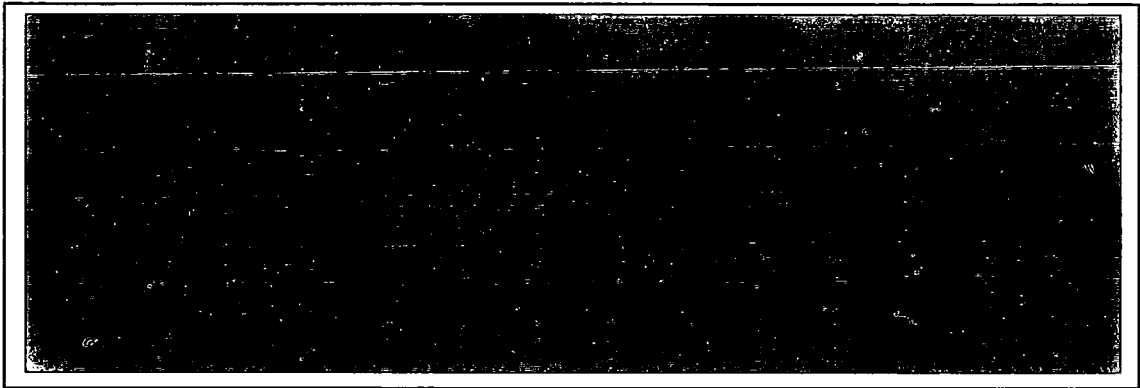


C

Complementation Lines

EM1 C24 77A 82 85 90 94B 113C 87A 93

GST2



28S
RNA

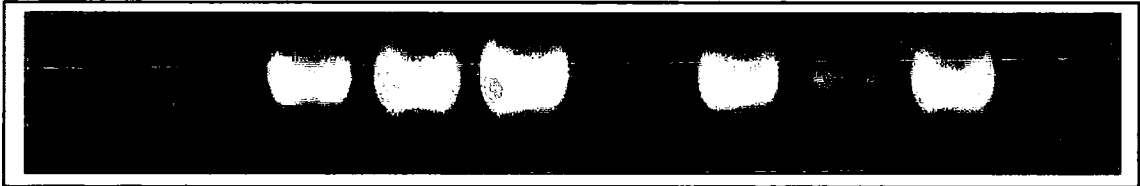


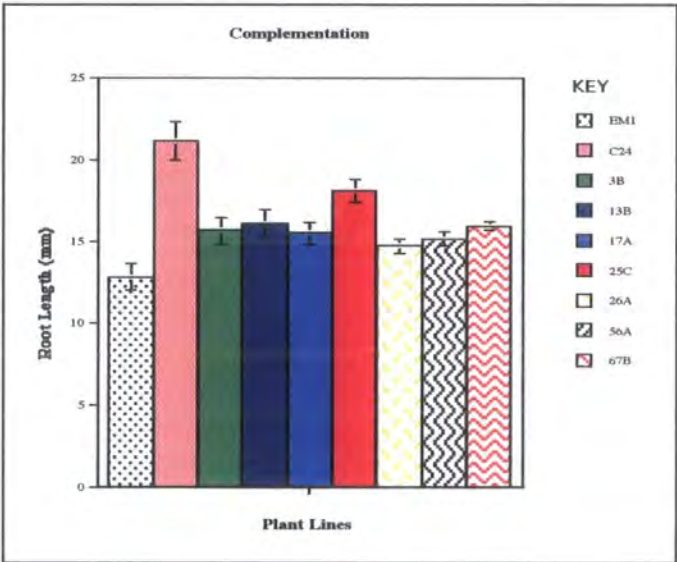
Figure 6.3. Root Lengths of Independent AtEM101 Lines
Retransformed with a Wild-Type Allele of *POLARIS*

Seedlings were germinated on 1/2MS10 medium and root lengths were measured at either 6 days or 9 days post-germination.

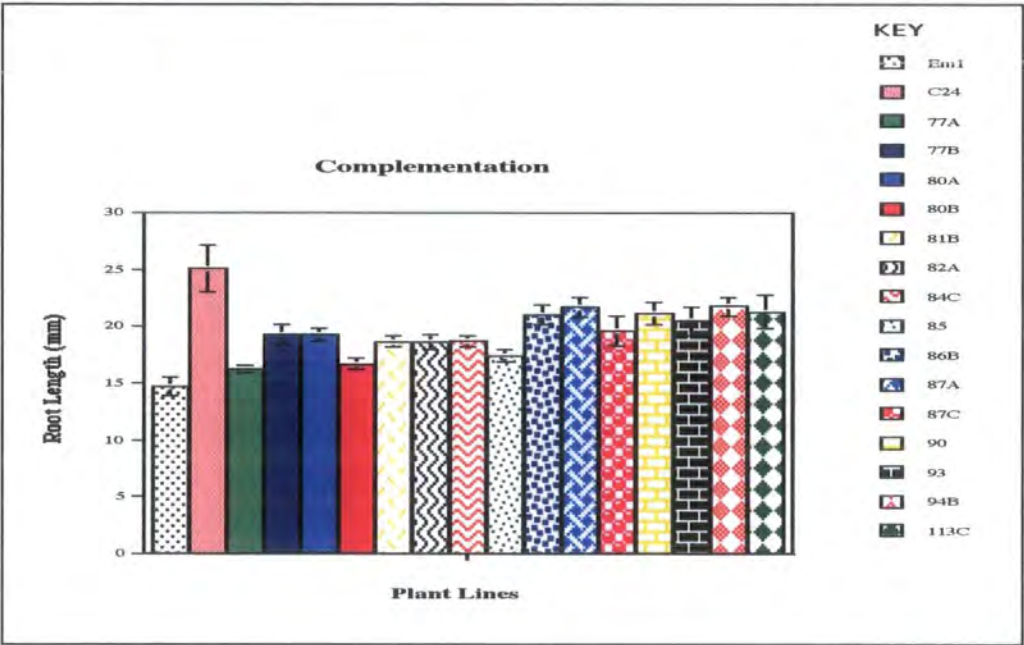
A) 6 days.

B) 9 days.

A



B



unequal it seems apparent that the majority of these lines do not show reduced *GST2* expression. However, line 113C does appear to have reduced levels of this transcript compared to *pls* even though slightly more of its RNA was blotted compared to *pls* (Figure 6.2 c). This correlates with the root length data (Figure 6.3 b) which indicated that this line shows one of the strongest reversions to a mean wild-type root length. Line 113C is therefore likely to represent a complementation of the mutant phenotype by a wild-type copy of the *POLARIS* gene (Figure 6.4).

6.2 35S:*POLARIS* seedlings overexpress the *POLARIS* gene

In order to further examine the role of the *POLARIS* gene, transgenic *Arabidopsis* plants were generated in which a 270bp fragment of the *POLARIS* gene containing the open reading frame for the putative 36 amino acid polypeptide was expressed under the control of the strong CaMV 35S promoter. The *pls* line, in which the *POLARIS* gene is interrupted by a T-DNA, has been shown to have shorter roots than wild-type C24 seedlings which is possibly due to increased ethylene levels in the root (Paul Chilley, unpublished results), and hypersensitivity to both cytokinins and ethylene. This implicates a role for *POLARIS* in regulating sensitivity to ethylene and cytokinin, especially with regards to root growth. It was therefore determined to examine the effect on root growth of overexpressing *POLARIS*.

For production of transgenic plants overexpressing *POLARIS*, a 270bp partial cDNA was amplified from the p λ EM1 by PCR using the Expand™ High Fidelity PCR system (section 2.11.2) using the primers Xba-For and Xba-Rev (10 μ M stocks). 30 cycles were performed with primer annealing at 60°C for 30 seconds and 1 minute extension at 72°C (Figure 6.5 a). These primers contain a recognition site for the restriction enzyme *Xba*I. The PCR product was purified using the *High Pure* PCR Product Purification kit (section 2.5.8) and 20 μ l was digested with *Xba*I. The digested PCR products were then purified again using the *High Pure* PCR Product Purification kit. The vector pDH51, which contains the CaMV 35S promoter and terminator between which is a multiple cloning site, was digested with *Xba*I and the digested PCR product was ligated into the vector. The cDNA could insert in both the sense and antisense orientations. Plasmids in which insertion had occurred in the sense orientation were identified by colony PCR using the primer pairs of Xba-For and -21M13 forward. The -21M13 forward primer site occurs after the CaMV 35S terminator, therefore a product with the Xba-For and -21M13 forward pair indicated a sense orientation. The cDNA was then sequenced and the whole cassette of CaMV 35S promoter-cDNA-CaMV 35S

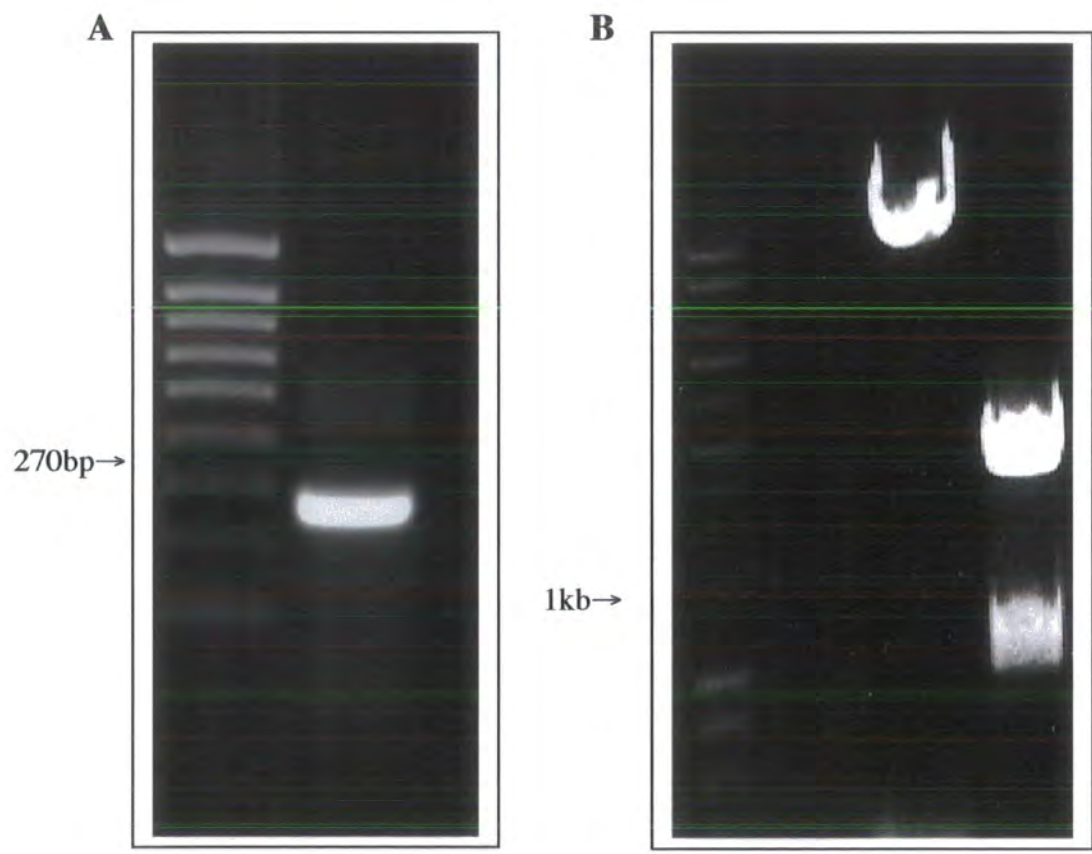
**Figure 6.4 Complementation of the AtEM101 Mutant Phenotype
in Line 113C**



Figure 6.5. Cloning of a Partial *POLARIS* cDNA for Overexpression

A partial *POLARIS* cDNA was amplified from the pλEM1 clone using the primers XbaFor and XbaRev. The product was cut with *XbaI* and inserted into the *XbaI* site of the vector pDH51, downstream of the CaMV35S promoter. The 35S*POLARIS* cassette was then transferred into the binary vector pBIN19 which was then mobilised into *Agrobacterium*, ready for transformation into *Arabidopsis*. For further details see main text.

- A)** Amplification of a 270bp partial *POLARIS* cDNA by PCR (lane 2). Lane 1, Hyperladder IV (Bioline).
- B)** *EcoRI-SacI* digests of the binary vector pBIN19 (lane 3) and pDH51 containing the partial *POLARIS* cDNA. The 35S*POLARIS* cassette is excised as a ~1kb fragment (lane 4).



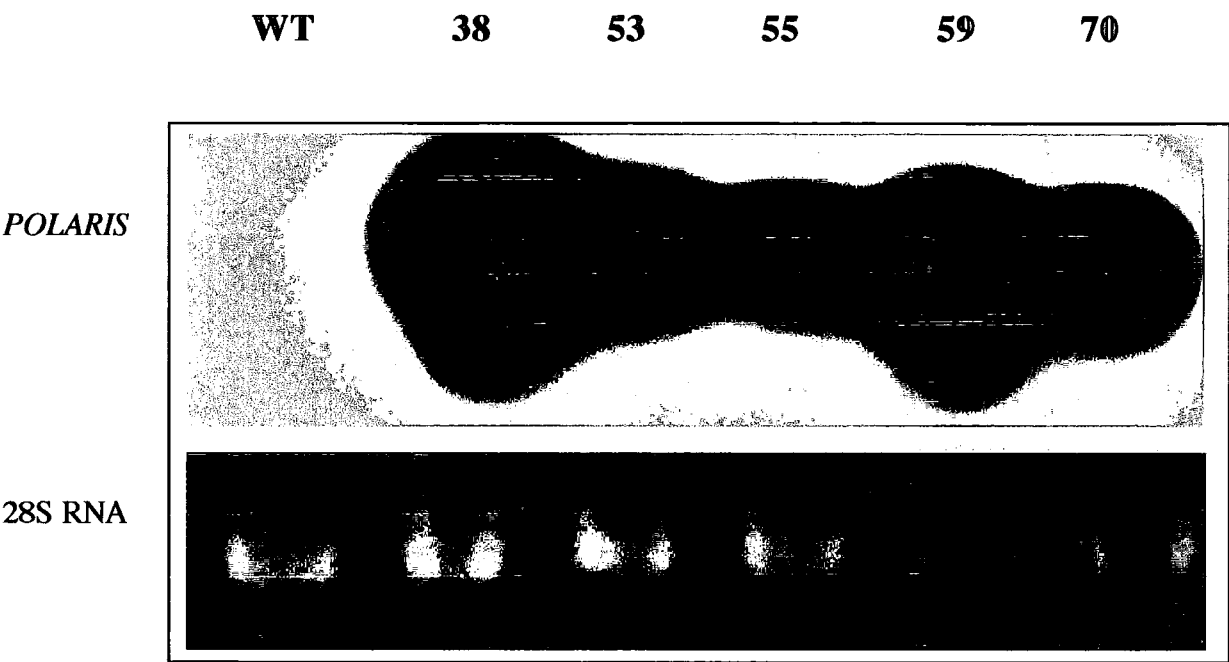
terminator was excised as an *EcoRI*-*SacI* fragment and inserted into digested pBIN19 (Figure 6.5 b). The binary vector, named pPol-Sense, was then introduced into *Agrobacterium tumefaciens* strain C58C3 by tri-parental mating (section 2.2.1). For the plant transformation, wild-type Columbia (Col-O) plants were used, and transformed using the floral-dip method (Clough and Bent, 1998; section 2.2.4). Following transformation, dipped plants were allowed to grow to maturity and seed was collected. Primary T1 transformants were selected on 1/2MS10 medium containing kanamycin, selection for which was conferred by the pPol-Sense T-DNA. These independent T1 lines were transferred to soil and allowed to self-fertilise. T2 seed from these lines was grown on 1/2MS10 medium containing kanamycin and seedlings showing resistance were again transferred to soil and allowed to self-fertilise. The process was repeated for T3 seed, and segregation for kanamycin resistance was again examined. Independent lines in which all seedlings were kanamycin resistant were presumed to be homozygous for the pPol-Sense T-DNA. Seedlings from these lines were transferred to soil and allowed to self-fertilise. In total, five independent T4 lines (line numbers 38, 53, 55, 59 and 70) were generated and were presumed to be homozygous for the transgene following segregation analysis for the kanamycin resistance marker conferred by the pPol-Sense T-DNA (data not shown). The presence of the T-DNA was also confirmed by PCR on genomic DNA extracted from the transgenic lines using primers to the NOS terminator and *POLARIS* sequence (data not shown). All analysis described in this, and future sections, was performed using this T4 seed.

Having established that these lines carried the T-DNA, total RNA was extracted from each of the transgenic lines and from the wild-type (ecotype Columbia), and expression of the transgene was determined by northern blotting using a radiolabelled *POLARIS* probe. Figure 6.6 shows that the transgenic lines are producing a transcript of approximately 350bp which is not visible in the wild-type. The low abundance of the wild-type *POLARIS* transcript is apparent by the lack of signal after overnight exposure. Unfortunately, this makes an accurate comparison of transcript levels between the transgenic lines and the wild-type impossible. However, this does indicate that each transgenic line is producing relatively very large amounts of the truncated *POLARIS* transcript.

As described in section 4.3.2 a polyclonal antibody raised to the N-terminus of the putative 36 amino acid *POLARIS* polypeptide had been unable to detect a polypeptide of the predicted size in protein extracts from wild-type seedlings. The 35S:*POLARIS* lines express the transcript at much higher levels in the wild-type and so total protein was extracted from two of the transgenic lines to determine if the putative

Figure 6.6. Overexpression of a Partial *POLARIS* cDNA in Transgenic Plants

RNA gel blot analysis was performed with 10μg of total RNA from both wild-type Columbia and 5 independent overexpressing lines and probed with a randomly labelled *POLARIS* cDNA. The lower panel shows ethidium bromide staining of the 28S RNA.



POLARIS polypeptide was being overproduced in these lines and if so whether it could be detected. Unfortunately, no protein of the predicted size was detected in these lines which may indicate a rapid turnover of the protein or an inability of the antibody to recognise the native polypeptide.

6.3 The effect of overexpressing *POLARIS* on root growth in light grown seedlings

Seedlings of both wild-type Columbia and 35S:*POLARIS* transgenic lines were grown for 7 days on the same plate in the light. A random sample of twenty seedlings for each line were then removed and the length of the primary root (from the root/hypocotyl junction to the root tip) was measured using a dissecting microscope and ruler (0.5mm divisions). The measurements for each of the five transgenic lines was compared to those of the wild-type using the Student T-test (Figure 6.7, appendix III). The results indicate that overexpression of *POLARIS* appears to have no significant effect on root growth in light grown seedlings with root lengths being reasonably uniform. Closer examination of the roots did not reveal any noticeable morphological differences to the wild-type.

6.4 Root growth of 35S:*POLARIS* seedlings grown in the presence of ACC and BA in the dark

The *pls* line has a shorter root phenotype than the wild-type which may be attributed to increased ethylene levels which would suggest that the *POLARIS* gene may be a negative regulator of the ethylene synthesis or sensitivity. If this was the case one possibility is that plants overexpressing *POLARIS* would display a degree of insensitivity to ethylene. When seedlings are grown in the dark in the presence of exogenous ethylene they display a triple response phenotype which includes a reduction in root growth (Guzman and Ecker, 1990). Like ethylene, cytokinin application results in a triple response-like phenotype in dark grown seedlings, which is likely to be caused by an enhancement of ethylene biosynthesis (Cary *et al.*, 1995; Vogel *et al.*, 1998).

To determine if overexpression of *POLARIS* alters sensitivity to these hormones seedlings of wild-type Columbia and the five 35S:*POLARIS* lines were grown in the dark for 7 days in the presence or absence of various concentrations of the ethylene precursor, ACC, or the cytokinin BA. As with previous experiments ACC was chosen because of its ease of application. For each treatment seedlings were grown on the same

Figure 6.7. Root Growth of 35SPOLARIS Transgenic Lines in Light

Conditions

Seedlings were grown in the light on 1/2MS10 medium. Root lengths were measured 7 days after germination.

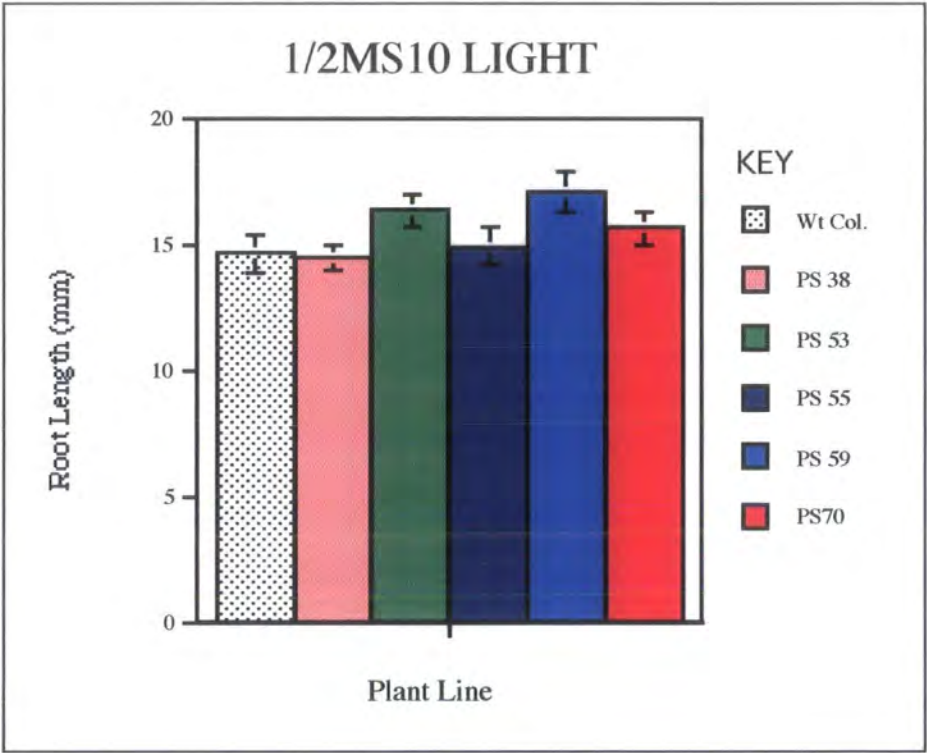


plate and a random sample of twenty seedlings from each line was then removed and the length of the primary root determined.

When grown in the dark in the absence of ACC or BA the roots of each of the 35S:*POLARIS* lines were on average longer than those of the wild-type (Figures 6.8 a; 6.9 a) though the difference in length was only statistically significant in the case of line 70 (22.725mm versus 17.875mm for wild-type).

The addition of micromolar concentrations of ACC to the media resulted in significant reductions in root length in both the wild-type and the 35S:*POLARIS* lines (Figures 6.8 b, d, f & h; 6.9 b). However, over the range of ACC concentrations used (1µM, 10µM, 50µM and 100µM) the overexpressing lines were each found to have significantly longer roots compared to wild-type seedlings, and this effect was greater on 1µM and 10µM ACC (Figures 6.8 b & d; 6.9 b, appendix II). Though only root growth was assayed it would appear from these results that the transgenic lines have reduced sensitivity to exogenous ACC and therefore probably to ethylene at concentrations of this compound that are inhibitory to root growth.

Addition of the cytokinin BA (0.1µM, 0.5µM, 1µM and 5µM) to the medium, like ACC, resulted in reductions in root length of all seedlings. The transgenic lines were each found to have significantly longer roots than the wild-type with the most noticeable differences seen on 1µM BA (Figures 6.8 c, e, g & I; 6.9 c, appendix II). Since cytokinin application increases ethylene synthesis (Cary *et al.*, 1995; Vogel *et al.*, 1998) it is possible that this accounts for much of the reduced sensitivity to BA by the transgenic lines.

6.5 The effect of auxin treatment on root growth of wild-type and 35S:*POLARIS* seedlings

Application of exogenous auxin to *pls* seedlings results in significant increases in GUS-fusion transcript levels and suggests that transcription of the wild-type *POLARIS* gene may be regulated by auxin levels, though this is yet to be proven. If *POLARIS* is an early auxin response gene what is its function? Though *pls* roots show normal sensitivity to low levels of synthetic auxins there is still the possibility that *POLARIS* is involved in a negative feedback pathway regulating the sensitivity of the cells at the root tip to auxin or alternatively, regulating downstream auxin responses such as cell division or elongation. Also, the similarities of the *pls* phenotype to some aspects of the *eto* mutants suggest that it may be that *POLARIS* is involved in regulating auxin mediated ethylene production. The reduced sensitivity of the 35S:*POLARIS* lines to the ethylene precursor

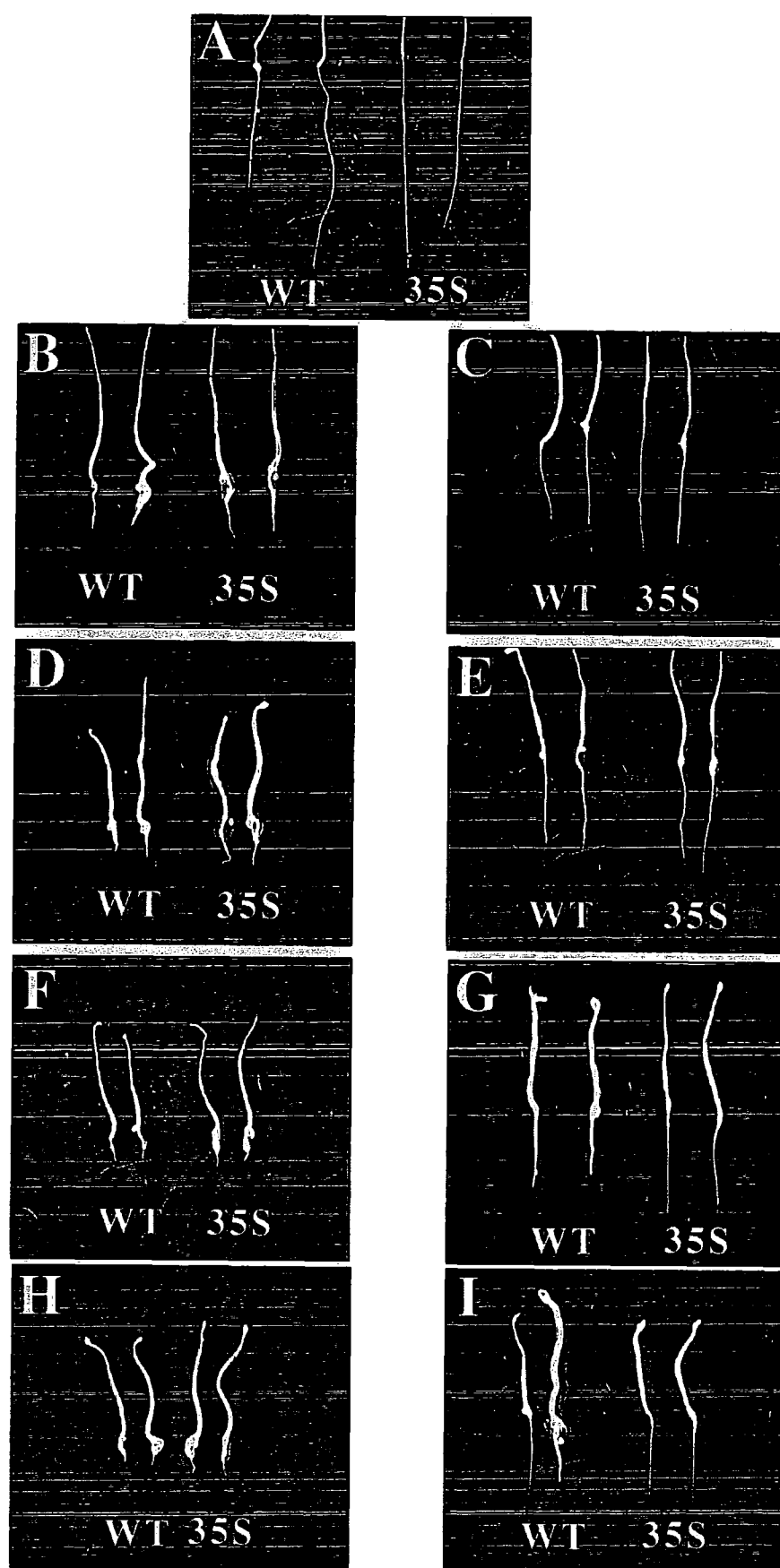
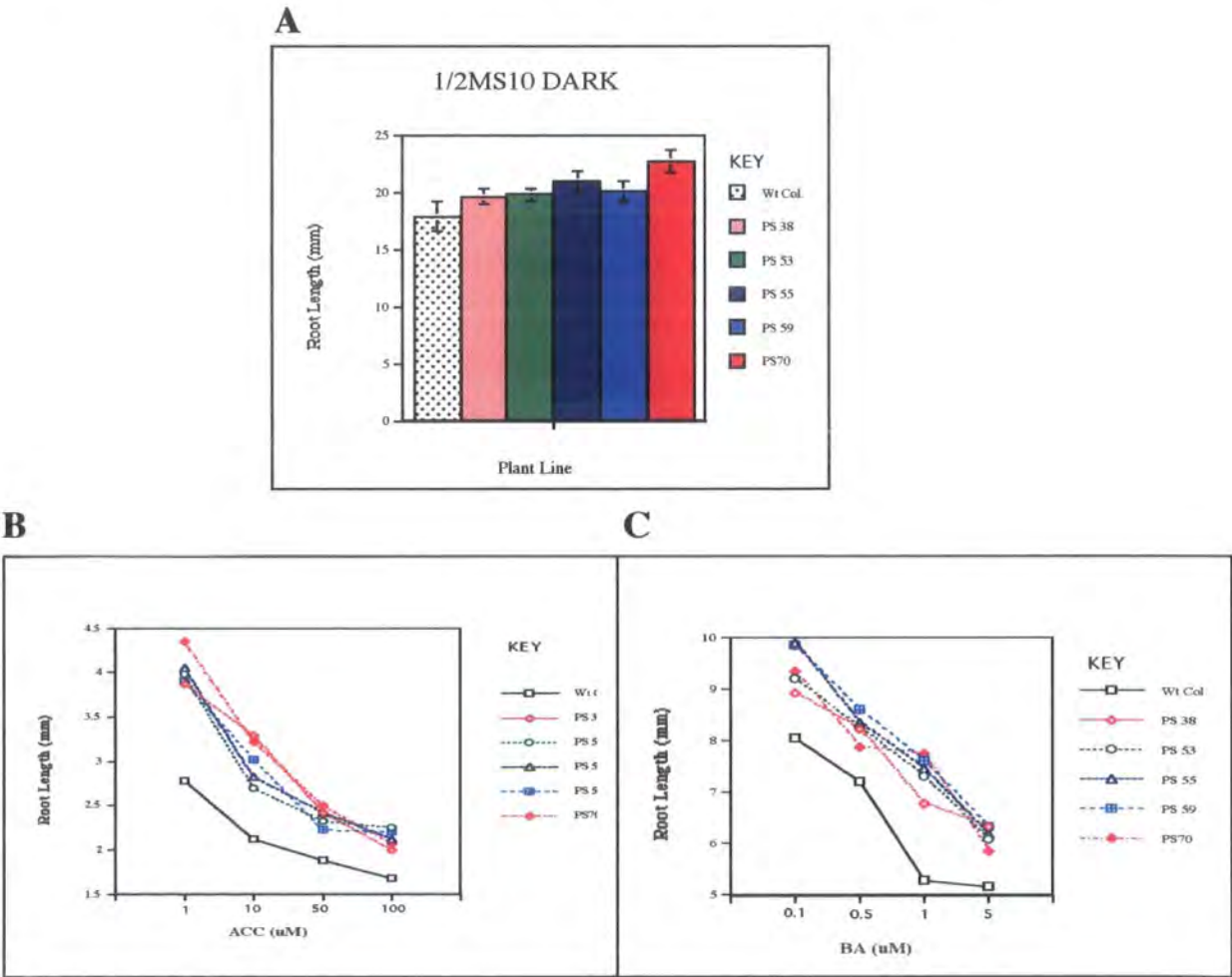


Figure 6.9. The Effect of Overexpressing *POLARIS* on ACC and BA Sensitivity

- A) 35*SPOLARIS* and wild-type seedlings were grown in the dark for 7days on 1/MS10 media following which the length of the primary root was measured for 20 seedlings of each line. The graph indicates the average root length with error bars indicating the SEM.
- B) 35*SPOLARIS* and wild-type seedlings were grown in the dark for 7days on 1/MS10 supplemented with the indicated concentrations of the ethylene precursor ACC. Each point represents the average length of 20 seedlings.
- C) 35*SPOLARIS* and wild-type seedlings were grown in the dark for 7days on 1/MS10 supplemented with the indicated concentrations of the cytokinin BA.



ACC supports a role for *POLARIS* in regulating ethylene response. Therefore the sensitivity of the 35S:*POLARIS* lines to exogenous auxin was examined in order to determine what, if any, the role of *POLARIS* has in regulating auxin responses.

Seedlings were grown in the light in the presence of the auxin, 1-NAA, with concentrations ranging from 10pM to 5μM (concentrations used; 10pM, 100pM, 1nM, 100nM, 1μM, 2μM, 3μM, 4μM and 5μM) and the length of the primary root was determined 7 d.p.g. As expected higher concentrations of auxin between 0.1μM to 5μM resulted in the inhibition of root growth whereas lower concentrations promoted root growth. Root growth of the 35S:*POLARIS* lines on auxin concentrations between 10pM and 0.1μM did not differ significantly from that of the wild-type (data not shown). The roots of both the wild-type and overexpressing lines were too short and fragile to be measured accurately on auxin concentrations higher than 1μM. Though not statistically significant, except in the case of line 38, the root lengths of the transgenic lines were longer than the wild-type on 1μM auxin, a feature not observed on lower concentrations of auxin that were still inhibitory to root growth (compare Figure 6.10 a & b, appendix III). It may be that at this concentration of auxin there is an elevation of ethylene biosynthesis and the difference in root lengths is due to this and not the auxin. It would appear however, that unlike ACC and BA, lines overexpressing *POLARIS* do not show altered sensitivity to a wide concentration range of auxin

6.6 Summary

It has been shown that reintroduction of a wild-type copy of the *POLARIS* gene under the control of its own promoter is able to partially complement the short root phenotype of the *pls* line. This would suggest that it is most probably the knockout of *POLARIS* in the *pls* line and not disruption of the expression of other tightly linked genes that is the cause of this phenotype. Given that the *pls* line is likely to represent a novel constitutive ethylene response mutant this would suggest that *POLARIS* may be considered a negative regulator of ethylene (and cytokinin) synthesis or sensitivity.

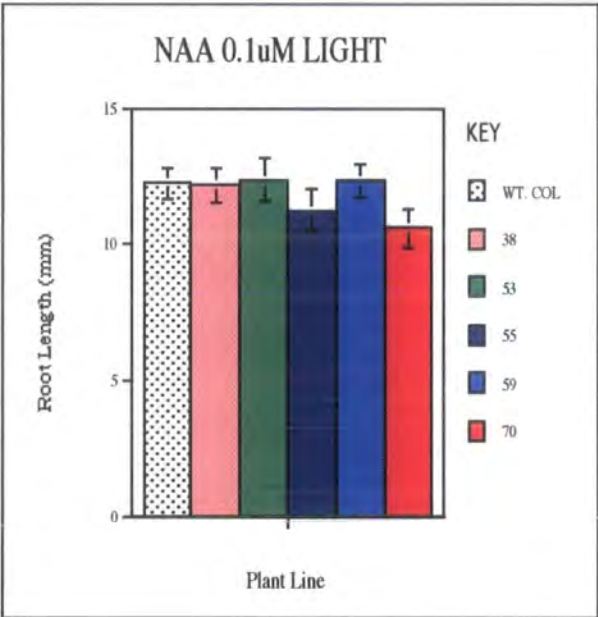
This hypothesis is supported by the examination of transgenic plants overexpressing *POLARIS*. These plants show a degree of insensitivity to the ethylene precursor ACC at varying concentrations and also to the cytokinin, BA, compared to wild-type plants in root growth experiments. At low concentrations of auxin, the root growth of the transgenic lines and the wild-type is the same. At a concentration of 1μM auxin however the transgenic plants have slightly longer roots, an effect which could be attributed to auxin-induced ethylene.

Figure 6.10. Root Growth of 35SPOLARIS Transgenic Lines in the Presence of NAA

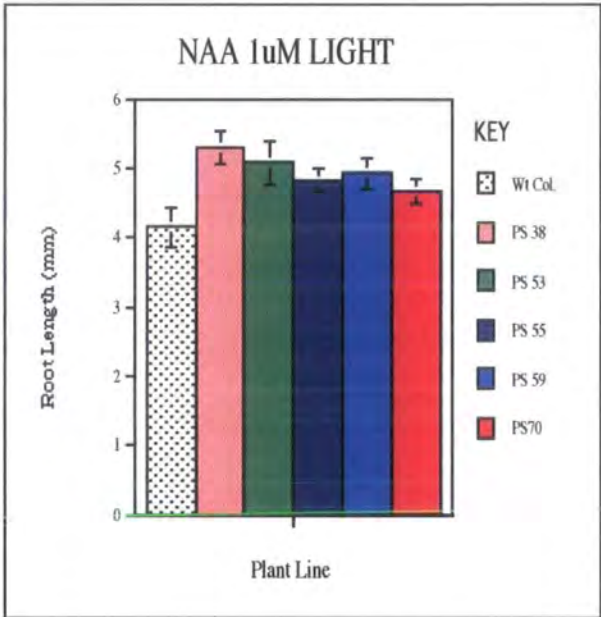
Seedlings were grown in the presence of the synthetic auxin NAA, at the concentrations shown, in the light. For each line, the root lengths of 20 seedlings were measured 7 days after germination.

- A) Seedlings grown in the presence of 0.1μM NAA.
- B) Seedlings grown in the presence of 1μM NAA.

A



B



Chapter 7 Discussion

This study has been concerned with the further characterisation of the *pls* promoter trap line and the subsequent cloning and molecular analysis of the T-DNA tagged *POLARIS* gene. The *pls* mutant line shows GUS activity throughout the root tip and also in various other organs. The short root phenotype of this line appears to correlate with an increase in either ethylene synthesis or sensitivity, though this does not appear to result in any obvious patterning differences between the *pls* root and that of the wild-type. The T-DNA promoter trap has integrated within a small gene called *POLARIS* which appears to function as a negative regulator of ethylene and cytokinin action in the root. This chapter is concerned with discussing a number of points raised by work performed in this study and will conclude with a model of the possible mode of action of the *POLARIS* gene, and a consideration of future work which may contribute to furthering our understanding of the function of this gene in root development.

7.1 Genomic Organisation of the *POLARIS* Locus

In eukaryotes, genes transcribed by RNA polymerase II are typically separated by intergenic non-coding regions of variable length which are thought to contain the regulatory elements required for transcription initiation and termination. Even in the yeast *Saccharomyces cerevisiae*, which has been shown to have tight packaging of genes on its chromosomes, this gene organisation appears to be the case. However, in this study, two transcripts have been identified which appear to show overlap between their 3' and 5' UTRs. The *POLARIS* transcript appears to have potentially two transcriptional initiation sites, as determined by 5' RACE and RPA, which extend between ~23bp and 117bp into the 3' end of the *GENE X* transcript. Such overlap is very unusual for eukaryotic genes, and also raises a number of questions regarding the expression of these two transcripts.

The experimental data support the view that *GENE X* and *POLARIS* are two separate transcriptional units. Firstly, *GENE X* was isolated by 3' RACE which mapped its polyadenylation site to within the 5'UTR of *POLARIS*. When this 3' RACE clone was used as a probe in northern blots using RNA from the *pls* transgenic line it identified a small transcript, presumably itself, but not the larger GUS-fusion transcript. Presumably the 20bp overlap between the major *POLARIS* transcript and *GENE X* was not enough to allow stable hybridisation. When a separate probe, which had considerable overlap between *POLARIS* and *GENE X* was used, it did hybridise to both the GUS-fusion

transcript and *GENE X*. Therefore, in the transgenic line *GENE X* is expressed as a separate transcript to that of GUS. There is no indication of an even larger transcript which could arise from transcriptional readthrough of *GENE X* and GUS. RS-PCR experiments performed on RNA from the wild-type was also not able to detect transcriptional linkage between *GENE X* and *POLARIS*. Other lines of evidence which demonstrate these are two separate genes comes from both the complementation analysis and the transgenic plants overexpressing *POLARIS*. The complementation of the *pls* mutant phenotype was performed using a genomic clone of *POLARIS* which lacked the putative start of the *GENE X* ORF. Overexpressing transgenic plants were able to show reduced sensitivity to ACC and BA, which would correlate with the putative ethylene overproducing phenotype of the *pls* mutant. Furthermore, promoter GUS constructs have shown that part of *GENE X* has promoter activity which correlates with the root tip expression of *POLARIS*. Therefore, whilst the genome organisation may be unusual, it would appear that taken together the experimental data demonstrates that this locus encodes two overlapping sense transcripts.

Such a situation is rare for eukaryotes, though a very similar organisation has been reported for the *EhMCM3* and *EhPAK* genes of *Entamoeba histolytica* (Gangopadhyay *et al.*, 1997). Indeed the *EhMCM3* gene, whose 5' UTR overlaps the *EhPAK* 3'UTR, may also have two transcriptional start sites. More common, though still very rare, is for overlapping convergent transcripts which are transcribed on separate DNA strands. The *OTC* and *AUL1* genes of *Arabidopsis* show just such an organisation with a 22bp overlap of their 3' UTRs (Quesada *et al.*, 1999) as do the *CCT8* and *TRP1* genes of *Candida albicans* where the gene overlap actually extends into the ORFs of both genes (Gerads and Ernst, 1998). Even in the more complex mouse and human genomes examples of gene overlap exist (Speek *et al.*, 1996; Koskimies *et al.*, 1997), a particularly unusual situation being that of the mouse *JAK3* and *Relaxin-like-factor (RLF)* genes. The *JAK3* gene is a complex gene which was initially thought to have 23 exons until it was determined that exon 23 was actually two exons separated by a 2.2kb intron. Within this intron and transcribed from the same strand is the promoter, exon 1 and intron 1 of the *RLF* gene. The second *RLF* exon actually shares the same acceptor splice site as the final *JAK3* exon though both exons have separate polyadenylation signals (Koskimies *et al.*, 1997).

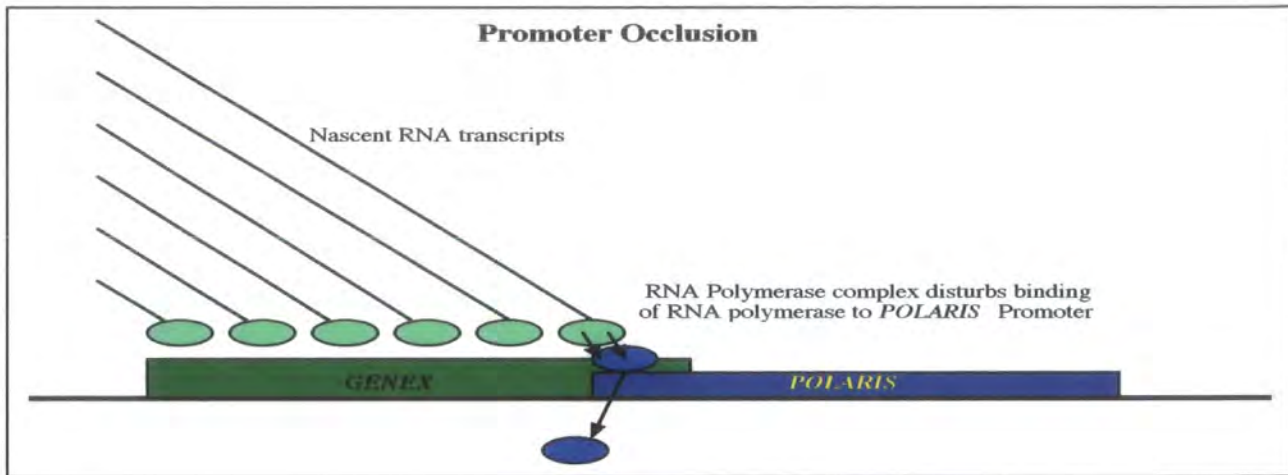
Overlapping transcripts, whether transcribed from the same or separate DNA strands, present particular problems. For convergently transcribed genes where the 3' end of both genes overlap, the problem of transcriptional termination is apparent. Such overlaps require that polyadenylation signals must be incorporated within the sequence

of the gene on the opposite strand and may also present the danger of hybridisation of nascent transcripts, potentially targeting them for degradation. There is also the potential of collision between RNA polymerase complexes though it has been shown for the *nmt1* and *nmt2* genes of *Schizosaccharomyces pombe* that, even though polymerases may extend well beyond the poly(A) signal into a downstream convergent transcriptional unit, the expression of the downstream gene is unaffected (Hansen *et al.*, 1998).

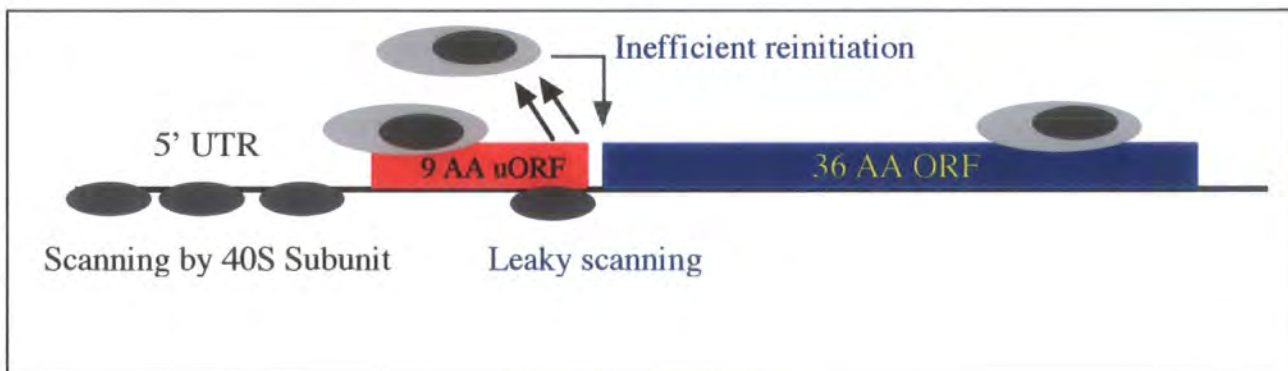
Of direct relevance to *POLARIS* and *GENE X* expression is the problem of promoter occlusion or transcriptional interference (Bateman and Paule, 1988; Irniger *et al.*, 1992). This arises when the RNA polymerase fails to terminate and reads into a downstream transcription unit resulting in reduced expression of this gene by disrupting interactions at the promoter (Figure 7.1 a). When this phenomenon was examined using two tandem RNA polymerase I promoters it was found that, when both promoters were loaded with transcription initiation factors (TIFs), upon addition of polymerase the TIFs on the downstream promoter would be displaced and subsequently transcription from this promoter was inhibited (Bateman and Paule, 1988). A natural example of this appears to occur in the *Saccharomyces cerevisiae* actin gene. The first intron appears to contain a cryptic promoter that is non-functional under normal conditions. However, deletion of the upstream actin promoter or the cloning of a 'strong' poly(A) signal within the intron upstream of the cryptic promoter results in activation of this cryptic promoter. Weaker poly(A) signals which are less efficient at transcription termination result in activity of both promoters (Irniger *et al.*, 1992). Therefore, though the expression pattern of the two genes appears to be subtly different, transcription of *GENE X* is likely to have an inhibitory effect on the transcription of *POLARIS* especially since it would appear that *GENE X* forms part of the *POLARIS* promoter. This may partially explain the apparent low abundance of the wild-type *POLARIS* message. However, this is not so apparent with the GUS-fusion transcript, and is thus likely to suggest other destabilising factors are involved.

It should be noted that whilst transcriptional interference can reduce downstream gene expression, expression of the downstream gene can still occur. One potential explanation for this is that either not all transcription factors are displaced by the elongating polymerase or that those that are displaced can quickly rebind. Also, in the case of *POLARIS*, part of its promoter is also likely to be shared and upstream of *GENE X*. It is therefore possible that the presence of bound upstream transcription factors is able to help stabilise or recruit factors that are displaced by transcription of *GENE X* thus maintaining an initiation complex ready for *POLARIS* transcription.

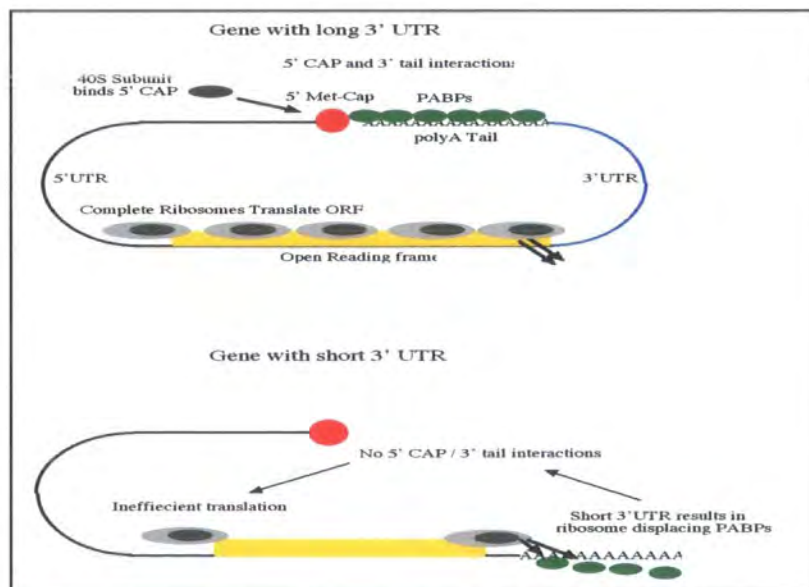
A



B



C



Given the unusual genome organisation of these two genes and the potential for transcriptional interference to inhibit expression of *POLARIS*, another factor that could be considered is how auxin appears to cause upregulation of *POLARIS* expression. Promoter GUS constructs have shown that the shorter p584POL promoter, which contains sequence downstream of the putative 92aa initiation codon, is able to mediate an auxin response and contains potential TGTCTC-like auxin response elements (AuxREs). This would suggest that the auxin response of *POLARIS* is mediated by ARF-like transcription factors binding at the promoter (Ulmasov *et al.*, 1997a). Transfection studies have indicated that ARFs occupy AuxREs regardless of the auxin status of the cell and activate transcription in response to high auxin potentially through interactions/dissociation with or from other factors (Ulmasov *et al.*, 1999a). If transcription interference does occur it may possibly affect ARF binding in this region of the *POLARIS* promoter which might inhibit auxin response. It is feasible therefore that auxin may cause upregulation of *POLARIS* by stabilising ARF binding either through interactions with other factors or even by causing a stalling of *GENE X* transcription due to a stabilisation of the *POLARIS* initiation complex which in turn would allow further loading of polymerase.

The likelihood that this locus has two overlapping divergent transcripts also raises the question of coordinate expression of the two transcripts. The expression pattern of GUS in seedlings of *pls* and p1635POL:GUS transgenics shows similarities to that of the *GENE X* promoter plants which seems to support this possibility. This would possibly be expected considering that the region upstream of the 92aa ORF of *GENE X* is common to the promoters of both transcripts. From closer examination of the GUS expression patterns of the various lines it would appear that the most simple scenario of one promoter controlling the expression of two transcripts cannot explain the differences observed. *pls* shows GUS expression throughout the root tip and meristem and more weakly in the hypocotyl, cotyledons and petioles, an expression pattern mimicked by the 1635POL promoter construct. The *GENE X* promoter construct shows a 900bp overlap with the 1635POL construct plus an additional 700bp of upstream region which does not appear to be required for correct *POLARIS* expression. This construct drives GUS expression in the columella, but apparently not in the meristem, and then after the elongation zone expression is seen in the rest of the root in several cell types. Expression is also observed in the cotyledons and more weakly in the first leaves and also to a weaker extent than in *pls* in the petioles and hypocotyl. In the *pls* line expression in the cotyledons is only observed after longer overnight stainings whereas such long periods were not required with the *GENE X* promoter constructs.

The question therefore is how essentially the same upstream region can give such similar and yet subtly different expression patterns? The most simple explanation is that the difference between the two construct lies in the regions not shared by both the 1635POL and *GENE X* promoter constructs. The downstream unshared region essentially consists of the 584POL construct though there is an 81bp overlap between this and the *GENE X* construct. Analysis of the 584POL:GUS seedlings showed that this region was most likely responsible for the auxin response of *POLARIS* and drove expression in the root tip, though this appeared to be restricted mainly to the young vasculature. Given that 1635POL:GUS expression is throughout the tip and the *GENE X* construct drives expression in the columella and lateral root cap it is tempting to speculate that the elements required for columella and root cap expression are in the shared upstream region whilst expression in the other regions of the root tip is governed by factors binding in the unshared downstream region.

It is more difficult to explain why GUS expression is seen strongly in the rest of the root with the *GENE X* construct but not in *pls* or 1635POL transgenics. It cannot simply be explained by the extra 700bp region of the *GENE X* construct since this is present in *pls*. It is therefore possible that the downstream unshared region of the 584POL construct is again potentially responsible for this difference. One possibility is that the factors that are required for expression in the rest of the root are unable to interact with the transcriptional initiation complex at the *POLARIS* start site but that interaction is possible with the *GENE X* initiation complex. This could be due to the extra factors bound to the 584POL downstream region already occupying the relevant positions in the initiation complex of *POLARIS*. An alternative explanation may relate to the auxin responsiveness of the *POLARIS* promoter. As suggested earlier, it is possible that the auxin response of *POLARIS* is caused by stabilisation of the initiation complex which allows heightened expression by countering transcriptional interference by *GENE X*. The auxin peak in the root (Sabatini *et al.*, 1999) correlates well with *POLARIS* expression whereas auxin levels are much lower further back in the root where *GENE X* expression appears to occur.

Therefore, it is feasible that in regions of high auxin, *POLARIS* is expressed regardless of *GENE X* expression but when the auxin levels fall below a threshold, *GENE X* expression inhibits *POLARIS* expression. This would allow both transcripts to share the same upstream (of *GENE X*) control region and still have different expression patterns. One factor that cannot be discounted and was not investigated in this study is that the p584POL region may also be required for *GENE X* expression. This would require an accurate analysis of the expression profiles of both transcripts by *in situ*

hybridisation, which may not be feasible because of their low abundance. As such it cannot be discounted that the same promoter elements are required for the expression of both transcripts and that they therefore show some degree of coordinate expression. If however, the p584POL region is specific to the expression of *POLARIS* then it is possible that this region is potentially responsible for countering the potential transcriptional interference of *GENE X* in response to auxin. A prediction of this model is that expression of *POLARIS* will be generally limited to regions of elevated auxin concentrations.

7.2 Structure of the *POLARIS* Transcript

The structure of the *POLARIS* genomic locus is unusual but the *POLARIS* transcript itself also shows some unusual features. Firstly there is the possibility of two alternative transcriptional initiation sites giving rise to transcripts that differ only in the length of their 5'UTRs. RNAP experiments indicate that the initiation site nearest to the *GENE X* poly(A) site is used much more frequently than the upstream site. The reason for having two start sites is unknown, and given the overlap with *GENE X* may simply be fortuitous, though the possibility remains that the expression pattern of the alternative transcripts is different.

Compared to the majority of eukaryote transcripts, *POLARIS* has a very long 5'UTR, a feature which was also noted for the overlapping *EhMCM3* and *EhPAK* genes of *Entamoeba histolytica* (Gangopadhyay *et al.*, 1997). By contrast the clustering of three poly(A) sites shortly after the TGA stop codon of the 36aa ORF results in an extremely short 3' UTR, though another poly(A) site 70bp further downstream also appears to be used. It was not determined which of these sites is favoured, though it would seem likely that the cluster represents the common termination region. The 5'UTR of *POLARIS* from the strong start site to the ATG of the 36aa ORF is AT-rich (59%), a feature which is even more noticeable with regards to the first 220bp. Such a high AT content is reminiscent of plant introns and yet there is no evidence from sequencing of RS-PCR clones, 5' RACE and RNAP that this region is spliced. The fact that the GUS-fusion transcript in *pls* is spliced is most likely due to the presence of a cryptic splice site in the T-DNA left-border. One possible consequence of the AT-richness of this region is that it may form weak secondary structure which may act to stall ribosome progression, but this remains to be tested.

Another interesting feature of the 5'UTR of *POLARIS* is the presence and positioning of two small ORFs upstream of the larger 36aa ORF. No other ATG codons are found in the rest of the 5' UTR from the more frequently used start site so the

presence of these two small ORFs may be significant. The presence of upstream ORFs (uORFs) is rare in most eukaryote messages and yet are found in a number of oncogenes (Kozak, 1986), the expression of which would be expected to be tightly regulated. The scanning model of translation (Kozak, 1978) suggests that the small 40S subunit of the ribosome binds the 5' cap of the transcript and then migrates to the first ATG start codon in a favourable context whereby it is joined by the larger ribosomal subunit and proceeds in the translation of the ORF. The presence of the uORF may therefore inhibit the identification of the main ORF and a number of studies in both plants (Damiani and Wessler, 1993; Wang and Wessler, 1998) and other eukaryotes (Oliveira and McCarthy, 1995; Linz *et al.*, 1997) indicate a role for uORFs in the regulation of both transcript stability and the expression of the main ORF. The maize *R* gene family encodes transcriptional activators required for activation of the anthocyanin biosynthetic pathway. The 5'UTR of a number of members of this family contain uORFs, which in the *Lc* transcript includes a 38 codon ORF which terminates 59bp from the main ORF (Damiani and Wessler, 1993). The effect of the *Lc* 5'UTR on expression of the luciferase reporter gene was examined (Wang and Wessler, 1998). It was found that the uORF had an inhibitory effect on luciferase translation that was independent of the amino acid content of the uORF. Much of this inhibition was determined to be due to inefficient reinitiation of ribosomes and not leaky scanning, a factor that seemed to be dependent on the sequence of the UTR between the uORF and luciferase ORF. The stability of the message did not appear to be affected by translation of the uORF (Wang and Wessler, 1998).

In yeast the presence of uORFs has been shown not only to inhibit expression of the main ORF but also to destabilise the message (Oliveira and McCarthy, 1995; Linz *et al.*, 1997). Minimal sequence changes in a 5'UTR linked to the *cat* reporter gene that generated uORFs were found to have significant inhibitory effects on the translation of the *cat* gene. Greater inhibition was observed if the uORF was not too close to the 5' end of the message and if the spacing between the uORF and the main ORF was reduced. This indicates that the closer the uORF is to the main ORF, the more ribosome reinitiation is relied upon for ORF translation. Coupled with this was the fact that the steady state levels of the uORF-bearing messages was lower than controls and this was shown to be due to reduced stability of the messages (Oliveira and McCarthy, 1995). Similar results have been observed in yeast using other reporters and 5'UTRs containing uORFs and it has been proposed that uORFs may destabilise messages via the nonsense-mediated decay mechanism (NMD; Linz *et al.*, 1997). In this mechanism, aberrant transcripts which contain nonsense mutations in the first two thirds of an ORF

are targeted for degradation. This mechanism is presumably part of a surveillance system that removes abnormal messages that may result in the production of truncated cytotoxic proteins, and genes required for this process have been identified (He *et al.*, 1997). It has been proposed that the termination and release of ribosomes by uORFs may target messages for NMD (Linz *et al.*, 1997). The significance of this is that evidence suggests that NMD may well be active in plants (Jofuku *et al.*, 1989; Voelker *et al.* 1986).

Given the ability of uORFs to affect both translation and message stability it would seem possible that the presence of the two small uORFs in the *POLARIS* transcript are acting in a similar fashion to regulate expression of the putative 36aa *POLARIS* polypeptide. This may be especially relevant to the 9aa ORF that is in frame with the 36aa ORF (Figure 7.1 b). The stop codon of the 9aa ORF may be considered by the NMD machinery to be a nonsense codon in a larger 46aa ORF and thus instigate destabilisation of *POLARIS*. There are however some observations that raise doubts over the potential effect these uORFs may have, especially regarding a destabilising effect. In both the *pls* mutant and the promoter-GUS transgenic lines, the GUS fusion transcript is moderately abundant and can be easily detected by northern blotting using total RNA, though they share virtually the same 5'UTR as *POLARIS*. It could be argued that position effects are responsible for the differences in steady state levels between the GUS-fusion transcripts and *POLARIS*. However, to explain the levels in *pls* it would have to be shown that the insertion of the T-DNA into *POLARIS* acts to open the whole locus making it more accessible for transcription. Yet, without the proper controls in which these uORFs are removed by mutagenesis, it cannot be ruled out that they are not affecting the stability of the fusion-transcripts. If they do destabilise the transcript, a crucial factor which may explain the differences in the steady state levels of *POLARIS* versus the fusion-transcripts, especially in the promoter-GUS lines where the whole *POLARIS* ORF is fused in frame with GUS, may be the length of either the ORF or transcript. Even if the uORFs reduce the translation of GUS it may be that the longer GUS ORF allows a build up of ribosomes on the fusion-transcript which partially blocks the decay mechanism. By comparison the small *POLARIS* ORF would not be able to accommodate many ribosomes and thus would be more susceptible to decay.

It cannot be ruled out that factors other than the uORFs are responsible for the apparent instability of the *POLARIS* transcript. The 3'UTRs of some genes contain sequence elements that are involved in transcript destabilisation. In plants the most characterised is the DST element found in the conserved region of the *SAUR* transcripts' 3' UTRs (Newman *et al.*, 1993; Gil and Green, 1996). A destabilising element in the *POLARIS* 3'UTR could explain the differences in steady-state levels with the fusion-

transcripts which do not share this region. However, if the 36aa main ORF is considered the principal translation product of *POLARIS* then the 3'UTR of the transcript ranges in size between only 10bp and 90bp. If this region does contain instability determinants then they are novel.

The cluster of three poly(A) sites so close to the stop codon of the 36aa ORF suggest that the signals for polyadenylation probably lie within the ORF. In plants polyadenylation appears to be controlled by a near-upstream element (NUE), an A-rich sequences of 6-10bp situated 10-40bp upstream of the poly(A) site and also a far-upstream element (FUE, Li and Hunt, 1997). Multiple poly(A) sites in plants are not uncommon (Dean *et al.*, 1986) and do not appear to be involved in differential expression but may rather reflect the nucleotide preference of the 3'UTR. Each poly(A) site is believed have its own NUE which might reflect the A/T richness of the 36aa ORF. The 3'UTR of most transcripts is between 100-200nt in length which makes the short 3'UTR of *POLARIS* unusual. However the significance of this is unknown. It has been shown in transient expression systems that an extremely short 3'UTR repressed expression from a polyadenylated reporter message (Tanguay and Gallie, 1996). The eukaryote ribosome spans some 30-35 nucleotides and therefore a terminating ribosome would extend some 15 nucleotides past the TGA stop codon of the 36aa ORF which would contact the cluster of poly(A) sites. It has been shown that interactions between the poly(A) tail and 5' methylated cap are required for efficient translation (Le *et al.*, 1997; Niepel *et al.*, 1999). It is possible that long 3'UTRs are favoured because they may prevent ribosomes from colliding and disturbing poly(A)-binding protein which in turn is required for interactions with the 5' cap. As with the uORFs, it is possible that the short 3'UTR of *POLARIS* acts to reduce the translation efficiency of the 36aa ORF (Figure 7.1 c). If this were the case then it would be expected that use of the farthest downstream poly(A) site would lead to an increased efficiency of translation, However, this was not examined in this study. It should be noted that reduction in the length of the 3'UTR of reporter RNAs did not affect the stability of these RNAs, only their translation efficiency (Tanguay and Gallie, 1996). This indicates that the stability determinants of the *POLARIS* transcript are probably not linked to sequences in the 3'UTR.

7.3 The *POLARIS* Polypeptide

The *POLARIS* transcript therefore displays a number of unusual features including its A/T-richness, long 5' UTR with uORFs, and short 3'UTR. The apparent instability of the transcript compared to the GUS-fusion transcript could therefore be due to a

number of possibilities. It would seem however that the structure of the transcript is designed towards reducing the level of translation of the 36aa ORF which appears to be the major polypeptide product of this transcript. This study has been unable to prove directly that this ORF is translated into a functional product and there are the other smaller uORFs which could be functional. Nevertheless, overexpression of *POLARIS* was performed with only a partial transcript, which included the 36aa ORF, and the full-length transcript was not required. This seems likely to discount the possibility of *POLARIS* being an active RNA. Further work is currently underway which is expected to distinguish between the possibilities of active RNA versus polypeptide.

If the 36aa polypeptide does represent the active product of the *POLARIS* transcript it would appear from the structure and abundance of the transcript that it is probably low abundance itself. It is also predicted that this polypeptide would be subject to a number of post-translational modifications. The basic arginine residues in the putative turn region between the two predicted β -sheets may form a cleavage site resulting in removal of the N-terminus, which may be required for generation of the active form of the polypeptide. These residues may also form part of a phosphorylation signal with serines 13 and 15 or tyrosine 18 and 23 being the possible targets (Pearson *et al.*, 1993). Potentially, phosphorylation may regulate cleavage or activate/deactivate the polypeptide by altering its conformation. Serine/tyrosine phosphorylation may be a means of modifying the activity of the polypeptide and it may be relevant that all six residues are predicted to lie in the second β -sheet. The C-terminal region of the polypeptide is predicted to form an amphipathic α -helix, with these motifs often involved in determining protein-protein interactions. It is possible that this polypeptide may form homodimers via interactions between the hydrophobic faces of two helices though interaction with an as yet unknown second polypeptide is under investigation (P. Chilley, unpublished data). If *POLARIS* does interact with other polypeptides, the interactions could be stabilised by disulphide bond formation involving cysteine 17.

The sequence of the polypeptide did not reveal any predicted localisation signals. Experiments in which the polypeptide was fused to the N-terminus of GFP and expressed in transgenic plants did not conclusively provide evidence for subcellular localisation (data not shown). The small size of the polypeptide means it is probably capable of diffusing through the nuclear pore without requiring the action of a transporter (Raikhel, 1992) but cytoplasmic localisation is also possible. Molecules between 1-3kDa can also diffuse through the plasmodesmata, the channels that connect cells (Jackson and Hake, 1997) and although this limit is slightly smaller than *POLARIS*, it is possible that a truncated version could move between cells.

The lack of homology to other known proteins makes conclusions about the function of POLARIS difficult but possibilities will be discussed in a later section. Functional studies could not be carried out due to the inability to express the polypeptide in bacteria, a problem which may be due to the differences in codon usage between plants and bacteria. However, the possibility that *POLARIS* encodes a small active polypeptide adds to the growing list of plant peptide factors. Polypeptide signalling molecules are common in animal systems with a noticeable feature being that they are all formed from larger prepolypeptides by cleavage events. To date, peptide factors belong to a very small family in plants consisting of CLAVATA3 (Fletcher *et al.*, 1999), phytosulfokines (Matsubayashi and Sakagami, 1996), Enod40 (reviewed in Bisseling, 1999) and systemin (Pearce *et al.*, 1991). There is also evidence that analogues of mammalian atrial natriuretic peptides exist in plants and mediate stomatal pore opening (Billington *et al.*, 1997).

Loss of function *CLAVATA3* mutants show enlarged shoot apical and floral meristems and act in the same pathway as the CLAVATA1 receptor kinase (Clark *et al.*, 1995; 1997). The gene itself encodes a 96aa polypeptide with a putative 18aa N-terminal signal peptide (Fletcher *et al.*, 1999). It is proposed that CLV3 is the ligand of CLV1 and yet the transcripts of both genes are expressed in different layers in the meristem which may indicate that CLV3 is secreted after processing (Fletcher *et al.*, 1999).

Phytosulfokines are short (4-5aa) disulphated peptides first isolated from asparagus cell cultures due to their ability to compensate for the cell growth inhibition observed in low-density cultures. These factors can act at very low concentrations and their biosynthesis appears to be regulated by auxin and cytokinin (Matsubayashi *et al.*, 1999). A phytosulfokine transcript has been isolated from rice which encodes a putative precursor polypeptide with the phytosulfokine sequence at the C-terminus. Though phytosulfokines have only been identified in suspension cultures and not plants, the transcript was localised to the meristems of rice seedlings consistent with a role for these peptides in cell proliferation (Sakagami *et al.*, 1999).

Enod40 genes have been identified in a number of legumes (reviewed in Bisseling, 1999) and is one of the first plant genes activated during nodule formation. It is predicted that these genes play a role in positioning of the nodule primordia by counteracting the negative effect of ethylene on cortical cell division; this hormone is known to block *Rhizobium* induced cortical cell division. The *Enod40* genes all appear to encode a conserved 10-13aa polypeptide which is translated though it is yet to be decisively proven that this is responsible for the gene activity.

Systemin was identified as a polypeptide factor that could induce wound-inducible proteinase inhibitor expression in unwounded tissue (Pearce *et al.*, 1991; reviewed in Ryan and Pearce, 1998). The 18aa active peptide is cleaved from a 200aa prosystemin precursor the gene for which, when expressed as an antisense transcript, inhibits the systemic wound response indicating the importance of this gene for wound response. The transcript itself is expressed following wounding within the vascular bundle which is consistent with systemin being transported through the phloem to unwounded tissues. Here it activates a signal transduction cascade resulting in the formation of jasmonic acid leading to proteinase inhibitor gene expression. Such responses are mediated by extremely low concentrations of systemin in the pico-femto molar range, indicating the powerful activity of this peptide. More recently a putative receptor has been identified on the plasma membrane of tomato suspension culture cells that may mediate the signalling cascade in response to systemin binding (Scheer and Ryan, 1999).

As with the multitude of animal peptide signalling molecules, it appears that plant peptides are cleaved from larger precursors and appear to be active at very low concentrations. These concentrations, certainly in the case of phytosulfokines and systemin, are generally lower than required for the classic plant hormones to elicit a response. The fact that very few peptide signalling factors have been identified in plants compared to animals may reflect a divergence in the nature of signalling perception and propagation. In contrast it may indicate that as yet a large proportion of these factors have yet to be identified and that a number of plant signalling cascades are mediated by their action. Given this fact it is interesting to note that at the same locus both *GENE X* and *POLARIS* appear to encode small polypeptides. Many features of the *POLARIS* transcript and the putative 36aa *POLARIS* polypeptide suggest that it may be a new addition to this family of plant peptide factors. The amino acid sequence and predicted structure strongly suggest processing of the N-terminus whilst the C-terminus may mediate interactions with other proteins. Its activity may also be mediated by phosphorylation indicating a signal cascade. The structure of the gene points strongly to tight regulatory mechanisms that result in inefficient translation of the polypeptide indicating that it may be active at very low concentrations. This factor, as well as its potential cleavage, may explain why a polyclonal antibody to the N-terminus could not detect the polypeptide. Further experiments are required to prove that the *POLARIS* gene does encode such a novel peptide factor.

7.4 The *pls* Phenotype

In the *pls* line the T-DNA has inserted within the 25th codon (leucine) of the putative POLARIS polypeptide and is therefore expected to produce a null allele of the gene. Complementation of the *pls* phenotype with a wild-type *POLARIS* allele indicates that it is this mutation which results in plants with shorter roots. This appears to be the result of reduced expansion of all the mature cell types of the root and not due to any major disruption in the patterning of the root. From the GUS staining and northern analysis of the fusion transcript in *pls* it would appear that *POLARIS* expression in the wild-type is mostly restricted to the root tip and the young vasculature. A relationship must therefore be drawn between the mutant phenotype of *pls*, the expression of *POLARIS*, and the activity of the gene product.

Expression of GUS in *pls* is first evident at the heart stage of embryogenesis in the region of the embryonic root primordia. As yet a detailed anatomical examination of embryogenesis of *pls* has not been performed and therefore it cannot be determined if there are phenotypic differences to the wild-type. It is therefore unknown whether the post-embryonic defects in *pls* root development have their origin in embryogenesis. In general, of the mutants identified so far in *Arabidopsis* that affect root development and polarity, those which have noticeable defects in embryogenesis such as *monopteros*, *bodenlos* and *hobbit* all result in severe post-embryonic root defects. The *pls* root phenotype is relatively weak in comparison which may indicate a predominantly post-embryonic role for *POLARIS*. Alternatively, the role of *POLARIS* in embryogenesis may be subtly different to its post-embryonic role in root development. It is also possible that the level of expression of factors which *POLARIS* interacts with or regulates is higher in the seedling than the embryo making the seedling more susceptible to mutations in *POLARIS*.

The observations that mature cells in the *pls* root are shorter than their wild-type counterparts indicates a defect in cell expansion/elongation in the mutant. However, unlike cell expansion mutants such as *cobra*, *cudgel* and *lion's tail* (Benfey *et al.*, 1993; Hauser *et al.*, 1995) the phenotype of the *pls* root is not dependent on maximal root growth (P. Chilley, unpublished data). The defects in cell length are also not more noticeable in one cell layer than another and although there is an increase in radial expansion (M. Souter, unpublished data), again it is not restricted to a single cell layer. Furthermore, unlike *lion's tail* in which reduction in cell expansion prevents cells achieving normal cell volumes, *pls* roots do not show abnormal expansion variably along the root.

The *pls* mutant does show similarities to both *sabre* (Benfey *et al.* 1993; Aeschbacher *et al.* 1995) and *stunted plant1* (Baskin *et al.* 1992; 1995). Unlike the other classes of expansion mutants, the *sabre* phenotype is not conditional on maximal root growth and can be partially rescued by growth in the presence of silver ions implicating a role for ethylene in the *sabre* phenotype. The roots of *stunted plant1* do not show any radial expansion and are shorter than the wild-type and like *pls*, root hairs develop closer to the tip than in the wild-type (P. Chilley, unpublished data). However, unlike *pls*, the defect in *sabre* roots is most significant in one cell layer, the cortex, and involves a change in the orientation of expansion rather than the degree of elongation. In *stp1* both the meristem and elongation zones are smaller than the wild-type whereas in *pls* only the elongation zone appears to be shorter accounting for the formation of root hairs closer to the tip. Furthermore, *stp1* is less sensitive to cytokinins whereas *pls* is hypersensitive to this hormone. Therefore, whilst the *pls* mutant is defective in cell expansion in the root it shows a number of differences to the expansion mutants described thus far.

The phenotype of *pls* can be phenocopied by treatment with low concentrations of auxin, NPA, ACC and cytokinin (P. Chilley, unpublished data; personal observations) indicating that interactions between these hormones is critical for correct growth of the root. Furthermore a number of other mutants defective in root pattern and morphology have been described which implicate these hormones (Dolan *et al.*, 1994; Aeschbacher *et al.*, 1995; Hardtke and Berleth, 1998; Hamann *et al.*, 1999; Hobbie *et al.*, 2000). An important feature of the *pls* phenotype is that it can be rescued by growth in the presence of silver ions, which are thought to block perception of ethylene by interactions with the receptors. This would most likely suggest that the production of ethylene is defective in *pls* putting this mutant in the overproducing class of constitutive ethylene response mutants. Increased levels of the ethylene-induced *GST2* transcript in *pls* compared to the wild-type provides further support for a defect in ethylene levels or perception in *pls*. Furthermore, *etr1/pls* double mutants have an *etr1* phenotype (P. Chilley, unpublished data) indicating that *pls* is genetically upstream of the ethylene receptors, which correlates again with defects in ethylene levels.

If increased ethylene levels are responsible for the short root phenotype of *pls* then this would suggest that *POLARIS* is a negative regulator of ethylene production. Complementation of the *pls* phenotype was achieved by reintroducing a wild-type allele of *POLARIS* which, at least in one line, 113C, resulted in downregulation of the ethylene-induced *GST2* transcript to near wild-type levels. Also, it would be predicted that if *POLARIS* does negatively regulate ethylene levels then overexpression would

reduce sensitivity to this hormone. This was indeed observed in the five independent lines that overexpress a partial *POLARIS* transcript.

However, the over-expressing lines are also partially resistant to exogenous cytokinin which could also be predicted given that *pls* roots are hypersensitive to this hormone. One possibility therefore is that the *pls* phenotype results from an increase in cytokinin-induced ethylene. It is well documented that seedlings grown in the dark in the presence of cytokinin exhibit a triple-response phenotype and cytokinin has been shown to modulate ethylene levels (Lieberman, 1979; Yang and Hoffman, 1984; Abeles *et al.*, 1992). The *cin5* mutant (Vogel *et al.*, 1998a; Section 1.7.8) exemplifies the link between cytokinin and ethylene. The *ACS5/CIN5* gene has been shown to be responsible for a significant proportion of the ethylene produced in response to low cytokinin levels. Hypersensitivity of *pls* to cytokinin and an apparent increase in ethylene levels combined with the partial insensitivity of the 35*SPOLARIS* lines to these hormones is consistent with *POLARIS* functioning to be a negative modulator ethylene production in response to cytokinins. It is also possible that *POLARIS* modulates cytokinin accumulation and/or sensitivity. It cannot be discounted that *POLARIS* acts independently of cytokinin to modulate ethylene levels.

Given this postulated role for *POLARIS* it is interesting that *pls* heterozygotes show a reduced root length, intermediate between *pls* and the wild-type (P. Chilley, unpublished data), indicating that a reduction of *POLARIS* levels is limiting to root growth. However, the decrease in sensitivity of the *POLARIS* over-expressing lines to exogenously applied BA and ACC is small. Northern analysis shows that each of these transgenic lines is expressing the partial *POLARIS* cDNA at levels many times greater than that of the wild-type *POLARIS* transcript. This would suggest that *POLARIS* is not rate-limiting for root growth when present at high concentrations, though this may apply to component(s) with which *POLARIS* may interact. It also cannot be discounted that whilst the over-expressing lines contain high levels of the truncated *POLARIS* transcript they do not have a similar increase in the amount of the gene product. The partial transcript still has the uORFs and though inserted upstream of a synthetic 3'UTR and poly(A) signal may still possess its own short 3'end. These factors combined may result in very inefficient translation of the transgene and thus only marginal changes in the sensitivity of the transgenic plants. The fact that high steady-state levels of the partial transcript are observed in the overexpressers raise doubts about the ability of the uORFs to destabilise the *POLARIS* mRNA.

The experimental evidence indicates that *POLARIS* is a negative regulator of cytokinin-induced ethylene biosynthesis and may also modulate sensitivity to these

hormones. Therefore, how does mutation of *POLARIS* result in the short root *pls* phenotype?, how does this correlate with the expression pattern and regulation of *POLARIS*?, and how is *POLARIS* involved in regulating cytokinin and ethylene responses?

The reduction in cell expansion and increased radial swelling (M. Souter, unpublished data) of the *pls* root is consistent with an ethylene overproducing phenotype which can be phenocopied by growth in the presence of either ethylene or ACC (Aeschbacher *et al.*, 1995). One means by which increased ethylene levels may cause reduced cell expansion and radial swelling is by inhibiting polar auxin transport in the root. Depending on the local concentration, auxin is able to both stimulate or inhibit cell expansion. Inhibition of polar auxin transport, by increased ethylene levels, may therefore result in either a reduction or accumulation of auxin in the root which would effect cell expansion.

Interestingly, mutations in the *AtPIN2/EIR1/AGR1* gene (Luschnig *et al.*, 1998; Muller *et al.*, 1998; Chen *et al.*, 1998), which encodes a putative auxin efflux carrier, results in roots that are insensitive to ethylene, are agravitropic and longer than their wild-type counterparts. In many ways, the *eir1/agr1* phenotype can be considered an opposite of that of *pls* since *pls* roots are short and hypersensitive to cytokinin and to a lesser extent, ACC. Localisation of the AtPIN2p to cortical and epidermal cells (Muller *et al.*, 1998; section 1.7.2) would suggest that mutations in this gene impair basipetal auxin transport. This would presumably result in lower auxin levels in the cortical and epidermal cell files in the elongation zone, with possible increases in auxin in the root cap. It has been postulated that the ethylene-insensitive phenotype of the *eir1/agr1* mutant is due to there being insufficient auxin in the cortex and epidermis of the elongation zone for ethylene to act (Leyser, 1999).

It could be argued that inhibition of auxin transport by ethylene would, as is likely in *eir1/agr1*, result in reduced auxin reaching the cortex and epidermis. Therefore, the short root phenotype of *pls* would not be due to inhibition of polar auxin transport by ethylene. However, ethylene has been shown to reduce the capacity of auxin movement but not its velocity of transport (Suttle, 1988). This is more likely to result in an accumulation of auxin in cells near to tip, where auxin is redistributed following transport from apical parts of the plant. This would include the cortex and epidermis in the elongation zone. Increases in the concentration of auxin in these cells could result in a reduction in expansion. Treatment of C24 seedlings with NPA, an auxin transport inhibitor, results in a short root phenotype similar to that of *pls*. It has been observed that treatment of *pls* roots with NPA results in an increase in GUS staining in the root tip

(P. Chilley, unpublished data; personal observations). Since auxin upregulates *POLARIS*, this could be interpreted as NPA treatment causing a local increase in the auxin concentration at the root tip. Also, a number of auxin resistant mutants are cross resistant to ethylene which combined with the *eir1* phenotype may indicate that if insufficient auxin is present (or sensed) in the elongation zone, ethylene is unable to effect cell expansion by inhibition of auxin transport.

Preliminary results, examining the localisation and expression of PIN proteins in the root tip, indicate increased levels of these proteins in *pls* compared to the wild-type (M. Souter, unpublished data). The increased levels of PIN proteins in *pls* root cells may be in response to an accumulation of auxin resulting from ethylene-induced inhibition of polar auxin transport.

Therefore, inhibition of polar auxin transport is a strong candidate for the means by which the proposed elevated ethylene levels of *pls* could cause the short root phenotype though further experimentation is required to verify this. It should be noted however, that the mechanism(s) by which ethylene inhibits auxin transport must be subtly different to that of the chemical inhibitors, NPA and TIBA. Prolonged treatment with these chemicals results in agravitropic roots and changes in cellular pattern (Sabatini *et al.*, 1999). These phenotypes are not observed in *pls* and also have not been reported for *ctr1*, though this mutant does have altered root hair patterning. Furthermore, analysis of *ein2-1/eir1-1* double mutants revealed that the roots of these plants were still agravitropic and yet when grown in the presence of ethylene, the roots were significantly longer than *eir1-1* roots but not those of *ein2-1*. This suggests that whilst EIN2 and EIR1/AtPIN2 act in the same pathway effecting ethylene-induced inhibition of root elongation, gravitropism is controlled by a separate EIR1/AtPIN2 dependent pathway (Roman *et al.*, 1995). The relationship between ethylene and auxin transport is therefore not likely to be a simple one.

There is mounting evidence for a small family of auxin export transporters in *Arabidopsis* (Palme *et al.*, unpublished data in Palme and Galweiler, 1999) and one possibility is that they respond differentially to ethylene, possibly via different ethylene signalling pathways. This may separate the action of ethylene from that of the auxin transport inhibitors such as NPA. Such chemicals may act in a 'global' manner to inhibit auxin transport resulting in accumulation of auxin in the root tip which as reported results in pattern changes (Sabatini *et al.*, 1999). By being responsive to ethylene in a differential manner, the different auxin transport proteins may allow ethylene to affect such processes as cell elongation without affecting meristem patterning. This would be beneficial to the plant since it would allow changes in root

elongation to be mediated by ethylene-induced inhibition of auxin transport without a detrimental accumulation of auxin at the meristem.

Ethylene is a positive regulator of root hair cell fate (Dolan *et al.*, 1994) but inhibits cortical cell division during nodule formation (Heidstra *et al.*, 1997). Plants which overproduce auxin whilst retaining wild-type ethylene levels (Romano *et al.*, 1993) have been used to distinguish the different roles of these two hormones, though the effects on root growth were not reported. Therefore, whilst inhibition of auxin transport by ethylene is a good candidate for the reduced cell expansion in the *pls* root it should not be discounted that ethylene may be acting in an auxin-independent manner.

7.5 Expression of *POLARIS* and the *pls* Phenotype

How then can the expression pattern of *POLARIS*, specifically with regards to the root, correlate with the mutant phenotype of *pls*. As described, the expression pattern of GUS in *pls* and the *POLARIS* promoter-GUS lines is similar to that of the DR5 synthetic auxin response promoter. This corresponds to an auxin peak in the root and also the predicted site of auxin efflux carrier localisation. If considering auxin transport, then *POLARIS* expression would be associated with unloading of auxin from the stele and also the initial aspects of the basi-petal transport machinery. Indeed, expression of GUS at the heart stage of embryogenesis can be correlated with the formation of the auxin transport machinery. It might also be used to explain the expression of GUS in a *gnom* mutant background. It has been shown that correct localisation of AtPIN1 requires functional GNOM protein and that in its absence, AtPIN1 localisation is defective (Steinmann *et al.*, 1999). GUS expression in the most severe ball-shaped *gnom* embryos is diffuse rather than localised which correlates with this defective localisation of the auxin transport machinery. This adds support to the growing body of evidence indicating that auxin is a positional signal required for polarity and pattern formation in the embryo. Therefore, as discussed previously in section 7.1, expression of *POLARIS* in the root tip is most likely in response to the high local concentration of auxin. This expression has been shown to be independent of cell division activity (Topping and Lindsey, 1997).

As discussed, it is proposed that *POLARIS* acts as a negative regulator of cytokinin-induced ethylene biosynthesis and may modulate sensitivity to these hormones. Due to the expression pattern of *POLARIS*, this role is likely to be restricted to the root tip. This correlates with studies which have immunolocalised cytokinins to the root tip in cells surrounding the quiescent centre (Zavala and Brandon, 1983). Furthermore, cytokinins are synthesised in the root tip whereafter they are transported through the vascular tissue

to the aerial parts of the plant (Davies, 1995). This is consistent with the fact that both cytokinins and auxin are required for cell division (Miller *et al.*, 1955; Riou-Khamlichi *et al.*, 1999) and therefore meristem activity in the root.

As well as cytokinin, members of the *ACS* family are also localised to the root tip (Rodrigues-Pousada *et al.*, 1999). Since cytokinin has been implicated in the post-transcriptional control of members of this family (Woeste *et al.*, 1999b) it might be expected that the presence of cytokinin in the root tip would induce ethylene production which in turn would result in the inhibition of auxin transport. The result of this may be changes in cell expansion, which in certain conditions, such as compact soil, may prove beneficial to the root. The increase in concentration of auxin at the root tip resulting from this inhibition of auxin transport could then act as a feedback mechanism to activate *POLARIS* which may then block cytokinin-induced ethylene in the root tip, resulting in normal cell expansion. The fact that cytokinins reduce whilst auxin rapidly increase *POLARIS* transcript levels (Topping and Lindsey, 1997; section 3.3) indicates that hormonal cross-talk is an important factor in the regulation of *POLARIS*. *POLARIS* is a low abundance transcript, which is also a feature of some of the *ACS* transcripts, and features of the transcript suggest inefficient translation of the putative *POLARIS* polypeptide. These features are consistent with a short-lived regulator involved in either feedback or cross-talk mechanisms.

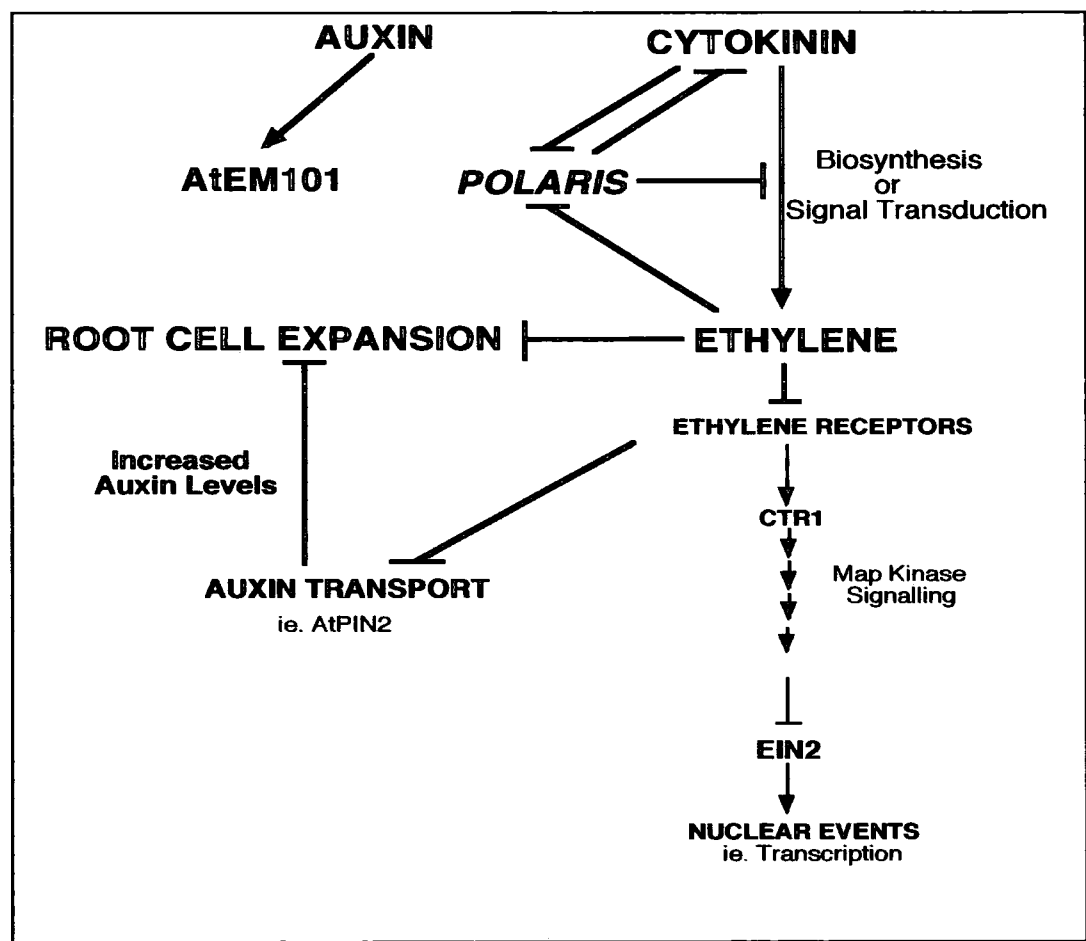
Taken together, the results of this study add support to previous reports that hormonal response pathways are not simple linear pathways and must be robust and diverse enough to integrate a number of separate signals, allowing for the plasticity of plant growth and development. *POLARIS* is likely to represent a gene required for integrating auxin, cytokinin and ethylene signals in order to regulate root growth. Based on the results of this study and ongoing work in our laboratory a simple model for the mode of action of *POLARIS* is presented in Figure 7.2.

7.6 Future Work

This study has raised a number of avenues for future investigation both at the molecular and plant level. Certainly one of the most important points is to clarify where the *POLARIS* gene is likely to act with regards to known auxin, cytokinin and ethylene pathways which will require double-mutant analysis. A number of these crosses have been performed or are underway and include *eir1-1*, *aux1-7* and *ein2-1* (P. Chilley, unpublished data) and should give valuable information. If *POLARIS* is involved in a pathway regulating cytokinin-induced ethylene then it would be expected that *eir1-1* would be epistatic. It would also be interesting to determine whether the roots of these

Figure 7.2. Model to Explain the Possible Mode of Action of *POLARIS* in the Root

The root tip is a region of auxin accumulation, and auxin may have a positive role in the regulation of *POLARIS* expression, though this is as yet only through analogy with AtEM101 expression. Cytokinin is synthesised in the root tip and is known to induce ethylene biosynthesis and inhibit expression of *POLARIS*. Ethylene can inhibit cell expansion, possibly by inhibition of auxin transport in the root, though this may be through another, direct pathway. A model is proposed in which *POLARIS* acts to block cytokinin-induced ethylene synthesis, therefore inhibiting the negative effects of ethylene on root cell expansion. It cannot be ruled out that *POLARIS* may act to inhibit cytokinin biosynthesis or alter the sensitivity of root tissue to either cytokinin or ethylene, or both.



double mutants are still agravitropic since evidence exists that gravitropism is controlled by an ethylene independent pathway. The unusual epistatic relationship between *eir1-1* and *ctr1-1* and *ein2-1* (Roman *et al.*, 1995) suggests that ethylene may act via more than one pathway to affect auxin transport and that auxin transport may conversely regulate ethylene signalling via *EIN2*. It will be interesting to determine therefore the relationship between *POLARIS* and *EIN2*. The *cin* class of mutants are defective in the induction of ethylene by cytokinin at low levels (Vogel *et al.* 1998a; 1998b). Given the model for *POLARIS* function it would be expected that examination of *cin/pls* double mutants would show *cin* phenotypes.

With regards to the ethylene phenotype of *pls* it will also be important to determine if ethylene levels are increased in this plant. Whilst the root phenotype of *pls* is rescued by silver suggesting ethylene overproduction versus signalling, the measurements would provide a definitive answer. Furthermore, this and previous examinations of *pls* have concentrated on the root phenotype and little study has been performed on the aerial parts of this mutant. *pls ctr1* double mutants exhibit a combinatorial phenotype that includes unusual development of aerial parts of the plant (P. Chilley, unpublished data). Therefore, though the aerial organs of *pls* appear wild-type, a detailed examination may indicate further features to correlate with the information already known. Indeed, preliminary examinations indicate irregular stomatal patterning which has been linked to ethylene overproduction (M. Souter, unpublished results). It would seem likely that other subtle defects will be identified since *POLARIS* /GUS expression is not limited to the root tip. Whether the role of *POLARIS* is the same in these other tissues will also require further investigation.

One of the predictions of this and other work on the *pls* mutant is that auxin transport is inhibited. This is expected to result in auxin accumulating in regions of the root, possibly the cells of the elongation zone. Whether auxin might be accumulating in its active form or in its various conjugated forms is unknown. Sensitive methods of accurately measuring auxin concentration in tissues has been reported (Uggla *et al.*, 1996). It would be interesting, upon collaboration with groups performing these measurements, to determine the distribution of auxin in the *pls* root. An alternative would be to use the auxin responsive synthetic DR5 promoter as a tool. Though the sensitivity of this promoter is not known, a GFP version of this reporter could be crossed into *pls* to compare its expression to the wild-type.

A further examination of the role auxin plays in the regulation of *POLARIS* could also be performed. Initially this could involve more detailed examination by northern analysis of the dose response and kinetics of GUS expression following auxin

treatment. Also, as yet it has not been determined what happens to expression following transfer from auxin media to unsupplemented media. If transcription of *POLARIS* is activated by an auxin signalling pathway then perhaps crosses with mutants effected in auxin response may clarify the nature of this pathway. Since mutations in the *axr3/iaa17* and *shy2/iaa3* genes show defects in root development they may be required for activation/repression of *POLARIS*. Other mutants in which GUS expression could be examined are the *age1* and *age2* (auxin-responsive gene expression, Oono *et al.*, 1998) which appear to be involved in auxin dependent gene expression. It is also possible that the putative *POLARIS* polypeptide is a target for auxin-mediated proteolysis resulting in a very short half-life. It would be interesting therefore to examine the effect of crossing the *POLARIS* overexpressing lines into an *axr1* or *tir1* mutant background.

It has been proposed that *POLARIS* is a marker of a positional information pathway in the root since it is expressed in mutants lacking functional root meristems (Topping and Lindsey, 1997; Willemsen *et al.*, 1998). Recent research has highlighted the importance of auxin as a positional signal in the root (Sabatini *et al.*, 1999). The *bdl* and *mp* mutants have also been implicated as having a role in auxin canalisation and root patterning. Crosses between these mutants and *pls* may reveal more of the role of auxin as a positional signal. Whilst epistatic relationships may be difficult to determine with such aberrant mutants, the expression pattern of GUS can be examined to determine the effect on localisation and polarity.

An important area that requires future experimentation is the identification of the gene(s) with which *POLARIS* interacts. One method of determining this has already been initiated (P. Chilley, unpublished results) and that is supressor/second site mutagenesis of the *pls* line. Promising lines have been identified but these require outcrossing to the wild-type and back-crossing to *pls* to determine their specificity to a *POLARIS* pathway. The mutations in these lines can then be mapped, and given the genome sequencing project, cloning of these genes will be easier than was previously possible.

A second method similar to supressor mutagenesis is activation tagging in which the transgenic line is transformed with a construct containing a powerful enhancer such as a tetramer of the CaMV 35S promoter enhancer (reviewed in Walden *et al.*, 1994). This, and related techniques has been successfully used to identify novel mutants and genes in a variety of processes (Schaffer *et al.*, 1998; Kardailsky *et al.*, 1999; Weigel *et al.*, 2000). Therefore, activation tagging could be used to identify genes downregulated in *pls*, genes required for the regulation of root elongation in response to hormonal signals as well as redundant genes. This approach has the advantage in that it doesn't

necessarily require the out-and-back-crossing required following EMS mutagenesis. Since an enhancer is used it does however mean that the activated gene may be several kilobases up or downstream of the T-DNA insertion site. An alternative would be to use a strong promoter instead of an enhancer creating transcriptional fusions. Such a method would create antisense lines as well but would require many more independent transformants than the enhancer system. Both suppressor mutagenesis and activation tagging have the advantage that they can identify genes that act at points both upstream and downstream of *POLARIS*. A more limited approach, though potentially just as informative, is to identify directly interacting proteins using the yeast-two hybrid system. However, if phosphorylation or cleavage of this polypeptide is required for such interactions there may be a number of technical difficulties to overcome.

As yet, the *POLARIS* gene product has not been identified, though the experimental evidence supports the functionality of a partial *POLARIS* transcript encoding the 36aa polypeptide. In order to address this problem a strategy has been designed in which a knockout of the 36aa ORF will be introduced into *pls*. The ATG of the 36aa ORF has been altered resulting in a modified transcript (full length rather than truncated as in the overexpressing lines) which cannot express the 36aa polypeptide. The first of the upstream ORFs is unaltered by this modification though the uORF that overlaps the 36aa ATG is altered. If this construct is unable to complement the short root phenotype of *pls* then this will provide strong evidence that the 36aa ORF is the functional gene product of *POLARIS*. The results of this experiment will unfortunately not be known for several months.

A number of studies have indicated the importance of both the 5' and 3'-UTR in regulating both transcript stability and translation efficiency (Damiani and Wessler, 1993; Tanguay and Gallie, 1996; Wang and Wessler, 1998). The effects of such features have been examined using reporter gene systems and both stable and transient expression systems. These techniques could be employed to examine the effect the UTRs of the *POLARIS* transcript have on reporter gene expression. One hypothesis presented in this work is that the structures of the UTRs of the *POLARIS* transcript result in inefficient translation of the 36aa ORF. One result of this is that, in the transgenic plants overexpressing the partial *POLARIS* transcript, the pathway in which *POLARIS* acts may not be saturated. Saturation of this pathway could be achieved by expression of the 36aa ORF in a favourable context for translation under the control of a strong promoter in plants. The sensitivity of these transgenic plants to both cytokinin and ethylene could be examined and compared to that of over-expressing lines discussed in this work.

The effect the position of *GENE X* has on *POLARIS* expression has not been determined in this work. As discussed, one hypothesis is that transcription of *GENE X* inhibits transcription of *POLARIS*. This hypothesis could be addressed by creating *POLARIS* promoter-GUS construct in which the transcription of *GENE X* is inhibited, potentially by removing putative TATA boxes, the expression of GUS could be examined in transient expression systems and compared to a control wild-type promoter-GUS construct. The function of *GENE X* is unknown, though preliminary promoter analysis indicates a role in the root. A reverse genetics approach could be used to identify putative null-alleles of this gene by screening membrane arrays of commercially available T-DNA tagged lines. One anticipated difficulty with this approach is that integration of a T-DNA or transposon in *GENE X* could disrupt expression of *POLARIS*. Therefore, to complement this approach, the 5' end of this gene could be mapped and the transcript overexpressed in plants. It is interesting, given the present rarity of small polypeptide signalling molecules in plant compared to animal systems, that this locus appears to encode two novel small polypeptides. It would suggest that as yet a number of similar genes have yet to be identified.

CHAPTER REFERENCES

- Abel S, Theologis A (1996) Early genes and auxin action. *Plant Physiol.* **111**: 9-17.
- Abel S, Ballas N, Wong L-W, Theologis A (1996) DNA elements responsive to auxin. *BioEssays* **18**: 647-654.
- Abeles FB, Morgan PW, Saltveit JR (1992) *Ethylene in plant biology*. Academic Press, New York.
- Abler ML, Green PJ (1996) Control of mRNA stability in higher plants. *Plant Mol. Biol.* **32**: 63-78.
- Achstetter T, Franzusoff A, Field C, Schekman R (1988) Sec7 encodes an unusual, high molecular-weight protein required for membrane traffic from the yeast golgi-apparatus. *J. Biol. Chem.* **263**: 11711-11717.
- Aeschbacher RA, Schiefelbein KW, Benfey PN (1994) The genetic and molecular basis of root development. *Annu. Rev. Plant Physiol. Plant Mol. Biol.* **45**: 25-45.
- Aeschbacher RA, Hauser M-T, Feldmann KA, Benfey PN (1995) The *SABRE* gene is required for normal cell expansion in *Arabidopsis*. *Genes Dev.* **9**: 330-340.
- Aida M, Ishida T, Tasaka M (1999) Shoot apical meristem and cotyledon formation during *Arabidopsis* embryogenesis: interaction among the *CUP-SHAPED COTYLEDON* and *SHOOT MERISTEMLESS* genes. *Development* **126**: 1563-1570.
- Allen ND, Cran DG, Barton SC, Hettle S, Reik W, Surani MA (1988) Transgenes as probes for active chromosomal domains in mouse development. *Nature* **333**: 852-855.
- Alonso JM, Hirayama T, Roma G, Nourizadeh S, Ecker JR (1999) EIN2, a bifunctional transducer of ethylene and stress responses in *Arabidopsis*. *Science* **284**: 2148-2152.
- Altschul SF, Gish W, Miller W, Myers EW, Lipmann DJ (1990) Basic local alignment search tool. *J. Mol. Biol.* **215**, 403-410.
- Ausubel FM, Brent R, Kingston RE, Moore DD, Seidman JG, Smith JA, Struhl K (1995) Current protocols in molecular biology. *Current Protocols, John Wiley & Sons Inc.*
- Bagyman IL, Revenkova EV, Pozmogova GE, Kraev AS, Skryabin KG (1995) 5'-regulatory region of *Agrobacterium tumefaciens* T-DNA gene 6b directs organ-specific, wound inducible and auxin-inducible expression in transgenic tobacco. *Plant Mol. Biol.* **25**: 1299-1304.

- Bai C, Sen P, Hofmann K, Ma L, Goebel M, Harper JW, Elledge SJ (1996) SKP1 connects cell cycle regulators to the ubiquitin proteolysis machinery through a novel motif, the F-box. *Cell* **86**: 263-274.
- Barbier-Brygoo H, Ephritikhine G, Klämbt D, Ghislain M, Guern J (1989) Functional evidence for an auxin receptor at the plasmalemma of tobacco mesophyll protoplasts *Proc. Nat. Acad. Sci. USA* **86**: 891-895.
- Barbier-Brygoo H, Ephritikhine G, Klämbt D, Maurel C, Palme K, Schell J, Guern J (1991) Perception of the auxin signal at the plasma membrane of tobacco mesophyll protoplasts. *Plant J.* **1**: 83-93.
- Baskin TI, Betzner AS, Hoggart R, Cork A, Williamson RE (1992) Root morphology mutants in *Arabidopsis thaliana*. *Aust. J. Plant Physiol.* **19**: 427-37.
- Baskin TI, Cork A, Williamson RE, Gorst JR (1995) *STUNTED PLANT 1*, A gene required for expansion in rapidly elongating but not dividing cells and mediating root growth responses to applied cytokinin. *Plant Physiol.* **107**: 233-243.
- Bateman E, Paule MR (1988) Promoter occlusion during RNA transcription. *Cell.* **54**: 985-992.
- Becraft PW (1998) Receptor kinases in plant development. *Trends in Plant Science.* **3**: 384-388.
- Bell CJ, Maher EP (1990) Mutants of *Arabidopsis thaliana* with abnormal gravitropic responses. *Mol. Gen. Genetics.* **220**: 289-293.
- Bellen HJ, O'Kane CJ, Wilson C, Grossniklaus U, Pearson RK, Gehring WJ (1989) P-element-mediated enhancer detection: a versatile method to study development in *Drosophila*. *Genes Dev.* **3**: 1288-1300.
- Benfey PN, Linstead PJ, Roberts K, Schiefelbein JW, Hauser M-T, Aeschbacher RA (1993) Root development in *Arabidopsis*: four mutants with dramatically altered root morphogenesis. *Development* **119**: 57-70.
- Benfey PN, Schiefelbein JW (1994) Getting to the root of plant development: the genetics of *Arabidopsis* root formation. *Trends in Genetics* **10**: 84-88.
- Benfey PN (1999) Is the shoot a root with a view? *Curr. Opinion Plant Biol.* **2**: 39-43.
- Bennett MJ, Marchant A, Green HG, May ST, Ward SP, Millner PA, Walker AR, Schulz B, Feldmann KA: *Arabidopsis AUX1* gene (1996) A permease-like regulator of root gravitropism. *Science* **273**: 948-950.
- Berger F, Brownlee C (1994) Photopolarization of the *Fucus* sp. zygote by blue light involves a plasma membrane redox chain. *Plant Physiol.* **105**: 519-527.

- Berger F, Taylor A, Brownlee C (1994) Cell fate determination by the cell wall in early *Fucus* development. *Science* **263**: 1421-1423.
- Berger F, Linstead P, Dolan L, Hasaloff J (1998) Stomata patterning on the hypocotyl of *Arabidopsis thaliana* is controlled by genes involved in the control of root epidermis patterning. *Dev. Biol.* **194**: 226-234.
- Berleth T, Jurgens G (1993) The role of the *monopteros* gene in organising the basal body region of the *Arabidopsis* embryo. *Development* **118**: 575-587.
- Bevan M (1984) Binary *Agrobacterium* vectors for plant transformation. *Nuc. Acids Res.* **12**: 8711-8721.
- Billington T, Pharmawati M, Gehring CA (1997) Isolation and immunoaffinity purification of biologically active plant natriuretic peptide. *Biochem. Biophys. Res. Comm.* **235**: 722-725.
- Bisseling T (1999) The role of plant peptides in intercellular signalling. *Curr. Opinion Plant Biol.* **2**: 365-368.
- Blancaflor EB, Hasenstein KH (1995) Time course and auxin sensitivity of cortical microtubule reorientation in maize roots. *Protoplasma* **185**: 72-82.
- Bleecker A, Estelle M, Somerville C, Kende H (1988) Insensitivity to ethylene conferred by a dominant mutation in *Arabidopsis thaliana*. *Science* **241**: 1086-1089.
- Bleecker AB, Esch JJ, Hall AE, Rodriguez FI, Binder BM (1998) The ethylene-receptor family from *Arabidopsis* : Structure and function. *Phil Trans. R. Soc. Lond. B* **353**: 1405-1412.
- Boerjan W, Cervera M-T, Delarue M, Beeckman T, Dewitte W, Bellini C, Caboche M, Onckelen HV, Montagu MV, Inze D (1995) *superroot* , a recessive mutation in *Arabidopsis* , confers auxin overproduction. *Plant Cell* **7**: 140-1419.
- Brandstatter I, Kieber JJ (1998) Two genes with similarity to bacterial response regulators are rapidly and specifically induced by cytokinin in *Arabidopsis*. *Plant Cell* **10**: 1009-1019.
- Brigham LA, Woo H-H, Wen F, Hawes MC (1998) Meristem-specific suppression of mitosis and a global switch in gene expression in the root cap of pea by endogenous signals. *Plant Physiol.* **118**: 1223-1231.
- Brownlee C, Bouget F-Y (1998) Polarity determination in *Fucus* : From zygote to multicellular embryo. *Cell Dev. Biol.* **9**: 179-185.
- Burg SP, Burg EA (1967) Molecular requirements for the biological activity of ethylene. *Plant Physiol.* **42**: 144-152.

- Busch M, er U, Jurgens G (1996) Molecular analysis of the *Arabidopsis* pattern formation gene *GNOM*: gene structure and intragenic complementation. *Mol. Gen. Genet.* **250**: 681-691.
- Bush DR (1993) Proton-coupled sugar and amino acid transporters in plants. *Ann. Rev. Plant Physiol. Plant Mol. Biol.* **44**: 513-542.
- Callis J, Carpenter T, Sun CW, Viersta RD (1995) Structure and evolution of genes encoding polyubiquitin and ubiquitin-like proteins in *Arabidopsis thaliana* ectotype Columbia. *Genetics* 1995 **139**: 921-939.
- Carland FM, McHale NA: *LOP1* (1996) a gene involved in auxin transport and vascular patterning in *Arabidopsis*. *Development* **122**: 1811-1819.
- Cary AJ, Liu W, Howell SH (1995) Cytokinin action is coupled to ethylene in its effects on the inhibition of root and hypocotyl elongation in *Arabidopsis thaliana* seedlings. *Plant Physiol.* **107**: 1075-1082.
- Celenza JL, Grisafi PL, Fink GR (1995) A pathway for lateral root formation in *Arabidopsis thailana*. *Genes and Develop.* **9**: 2131-2142.
- Cernac A, Lincoln C, Lammer D, Estelle M (1997) The *SAR1* gene of *Arabidopsis* acts downstream of the *AXR1* gene in auxin response. *Development* **124**: 1583-1591.
- Chao Q, Rothenberg M, Solano R, Roma G, Terzaghi W, Ecker JR (1997) Activation of the ethylene gass response pathway in *Arabidopsis* by the nuclear protein ETHYLENE-INSENSITIVE3 and related proteins. *Cell* **89**: 1133-1144.
- Cheng J-C, Seeley KA, Sung ZR (1995) *RML1* and *RML2*, *Arabidopsis* genes required for cell proliferation at the root tip. *Plant Physiol.* **107**: 365-376.
- Chen R, Hilson P, Sedbrook J, Rosen E, Caspar T, Masson PH (1998) The *Arabidopsis thaliana* *AGARVITROPIC 1* gene encodes a component of the polar-auxin-transport efflux carrier. *Proc. Natl. Acad. Sci. USA.* **95**: 15112-15117.
- Chory J, Li J (1997) Gibberellins, brassinosteroids and light-regulated development. *Plant , Cell Env.* **20**: 801-806.
- Chuck G, Lincoln C, Hake S (1996) *KNAT1* induces lobed leaves woth ectopic meristems when overexpressed in *Arabidopsis*. *Plant Cell.* 1996 **8**: 1277-1289.
- Clark DG, Gubrium EK, Barret JE, Nell TA, Klee HJ (1999) Root formation in ethylene-insensitive plants. *Plant Physiol.* **121**: 53-59.
- Clark SE, Running MP, Meyerowitz EM (1995) *CLAVATA3* is a specific regulator of shoot and floral meristem development affecting the same processes as *CLAVATA1*. *Development* **121**: 2057.

- Clark SE, Williams RW, Meyerowitz EM (1997) The *CLAVATA1* gene encodes a putative receptor kinase that controls shoot and floral meristem size in *Arabidopsis*. *Cell* 1997, **89**: 575-585.
- Clarke MC, Wei W, Lindsey K (1992) High-frequency transformation of *Arabidopsis thaliana* by *Agrobacterium tumefaciens*. *Plant Mol. Biol. Report.* **10** : 178-189.
- Cleland RE, Buckley G, Nowbars S, Lew NM, Stinemetz C, Evans ML, Rayle DL (1991) The pH profile for acid-induced elongation of coleoptile and epicotyl sections is consistent with the acid-growth theory. *Planta* **186**: 70-74.
- Clough SJ, Bent AF (1998) Floral dip: a simplified method for *Agrobacterium* - mediated transformation of *Arabidopsis thaliana*. *Plant J.* **16**: 735-743.
- Clouse SD, Langfor M, McMorris TC (1996) A brassinosteroid-insensitive mutant in *Arabidopsis thaliana* exhibits multiple defects in growth and development. *Plant Physiol.* **111**: 671-678.
- Cobb MH, Xu SC, Hepler JE, Hutchison M, Frost J, Robbins DJ (1994) Regulation of the MAP kinase cascade. *Cell. Mol. Biol. Res.* **40**: 253-256.
- Coenen C, Lomax TL (1998) The *Diageotropica* gene differentially affects auxin and cytokinin responses throughout development in tomato. *Plant Physiol.* **117**: 63-72.
- Conner TW, Goekjian VH, LaFayette PR, Key JL (1990) Structure and expression of two auxin-inducible genes from *Arabidopsis*. *Plant Mol. Biol.* **15**: 623-632.
- Dale PJ, Marks MS, Brown MM, Woolston Cj, Gunn HV, Mullineaux PM, Lewis DM, Kemp JM, Chen DF (1989) Agroinfection of wheat - inoculation of *in vitro* grown seedlings and embryos. *Plant Science* **63**: 237-245.
- Davies PJ (ed.) (1995) Plant Hormones: physiology, biochemistry and molecular biology (2nd editions) Kluwer Academic Publishers.
- Davies RT, Goetz DH, Lasswell J, Anderson MN, Bartel B (1999) *IAR3* encodes an auxin conjugate hydrolase from *Arabidopsis*. *Plant Cell* **11**: 365-376.
- Davis SJ, Viersta RD (1998) Soluble, highly fluorescent variants of green fluorescent protein (GFP) for use in higher plants. *Plant Mol. Biol.* **36**: 521-528.
- Dean C, Tamaki S, Dunsmuir P, Favreau M, Katayama C, Dooner H, Bedbrook J (1986) mRNA transcripts of several plant genes are polyadenylated at multiple sites *in vivo*. *Nuc. Acids Res.* **5**: 2229-2240.
- Delarue M, Prinsen E, Onckelen HV, Caboche M, Bellinin C (1998) *Sur2* mutations in *Arabidopsis thaliana* define a new locus involved in the control of auxin homeostasis. *Plant J.* **14**: 603-611.

- Delbarre A, Muller P, Guern J (1998) Short-lived and phosphorylated proteins contribute to carrier-mediated efflux, but not to influx, of auxin in suspension-cultured tobacco cells. *Plant Physiol.* **116**: 833-844.
- Diekmann W, Venis MA, Robinson DG (1995) Auxins induce clustering of the auxin-binding protein at the surface of maize coleoptiles. *Proc. Nat. Acad. Sci. USA* **92**: 3425-3429.
- Di Laurenzio L, WysockaDiller J, Malamy JE, Pysh L, Helariutta Y, Freshour G, Hahn MG, Feldmann KA, Benfey PN (1996). The SCARECROW gene regulates an asymmetric cell division that is essential for generating the radial organization of the *Arabidopsis* root *Cell* **86**, 423-433.
- Ditta G, Stanfield S, Corbin D, Helinski DR (1980) Broad host range DNA cloning system for Gram-negative bacteria - construction of a gene bank of *Rhizobium meliloti*. *PNAS* **77**: 7347-7351.
- Doerner P, Jorgensen J-E, You R, Steppuhn J, Lamb C (1996) Control of root growth and development by cyclin expression. *Nature* **380**: 520-523.
- Dolan L, Janmaat K, Willemssen V, Linstead P, Poethig S, Roberts K, Scheres B (1993) Cellular organisation of the *Arabidopsis thaliana* root. *Development* **119**: 71-84.
- Dolan L, Duckett CM, Grierson C, Linstead P, Schneider K, Lawson E, Dean C, Poethig S, Roberts K (1994) Clonal relationships and patterning in the root epidermis of *Arabidopsis*. *Development* **120**: 2465-2474.
- Dolan L, Roberts K (1995) Plant development: pulled up by the roots. *Curr. Opin. Genet. Dev.* **5**: 432-438.
- Dolan L (1996) Pattern in the root epidermis: an interplay of diffusible signals and cellular geometry. *Ann. Botany.* **77**: 547-553.
- Dolan L (1997) SCARECROW: specifying asymmetric cell divisions throughout development. *Trends Plant Science.* **2**: 1-2.
- Dolan L, Roberts K (1995) The development of cell pattern in the root epidermis. *Phil. Trans. R. Soc. Lond B.* **350**: 95-99.
- Dolan L, Scheres B (1998) Root pattern: shooting in the dark? *Cell Dev. Biol.* **9**: 201-206.
- Duckett CM, Oparka KJ, Prior DAM, Dolan L, Roberts K (1994) Dye-coupling in the root epidermis of *Arabidopsis* is progressively reduced during development. *Development* **120**: 3247-3255.

- Eady C, Lindsey K, Twell D (1995) The significance of microspore division and division symmetry for vegetative cell-specific transcription and generative cell differentiation. *Plant Cell*. **7**: 65-74.
- Ecker JR (1995) The ethylene signal transduction pathway in plants. *Science* **268**: 667-675.
- Ephritikhine G, Barbier-Brygoo H, Muller JF, Guern J (1987) Auxin effect on the transmembrane potential difference of wild-type and mutant tobacco protoplasts exhibiting a differential sensitivity to auxin. *Plant Physiol.* **84**: 801-804.
- Esau K (1977) Anatomy of seed plants (2nd edition) John Wiley Publishers.
- Estelle M (1998a) Polar auxin transport: new support for an old model. *Plant Cell* **10**: 1775-1777.
- Estelle M (1998b) Two receptors better than one? *Curr. Biol.* **8**: 539-541.
- Evans ML (1991) Gravitropism – interaction of sensitivity modulation and effector redistribution. *Plant Physiol.* **95**: 1-5.
- Farrel RE (1993) RNA Methodologies: A laboratory guide for isolation and characterisation (San Diego: Academic Press).
- Fisher RH, Barton MK, Cohen JD, Cooke TJ (1996) Hormonal studies of *fass*, an *Arabidopsis* mutant that is altered in organ elongation. *Plant Physiol.* **110**: 1109-1121.
- Fletcher JC, Brand U, Running MP, Simon R, Meyerowitz EM (1999) Signalling of cell fate decisions by *CLAVATA3* in *Arabidopsis* shoot meristems. *Science* **283**: 1911-1914.
- Fluhr R: Ethylene perception (1998) from two-component signal transducers to gene induction. *Trends Plant Science* **3**: 141-146.
- Franzmann LH, Yoon ES, Meinke DW (1995) Saturating the genetic map of *Arabidopsis thaliana* with embryonic mutations. *Plant J.* **7**: 341-350.
- Freshour G, Clay RP, Fuller MS, Albersheim P, Darvill AG, Hahn MG (1996) Developmental and tissue-specific structural alterations of the cell-wall polysaccharides of *Arabidopsis thaliana* roots. *Plant Physiol.* **110**: 1413-1429.
- Fujita H, Syono K (1997) PIS1, a negative regulator of the action of auxin transport in *Arabidopsis thaliana*. *Plant J.* **12**: 583-595.
- Futterer J, Hohn T (1992) Role of an upstream open reading frame in the translation of polycistronic mRNAs in plant cells. *Nuc. Acids Res.* **20** : 3851-3857.
- Gallagher K, Smith LG (1997) Asymmetric cell division and cell fate in plants *Curr. Opinion Cell Biol.* **7**: 842-848.

- Galweiler L, Guan C, Muller A, Wisman E, Mendgen K, Yephremov A, Palme K (1998) Regulation of polar auxin transport by AtPIN1 in *Arabidopsis* vascular tissue. *Science* **282**: 2226-2230.
- Gangopahyay SS, Ray SS, Sinha P, Lohia A (1997) Unusual genome organisation in *Entamoeba histolytica* leads to two overlapping transcripts. *Mol. Bioch. Parasitol.* **89**: 73-83.
- Garbers C, DeLong A, Deruere J, Bernasconi P, Soll D (1996) A mutation in protein phosphatase 2A regulatory subunit A affects auxin transport in *Arabidopsis*. *EMBO J.* **9**: 2115-2124.
- Gerads M, Ernst JF (1998) Overlapping coding regions and transcriptional units of two essential chromosomal genes (*CCT8*, *TRP1*) in the fungal pathogen *Candida albicans*. *Nuc. Acids Res.* **26**: 5061-5066.
- Gil P, Liu Y, Orbovic V, Verkamp E, Poff KL, Green PJ (1994) Characterisation of the auxin-inducible *SAUR-AC1* gene for use as a molecular genetic tool in *Arabidopsis*. *Plant Physiol.* **104**: 777-784.
- Gil P, Green PJ (1996) Multiple regions of the *Arabidopsis SAUR-AC1* gene control transcript abundance: the 3' untranslated region functions as an mRNA instability determinant. *EMBO J.* **15**: 1678-1686.
- Goodner B, Quatrano RS (1993) *Fucus* embryogenesis: a model to study the establishment of polarity. *Plant Cell* **5**: 1471-1481.
- Goto N, Katoh N, Kranz AR (1991) Morphogenesis of floral organs in *Arabidopsis* predominant carpel formation of the *PIN-FORMED* mutant. *Jap. J. Genetics* **66**: 551-567.
- Grant SGN, Jessee J, Bloom FR, Hanahan D (1990) Differential plasmid rescue from transgenic mouse DNAs into *Escherichia coli* methylation-restriction mutants. *PNAS.* **87**: 4645-4649
- Gray WM, del Pozo JC, Walker L, Hobbie L, Risseuw E, Banks T, Crosby WL, Yang M, Ma H, Estelle M (1999) Identification of an SCF ubiquitin-ligase complex required for auxin response in *Arabidopsis thaliana*. *Genes Dev.* **13**: 1678-1691.
- Hadfi K, Speth V, Neuhaus G (1998) Auxin-induced developmental patterns in *Brassica juncea* embryos. *Development* **125**: 879-887.
- Hamann T, Mayer U, Jurgens G (1999) The auxin-insensitive *bodenlos* mutation affects primary root formation and apical-basal patterning in the *Arabidopsis* embryo. *Development* **126**: 1387-1395.

- Hansen K, Birse CE, Proudfoot NJ (1998) Nascent transcription from the *nmt1* and *nmt2* genes of *Schizosaccharomyces pombe* overlaps neighbouring genes. *EMBO J.* **17**: 3066-3077.
- Harada JJ (1999) Signalling in plant embryogenesis. *Curr. Opinon Plant Biol.* **2**: 23-27.
- Hardtke CS, Berleth T (1998) The *Arabidopsis* gene *MONOPTEROS* encodes a transcription factor mediating embryo axis formation and vascular development. *EMBO J.* **17**: 1405-1411.
- Hauser M-T, Morikami A, Benfey PN (1995) Conditional root expansion mutants of *Arabidopsis*. *Development* **121**: 1237-1252.
- He F, Brown A, Jacobson A (1997) Upf1p, Nmd2p, and Upf3p are interacting components of the yeast nonsense-mediated mRNA decay pathway. *Mol. Cell. Biol.* **17**: 158-1594.
- Hebsgaard SM, Korning PG, Tolstrup N, Engelbrecht J, Rouze P, Brunak S (1996) Splice site prediction in *Arabidopsis thaliana* DNA by combining local and global sequence information. *Nuc. Acids Res.* **24**: 3439-3452.
- Heidstra R, Yang WC, Yalcin Y, Peck S, Emons A, van Kammen A, Bisseling T (1997) Ethylene provides positional information on cortical cell division but is not involved in Nod factor-induced root hair tip growth in *Rhizobium*-legume interaction. *Development* **124**: 1781-1787.
- Hirayama T, Kieber JJ, Hirayama N, Kogan M, Guzman P, Nourizadeh S, Alonso JM, Dailey WP, Dancis A, Ecker JR (1999) RESPONSE-TO-ANTAGONIST1, a Menkes/Wilson disease-related copper transporter, is required for ethylene signalling in *Arabidopsis*. *Cell* **97**:383-393.
- Hobbie L, Estelle M (1995) The *axr4* auxin-resistant mutants of *Arabidopsis thaliana* define a gene important for root gravitropism and lateral root initiation. *Plant J.* **7**: 211-220.
- Hobbie LJ (1998) Auxin: molecular genetic approaches in *Arabidopsis*. *Plant Physiol. Biochem.* **36**: 91-102.
- Hobbie L, McGovern M, Hurwitz LR, Pierro A, Liu NY, Bandyopadyay A, Estelle M (2000) The *axr6* mutants of *Arabidopsis thaliana* define a gene involved in auxin response and early development. *Development* **127**: 23-32.
- Hoekema A, Hirsch PR, Hooykaas PJJ, Schilperoort RA (1983) A binary plant vector strategy based on seperation of VIR-region and T-region of the *Agrobacterium tumefaciens* Ti-plasmid. *Nature* **303**: 179-180.

- Holding DR, McKenzie RJ, Coomber SA (1994) Genetic and structural analysis of five *Arabidopsis* mutants with abnormal root morphology generated by the seed transformation method. *Ann Bot.* **74**: 193-204.
- Hope IA (1991) 'Promoter trapping' in *Caenorhabditis elegans*. *Development* **113**: 399-408.
- Hua J, Meyerowitz EM (1998) Ethylene responses are negatively regulated by a receptor gene family in *Arabidopsis thaliana*. *Cell* **94**: 261-271.
- Hua J, Sakai H, Nourizadeh S, Chen QG, Bleecker AB, Ecker JR, Meyerowitz EM (1998) *EIN4* and *ERS2* are members of the putative ethylene receptor gene family in *Arabidopsis*. *Plant Cell* **10**: 1321-1332.
- Hung C-Y, Lin Y, Zhang M, Pollock S, Marks MD, Schiefelbein J (1998) A common position-dependent mechanism controls cell-type patterning and *GLABRA2* regulation in the root and hypocotyl epidermis of *Arabidopsis*. *Plant Physiol.* **117**: 73-84.
- Huynh TV, Young RA, Davis RH: (1985) DNA cloning: a practical approach (D. M. Glover, ed.) Vol. 1, IRL Press, Oxford, England
- Irniger S, Egli CM, Kuenzler M, Braus GH (1992) The yeast actin intron contains a cryptic promoter that can be switched on by preventing transcriptional interference. *Nuc. Acids Res.* **20**: 4733-4739.
- Jackson D, Hake S (1997) Morphogenesis on the move: cell-to-cell trafficking of plant regulatory proteins. *Curr. Opin. Gen. Dev.* **7**: 495-500.
- Jensen PJ, Hangarter RP, Estelle M (1998) Auxin transport is required for hypocotyl elongation in light-grown but not dark-grown *Arabidopsis*. *Plant Physiol.* **116**: 455-462.
- Jerpseth B, et al. (1992) *Strategies* **5**: 2-3.
- Jofuku KD, Schipper RD, Goldberg RB (1989) A frameshift mutation prevents Kunitz trypsin inhibitor mRNA accumulation in soybean embryos. *Plant Cell* **1**: 427-435.
- Johnson ES, Schwienhorst I, Dohmen RJ, Blobel G (1997) The ubiquitin-like protease Smt3p is activated for conjugation to other proteins by an Aos1p/Uba2p heterodimer. *EMBO J.* **16**: 5509-5519.
- Jones AM; Lamerson P; Venis MA (1989) Comparison of site-1 auxin binding and a 22-kilodalton auxin-binding protein in maize. *Planta* **179**: 409-414.
- Jones Am, Herman EM (1993) KDEL-containing auxin-binding protein is secreted to the plasma membrane and cell wall *Plant Physiol.* **101**: 595-606.

- Jones AM (1994) Auxin-binding proteins. *Ann. Rev. Plant Physiol. Mol. Biol.* **45**: 393-420.
- Jones AM, IM K-H, Savka MA, Wu M-J, DeWitt G, Shillito R, Binnes AN (1998) Auxin-dependent cell expansion mediated by overexpressed auxin-binding protein 1 *Science* **282**: 1114-1117.
- Joshi CP (1987) An inspection of the domain between putative TATA box and translation start site in 79 plant genes. *Nuc. Acids Res.* **15**: 6643-6653
- Jurgens G (1995) Axis formation in plant embryogenesis: cue and clues. *Cell* **81**: 467-470.
- Jurgens G, Mayer U, Torrese-Ruiz RA, Berleth T, Misera S (1991) Genetic analysis of pattern formation in the *Arabidopsis* embryo. *Development Supp.* **1**: 27-38.
- Jurgens G, Mayer U, Busch M, Lukowitz W, Laux T (1995) Pattern formation in the *Arabidopsis* embryo: a genetic perspective. *Phil. Trans. R. Soc. Lond. B* **350**: 19-25.
- Jurgens G, Grebe M, Steinmann T (1997) Establishment of cell polarity during early plant development. *Curr. Opinion Cell Biol.* **9**: 849-852.
- Kakimoto T (1998) Cytokinin signalling. *Curr. Opinion Plant Biol.* **1**: 399-403.
- Kardailsky I, Shukla VK, Ahn JH, Dagenais N, Christensen SK, Nguyen JT, Chory J, Harrison MJ, Weigel D (1999) Activation tagging of the floral inducer *FT*. *Science* **286**: 1962-1965.
- Katekar GF, Geissler AE (1977) Auxin transport inhibitors III. Chemical requirements of a class of auxin transport inhibitors. *Plant Physiol.* **60**: 826-829.
- Keddie JS, Carroll BJ, Thomas CM, Reyes MEC, Klimyuk V, Holtan H, Grissem W, Jones JDG (1998) Transposon tagging of the *Defective embryo and meristems* gene of tomato. *Plant Cell* **10**: 877-887.
- Keller CP, Van Volkenburgh E (1997) Auxin-induced epinasty of tobacco leaf tissues. A non-ethylene mediated response. *Plant Physiol.* **113**: 603-610.
- Keller CP, Van Volkenburgh E (1998) Evidence that auxin-induced growth of tobacco leaf tissue does not involve cell wall acidification *Plant Physiol.* **118**: 557-564.
- Kieber JJ, Rothenberg M, Roman G, Feldmann KA, Ecker JR (1993) *CTR1*, a negative regulator of the ethylene response pathway in *Arabidopsis*, encodes a member of the Raf family of protein kinases. *Cell* **72**: 427-441.
- Kim J, Harter K, Theologis A (1997) Protein-protein interactions among the Aux/IAA proteins. *Proc. Natl. Acad. Sci. USA* **94**: 11786-11791.

- King JJ, Stimart DP, Fisher RH, Bleecker AB (1995) A mutation altering auxin homeostasis and plant morphology in *Arabidopsis*. *Plant Cell* **7**: 2023-2037.
- Koskimies P, Spiess A-N, Lahti P, Huhtaniemi I, Ivell R (1997) The mouse relaxin-like factor gene and its promoter are located within the 3' region of the JAK3 genomic sequence. *FEBS Letters*. **419**: 186-190.
- Kozak M (1978) How do eukaryotic ribosomes select initiation regions in messenger RNA? *Cell* **15**: 1109-1123.
- Kozak M (1986) Bifunctional messenger RNAs in eukaryotes. *Cell* **47**: 481-483.
- Kozak M (1987a) An analysis of 5'-noncoding sequences from 699 vertebrate messenger RNAs. *Nuc. Acids Res.* **15**: 8125-8148.
- Kozak M (1987b) At least six nucleotides preceding the AUG initiator codon enhance translation in mammalian cells. *J. Mol. Biol.* **196**: 947-950.
- Kozak M (1989) The scanning model for translation: An update. *J. Cell Biol.* **108**: 229-241.
- Kubo H, Peeters AJM, Aarts MGM, Pereira A, Koornneef M (1999) *ANTHOCYANINLESS2*, a homeobox gene affecting anthocyanin distribution and root development in *Arabidopsis*. *Plant Cell* **11**: 1217-1226.
- Kuhlemeier C (1992) Transcriptional and post-transcriptional regulation of gene expression in plants. *Plant Mol. Biol.* **19**: 1-14.
- Lacks S, Greenberg JR (1977) Complementary specificity of restriction endonucleases of *Diplococcus pneumoniae* with respect of DNA methylation. *J. Mol. Biol.* **114**: 153-168.
- Lammer D, Mathias N, Laplaza JM, Jiang WD, Liu Y, Callis J, Goebel M, Estelle M (1998) Modification of yeast Cdc53p by the ubiquitin-related protein Rub1p affects the function of the SCF Cdc4 complex. *Genes Dev.* **12**: 914-926.
- Laskowski MJ, Williams ME, Nusbaum HC, Sussex IM (1995) Formation of lateral root meristems is a two-stage process. *Development* **121**: 3303-3310.
- Lauber MH, Waizenegger I, Steinmann T, Schwarz H, Mayer U, Hwang I, Lukowitz W, Jurgens G (1997) The *Arabidopsis* KNOLLE protein is a cytokinesis-specific syntaxin. *J. Cell Biol.* **139**: 1485-1493.
- Laux T, Jurgens G (1997) Embryogenesis: a new start in life. *Plant Cell* **9**: 989-1000.
- Le H, Tanguay RL, Balasta ML, ML, Wei C-C, Browning KS, Metz AM, Goss DJ, Gallie DR (1997) Translation initiation factors eIF-iso4G and eIF-4B interact with the poly(A)-binding protein and increase its RNA binding activity. *J. Biol. Chem.* **272**: 16247-16255.

- Leblanc N; Roux C; Pradier JM; Perrot-Rechenmann C (1997) Characterization of two cDNAs encoding auxin-binding proteins in *Nicotiana tabacum*. *Plant Mol. Biol.* **33**: 679-689
- Leblanc N, Perrot-Rechenmann C, Barbier-Brygoo H (1999) The auxin-binding protein Nt-ERabp1 alone activates an auxin-like transduction pathway. *FEBS Letters* **449**: 57-60.
- Lee MM, Schiefelbein J (1999) WEREWOLF, a MYB-related protein in *Arabidopsis*, is a position-dependent regulator of epidermal cell patterning. *Cell* **99**: 473-483.
- Leyser O (1998) Auxin signalling: protein stability as a versatile control target. *Curr. Biol.* **8**: 305-307.
- Leyser O (1999) Ins and outs of auxin transport *Curr. Biol.* **9**: 8-20.
- Leyser O, Berleth T (1999) A molecular basis for auxin action. *Cell Dev. Biol.* **10**: 131-137.
- Li J, Chory J (1997) A putative leucine-rich repeat receptor kinase involved in brassinosteroid signal transduction. *Cell* **90**: 929-938.
- Li Q, Hunt AG (1997) The polyadenylation of RNA in plants. *Plant Physiol.* **115**: 321-325.
- Li Y, Liu Z-B, Shi X, Hagen G, Guifoyle TJ (1994) An auxin-inducible element in soybean SAUR promoters. *Plant Physiol.* **106**: 37-43.
- Liakopoulos D, Doenges G, Matuschewski K, Jentsch S (1998) A novel protein modification pathway related to the ubiquitin system. *EMBO J.* **17**: 2208-2214.
- Liang X, Abel S, Keller JA, Shen NF, Theologis A (1992) The 1-Aminocyclopropane-1-carboxylate synthase gene family of *Arabidopsis thaliana*. *Proc. Natl. Acad. Sci. USA* **89**: 11046-11050.
- Lieberman M (1979) Biosynthesis and action of ethylene. *Annu. Rev. Plant Physiol.* **30**: 533-591.
- Lincoln C, Britton JH, Estelle M (1990) Growth and development of the *Axr1* mutants of *Arabidopsis*. *Plant Cell* **2**: 1071-1080.
- Lindsey K, Wei W, Clarke MC, McArdle HF, Rooke LM, Topping JF (1993) Tagging genomic sequences that direct transgene expression by activation of a promoter trap in plants. *Transgenic Research* **2**: 33-47.
- Lindsey K, Topping JF (1993) Embryogenesis: a question of pattern. *J. Exp. Biol.* **44**: 359-374.
- Lindsey K, Topping J (1998) On the relationship between the plant cell and the plant. *Cell Dev. Biol.* **9**: 171-177.

- Linz B, Koloteva N, Vasilescu S, McCarthy JEG (1997) Disruption of ribosomal scanning on the 5'-untranslated region, and not restriction of translational initiation *per se*, modulates the stability of nonaberrant mRNAs in the yeast *Saccharomyces cerevisiae*. *J. Biol. Chem.* **272**: 9131-9140.
- Liu C-M, Xu Z-h, Chua N-H (1993) Auxin polar transport is essential for the establishment of bilateral symmetry during early embryogenesis. *Plant Cell* **5**: 621-630.
- Liu Z-B, Ulmasov T, Shi X, Hagen G, Guifoyle T (1994) Soybean *GH3* promoter contains multiple auxin-inducible elements. *Plant Cell* **6**: 645-657.
- Liu Z-B, Hagen G, Guifoyle T (1997) A G-box-binding protein from soybean binds to the E1 auxin-response element in the soybean *GH3* promoter and contains a proline-rich repression domain. *Plant Physiol.* **115**: 397-407.
- Löbner M and Klämbt D (1985a) Auxin-binding protein from coleoptile membranes of corn (*Zea mays* L.) I. Purification by immunological methods and characterization. *J. Biol. Chem.* **260**: 9848-9853.
- Löbner M and Klämbt D (1985b) Auxin-binding protein from coleoptile membranes of corn (*Zea mays* L.) II. Localization of a putative auxin receptor. *J. Biol. Chem.* **260**: 9854-9859.
- Logemann J, Schell J, Willmitzer L (1987) Improved method for the isolation of RNA from plant-tissues. *Analyt. Biochem.* **163**: 16-20.
- Long JA, Moan EI, Medford JI, Barton MK (1996) A member of the KNOTTED class of homeodomain proteins encoded by the *STM* gene of *Arabidopsis*. *Nature* **379**: 66-69.
- Ludwig SR, Habera LF, Dellaporta SL, Wessler SR (1989) *LC*, a member of the maize *R*- gene family responsible for tissue-specific anthocyanin production, encodes a protein similar to transcriptional activators and contains the MYC-homology region. *PNAS* **86**: 7092-7096.
- Lukowitz W, Mayer U, Jurgens G (1996) Cytokinesis in the *Arabidopsis* embryo involves the syntaxin-related KNOLLE gene product. *Cell* **84**: 61-71.
- Luschnig C, Gaxiola RA, Grisafi P, Fink GR (1998) EIR1, a root-specific protein involved in auxin transport, is required for gravitropism in *Arabidopsis thaliana*. *Genes Dev.* **12**: 2175-2187.
- Maniatis T, Fritsch EF, Sambrook J: Molecular cloning (1982) A laboratory manual (Cold Spring Harbor, New York: Cold Spring Harbor Laboratory Press).

- Marchant A, Kargul J, May ST, Muller P, Delbarre A, Perrot-Rechenmann C, Bennett MJ (1999) AUX1 regulates root gravitropism in *Arabidopsis* by facilitating auxin uptake within root apical tissue *EMBO J.* **18**: 2066-2073.
- Masucci JD, Schiefelbein JW (1994) The *rdh6* mutation of *Arabidopsis thaliana* alters root-hair initiation through an auxin-and-ethylene-associated process. *Plant Physiol.* **106**: 1335-1346.
- Masucci JD, Rerie WG, Foreman DR, Zhang M, Galway ME, Marks MD, Schiefelbein JW (1996) The homeobox gene *GLABRA 2* is required for position-dependent cell differentiation in the root epidermis of *Arabidopsis thaliana*. *Development* **122**: 1253-1260.
- Masucci JD, Schiefelbein JW (1996) Hormones act downstream of *TTG* and *GL2* to promote root hair outgrowth during epidermis development in the *Arabidopsis* root. *Plant Cell* **8**: 1505-1517.
- Matsubayashi Y, Sakagami Y (1996) Phytosulfokine, sulfated peptides that induce the proliferation of single mesophyll cells of *Asparagus officinalis* L. *PNAS* **93**: 7623-7627.
- Matsubayashi Y, Morita A, Matsunaga E, Furuya A, Hanai N, Sakagami Y (1999) Physiological relationships between auxin, cytokinin, and a peptide growth factor, phytosulfokine- α , in stimulation of asparagus cell proliferation. *Planta* **207**: 559-565.
- Mattsson J, Sung ZR, Berleth T (1999) Responses of plant vascular systems to auxin transport inhibitors. *Development* **126**: 2979-2991.
- Mayer U, Torrese Ruiz RA, Berleth T, Misera S, Jurgens G (1991) Mutations affecting body organisation in the *Arabidopsis* embryo. *Nature* **353**: 402-407.
- Mayer U, Buttner G, Jurgens G (1993) Apical-basal pattern formation in the *Arabidopsis* embryo: studies on the role of the *gnom* gene. *Development* **117**: 149-162.
- Mayer U, Jurgens G (1998) Pattern formation in plant embryogenesis: a reassessment. *Cell Dev. Biol.* **9**: 187-193.
- McClure BA, Guifoyle T (1987) Characterisation of a class of small auxin-inducible soybean polyadenylated RNAs. *Plant Mol. Biol.* **9**: 611-623.
- McClure BA, Hagen G, Brown CS, Gee MA, Guifoyle TJ (1989) Transcription, organisation, and sequence of an auxin-regulated gene cluster in soybean. *Plant Cell* **1**: 229-239.
- McClure BA, Guifoyle T (1989) Rapid redistribution of auxin-regulated RNAs during gravitropism. *Science* **243**: 91-93.

- McCourt P (1999) Genetic analysis of hormone signalling. *Ann. Rev. Plant Physiol. Plant Mol. Biol.* **50**: 219-43.
- McGrath RB, Ecker JR (1998) Ethylene signalling in *Arabidopsis*: events from the membrane to the nucleus. *Plant Physiol. Biochem.* **36**: 103-113.
- Meinke DW, Cherry JM, Dean C, Rounsley SD, Koornneef M (1998) *Arabidopsis thaliana*: A model plant for genome analysis *Science* **282** 662-666.
- Meller Y, Sessa G, Eyal Y, Fluhr R (1993) DNA-protein interactions on a cis-DNA element essential for ethylene regulation. *Plant Mol. Biol.* **23**: 453-463.
- Miller Co, Skoog F, von Saltza HM, Okumera FS, Strong FM (1955) Kinetin: Structure and synthesis of kinetin. *J. Am. Chem. Soc.* **77**: 2662-2663.
- Morgan PW, Gausman HW (1966) Effects of ethylene on auxin transport. *Plant Physiol.* **41**: 45-52.
- Morris DA, Rubery PH, Jarman J, Sabater M (1991) Effects of inhibitors of protein-synthesis on transmembrane auxin transport in *Cucubita-pepo L* hypocotyl segments. *J. Exp. Bot.* **42**: 773-783.
- Muday GK, Brunn SA, Haworth P, Subramanian M (1993) Evidence for a single naphthylphthalamic acid-binding site on the zucchini plasma membrane. *Plant Physiol.* **103**: 449-456.
- Muller A, Guan C, Galweiler L, Tanzler P, Huijser P, Marchant A, Parry G, Bennett M, Wisman E, Palme K (1998) *AtPIN2* defines a locus of *Arabidopsis* for root gravitropism control. *EMBO J.* **17**: 6903-6911.
- Nelson T (1998) Polarity, vascularisation and auxin. *Trends Plant Science* 1998, **3**: 245-246.
- Newman TC, Ohme-Takagi M, Taylor CB, Green PJ (1993) DST sequences, highly conserved among plant *SAUR* genes, target reporter transcripts for rapid decay in tobacco. *Plant Cell* **5**: 701-714.
- Niepel M, Ling J, Gallie DR (1999) Secondary structure in the 5'-leader or 3'-untranslated region reduces protein yield but does not affect the functional interaction between the 5'-cap and the poly(A) tail. *FEBS Letters* **462**: 79-84.
- Oliveira CC, McCarthy JEG (1995) The relationship between eukaryotic translation and mRNA stability. *J. Biol. Chem.* **270**: 8936-8943.
- Ooms G, Hooykaas PJJ, Vanveen RJM, Vanbeelen P, Regensburgtuink TJG, Schilperoort RA (1982) Octopine Ti-plasmid deletion mutants of *Agrobacterium tumefaciens* with emphasis on the right side of the T-region. *Plasmid* **7**: 15-29.

- Oono Y, Chen QG, Overvoorde PJ, Kohler C, Theologis A (1998) *age* mutants of *Arabidopsis* exhibit altered auxin-regulated gene expression. *Plant Cell* **10**: 1649-1662.
- Palme K; Hesse T; Campos N; Garbers C; Yafnosky MF; Schell J (1992) Molecular analysis of an auxin-binding protein gene located on chromosome 4 of *Arabidopsis*. *Plant Cell* **4**: 193-201.
- Palme K, Galweiler L (1999) PIN-pointing the molecular basis of auxin transport. *Curr. Opinion Plant Biol.* **2**: 375-381.
- Pearce G, Strydom D, Johnson S, Ryan CA (1991) A polypeptide from tomato leaves induces wound-inducible proteinase inhibitor proteins. *Science* **253**: 895-898.
- Pearson RB, Mitchelhill KI, Kemp BE (1993) Studies of protein kinase/phosphatase specificity using synthetic peptides in *Protein Phosphorylation: A practical approach*, Oxford University Press. pp 265-291.
- Peyroche A, Paris S, Jackson CL (1996) Nucleotide exchange on ARF mediated by yeast Gea1 protein. *Nature* **384**: 479-481.
- Pietrzak M, Shillito RD, Hohn T, Potrykus I (1986) Expression in plants of 2 bacterial antibiotic resistance genes after protoplast transformation with a new transformation vector. *Nuc. Acids Res.* **14**: 5857-5868.
- Porat R, Lu PZ, Oneil SD (1998) *Arabidopsis SKP1*, a homologue of a cell cycle regulator gene, is predominantly expressed in meristematic cells. *Planta* **204**: 345-351.
- del Pozo JC, Timpte C, Tan S, Callis J, Estelle M (1998) The ubiquitin-related protein RUB1 and auxin responses in *Arabidopsis*. *Science* **280**: 1760-1763.
- del Pozo JC, Estelle M (1999) Function of the ubiquitin-proteasome pathway in auxin response. *Trends Plant Science* **4**: 107-112.
- Praekelt UM, Meacock PA (1990) HSP12, a new small heat-shock gene of *Saccharomyces cerevisiae* - analysis of structure, regulation and function. *Mol. Gen. Genet.* **223**: 97-106.
- Przemeck GKH, Mattsson J, Hardtke CS, Sung ZR, Berleth T (1996) Studies on the role of the *Arabidopsis* gene *MONOPTEROS* in vascular development and plant cell axialization. *Planta* **200**: 229-237.
- Quatrano RS, Shaw SL (1997) Role of the cell wall in the determination of cell polarity and the plane of cell division in *Fucus* embryos. *Trends Plant Science* **2**: 15-21.

- Quesada V, Ponce MR, Micol JL (1999) *OTC* and *AUL1*, two convergent and overlapping genes in the nuclear genome of *Arabidopsis thaliana*. *FEBS Letters*. **461**: 101-106.
- Raikhel N (1992) Nuclear targeting in plants. *Plant Physiol.* **100**: 1627-1632.
- Raven JA (1975) transport of indoleacetic acid in plant cells in relation to pH and electrical potential gradients, and its significance for polar IAA transport. *New Phytol.* **74**: 163-172.
- Rayle DL, Cleland R (1977) Control of plant cell enlargement by hydrogen ions. *Curr Top Dev Biol* **11**: 187-214
- Reed RC, Brady SR, Muday GK (1998) Inhibition of auxin movement from the shoot into the root inhibits lateral root development in *Arabidopsis*. *Plant Physiol.* **118**: 1369-1378.
- Rerie WG, Feldmann KA, Marks MD (1994) The *GLABRA2* gene encodes a homeodomain protein required for normal trichome development in *Arabidopsis*. *Genes Dev.* **8**: 1388-1399.
- Riechmann JL, Meyerowitz EM (1998) The AP2/EREBP family of plant transcription factors. *Biol. Chem.* **379**: 633-646.
- Riou-Khamlichi C, Huntly R, Jacqumard A, Murray JAH (1999) Cytokinin activation of *Arabidopsis* cell division through a D-type cyclin. *Science* **283**: 1541-1544.
- Rodrigues-Pousada R, Caeneghem WV, Chauvaux N, Onckelen HV, Montagu MV, Straeten DVD (1999) Hormonal cross-talk regulates the *Arabidopsis thaliana* 1-aminocyclopropane-1-carboxylate synthase gene 1 in a developmental and tissue-dependent manner. *Physiol.Plant.* **105**: 312-320.
- Roman G, Lubarsky B, Kieber JJ, Rothenberg M, Ecker JR (1995) Genetic analysis of ethylene signal transduction in *Arabidopsis thaliana* : five novel mutant loci integrated into a stress response pathway. *Genetics* **139**: 1393-1409.
- Romano CP, Cooper ML, Klee HJ (1993) Uncoupling auxin and ethylene effects in transgenic tobacco and *Arabidopsis* plants. *Plant Cell* **5**: 181-189.
- Ross J (1996) Control of messenger RNA stability in higher eukaryotes. *Trends Genetics* **12**: 171-175.
- Rothnie HM, Reid J, Hohn T (1994) The contribution of AAUAAA and the upstream element UUUGUA to the efficiency of mRNA 3'-end formation in plants. *EMBO J.* **9**: 2200-2210.
- Rouse D, Mackay P, Stirnberg P, Estelle M, Leyser O (1998) Changes in auxin response from mutations in an *AUX/IAA* gene. *Science* **279**: 1371-1373.

- Rubery PH, Sheldrake AR (1974) Carrier mediated auxin transport. *Planta* **188**: 101-121.
- Ruegger M, Dewey E, Gray WM, Hobbie L, Brown D, Bernasconi P, Turner J, Muday G, Estelle M (1997) Reduced naphthylphthalamic acid binding in the *tir3* mutant of *Arabidopsis* is associated with a reduction in polar auxin transport and diverse morphological defects. *Plant Cell* **9**: 745-757.
- Ruegger M, Dewey E, Gray WM, Hobbie L, Turner J, Estelle M (1998) The TIR1 protein of *Arabidopsis* functions in auxin response and is related to human SKP2 and yeast Grr1p. *Genes Dev.* **12**: 198-207.
- Ryan CA, Pearce G (1998) SYSTEMIN: a polypeptide signal for plant defensive genes. *Ann. Rev. Cell Dev. Biol.* **14**: 1-17.
- Sabatini S, Beis, Wolkenfelt H, Murfett J, Guifoyle T, Malamy J, Benfey P, Leyser O, Bechtold N, Weisbeek P, Scheres B (1999) An auxin-dependent organizer of pattern and polarity in the *Arabidopsis* root. *Cell* **99**: 463-472.
- Sakagami Y, Matsubayashi Y, Young H (1999) A novel plant growth factor, phytosulfokine, its discovery, cDNA cloning and receptor. *XVI International Botanical Congress St. Louis, USA, Aug 1-7*. <http://www.ibc99.org>.
- Sakai T, Takahashi Y, Nagata T (1996) Analysis of the promoter of the auxin-inducible gene, *parC*, of tobacco. *Plant Cell Physiol.* **37**: 906-913.
- Sambrook J, Fritsch EF, Maniatis T (1989). Molecular cloning, a laboratory manual, 2nd edition (New York, Cold Spring Harbour Laboratory Press).
- Sanyal A, O'Driscoll SW, Bolander MA, Sarkar G (1997) An effective method of completely removing contaminating genomic DNA from an RNA sample to be used for PCR. *Mol. Biotech.* **8**: 135-137.
- Sato F, Kitajima S, Koyama T, Yamada Y (1996) Ethylene-induced gene expression of osmotin-like protein, a neutral isoform of tobacco PR-5, is mediated by the AGCCGCC cis-sequence. *Plant Cell Physiol.* **37**: 249-255.
- Schaffer R, Ramsay N, Samach A, Corden S, Putterill J, Carre IA, Coupland G (1998) The *late elongated hypocotyl* mutation of *Arabidopsis* disrupts circadian rhythms and the photoperiodic control of flowering. *Cell* **93**: 1219-1229.
- Schagger H, von Jagow G (1987) Tricine sodium-dodecyl sulphate polyacrylamide-gel electrophoresis for the separation of proteins in the range from 1-kDa to 100kDa. *Analyt. Biochem.* **166**: 368-379.
- Schaller GE (1997) Ethylene and cytokinin signalling in plants: the role of two-component systems. *Essays Biochem.* **32**: 101-111.

- Scheer JM, Ryan CA (1999) A 160 kDa systemin receptor on the cell surface of *Lycopersicon peruvianum* suspension culture cells: kinetic analyses, induction by methyl jasmonate and photaffinity labelling. *Plant Cell* **11**: 1525-1535.
- Scheres B, Wolkenfelt H, Willemsen V, Terlouw M, Lawson E, Dean C, Weisbeek P (1994) Embryonic origin of the *Arabidopsis* primary root and root meristem initials. *Development* **120**: 2475-2487.
- Scheres B, Di Laurenzio L, Willemsen V, Hauser M-T, Janmaat K, Weisbeek P, Benfey PN (1995) Mutations affecting the radial organisation of the *Arabidopsis* root display specific defects throughout the embryonic axis. *Development* **121**: 53-62.
- Scheres B (1996) Embryo patterning genes and reinforcement cues determine cell fate in the *Arabidopsis thaliana* root. *Cell Dev. Biol.* **7**: 857-865.
- Scheres B, McKhann HI, van den Berg C (1996) Roots redefined: anatomical and genetic analysis of root development. *Plant Physiol.* **111**: 959-964.
- Scheres B (1997) Cell signalling in root development. *Curr. Opin. Gen. Dev.* **7**: 501-506.
- Scheres B, Wolkenfelt H (1998) The *Arabidopsis* root as a model to study plant development. *Plant Physiol. Biochem.* **36**: 21-32.
- Schiefelbein JW, Masucci JD, Wang H (1997) Building a root: the control of patterning and morphogenesis during root development. *Plant Cell* **9**: 1089-1098.
- Schneider K, Wells B, Dolan L, Roberts K (1997) Structural and genetic analysis of epidermal cell differentiation in *Arabidopsis* primary roots. *Development* **124**: 1789-1798.
- Schneider K, Mathur J, Boudonck K, Wells B, Dolan L, Roberts K (1998) The *root hairless 1* gene encodes a nuclear protein required for root hair initiation in *Arabidopsis*. *Genes Dev.* **12**: 2013-2021.
- Seo M, Akaba S, Oritani T, Delarue M, Bellini C, Caboche M, Koshida T (1998) Higher activity of an aldehyde oxidase in the auxin-overproducing *superroot1* mutant of *Arabidopsis thaliana*. *Plant Physiol.* **116**: 687-693.
- Sessa G, Meller Y, Fluhr R (1995) A GCC element and a G-box motif participate in ethylene-induced expression of the *PRB-1B* gene. *Plant Mol. Biol.* **28**: 145-153.
- Shaw SL, Quatrano RS (1996) The role of targeted secretion in the establishment of cell polarity and the orientation of the division plane in *Fucus* zygotes. *Development* **122**: 2623-2630.
- Shimomura S; Inohara N; Fukui T; Futai M (1988) Different properties of 2 types of auxin-binding sites in membranes from maize coleoptiles. *Planta* **175**: 558-566.

- Short JM, Fernandez JM, Sorge JA, Huse WD (1988) Lambda-Zap - a bacteriophage lambda-expression vector with *in vivo* excision properties. *Nuc. Acids Res.* **16**: 7583-7600.
- Shevell DE, Leu W-M, Gillmor CS, Xia G, Feldmann KA, Chua N-H (1994) *EMB30* is essential for normal division, cell expansion, and cell adhesion in *Arabidopsis* and encodes a protein that has similarity to Sec7. *Cell* **77**: 1051-1062.
- Simmons C, Migliaccio F, Masson P, Caspar T, Soll D (1995) A novel root gravitropism mutant of *Arabidopsis thaliana* exhibiting auxin physiology. *Physiol. Plant.* **93**: 790-798.
- Sisler Ec, Serek M (1997) Inhibitors of ethylene responses in plants at the receptor level: recent developments. *Physiol. Plant.* **100**: 577-582.
- Skowrya D, Craig KL, Tyers M, Elledge SJ, Harper JW (1997) F-box proteins are receptors that recruit phosphorylated substrates to the SCF ubiquitin-ligase complex. *Cell* **91**: 209-219.
- Slabas AR, Forgham-Skelton AP, Fletcher D, Martinezrivas JM, Swinhoe R, Croy RRD, Evans IM (1994) Characterisation of cDNA and genomic clones encoding homologs of the 65-kDa regulatory subunit. *Plant Mol. Biol.* **26**: 1125-1138.
- Small I, Wintz H, Akashi K, Mireau H (1998) Two birds with one stone: genes that encode products targeted to two or more compartments. *Plant Mol. Biol.* **38**: 265-277.
- Solano R, Stepnova A, Chao Q, Ecker JR (1998) Nuclear events in ethylene signalling: a transcriptional cascade mediated by ETHYLENE-INSENSITIVE3 and ETHYLENE-RESPONSE-FACTOR1. *Genes Dev.* **12**: 3703-3714.
- Speek M, Barry F, Miller WL (1996) Alternate promoters and alternate splicing of human tenascin-X, a gene with 5' and 3' ends buried in other genes. *Hum. Mol. Gen.* **5**: 1749-1759.
- Steinmann T, Geldner N, Grebe M, Mangold S, Jackson CL, Paris S, Galweiler L, Palme K, Jurgens G (1999) Coordinated polar localisation of auxin efflux carrier PIN1 by GNOM ARF GEF. *Science* **286**: 316-318.
- Stomp A-M (1990) Use of X-Gluc for histochemical localisation of glucuronidase. Editorial comments (Cleveland: United State Biochemical) **16**:5.
- Sullivan ML, Green PJ (1993) Post-transcriptional regulation of nuclear-encoded genes in higher plants: the roles of mRNA stability and translation. *Plant Mol. Biol.* **23**: 1091-1104.

- Suttle JC (1988) Effect of ethylene treatment on polar IAA transport, net IAA uptake and specific binding of *N*-1-naphthylphthalamic acid in tissues and microsomes isolated from etiolated pea epicotyls. *Plant Physiol.* **88**: 795-799.
- Tanguay RL, Gallie DR (1996) The effect of the length of the 3'-untranslated region on expression in plants. *FEBS Letters* **394**: 285-288.
- Tanimoto M, Roberts K, Dolan L (1995) Ethylene is a positive regulator of root hair development in *Arabidopsis thaliana*. *Plant J.* **8**: 943-948.
- Theologis A (1996) Plant hormones: more than one way to detect ethylene. *Curr. Biol.* **6**: 144-145.
- Theologis A (1998) Ethylene signalling: redundant receptors all have their say. *Curr. Biol.* **8**: 875-878.
- Tian H, Klämbt D, Jones AM (1995) Auxin-binding protein 1 does not bind auxin within the endoplasmic reticulum despite this being the predominant subcellular location for this hormone. *J. Biol. Chem.* **270**: 26962-26969.
- Tian Q, Reed JW (1999) Control of auxin-regulated root development by the *Arabidopsis thaliana* *SHY2/IAA3* gene. *Development* **126**: 711-721.
- Tillmann U; Viola G; Kayser B; Siemiester G; Hesse T; Palme K, Löbner M; Klämbt D (1989) cDNA clones of the auxin-binding protein from corn coleoptiles (*Zea Mays*-L) – isolation and characterisation by immunological methods. *EMBO J.* **8**: 2463-2467.
- Timpte C, Lincoln C, Pickett FB, Turner J, Estelle M (1995) The *AXR1* and *AUX1* genes of *Arabidopsis* function in separate auxin-response pathways. *Plant J.* **8**: 561-569.
- Topping JF, Wei W, Lindsey K (1991) Functional tagging of regulatory elements in the plant genome. *Development* **112**: 1009-1019.
- Topping JF, Agyeman F, Henricot B, Lindsey K (1994) Identification of molecular markers of embryogenesis in *Arabidopsis thaliana* by promoter trapping. *Plant J.* **5**: 895-903.
- Topping JF, Lindsey K (1995) Insertional mutagenesis and promoter trapping in plants for the isolation of genes and the study of development. *Transg. Res.* **4**: 291-305.
- Topping JF, Lindsey K (1997) Promoter trap markers differentiate structural and positional components of polar development in *Arabidopsis*. *Plant Cell* **9**: 1713-1725.

- Topping JF, May VJ, Muskett PR, Lindsey K (1997) Mutations in the *HYDRA1* gene of *Arabidopsis* perturb cell shape and disrupt embryonic and seedling morphogenesis. *Development* **124**: 4414-4424.
- Torres-Ruiz RA, Jurgens G (1994) Mutations in the *FASS* gene uncouple pattern formation and morphogenesis in *Arabidopsis* development. *Development* **120**: 2967-2978.
- Torres-Ruiz RA, Lohner A, Jurgens G (1996) The *GURKE* gene is required for normal organisation of the apical region in the *Arabidopsis* embryo. *Plant J.* **10**: 1005-1016.
- Towbin H, Strahelin T, Gordon J (1979) Electrophoretic transfer of proteins from polyacrylamide gels to nitrocellulose sheets: procedure and some applications. *PNAS*. **76**: 4350-4354.
- Traas J, Bellini C, Nacry P, Kronenberger J, Bouchez D, Caboche M (1995) Normal differentiation patterns in plants lacking microtubular preprophase bands. *Nature* **375**: 676-677.
- Trotochaud AE, Hao T, Wu G, Yang Z, Clark SE (1999) The CLAVATA1 receptor-like kinase requires CLAVATA3 for its assembly into a signalling complex that includes KAPP and a Rho-related protein. *Plant Cell* **11**: 393-405.
- Tsugeki R, Federoff NV (1999) Genetic ablation of root cap cells in *Arabidopsis*. *PNAS* **96**: 12941-12946.
- Uggla C, Moritz T, Sandberg G, Sundberg B (1996) Auxin as a positional signal in pattern formation in plants. *PNAS* **93**: 9282-9286.
- Ulmasov T, Hagen G, Guifoyle TJ (1997a) ARF1, a transcription factor that binds to auxin response elements. *Science* **276**: 1865-1868.
- Ulmasov T, Murfett J, Hagen G, Guifoyle TJ (1997b) AUX/IAA proteins repress expression of reporter genes containing natural and highly active synthetic auxin response elements. *Plant Cell* **9**: 1963-1971.
- Ulmasov T, Hagen G, Guifoyle TJ (1999a) Activation and repression of transcription by auxin-response factors. *PNAS* **96**: 5844-5849.
- Ulmasov T, Hagen G, Guifoyle TJ (1999b) Dimerization and DNA binding of auxin response factors. *Plant J.* **19**: 309-319.
- van den Berg C, Willemsen V, Hage W, Weisbeek P, Scheres B (1995) Cell fate in the *Arabidopsis* root meristem determined by directional signalling. *Nature* **378**: 62-65.

- van den Berg C, Willemsen V, Hendriks G, Weisbeek P, Scheres B (1997) Short-range control of cell differentiation in the *Arabidopsis* root meristem. *Nature* **390**: 287-289.
- van den Berg C, Weisbeek P, Scheres B (1998) Cell fate and cell differentiation status in the *Arabidopsis* root. *Planta* **205**: 483-491.
- Van Der Straeten D, Djudzman A, Caeneghem WV, Smalle J, Montagu MV (1993) Genetic and physiological analysis of a new locus in *Arabidopsis* that confers resistance to 1-aminocyclopropane-1-carboxylic acid and ethylene and specifically affects the ethylene signal transduction pathway. *Plant Physiol.* **102**: 401-408.
- Voelker TA, Staswick P, Chrispeels MJ (1986) Molecular analysis of two phytohemagglutinin genes and their expression in *Phaseolus vulgaris* cv. Pinto, a lectin-deficient cultivar of the bean. *EMBO J.* **5**: 3075-3082.
- Vogel JP, Woeste KE, Theologis A, Kieber JJ (1998a) Recessive and dominant mutations in the ethylene biosynthetic gene *ACS5* of *Arabidopsis* confer cytokinin insensitivity and ethylene overproduction, respectively. *PNAS* **95**: 4766-4771.
- Vogel JP, Schuerman P, Woeste K, Brandstatter I, Kieber JJ (1998b) Isolation and characterisation of *Arabidopsis* mutants defective in the induction of ethylene biosynthesis by cytokinin. *Genetics* 1998b, **149**: 417-427.
- Vroemen CW, Langeveld S, Mayer U, Ripper G, Jurgens G, Kammen AV, De Vries SC (1996) Pattern formation in the *Arabidopsis* embryo revealed by position-specific lipid transfer protein gene expression. *Plant Cell* **8**: 783-791.
- Wada T, Tachibana T, Shimura Y, Okada K (1997) Epidermal cell differentiation in *Arabidopsis* determined by a *Myb* homolog, *CPC*. *Science* **277**: 1113-1116.
- Walden R, Fritze K, Hayashi H, Miklashevichs E, Harling H, Schell J (1994) Activation tagging: a means of isolating genes implicated as playing a role in plant growth and development. *Plant Mol. Biol.* **26**: 1521-1528.
- Walker AR, Davison PA, Bolognesi-Winfield AC, James CM, Srinivasan N, Blundell TL, Esch JJ, Marks MD, Gray JC (1999) The *TRANSPARENT TESTA GLABRA1* locus, which regulates trichome differentiation and anthocyanin biosynthesis in *Arabidopsis*, encodes a WD40 repeat protein. *Plant Cell* **11**: 1337-1349.
- Wang L, Wessler SR (1998) Inefficient reinitiation is responsible for upstream open reading frame-mediated translational repression of the maize *R* gene. *Plant Cell* **10**: 1733-1745.
- Weigel D, Ahn JH, Blazquez MA, Borevitz JO, Christensen SK, Fankhauser C, Ferrandiz C, Kardailsky I, Malanchruvil EJ, Neff MM, Nguyen JT, Sato S, Wang

- Z-Y, Xia Y, Dixon RA, Harrison MJ, Lamb CJ, Yanofsky MF, Chory J (2000) Activation tagging in *Arabidopsis*. *Plant Physiol.* **122**: 1003-1013.
- West MAL, Harada JJ (1993) Embryogenesis in higher plants: an overview. *Plant Cell* **5**: 1361-1369.
- West MAL, Yee KM, Danao J, Zimmerman JL, Fischer RL, Goldberg RB, Harada JJ (1994) *LEAFY COTYLEDON1* is an essential regulator of late embryogenesis and cotyledon identity in *Arabidopsis*. *Plant Cell* **6**: 1731-1745.
- Willemsen V, Wolkenfelt H, de Vrieze G, Weisbeek P, Scheres B (1998) The *HOBBIT* gene is required for formation of the root meristem in the *Arabidopsis* embryo. *Development* **125**: 521-531.
- Woeste K, Kieber JJ (1998) The molecular basis of ethylene signalling in *Arabidopsis*. *Phil. Trans. R. Soc. Lond. B* **353**: 1431-1438.
- Woeste K, Ye C, Kieber JJ (1999a) Two *Arabidopsis* mutants that overproduce ethylene are affected in the posttranscriptional regulation of 1-aminocyclopropane-1-carboxylic acid synthase. *Plant Physiol.* **119**: 521-529.
- Woeste K, Vogel JP, Kieber JJ (1999b) factors regulating ethylene biosynthesis in etiolated *Arabidopsis thaliana* seedlings. *Physiol. Plant.* **105**: 478-484.
- Wong LM, Abel S, Shen N, de la Foata M, Mall Y, Theologis A (1996) Differential activation of the primary auxin response genes *PS-IAA4/5* and *PS-IAA6*, during early plant development. *Plant J.* **9**: 587-599.
- Yang S, Hoffman N (1984) Ethylene biosynthesis and its regulation in higher plants. *Ann. Rev. Plant Physiol.* **35**: 155-189.
- Young R, Davies RW (1983) *Science (Washington D. C.)* **222**: 778-789.
- van der Zaal EJ, Droog FNJ, Boot CJM, Hensgens LAM, Hoge JHC, Schilperoort RA, Libbenga KR (1991) Promoters of auxin-induced genes from tobacco can lead to auxin-inducible and root tip-specific expression. *Plant Mol. Biol.* **16**: 983-998.
- Zavala ME, Brandon DL (1983) Localization of a phytohormone using immunocytochemistry. *J. Cell Biology* **97**: 1235-1239.
- Zhou JM, Goldsbrough PB (1993) An *Arabidopsis* gene with homology to glutathione-S-transferases is regulated by ethylene. *Plant Mol. Biol.* **22**: 517-523.

APPENDIX 1 Primers

C-GFPR_v – CGGGATCCTTTGTATAGTTCATCCATGC

C-POLF – CGGGATCCATGAAACCCAGACTTTGT

C-POLR_v – CGGAATTCTCATCAATGGATTTTAAAAAG

POL-RS-PCR - CTTATACGGATATCCTGGCAATTCGGACTTGATAGGGTGA
TCAATGGA

RS-PCR AD – CTTATACGGATATCCTGGCAATTCGGACTT

GENEX_{for} – AGTGGATCCCCAAAATCTGAGCCGTCCG

GENEX_{Rev} – AGTGGATCCCCTAACAACGTCTCCTTCC

35SGFP_{REV} – GCCTGCAGCTTATTTGTATAGTTCATCC

35SGFP FOR - CGGGATCCATGAGTAAAGGAGAAGAAC

HYG FOR – GTTGCAAGACCTGCCTGAAACC

HYG REV – CTGCTGCTCCATACAAGCCAACC

GUS PA – CCAGGTGTTTCGGCGTGGTGTAGAGC

GUS PB – GGCGTGACATCGGCTTCAAATGGCG

RACE Anchor – GCCAAGCTTCTGCAGGAGCTC

Oligo d(T)₁₅ anchor – CCAAGCTTCTGCAGGAGCTCTTTTTTTTTTTTTTTT

3.0 prom – GGAACACGAAATCCGAAGAGCGAG

3.1 prom - GTTGTGGTGATGTTGGCGCAGTG

EM1 RT3 – GGAAGTTTCCGACAAGAACAG

RT 35/55 – CGCTGAAACTGTGGAAGAAG

ACT-FOR – GATCCTAACCGAGCGTGGTTAC

ACT-REV – GACCTGACTCGTCATACTCTGC

NOS FOR – CAGGTACCCCGATCGTTCAAACATTTGGC

NOS REV – CAGGTACCCCAATTCCCGATCTAGTAAC

GST for – CCATTGCCAGGAGAGTCCTC
GST rev – CCACTCATTGACACGTGGACGC
PROM1635 – GACAAACAAGCTTTAGCCCGTGCG
PolProm – GCGAGCTCAAGCTTGAGGGAAAGAGAGGAAG
NH-POLR – CGGGATCCATGGATTTTAAAAAGTTTAAAC
NH-GFPF – CGGGATCCAGTAAAGGAGAAGAAGAACTTTTC
NH-GFPRv – CGGAATTCCTTATTTGTATAGTTCATCC
5'UTR-Rv – GCTCTAGATCATGTTTCAGTGAGACAC
C-GFPF – GCTCTAGAATGAGTAAAGGAGAAGAAC
POL5'TEST – GGAGACTAAAGCGAACATATAAAACC
POL5'EXT – CTCACTACTACCCAAACTAAAACAC
POL121 – GTGTTTTAGTTTGGGTAGTAGTGAG
Xba-For – GCATCTAGAGGAACACGAAATCCGAAGAGC
Xba-Rev – GTCTCTAGAATTGAAAATGATAGGGTGATC
2.85prom – CCACTTAATATATTAGTATTGGAG
EXT-S1 – GTGTGCCTCACGTGCTCTTCTC
EcoR1-220 – GACGAATTCGAAATCCATGATCATATAG
RACE1 – CATGGAGAAATGGACCTTCGCC
RACE2 – GGTTTCATTCATGTTTCAGTGAG
POL+RT – GGAACACGAAATCCGAAGAGCGAG
POL-RT – GAAAATGATAGGGTGATCAATGG
POLRT+1 – GAGCGAGGGGAGCGAAGACAG
POLRT+2 – GAAAGAGAAGAGCACGTGAGG
POLREV1 – CATGGAGAAATGGACCTTCGC
584prom – GAGGGAAAGAGAGGAAGAGGTC

NESTED1 – GCGATCCAGACTGAATGC

P40.N2 - TTCACGGGTTGGGGTTTCTACAGG

-VE PROM – GTGGACTGTCTTCGCTCCCTCGC

T7 Primer – CGGGATATCACTCAGCATAATG

M13 FOR – GTAAAACGACGGCCAG

M13 REV - CAGGAAACAGCTATGAC

Appendix II Complementation Root Length Data

The roots of 10 seedlings were measured following
6 days growth in the light on 1/2MS10 Media

LINE	ROOT LENGTH (mm)	STAND. DEV.
AtEM101	12.85	2.6
C24	21.2	3.6
3B	15.7	2.7
13B	16.15	3.1
17A	15.55	1.7
25C	18.15	2.1
26A	14.75	1.3
56A	15.2	1.3
67B	16	0.7

The roots of 10 seedlings were measured following
9 days growth in the light on 1/2MS10 Media

LINE	ROOT LENGTH (mm)	STAND. DEV.
AtEM101	14.7	2.6
C24	25.1	6.5
77A	16.2	1.1
77B	19.3	2.8
80A	19.3	1.7
80B	16.7	1.5
81B	18.7	1.5
82A	18.6	2.2
84C	18.7	1.5
85	17.4	1.6
86B	21	2.7
87A	21.7	2.7
87C	19.7	4.1
90	21.1	3.1
93	20.5	3.9
94B	21.8	2.7
113C	21.3	4.7

Appendix III 35SPOLARIS Data

Tables show the data for experiments involving the plant lines overexpressing *POLARIS*, as described in Chapter 6. For each treatment the table shows the mean root length in mm of 20 seedlings. Standard deviations are shown in brackets.

- A) 7 day dark grown seedlings grown on either the cytokinin BA or ACC.
- B) 7 day light grown seedlings grown on NAA.

A

Treatment	PLANT LINE Root Length (mm) + Stand. Dev.					
	Columbia	35SPOL 38	35SPOL 53	35SPOL 55	35SPOL 59	35SPOL 70
1/2MS10	17.9 (5.7)	19.6 (2.9)	19.8 (2.5)	20.9 (4.2)	20.1 (3.8)	22.8 (4.4)
BA 0.1uM	8.1 (1.7)	8.9 (0.8)	9.2 (1)	9.9 (0.9)	9.9 (0.9)	9.4 (0.8)
BA 0.5uM	7.2 (1.3)	8.2 (0.8)	8.3 (0.9)	8.4 (0.6)	8.6 (0.8)	7.9 (1)
BA 1uM	5.3 (1.6)	6.8 (1.5)	7.3 (0.9)	7.5 (0.9)	7.6 (1.1)	7.8 (0.8)
BA 5uM	5.2 (1.7)	6.3 (1.1)	6.1 (1.1)	6.2 (1.2)	6.3 (1)	5.9 (1.1)
ACC 1uM	2.8 (0.8)	3.9 (1.2)	4.0 (0.8)	4.1 (0.4)	3.9 (1.1)	4.4 (1.0)
ACC 10uM	2.1 (0.7)	3.3 (0.6)	2.7 (0.5)	2.9 (0.5)	3.0 (0.8)	3.2 (1.0)

B

Treatment	PLANT LINE Root Length (mm) + Stand. Dev.					
	Columbia	35SPOL 38	35SPOL 53	35SPOL 55	35SPOL 59	35SPOL 70
1/2MS10	14.6 (3.4)	14.5 (2.4)	16.3 (2.9)	14.9 (3.3)	17.1 (3.4)	15.7 (2.9)
NAA 0.1uM	12.3 (2.5)	12.2 (2.9)	12.4 (3.6)	11.2 (3.5)	12.3 (2.8)	10.6 (3.2)
NAA 1uM	4.2 (1.3)	5.3 (1.1)	5.1 (1.4)	4.8 (0.7)	4.9 (1.0)	4.7 (0.8)

